Dynamique des communautés bactériennes detapis microbiens soumis aux stressenvironnementaux

Aude Fourçans

N° d'ordre : 2004PAUU3007

THÈSE

présentée à

L'UNIVERSITÉ DE PAU ET DES PAYS DE L'ADOUR

École doctorale des Sciences exactes et de leurs applications

par **Aude FOURÇANS**

pour obtenir le grade de

DOCTEUR

Spécialité : **Microbiologie**

Dynamique des communautés bactériennes de tapis microbiens soumis aux stress environnementaux

Soutenue le : ***9 avril 2004***

Après avis de :

Philippe Normand (DR, UMR 5557 CNRS UCBL, Lyon I)	*Rapporteur*
Jean Claude Bertrand (Pr, LOB UMR 6535, Aix-Marseille II)	*Rapporteur*

Devant la commission d'examen formée de :

Philippe GOULAS (Pr, LEM EA 3525, Université de Pau)	*Président*
Gerard MUYZER (Pr Associé, Delft University of Technology – Netherlands)	*Examinateur*
Pierre CAUMETTE (Pr, LEM EA 3525, Université de Pau)	*Directeur de thèse*
Robert DURAN (MCF HDR, LEM EA 3525, Université de Pau)	*Co-directeur de thèse*

Mes premiers remerciements s'adressent en premier lieu à mes Directeurs de thèse pour avoir répondu favorablement à mon souhait appuyé d'effectuer une thèse ; pour leur accueil au sein du Laboratoire d'Ecologie Moléculaire ; pour m'avoir dirigée de manière si complémentaire, et surtout pour toute la confiance qu'ils m'ont accordée dans ce travail de thèse :

Pierre Caumette, Professeur à l'Université de Pau et des Pays de l'Adour, pour son accueil chaleureux au sein du Laboratoire d'Ecologie Moléculaire, pour ses conseils, pour les possibilités d'ouverture au milieu scientifique et de collaboration, par le biais du projet européen MATBIOPOL et l'accès à divers congrès.

Robert Duran, Maître de Conférence à l'Université de Pau et des Pays de l'Adour, pour son encadrement avisé pendant cette thèse, pour sa présence judicieuse, pour l'indépendance qu'il m'a laissé prendre et dans laquelle j'ai su m'épanouir, pour sa disponibilité et ses conseils précieux, tout simplement pour le bel exemple de chercheur qu'il a su me donner.

Je tiens également à remercier les rapporteurs de cette thèse, Philippe Normand, Directeur de recherche CNRS à l'Université Claude Bernard de Lyon, et Jean Claude Bertrand, Professeur à l'Université d'Aix Marseille, pour avoir accepté de juger ce travail, et aussi pour leur réelle patience dans l'attente du manuscrit !
Merci aussi à Philippe Goulas, Professeur à l'Université de Pau et des Pays de l'Adour, d'avoir présidé ce jury de thèse ; Gerard Muyzer, Professeur associé à l'Université de Delft, qui malgré la distance à volontiers accepté de participer à ce jury de thèse et d'examiner mon travail..

Ce travail de recherche n'aurait pu avoir lieu sans le soutien financier du Conseil Général des Pyrénées Atlantiques et de la Communauté Economique Européenne.

Evidemment cette thèse ne serait pas ce qu'elle est sans l'aide, la disponibilité et la bonne humeur sans cesse renouvelée de tous les membres du laboratoire. Je vous en suis reconnaissante car cela m'a permis d'évoluer dans un environnement de confiance et de sérénité.
Je commencerais par citer la bande des jeunes MC de l'équipe Microbio, Régis et ses longues discussions devant un café, le calme olympien de Rémy face au speed de Marisol,…et un MC adoptif…Patrice, peut-être un bureau dans le futur labo !?
Les étudiants, fort nombreux pendant ces 4 années, alors ne m'en veuillez pas si je ne peux tous vous citer ! Plus particulièrement une pensée pour mes deux « p'tits » DEA devenus grands (thésards !), Tony toujours assorti à son mobile, et Sylvain perdu sans son surf et ses skis! A vous les joies de la thèse ! Merci aussi au « club » des thésards Microbio :Odile (ah ! …Marseille !), Guillaume (c'est pas mal aussi Préchacq !) et Benji (t'as pas changé depuis le collège !).
De gros bisous aux « jumelles », thésardes adoptives du LEM, Odile, Miss Montpellier (dur, dur la bio mol chère docteur !) et Séraphine alias Séverine, Miss Nouméa (courage plus qu'un an !).
Merci en dernier lieu à Christine, Béatrice, Pat, Solange, Arnaud et Marie-Jo pour votre aide, vos conseils et vos coups de mains réguliers !
Enfin, un grand merci à Sophie et Guille, vous avez été présentes au sein du laboratoire au cours de ma thèse. J'ai pu apprécier votre présence, votre expérience, et tout particulièrement votre amitié. Et je les apprécie toujours !

Une tendresse toute particulière à mes parents, et à mon frère, pour vos encouragements tout au long de mes études et vis à vis de mes choix, pour votre présence aimante de tous les instants, surtout durant cette dernière année que je vous ai fait vivre …ou subir ! Vous pourriez presque dire « on a fait une thèse ! ».

Le principal objectif de ce travail de recherche était l'étude de la dynamique des communautés bactériennes de tapis microbiens afin de comprendre leurs fonctionnements et leur mécanismes d'adaptation face aux stress environnementaux. De part le développement dans des habitats très variés et soumis à des variations des conditions environnementales importantes, les tapis microbiens constituent des modèles de choix pour ce type d'études. La biodiversité bactérienne a principalement été abordée par T-RFLP (Terminal Restriction Fragment Length Polymorphism), approche moléculaire d'écologie microbienne.

Premièrement, ce travail a porté sur la description de deux tapis microbiens photosynthétiques présents sur deux sites différents de salinité distinctes, marin (Iles Orcades), et hypersalé (Marais salants de Camargue). La combinaison de différentes approches d'analyses ont permis d'obtenir une image à l'échelle du micromètre de ces tapis. Ainsi, la diversité bactérienne des principales communautés (eubactéries, bactéries phototrophes pourpres, bactéries sulfato-réductrices) de ces tapis microbiens a été décrite par l'approche moléculaire de T-RFLP. Les résultats de cette analyse, associés à ceux d'analyses biogéochimiques, moléculaire DGGE (Denaturing Gradient Gel Electrophoresis), microscopiques (CLSM), et de biomarqueurs lipidiques a permis de relier les communautés bactériennes présentes et d'appréhender leurs rôles écologiques au sein de ces écosystèmes complexes. Ces deux tapis bien que très différents révèlent une organisation très fine, constituée de couches distinctes verticales de quelques micromètres, où s'agencent les populations bactériennes en fonction de leurs caractéristiques physiologiques et des conditions environnementales. Le tapis de Camargue est dominé en surface par les cyanobactéries filamenteuses, principalement *Microcoleus chthonoplastes*. De plus, la distribution des bactéries phototrophes pourpres et sulfato-réductrices est répartie en fonction des gradients mesurés de sulfure, oxygène et lumière. Le tapis des îles Orcades est au contraire dominé par les bactéries pourpres, très diversifiées, principalement du genre *Thiocapsa.* Les cyanobactéries y sont faiblement représentées. La diversité bactérienne phototrophes et sulfato-réductrices est très finement organisée le long de gradients physico-chimiques.

Dans un deuxième temps, la distribution spatio-temporelle du tapis microbien de Camargue en fonction du cycle nycthéméral a été étudiée. Des comportements adaptatifs chez les bactéries pourpres, les cyanobactéries et les bactéries sulfato-réductrices ont ainsi pu être révélés. Parmi ces réponses aux variations des microgradients de sulfure et d'oxygène, la migration a été mise en évidence chez un grand nombre de ces microorganismes.

L'analyse de l'impact d'hydrocarbures sur les tapis microbiens de Guérande et de Camargue a été le troisième point abordé. L'influence des paramètres environnementaux sur la dégradation naturelle du pétrole Erika a pu être démontrée. De plus, l'impact réel de la pollution sur les communautés du tapis a été observé montrant une succession de différentes communautés bactériennes. Ceci révèle les capacités d'adaptation de ces écosystèmes face à ce stress d'hydrocarbures. Même si la dégradation par voie microbiologique n'a pu être mise en évidence dans ces systèmes, l'analyse de la diversité des gènes codant pour les dioxygénases montre une grande diversité, suggérant que les tapis microbiens possèdent un potentiel de dégradation important.

Ce travail a permis de mettre en évidence l'organisation dynamique des bactéries au sein de tapis microbiens, et d'approcher leurs comportements adaptatifs vis à vis des stress soumis.

Mots clés : Biodiversité bactérienne, tapis microbien, T-RFLP, hypersalé, structure verticale, gradients physico-chimiques, pollution d'hydrocarbures.

Introduction

Introduction :

Les tapis microbiens, écosystèmes sédimentaires complexes, mettent en jeu de nombreux processus biologiques différents. Leurs compositions variées en communautés bactériennes, cyanobactéries, bactéries chimiolithotrophes sulfo-oxydantes, bactéries phototrophes anoxygéniques, bactéries sulfato-réductrices, et la nature compacte de leurs organisations sont les caractéristiques principales de ce type d'écosystème.

De plus, ils sont, entre autres, le siège des cycles du carbone, du soufre et de l'azote. Ils participent donc étroitement au processus dynamique du renouvellement des molécules utilisées comme donneurs et accepteurs d'électrons par les diverses communautés bactériennes qui les composent. Ces consortiums microbiens constituent des modèles d'étude et de compréhension des nombreuses interactions existantes entre les communautés et leur environnement.

Depuis ces dernières années, l'essor de nouveaux outils moléculaires d'analyse de la biodiversité ont permis d'appréhender ces systèmes de manière intégrée, s'affranchissant ainsi des méthodes de cultures classiques. Alors que plus de 99% des microorganismes présents dans la nature ne sont pas accessibles par les méthodes de microbiologie classique, les méthodes d'écologie moléculaire permettent d'améliorer les études de la diversité. Ainsi, il en découle une meilleure compréhension et connaissance de ces écosystèmes complexes.

D'un point de vue écologique, l'étude présentée vise à étudier la place et le rôle des microorganismes à deux niveaux :

- de l'écosystème, en intégrant à l'étude de biodiversité les aspects métaboliques, et physico-chimiques du tapis microbien.
- des communautés bactériennes, analysant la biodiversité du tapis microbien et le comportement des différentes communautés face à divers stress.

Le travail présenté ici porte sur l'étude de la diversité des principales communautés bactériennes de tapis microbiens par une approche moléculaire de polymorphisme de restriction la T-RFLP (Terminal Restriction Fragment Length Polymorphism).

Le chapitre introductif est consacré à la présentation des tapis microbiens, de leurs communautés bactériennes majeures, et des connaissances actuelles sur les comportements de ces communautés face à divers stress physico-chimiques, salin ou par pollution.

Face au stress salin, leurs adaptations en terme de diversité a été abordée par l'étude de deux tapis microbiens distincts, l'un hypersalé (Salins-de-Giraud, Camargue), l'autre marin (Iles Orcades, Ecosse). Cette étude descriptive associant l'analyse de la diversité bactérienne et des facteurs environnementaux fait l'objet de deux articles au sein du chapitre III.

Les gradients physico-chimiques naturellement présents au sein des tapis microbiens sont source de stress régulier par leurs fluctuations quotidiennes. L'impact de ces gradients sur les bactéries sulfato-réductrices et phototrophes (anoxygéniques et oxygéniques) a été étudié en détails, et les résultats sont présentés dans deux articles.

Les pollutions par des hydrocarbures, accidentelles ou non, ont des conséquences importantes sur la diversité des bactéries. De nombreux microorganismes sont connus pour leur capacité à métaboliser les hydrocarbures. Vu le potentiel métabolique que constituent les tapis microbiens, l'impact de cette pollution a été étudié sur deux tapis microbiens hypersalés (Guérande et Camargue), et les résultats sont présentés sous forme d'article.

Chapitre I : Etude bibliographique

I. Etude bibliographique

I.1. Le tapis microbien

I.1.1. Description générale

Dans la nature, les microorganismes ont la capacité, de part leur grande diversité métabolique, de coloniser différents types d'habitats et d'interagir entre eux formant de ce fait des écosystèmes plus ou moins complexes. Ainsi, la présence de tapis microbiens dans de nombreux sites couvrant toutes les zones climatiques et géographiques, en est un bel exemple. Ils se développent à l'interface eau-sédiment, d'environnements peu profonds tels que les estuaires (Mir *et al.*, 1991), les sources hydrothermales (Ferris *et al.*, 1996), les lacs (Brambilla *et al.*, 2001), les déserts, les plages sablonneuses abritées (van Gemerden *et al.*, 1989a; Wieland *et al.*, 2003), ou bien les environnements hypersalés comme les marais salants (Caumette *et al.*, 1994; Giani *et al.*, 1989).

Souvent décrit depuis de nombreuses années (Castenholz, 1994; Caumette *et al.*, 1994; Esteve *et al.*, 1992; Giani *et al.*, 1989; Guerrero *et al.*, 1993; Mir *et al.*, 1991; Stal, 1994; Stal *et al.*, 1985 ; van Gemerden *et al.*, 1989a; van Gemerden *et al.*, 1989b), les tapis microbiens correspondent à l'association de différentes populations microbiennes organisées selon leurs physiologies, sous forme d'une structure verticale composée de strates successives. Les tapis bactériens, généralement photosynthétiques, s'organisent de la surface vers la profondeur, depuis les cyanobactéries, les bactéries hétérotrophes aérobies, les bactéries chimiolithotrophes sulfo-oxydantes, les bactéries phototrophes anoxygéniques (pourpres et vertes) jusqu'aux bactéries sulfato-réductrices (Figure 1). Les microorganismes fermentatifs, méthanogènes, nitrifiants ou dénitrifiants sont aussi présents au sein de ces tapis microbiens, mais en quantités moins importantes (van Gemerden, 1993). Ainsi, sous l'influence des activités métaboliques des différents membres de ces communautés bactériennes, des gradients physico-chimiques verticaux d'oxygène, de sulfure et d'intensité lumineuse sont formés (Jørgensen *et al.*, 1983; Revsbech *et al.*, 1983).

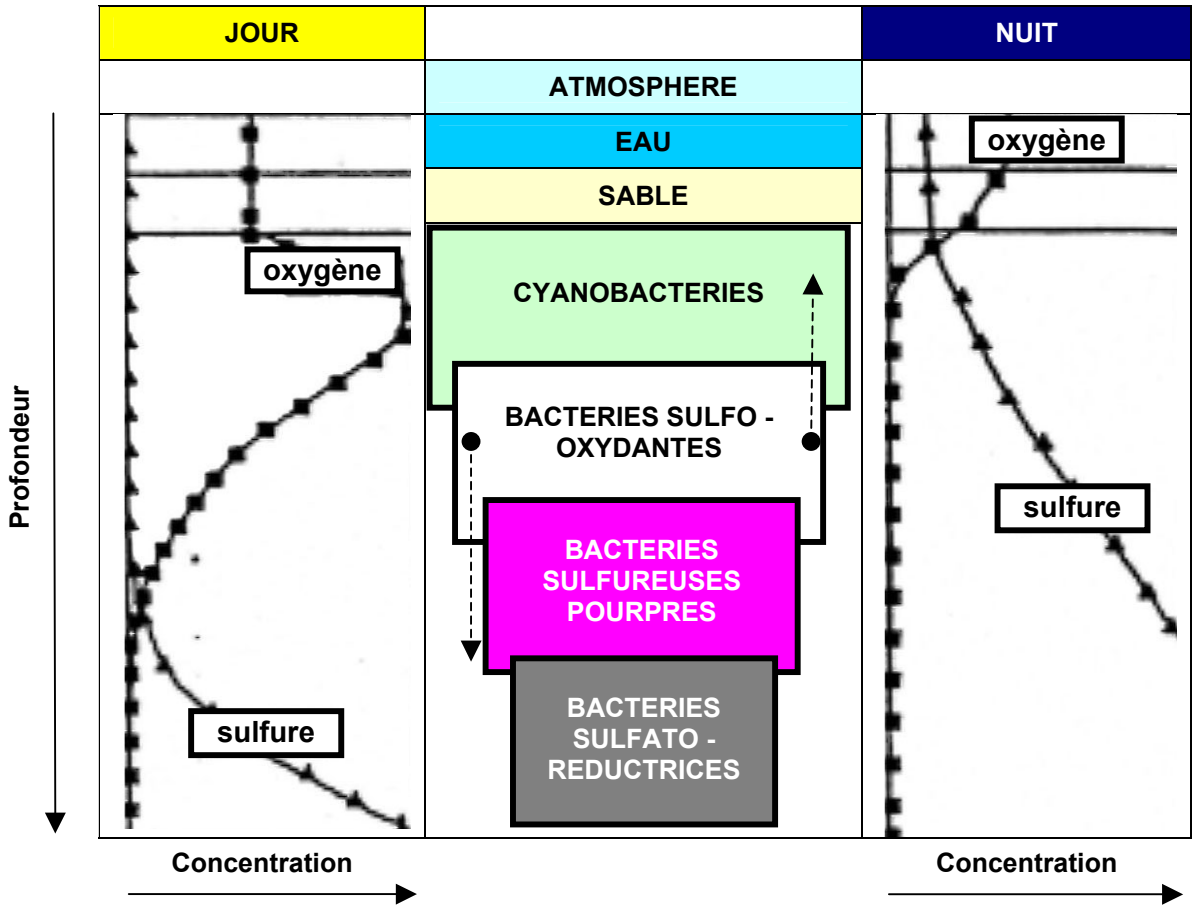

Figure 1 : Représentation schématique de l'organisation des communautés bactériennes au sein d'un tapis microbien, en fonction des gradients physico-chimiques d'oxygène et de sulfure. D'après van Gemerden (1993).

Les tapis microbiens sont donc le résultat de croissances et d'activités bactériennes conjointes (Tableau 1). La colonisation des sédiments par ces écosystèmes bactériens dépend essentiellement de paramètres environnementaux tels que la granulométrie, le taux de sédimentation et d'érosion (par le vent et l'eau), la rétention par capillarité de l'eau, la pénétration de la lumière, et la prédation par des organismes eucaryotes. Les tapis microbiens participent ainsi à la stabilisation des sédiments (van Gemerden, 1993; Walter, 1976). Les tapis microbiens sont considérés comme les analogues récents des stromatolites du Précambrien. Des microfossiles provenant de ces stromatolites ont en effet été datés à 3,5 milliards d'années (Margulis *et al.*, 1980; Walter *et al.*, 1992b). Ces structures stratifiées fossilisées peuvent être observées dans les zones riches en fer, calcaires, phosphorites, magnésites. Ils sont considérés comme faisant partie des plus anciens écosystèmes structurés observés sur la planète (Walter, 1976; Walter *et al.*, 1992a; Walter *et al.*, 1992b).

Tableau 1 : Différents métabolismes bactériens existants au sein des tapis microbiens. D'après van Gemerden (1993).

1.a Cyanobacteria: oxygenic photosynthesis	
energy source: light e^- donor: H_2O carbon source: CO_2	
e^- donor for CO_2 fixation	$2H_2O \rightarrow O_2 + 4[H]$
CO_2-fixation	$CO_2 + 4[H] \rightarrow \langle CH_2O \rangle + H_2O$
Total	$CO_2 + H_2O \rightarrow \langle CH_2O \rangle + O_2$
1.b Cyanobacteria: anoxygenic photosynthesis	
energy source: light e^- donor: H_2S carbon source: CO_2	
e^- donor for CO_2 fixation	$2H_2S + 3H_2O \rightarrow H_2S_2O_3 + 8[H]$
CO_2-fixation	$2CO_2 + 8[H] \rightarrow 2\langle CH_2O \rangle + 2H_2O$
Total	$2CO_2 + 2H_2S + H_2O \rightarrow 2\langle CH_2O \rangle + H_2S_2O_3$
1.c Cyanobacteria: fermentation, sulfur respiration	
energy source: glycogen, trehalose e^- acceptor: S^0	
Total	$C_6H_{12}O_6 \rightarrow CH_3CHOHCOOH + CH_3CH_2OH + CO_2$
	(approximation) $C_6H_{12}O_6 + H_2O \rightarrow 2CH_3COOH + 2CO_2 + 3H_2 + 2[H]$
	$2[H] + S^0 \rightarrow H_2S$
Total	(approximation) $C_6H_{12}O_6 + H_2O + S^0 \rightarrow 2CH_3COOH + 2CO_2 + 3H_2 + H_2S$
2 Colourless sulfur bacteria: chemosynthesis	
energy source: H_2S/O_2 principal e^- donor: H_2S principal carbon source: CO_2	
	$3H_2S + 1\frac{1}{2}O_2 \rightarrow 3S^0 + 3H_2O$
	$3S^0 + 4\frac{1}{2}O_2 + 3H_2O \rightarrow 3H_2SO_4$
energy	$3H_2S + 6O_2 \rightarrow 3H_2SO_4$
	$H_2S \rightarrow S^0 + 2[H]$
	$S^0 + 4H_2O \rightarrow H_2SO_4 + 6[H]$
e^- donor for CO_2-fixation	$H_2S + 4H_2O \rightarrow H_2SO_4 + 8[H]$
CO_2-fixation	$2CO_2 + 8[H] \rightarrow 2\langle CH_2O \rangle + 2H_2O$
Total	$2CO_2 + 4H_2S + 6O_2 + 2H_2O \rightarrow 2\langle CH_2O \rangle + 4H_2SO_4$
3.a Purple sulfur bacteria: anoxygenic photosynthesis	
energy source: light principal e^- donor: H_2S principal carbon source: CO_2	
	$H_2S \rightarrow S^0 + 2[H]$
	$S^0 + 4H_2O \rightarrow H_2SO_4 + 6[H]$
e^- donor for CO_2-fixation	$H_2S + 4H_2O \rightarrow H_2SO_4 + 8[H]$
CO_2-fixation	$2CO_2 + 8[H] \rightarrow 2\langle CH_2O \rangle + 2H_2O$
Total	$2CO_2 + H_2S + 2H_2O \rightarrow 2\langle CH_2O \rangle + H_2SO_4$
3.b Purple sulfur bacteria, chemosynthesis	
energy source: H_2S/O_2 principal e^- donor: H_2S principal carbon source: CO_2	
4 Sulfate-reducing bacteria: dissimilatory sulfate reduction, sulfate respiration	
energy source: organic C, H_2 e^- donor: organic C, H_2 carbon source: organic C	
4.a incomplete oxidation[1]	$2CH_3CHOHCOOH + 2H_2O \rightarrow 2CH_3COOH + 2CO_2 + 8[H]$
e^- acceptor	$H_2SO_4 + 8[H] \rightarrow H_2S + 4H_2O$
Total	$2CH_3CHOHCOOH + H_2SO_4 \rightarrow 2CH_3COOH + 2CO_2 + H_2S + 2H_2O$
4.b complete oxidation[2]	$2CH_3CHOHCOOH + 6H_2O \rightarrow 6CO_2 + 24[H]$
e^- acceptor	$3H_2SO_4 + 24[H] \rightarrow 3H_2S + 12H_2O$
Total	$2CH_3CHOHCOOH + 3H_2SO_4 \rightarrow 6CO_2 + 3H_2S + 6H_2O$
4.c e^- donor[3]	$4H_2 \rightarrow 8[H]$
e^- acceptor	$H_2SO_4 + 8[H] \rightarrow H_2S + 4H_2O$
Total	$4H_2 + H_2SO_4 \rightarrow H_2S + 4H_2O$

I.1.2. Les groupes bactériens fonctionnels majeurs

I.1.2.1. Les cyanobactéries

Les cyanobactéries, filamenteuses ou unicellulaires, forment un groupe complexe de microorganismes présentant une large diversité. Parmi les nombreux genres qui constituent la grande diversité de ce groupe bactérien, *Aphanothece, Chroococcus, Gloeocapsa, Halomicronema, Leptolyngbya, Microcoleus, Oscillatoria, Pleurocapsa, Spirulina,, Synechocystis* sont les plus représentés au sein de tapis microbiens, *Microcoleus chthonoplastes* étant l'espèce dominante des tapis cyanobactériens hypersalés (Caumette *et al.*, 1994; Giani *et al.*, 1989; Nübel *et al.*, 2000a).

Le métabolisme principal des cyanobactéries correspond à la photosynthèse oxygénique. Ces bactéries réalisent la photolyse de l'eau en utilisant les radiations lumineuses du spectre visible pour produire du dioxygène. Elles possèdent deux photosystèmes membranaires, PSI et PSII, qui contiennent différents pigments : la chlorophylle *a*, des caroténoïdes et des phycobylines (Blankenship and Hartman, 1998; Grossman *et al.*, 1995).

Dans l'environnement, elles colonisent volontiers la surface d'habitats pauvres en matières organiques, tels que les sédiments (van Gemerden, 1993). Leurs différentes potentialités font de ces microorganismes des précurseurs dans la constitution des tapis microbiens. En effet, leurs capacités à réaliser une photosynthèse oxygénique et à fixer l'azote atmosphérique permettent d'enrichir le sédiment en oxygène, en matière organique et en composés azotés favorisant ainsi le développement d'autres espèces bactériennes (Stal, 1994; Stal *et al.*, 1985). Ainsi, les cyanobactéries délimitent au sein des tapis une zone oxique riche en nutriments, favorisant le développement d'autres microorganismes. Leur capacité à glisser leurs permet de se maintenir en surface, et de se placer à des niveaux où leurs pigments peuvent capter les radiations lumineuses (Donkor and Häder, 1991).

D'autre part, les cyanobactéries en excrétant des polysaccharides ou EPS (extracellular polymeric substances) forment une matrice autour des bactéries (Decho, 1990). Cette gaine polysaccharidique, en se liant aux particules de sédiments, contribue à la stabilisation du tapis microbien et prévient les phénomènes d'érosion (Dade *et al.*, 1990; Paterson, 1989). Les cyanobactéries filamenteuses participent en grande partie au maintien de ce réseau en piégeant les particules du sédiment au sein de leurs filaments (D'Amelio *et al.*, 1987).

I.1.2.2. Les bactéries chimiolithotrophes sulfo-oxydantes

Les bactéries chimiolithotrophes sulfo-oxydantes trouvent leur place au sein du tapis microbien au niveau de l'interface entre la zone oxique, délimitée par les cyanobactéries, et la zone anoxique inférieure riche en sulfure. Ces microorganismes ont la capacité d'oxyder le sulfure et d'autres composés inorganiques soufrés, en sulfate à l'issue d'une réaction de sulfato-réduction. Ce sulfure est utilisé à la fois comme source d'énergie et donneur d'électrons pour réduire le dioxyde de carbone en carbone organique. L'oxygène et le nitrate sont les accepteurs terminaux d'électrons de cette oxydation (Jørgensen, 1982; Nelson *et al.*, 1986a; Nelson *et al.*, 1986b; van Gemerden, 1993).

Parmi ces microorganismes sulfo-oxydants, le genre *Beggiatoa* est particulièrement présent dans les tapis microbiens (Martinez *et al.*, 1997). Ces bactéries montrent une bonne adaptation au rythme nycthéméral. En effet, elles ont la propriété de suivre les fluctuations de l'interface oxygène-sulfure par des déplacements verticaux (García-Pichel *et al.*, 1994; Richardson, 1996). De plus, elles peuvent entrer en compétition avec les bactéries photosynthétiques sulfo-oxydantes, selon la localisation de cette interface par rapport à la surface du tapis. Dans les tapis microbiens où l'oxygène, produit par une forte activité photosynthétique, pénètre au-delà de la zone irradiée, le développement de ces bactéries chimiolithotrophes est favorisé. Au contraire, lorsque l'interface oxygène-sulfure se situe au niveau de la zone irradiée, les bactéries sulfureuses sont alors les organismes sulfo-oxydants dominants (Jørgensen and Des Marais, 1986).

I.1.2.3. Les bactéries phototrophes anoxygéniques (BPA)

Les bactéries phototrophes anoxygéniques (pourpres ou vertes) se développent en surface de la zone anoxique des tapis microbiens, où pénètrent encore les radiations lumineuses nécessaires à leur métabolisme photosynthétique. Utilisant les mêmes sources d'énergie et d'électrons, les bactéries vertes et pourpres se trouvent souvent en compétition (van Gemerden, 1993). Cependant, les bactéries pourpres utilisent des longueurs d'ondes différentes de celles des bactéries vertes en raison des différences de leurs contenus pigmentaires (Pfennig, 1967). Grâce à la présence des bactériochlorophylles *c*, *d* et *e*, les bactéries vertes peuvent capter les photons à des longueurs d'ondes différentes de celles utilisées par les bactéries pourpres (Tableau 2). Ainsi, on peut observer au sein d'un tapis

microbien une stratification verticale des ces bactéries phototrophes anoxygéniques, les bactéries pourpres se localisant au-dessus des bactéries vertes.

Tableau 2 : Les bactériochlorophylles présentes chez les bactéries phototrophes anoxygéniques et leurs longueurs d'ondes d'absorption maximum. D'après Gloe *et al.* (1975) ; Matheron (1976) ; Pfennig and Trüper (1974).

Bactériochlorophylle	Longueur d'onde d'absorption maximum *in vivo* (nm)	Bactéries phototrophes anoxygéniques
a	375, 590, 800-805, 830-890	Pourpres et vertes
b	400, 605, 850, 1020-1040	Pourpres
c	745-755	Vertes
d	725-745	Vertes
e	715-725	Vertes

Ces microorganismes réalisent une photosynthèse anaérobie dite anoxygénique, sans dégagement d'oxygène. Contrairement aux cyanobactéries elles sont incapables de réaliser la photolyse de l'eau, par manque du photosystème II. Elles utilisent comme donneur d'électron les produits terminaux de la dégradation de la matière organique des producteurs primaires et certains composés issus de la fermentation et de la respiration anaérobie. Parmi les producteurs primaires, les cyanobactéries fournissent de l'hydrogène, du sulfure, et des carbonates. Ces bactéries phototrophes sont considérées comme des producteurs primaires « secondaires » selon Pfennig (1975).

Sur le plan taxonomique (Figure 2), les bactéries pourpres sont regroupées en trois familles distinctes, les *Chromatiaceae* (pourpres sulfureuses), les *Ectothiorhodospiraceae* (pourpres sulfureuses) et les pourpres non sulfureuses. Les bactéries vertes se partagent en 2 familles, Les *Chlorobiaceae* (vertes sulfureuses) et les *Chloroflexaceae* (vertes non sulfureuses) (Imhoff, 1992; Pfennig, 1989; Pfennig and Truper, 1983).

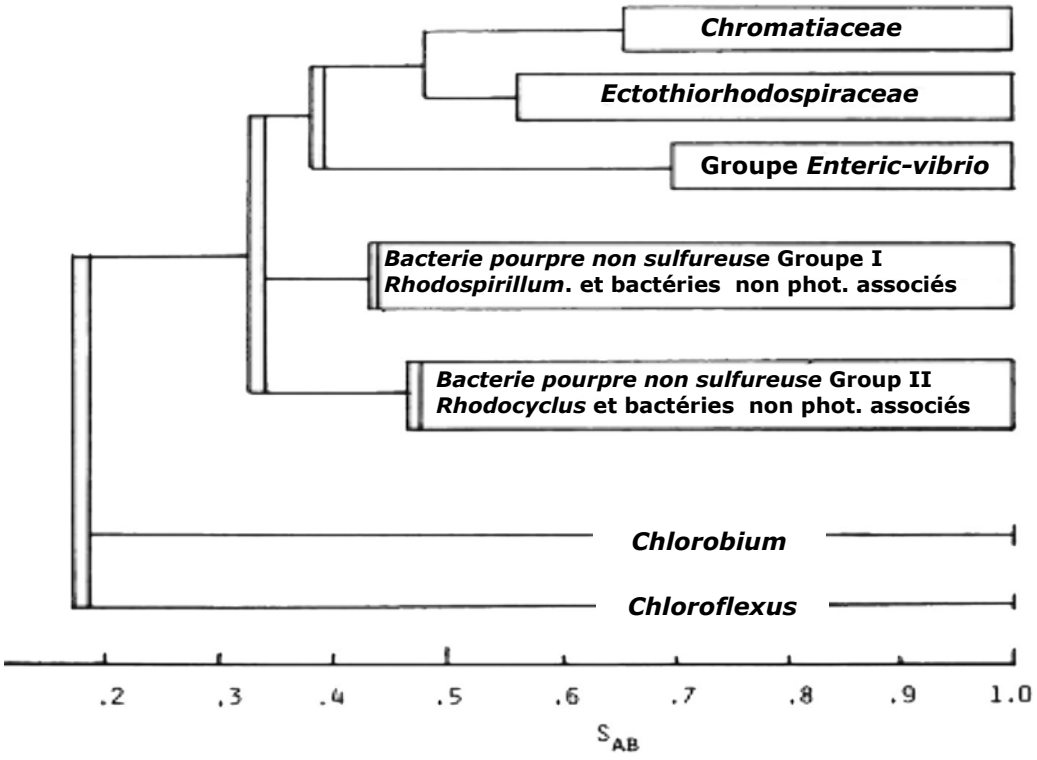

Figure 2 : Arbre phylogénétique montrant les relations entre les principaux groupes anoxygéniques phototrophes et non phototrophes associés. L'analyse phylogénétique est basée sur la comparaison des séquences du gène *ADNr 16S.* Modifié d'après Gibson *et al.* (1979) ; Stackebrandt and Woese (1984).

Les caractéristiques principales de ces microorganismes phototrophes anoxygéniques sont résumées dans le tableau 3. La nature des pigments chlorophylliens, et la structure de leurs appareils photosynthétiques permettent de différencier, d'un point de vue phénotypique, les bactéries pourpres des bactéries vertes. Chez les bactéries pourpres, les pigments (bactériochlorophylles et caroténoïdes) sont contenus au sein d'un système d'invaginations cytoplasmiques. Au contraire, les bactéries vertes possèdent des vésicules intra-cytoplasmiques appelées chlorosomes renfermant ces pigments.

Au sein des tapis microbiens, une grande diversité en bactéries pourpres est observée, où les genres *Thiocapsa* et *Chromatium* sont fortement représentés (Caumette *et al.*, 1994; Giani *et al.*, 1989; Herbert, 1985; van Gemerden *et al.*, 1989b).

Tableau 3 : Principales caractéristiques des bactéries phototrophes anoxygéniques.

Microorganismes phototrophes	Donneurs d'électrons	Source de carbone	Réserves de soufre	Bactério-chlorophylles	Croissance
Pourpres sulfureuses (*Chromatiaceae*, *Ectothiorhospiraceae*)	H_2, H_2S, S°, composés soufrés	CO_2, composés organiques	Globules intracellulaires ou extracellulaires	Bchl *a, b*	Photolithotrophe en anaérobiose, chimiotrophes en aérobiose et à l'obscurité
Pourpres non-sulfureuses	Composés organiques, (H_2, H_2S, S°, composés soufrés)	CO_2, composés organiques	Globules extracellulaires	Bchl *a, b*	Photohétérotrophe en anaérobiose, chimiotrophes en aérobiose et à l'obscurité
Vertes sulfureuses (*Chlorobiaceae*)	H_2S, S°, H_2, composés soufrés,	CO_2	Globules extracellulaires	Bchl *a, c, d, e*	Photolithotrophe anaérobie stricte
Vertes non- sulfureuses (*Chloroflexaceae*)	Composés organiques, (H_2S, S°, H_2)	CO_2, composés organiques	aucune	Bchl *a, c, d*	Photohétérotrophe en anaérobiose, chimiotrophes en aérobiose et à l'obscurité

I.1.2.4. Les bactéries sulfato-réductrices (BSR)

Les bactéries sulfato-réductrices se localisent dans les zones anoxiques des sédiments. La respiration aérobie des bactéries hétérotrophes du tapis appauvrit le sédiment en oxygène conduisant à l'anoxie du tapis microbien en profondeur (Marshall, 1989). Cette zone est également enrichie en matière organique, composés simples provenant des processus de dégradation aérobies et anaérobies, et en sulfate issu de l'oxydation des sulfures par les bactéries phototrophes anoxygéniques. Les bactéries sulfato-réductrices s'y développent aisément en utilisant les composés organiques simples comme donneurs d'électrons et sources de carbone, et le sulfate comme accepteur terminal d'électrons. Cette respiration dissimilatrice du sulfate entraîne la production de sulfure et la formation d'un gradient associé (Barton and Tomei, 1995 ; Fauque, 1995). La sulfato-réduction est un processus important de minéralisation de la matière organique au sein d'environnements anoxiques, tels que les écosystèmes hypersalés et marins (Ollivier *et al.*, 1994).

Les bactéries sulfato-réductrices d'un point de vue phylogénétique représentent un groupe complexe. Le tableau 4, ci-dessous, récapitule les différentes caractéristiques permettant leur classification (Castro *et al.*, 2000).

Tableau 4 : Caractéristiques de classification des principales bactéries sulfato-réductrices. D'après Castro *et al.* (2000).

	Shape	Motility	GC content of DNA (%)	Desulfovirin	Cytochromes	Oxidation of acetate	Growth temp. (°C)
Gram-negative mesophilic SRB							
Desulfobulbus	lemon to rod	−/+	59–60	−	b, c, c_3	I[a]	25–40
Desulfomicrobium	ovoid to rod	+/−	52–67	−	b, c	I	25–40
Desulfomonas	rod	−	66	+	c	I	30–40
Desulfovibrio	spiral to vibrioid	+	49–66	+/−	c_3, b, c	I	25–40
Desulfobacter	oval to rod	+/−	44–46	−		C[b]	20–33
Desulfobacterium	oval to rod	+/−	41–52	−	b, c	C	20–35
Desulfococcus	spherical or lemon	−/+	46–57	+/−	b, c	C	28–35
Desulfomonile	rod	−	49	+	c_3	C	37
Desulfonema	filaments	gliding	35–42	+/−	b, c	C	28–32
Desulfosarcina	oval rods or coccoid, packages	+/−	51	−	b, c	C	33
Gram-positive spore-forming SRB							
Desulfotomaculum	straight to curved rods	+	48–52	−	b, c	I/C	most 25–40, some 40–65
Bacterial thermophilic SRB							
Thermodesulfobacterium	vibrioid to rod	−/+	30–38	−	c_3, c	I	65–70
Archaeal thermophilic SRB							
Archaeoglobus	coccoid	+/−	41–46	−	n.r.[c]	I	64–92

[a]I, incomplete.
[b]C, complete.
[c]n.r., not reported.

Longtemps considérées comme des bactéries anaérobies strictes (Widdel, 1988), de nombreuses études actuelles remettent en question ce dogme par la description de leur présence dans des zones riches en oxygène et leur capacité pour certaines d'entre elles à respirer en présence d'oxygène (Cypionka, 2000; Cypionka *et al.*, 1985; Krekeler *et al.*, 1998; Minz *et al.*, 1999a; Minz *et al.*, 1999b; Sigalevich *et al.*, 2000a; Sigalevich *et al.*, 2000b; Teske *et al.*, 1998).

I.1.2.5. Les autres groupes bactériens fonctionnels

Les microorganismes hétérotrophes aérobies présents à la limite de la zone oxique / anoxique participent à l'appauvrissement en oxygène du sédiment. Les bactéries fermentatives jouent également un rôle important au niveau fonctionnel, puisqu'elles réalisent

les étapes préliminaires de la dégradation de la matière organique et fournissent des substrats aux bactéries sulfato-réductrices. Les bactéries nitrifiantes (bactéries aérobies oxydant l'azote), dénitrifiantes (bactéries aéro-anaérobies facultatives pouvant utiliser des formes oxydées de l'azote comme accepteur final d'électrons) et méthanogènes (bactéries anaérobies productrices de méthane) sont présentes au sein des tapis microbiens mais en moindre abondance (van Gemerden, 1993).

I.1.3. Structure verticale des communautés

I.1.3.1. Gradients physico-chimiques

Ces écosystèmes microbiens, comprenant des bactéries sulfato-réductrices, des phototrophes des chimiolithotrophes sulfo-oxydantes, associées à des couches denses de cyanobactéries productrices d'oxygène, sont le siège de gradients physico-chimiques étroits. La nature compacte des tapis combinée aux divers processus biologiques tels que la photosynthèse, la respiration, la fermentation, et la sulfato-réduction créent des micro-gradients de concentrations d'oxygène, de sulfure soluble, d'ions hydrogène, et d'autres espèces chimiques (Revsbech *et al.*, 1983). De plus, les gradients liés à l'intensité de la lumière et à son spectre apparaissent avec la forte absorption des radiations lumineuses (Jørgensen and Des Marais, 1988; Kühl, 1992; Kühl and Fenchel, 2000; Lassen *et al.*, 1992; Pierson *et al.*, 1987).

Ces gradients environnementaux présentent de fortes fluctuations au cours du cycle nycthéméral (jour / nuit), en fonction de la grande variété de métabolismes bactériens mis en jeu (Jørgensen *et al.*, 1983; Wieland *et al.*, 2004) (Figure 3).

Ainsi, en journée, les radiations lumineuses disponibles en surface pour les cyanobactéries induisent une production d'oxygène importante, par la photosynthèse. Cette forte concentration en oxygène pénètre jusqu'au niveau du premier millimètre du tapis, puis diminue fortement et disparaît sous l'action des bactéries hétérotrophes aérobies qui le consomment. Il s'est donc défini au-delà de ce millimètre une zone totalement anoxique. A l'opposé, il apparaît un gradient de sulfure par le biais de la réduction du sulfate, réalisée par les bactéries sulfato-réductrices situées dans les profondeurs du sédiment. Cette forte concentration en sulfure disparaît brutalement entre le 1er et le 2ème millimètre, sous l'action des bactéries sulfo-oxydantes phototrophes ou non. Il en résulte une zone anaérobie riche en

sulfure séparée d'une zone aérobie. Le pH augmente en surface suite à la forte activité photosynthétique des cyanobactéries et au faible pouvoir tampon du tapis, puis diminue en profondeur. Les fortes radiations lumineuses de la journée pénètrent le long du tapis microbien établissant un gradient lumineux utilisable par les bactéries phototrophes. L'atténuation des longueurs d'ondes dans les tapis est essentiellement due à l'absorption par les pigments des bactéries phototrophes sulfo-oxydantes présentent.

Au cours de la nuit, aucun gradient lumineux n'existe, l'absence d'activité photosynthétique des cyanobactéries provoque un appauvrissement très rapide en oxygène dans la totalité du tapis. Celui ci est donc majoritairement anoxique. Les métabolismes anaérobies de sulfato-réduction dissimilatrice deviennent dominants, le sulfure envahi donc tout le tapis même en surface. Sans activité de photosynthèse oxygénique, le tapis présente un pH plus acide qu'en journée (Wieland *et al.*, 2004).

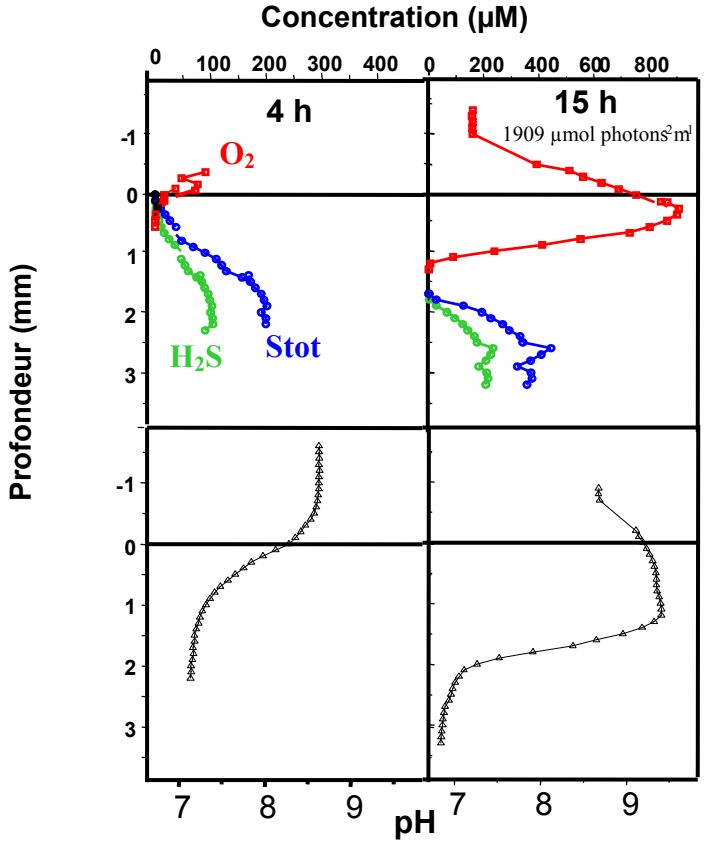

Figure 3 : Exemple de gradients physico-chimiques (H_2S, O_2, S_{tot}, pH, lumière) mesurés *in situ* sur le tapis microbien hypersalé de Camargue (Salins-de-Giraud). D'après Wieland *et al.* (2004).

I.1.3.2. Cycle du soufre

Les tapis microbiens sont caractérisés par la forte interaction entre les différents cycles biogéochimiques de l'oxygène, du soufre, et du carbone (Canfield and Des Marais, 1993) (Wieland and Kühl, 2000). Les communautés sulfato-réductrices, phototrophes anoxygéniques sulfureuses et sulfo-oxydantes constituent les trois principaux groupes physiologiques des tapis impliqués dans le cycle du soufre (Overmann and van Gemerden, 2000). Un tel écosystème représente un modèle idéal d'étude du cycle du soufre.

De part l'état d'oxydation variable du soufre de –2 (sulfure : S^{2-}) à +6 (sulfate : SO_4^{2-}), les différents composés soufrés existants (sulfate, sulfite, soufre, thiosulfate, polythionates) peuvent être oxydés en tant que donneur d'électrons ou réduit en tant qu'accepteur d'électrons. Les bactéries jouent un rôle important dans ces différents processus. Le soufre constitue un élément essentiel pour ces organismes vivants, puisqu'il intervient dans la composition d'acides aminés (cystéine, méthionine), la structure tertiaire de protéines (ponts disulfures), la constitution de coenzymes (thiamine, biotine) et d'osmolytes, mais aussi au niveau de centres réactionnels d'enzymes (en association avec le fer) impliqués dans divers métabolismes bactériens.

Le cycle du soufre correspond à la combinaison de plusieurs processus biologiques ou chimiques mis en jeu, assurant le renouvellement dynamique des donneurs et accepteurs d'électrons dans le tapis microbien (Figure 4). Au sein du tapis, les différents groupes bactériens sont très proches les uns des autres permettant ainsi une étroite relation entre les différents processus biologiques présents (van Gemerden, 1993). Le cycle du soufre correspond à l'association de trois processus principaux :

- la sulfato-réduction assimilatrice (1),
- la sulfato-réduction dissimilatrice (2),
- l'oxydation des composés soufrés (3).

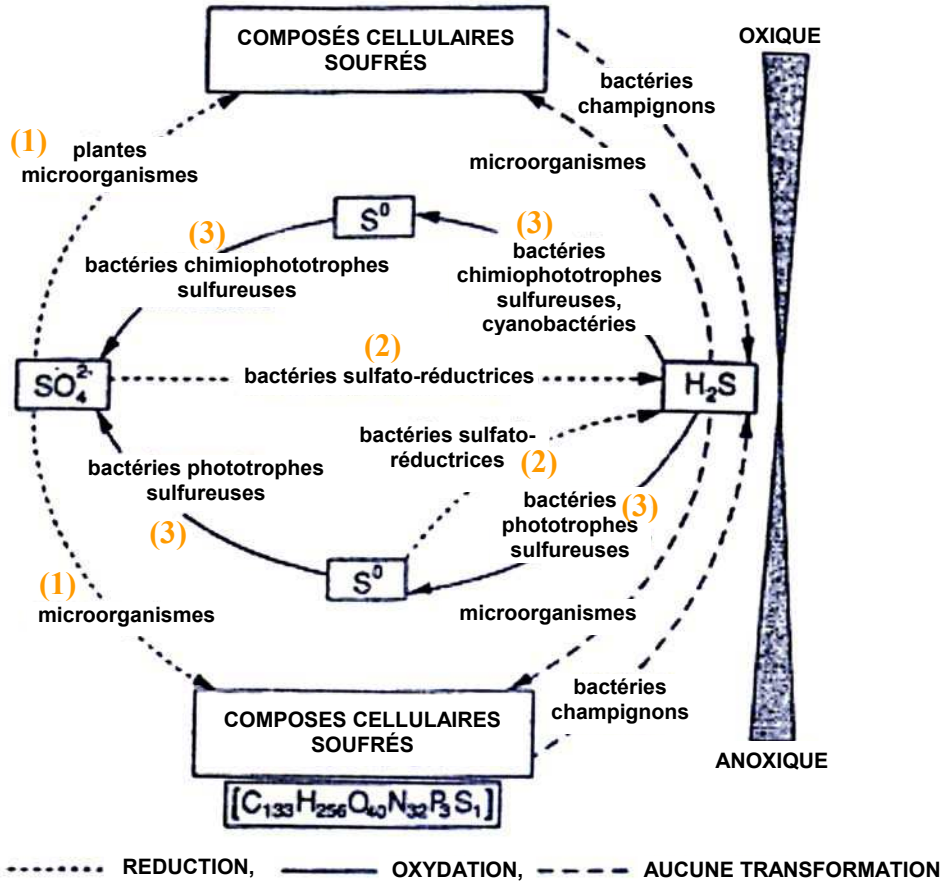

Figure 4 : Cycle biogéochimique du soufre au sein d'un écosystème sédimentaire ayant une compartimentation oxique / anoxique. Les numéros suivants correspondent aux principaux processus impliqués : (1) sulfato-réduction assimilatrice, (2) sulfato-réduction dissimilatrice, (3) oxydation des composés soufrés. Modifié d'après van Gemerden (1993).

Dans les tapis microbiens, le sulfure (H_2S, HS^-, S^{2-}) s'accumule principalement au niveau de la zone anoxique. En effet, au contact de la zone oxique le sulfure est rapidement réoxydé en soufre élémentaire (S°) stocké à l'intérieur de globules intracellulaire ou extracellulaire, et en sulfate (SO_4^{2-}) par l'action des bactéries sulfo-oxydantes et des cyanobactéries. En absence d'oxygène et en présence de lumière, ce sont les bactéries phototrophes sulfureuses qui réalisent l'oxydation du sulfure en soufre (bactéries pourpres) accumulé dans des réserves intra- ou extracellulaires, ou en thiosulfate ($S_2O_3^{2-}$) puis sulfate (bactéries vertes). Les bactéries pourpres sulfureuses ont toutefois la capacité de réaliser à l'obscurité la réduction dissimilatrice du soufre (en faible quantité) (van Gemerden, 1993).

I.1.3.3. Distribution spatiale des communautés : résultats d'interactions

La nature compacte des tapis microbiens et les paramètres physico-chimiques décrits, suggèrent des relations étroites, positives ou négatives, entre les différents microorganismes qui les composent. La figure 5 résume les principales relations mises en évidence entre ces bactéries. L'oxygène, le soufre, et les autres composés sulfurés en sont les principaux acteurs (van Gemerden, 1993).

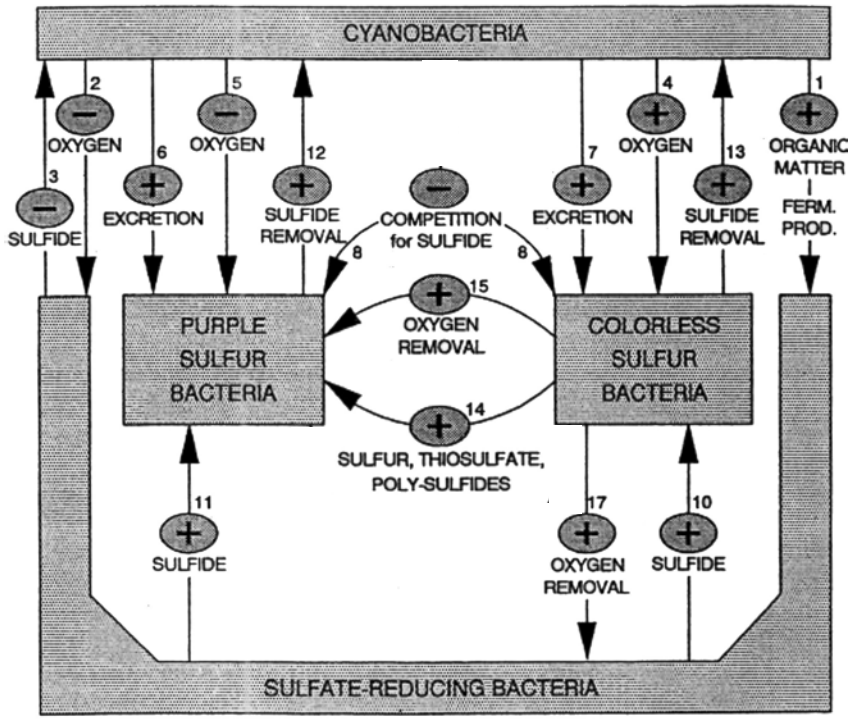

Figure 5 : Interactions entre les différents groupes bactériens d'un tapis microbien. Les flèches pointent vers les groupes affectés, les interactions négatives et positives sont indiquées respectivement par les symboles + et –. D'après van Gemerden (1993).

Par la photosynthèse oxygénique, les cyanobactéries favorisent le développement des différents groupes fonctionnels composant le tapis microbien :

- les bactéries sulfato-réductrices, en leur procurant des sources de carbone et d'énergie **(1),**
- les bactéries sulfo-oxydantes par l'apport d'oxygène **(4)** et de produits d'excrétions **(7)**,
- les bactéries phototrophes sulfureuses utilisant les produits d'excrétions **(6)**.

Au contraire, par leur production d'oxygène les cyanobactéries ont un rôle potentiellement néfaste vis à vis :

- des BSR, certaines sont très sensibles à l'oxygène produit **(2)**,
- des BPA, dont la synthèse de leurs pigments est inhibée induisant l'utilisation d'un métabolisme chimiolithotrophe moins productif **(5)**.

Les bactéries chimiolithotrophes sulfo-oxydantes permettent au contraire de protéger les BPA **(15)**, mais aussi les BSR **(17)** de cet important apport en oxygène, en l'utilisant pour oxyder le sulfure présent. De plus, celles-ci produisent des composés soufrés réduits utilisables par les BPA **(14)**.

Les BSR, par la sulfato-réduction, produisent du sulfure en grande quantité au sein du tapis. Celui-ci est toxique pour les cyanobactéries **(3)**, puisqu'il inhibe leur croissance. En contre partie, ce sulfure sera réoxydé par les différentes bactéries sulfo-oxydantes **(10) (11)**. Ceci est bénéfique à la prolifération des cyanobactéries **(12) (13)**, dont la croissance est inhibée par le sulfure. L'utilisation concomitante de ce même donneur d'électrons, fait entrer en compétition ces deux groupes fonctionnels**(8)**.

De Wit *et al.* (1995) ont cherché à modéliser les interactions existantes entre les différentes communautés d'un tapis microbien afin de cerner l'impact des paramètres biotiques et abiotiques sur la structuration des communautés. Ce modèle mathématique simule la croissance de microorganismes autotrophes d'un tapis microbien en relation avec les gradients d'oxygène, de sulfure et de lumière. Les microorganismes modèles choisis *M. chtonoplastes*, *Thiocapsa roseospersicina*, et *Thiobacillus tioparus*, sont respectivement représentatifs des cyanobactéries, des bactéries pourpres sulfureuses, et des bactéries sulfo-oxydantes. Il s'agit d'une simulation mathématique de 2 mois au cours desquelles un tapis microbien se développe en fonction de paramètres environnementaux donnés. Les résultats de cette étude révèlent une stratification typique de tapis microbiens très similaire à celle souvent décrite. Un tel modèle permet donc de décrire les relations complexes existantes entre les populations bactériennes et les paramètres environnementaux, à partir de connaissances écophysiologiques. De plus, il permet de déduire les impacts liés aux changements de conditions environnementales, sur la structure des communautés bactériennes.

I.2. Adaptations aux stress environnementaux

Les tapis microbiens comme décrits précédemment sont des structures complexes mettant en jeu de nombreuses interactions biologiques ou non. L'apport d'un stress extérieur qu'il soit récurant (fortes concentrations en sels dans les marais salants) ou accidentel (pollution chimique, pétrolière), induit un fort potentiel d'adaptation des communautés bactériennes présentes.

I.2.1. Salinité

De nombreux tapis microbiens se développent au niveau d'environnements hypersalés, tels que les marais salants (Caumette *et al.*, 1994; Giani *et al.*, 1989; Hirschler-Rea *et al.*, 2003; Nicholson *et al.*, 1987; Nubel *et al.*, 2001; Teal *et al.*, 1996). La production de sels, par évaporation de l'eau, induit la précipitation séquentielle des sels de calcium, puis de sodium. Ces habitats présentent donc une grande variabilité au niveau de leur concentration totale en sels, de leur composition ionique, et de leur pH.

Cette grande variabilité physico-chimique suggère un développement de tapis microbiens qui diffère selon les conditions du milieu (figure 6).

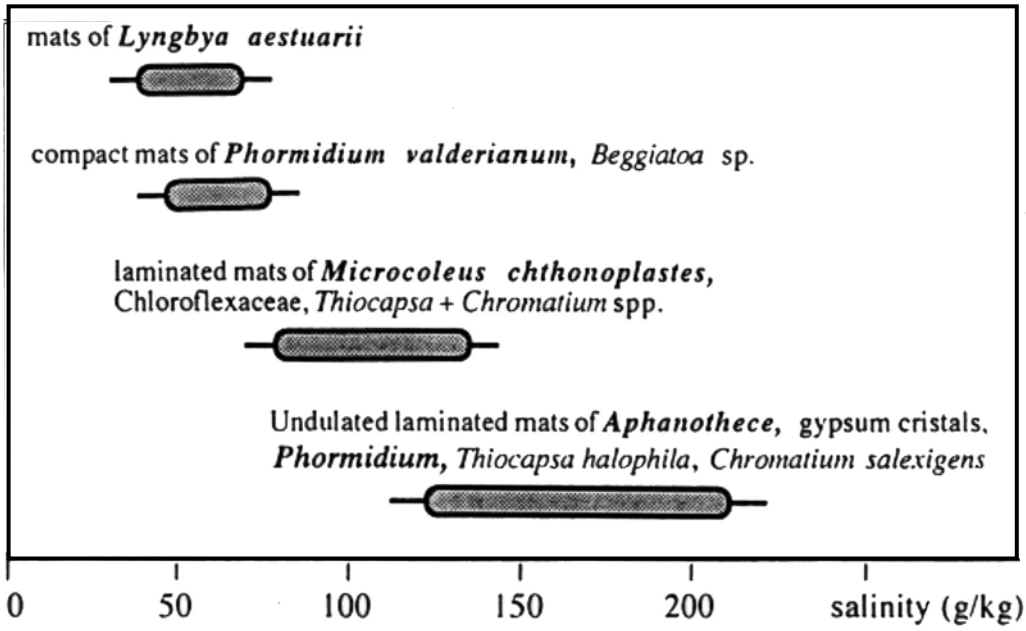

Figure 6 : Communautés microbiennes des marais salants présentes dans les tapis en fonction du gradient de salinité. D'après De Wit and Caumette (1994).

Les communautés bactériennes présentes sont capables de s'adapter au stress osmotique par une grande versatilité métabolique allant de l'halotolérance aux halophiles extrêmes (Ollivier *et al.*, 1994).

Les microorganismes sont dits halotolérants lorsqu'ils sont capables de se développer sans sels, tout en tolérant des concentrations variables en sels. Au contraire, ils sont halophiles lorsqu'ils ne peuvent se développer qu'en présence de sels. Parmi les microorganismes tolérants aux sels, trois groupes peuvent être définis en fonction de la concentration en sels nécessaire à une croissance optimale (Larsen, 1986) :

- groupe 1 : microorganismes légèrement halophiles (optimum se situant entre 2 et 5 %),
- groupe 2 : microorganismes halophiles modérés (optimum se situant entre 5 et 20 %),
- groupe 3 : microorganismes halophiles extrêmes (optimum se situant entre 20 et 30 %).

Il existe différents mécanismes d'osmorégulation chez les microorganismes leur permettant de se développer au sein d'environnements hypersalés :

- le transport d'ion à travers la membrane par des pompes ioniques
- la synthèse ou l'accumulation de molécules organiques.

Les osmolytes organiques permettent en effet de maintenir la pression de turgescence au sein des cellules soumises à un stress aux sels. Une grande variété de substrats est disponible dans les habitats hypersalés. Outre le potassium K^+, les bactéries halophiles, accumulent des composés de faibles poids moléculaires tel que la glycine-bétaïne. Les cyanobactéries sont aussi capables d'accumuler le sucrose et le thréalose. Les espèces d'*Ectothiorhodospira* synthétisent un acide aminé cyclique l'ectoïne (Ollivier *et al.*, 1994).

L'étude de différents tapis microbiens hypersalés a pu montrer l'impact de la salinité sur la diversité bactérienne. En effet, plus la salinité augmente, plus la biodiversité bactérienne de ces tapis diminue (Benlloch *et al.*, 2002; Casamayor *et al.*, 2002; Nübel *et al.*, 2000b).

Les tableaux 5 et 6 ci-dessous résument la tolérance aux sels des bactéries sulfato-réductrices et des bactéries phototrophes.

Tableau 5 : Bactéries sulfato-réductrices halophiles classées selon leurs tolérances au sel. D'après Ollivier *et al.* (1994).

Species	Salinity range (% NaCl)	Salinity optimum (% NaCl)
Slight halophiles		
Desulfovibrio desulfuricans subsp. *aestuarii*	0.5–6	2.5
Desulfovibrio salexigens	0.5–12	2–4
Desulfovibrio giganteus	0.2–6	2–3
Desulfobacter postgatei	0.5–4	0.7
Desulfobacter latus		2
Desulfobacter curvatus		2
Desulfobacter hydrogenophilus		1
Desulfococcus multivorans		0.5
Desulfococcus niacini		1.5
Desulfosarcina variabilis		1.5
Desulfobacterium autotrophicum		2
Desulfobacterium vacuolatum		2
Desulfobacterium phenolicum		2
Desulfobacterium indolicum		2
Desulfonema limicola		1.5
Desulfonema magnum		2–3
Moderate halophiles		
Desulfovibrio halophilus	3–18	6–7
Desulfohalobium retbaense	3–25	10

Tableau 6 : Bactéries phototrophes halophiles classées selon leurs tolérances au sel. D'après Ollivier *et al.* (1994).

I.2.2. Gradients physico-chimiques

Au cœur des tapis microbiens, les gradients physico-chimiques de sulfure, d'oxygène, de pH, et de lumière présents peuvent être source de stress. Comme l'ont montré plusieurs travaux (Revsbech *et al.*, 1983; Wieland *et al.*, 2004), ces gradients présentent de fortes fluctuations au cours d'un cycle nycthéméral, en terme de concentration et de localisation. Ponctuellement, mais régulièrement les bactéries sont donc soumises aux stress induits par l'oxygène, le sulfure, la lumière ou le pH.

I.2.2.1. Exemple du stress oxique

Le stress oxique est l'un des plus étudiés chez les bactéries sulfato-réductrices, microorganismes longtemps considérés comme des anaérobies strictes. En effet, de nombreuses études de biodiversité ont démontré la présence régulière de BSR dans la zone oxique de tapis microbiens (Canfield and Des Marais, 1991; Minz *et al.*, 1999a; Minz *et al.*, 1999b; Teske *et al.*, 1998).

Certaines BSR tolèrent la présence d'oxygène en s'adaptant par différents moyens :

- Présence d'enzyme de détoxication (catalase, superoxyde dismutase),
- Migration vers des conditions optimales de croissance. Des vitesses de migration allant de 1 à 69 $\mu m.s^{-1}$ont été mesurées, pour des souches de l'espèce *Desulfovirio oxyclinae* (Krekeler *et al.*, 1998).
- Agrégation, observée chez le genre *Desulfonema* lorsqu'il se retrouve en surface du tapis (Sigalevich *et al.*, 2000a).

Au contraire, d'autres BSR ont des métabolismes versatiles, puisqu'elles sont capables de respirer en présence d'oxygène (Cypionka, 2000; Cypionka *et al.*, 1985; Krekeler *et al.*, 1998; Sigalevich *et al.*, 2000b).

De nombreux autres stress, vis à vis de l'eau, de la lumière, du sulfure et de l'oxygène ont été étudiés chez les cyanobactéries (Bebout and Garcia-Pichel, 1995; Garcia-Pichel and Pringault, 2001; Kruschel and Castenholz, 1998; Pringault and Garcia-Pichel, 2003), les bactéries pourpres (*Rhodobacter sphaeroides, Marichromatium gracile*) (Romagnoli *et al.*, 2002; Thar and Kuhl, 2001), les bactéries sulfo-oxydantes (*Beggiatoa*) (García-Pichel *et al.*,

1994; Richardson, 1996). Un mécanisme général de migration a été décrit pour tous ces microorganismes afin d'échapper rapidement à ces conditions physico-chimiques extrêmes. Ce comportement s'appelle l'énergie tactisme.

I.2.2.2. L'énergie tactisme

Ce terme générique regroupe tous les comportements, positif ou négatif de mobilité bactérienne en réponse à divers stimuli : l'aéro-tactisme (réponse à l'oxygène), le photo-tactisme (réponse à la lumière), le redox-tactisme (réponse au potentiel redox), le tactisme lié aux accepteurs d'électrons, et le chimio-tactisme vers les sources de carbone (Taylor *et al.*, 1999).

Auparavant les réponses comportementales des microorganismes mobiles étaient définies à partir de gradients physico-chimiques distribués dans l'espace, le long desquels la mobilité était observée (Adler, 1988). Au contraire l'énergie tactisme décrit un mécanisme sensoriel et réfère aux mouvements actifs de la cellule le long de divers gradients associés au niveau d'énergie intracellulaire. Les paramètres physico-chimiques en affectant le transport d'électrons engendrent une réponse comportementale (Figure 7) (Alexandre and Zhulin, 2001; Alexandre *et al.*, 2004; Fenchel, 2002).

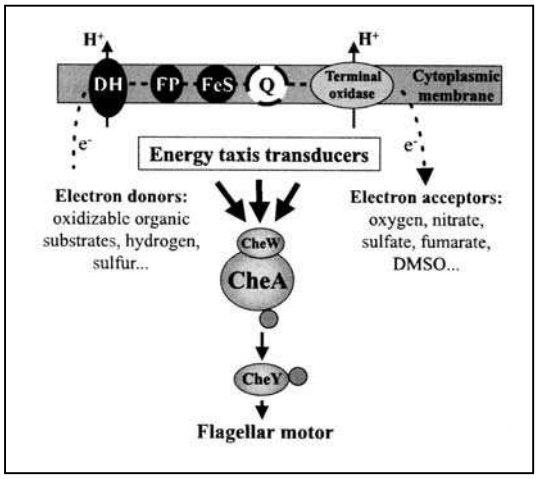

Figure 7 : Schéma général de l'énergie tactisme gouverné par une chaîne respiratoire de transport d'électrons. Les senseurs d'énergie reçoivent l'information à partir d'un système de transport d'électrons à l'état réduit et / ou de la force protomotrice. Les changements de concentrations des donneurs et accepteurs d'électrons affectent ces deux paramètres. Les petits cercles gris représentent les groupements phosphates. Abréviations : DH, déhydrogenases ; FP, flavoprotéines ; FeS, protéines fer-soufre ; Q, quinones ; DMSO, diméthyl sulfoxyde. D'après Alexandre *et al.* (2004).

I.2.3. Pollution d'hydrocarbures

Le développement industriel a entraîné un accroissement de la pollution des écosystèmes naturels. Les pollutions chimiques, dans le cas des pétroles, peuvent être soit naturelles (par transformation de la matière organique), soit accidentelles (dégazage ou naufrage de pétroliers). La présence d'hydrocarbures dans les habitats naturels peut-être source de toxicité pour la flore microbienne présentes.

Au sein d'écosystèmes contaminés, comme les tapis microbiens, l'association des organismes semble bénéfique à la dégradation des hydrocarbures. En effet, Höpner *et al.* (1996) ont pu mettre en évidence, suite à la pollution pétrolière du golfe Arabo-Persique, le développement de tapis microbiens sur les zones contaminées. Cette prolifération de tapis a été associée à une dégradation des hydrocarbures sur quelques mois.

I.2.3.1. Origine et Composition des pétroles

Les hydrocarbures de l'environnement se trouvent en grande quantité dans les gisements naturels profonds. Ils proviennent de diverses origines après transformation, sous l'effet de la chaleur et de la pression, de substances organiques végétales (diagénèse, catagénèse). La formation de pétrole dans les gisements est influencée en premier lieu par la nature de la matière qui a été enfouie. On distingue quatre fractions principales : les hydrocarbures saturés, les hydrocarbures aromatiques, les résines, les asphaltènes (Harayama *et al.*, 1999).

Durant la phase de maturation du pétrole, l'influence thermique et biologique peut agir très sensiblement sur sa composition et ses propriétés par exemple en raison de la biotransformation des fractions légères d'hydrocarbures en composés gazeux.

Les hydrocarbures aromatiques polycycliques (HAP) peuvent représenter jusqu'à 45 % en poids des hydrocarbures selon les types de pétroles. Les composés aromatiques soufrés (dérivés thiophéniques) peuvent représenter 23 % de la fraction aromatique d'une huile (Tissot and Welte, 1984). Les naphtalènes, les phénanthrènes et les dibenzothiophènes font partie des HAP les plus abondants au sein d'un pétrole.

I.2.3.2. Dégradation des hydrocarbures

I.2.3.2.1. Par les microorganismes

❋ ***La « réponse hydrocarbure »***

Les microorganismes développent différents mécanismes pour faire face à la présence d'hydrocarbures. Ces mécanismes sont essentiels pour leurs permettre de tolérer et résister à la présence d'hydrocarbures, d'atteindre des substrats très peu solubles et parfois même de transporter des molécules volumineuses à l'intérieur des cellules.

De nombreuses études ont permis de mettre en évidence différents processus utilisés par les microorganismes pour métaboliser les hydrocarbures :

- Les modifications des membranes biologiques (composition en phospholipides) permettent d'éviter les altérations causées par les hydrocarbures (Pinkart and White, 1997; Tsitko *et al.*, 1999).
- La formation de biofilms permettant le positionnement des bactéries à l'interface eau/huile, assurant ainsi le contact avec le substrat (Van Hamme *et al.*, 2003).
- Le transport actif des hydrocarbures à travers les membranes biologiques permet l'entrée des molécules dans les cellules et par conséquent leur dégradation (Kim *et al.*, 2002; Story *et al.*, 2000; Whitman *et al.*, 1998).
- La tolérance aux hydrocarbures grâce à des systèmes de pompes de flux (Duque *et al.*, 2001; Kieboom *et al.*, 1998a; Kieboom *et al.*, 1998b; Rojas *et al.*, 2001).
- Le chimiotactisme permet aux bactéries de se diriger par rapport aux hydrocarbures (Pandey and Jain, 2002).
- La production de surfactants permet de rendre accessibles certaines molécules (Makkar and Cameotra, 1998; Makkar and Cameotra, 2002; Van Hamme and Ward, 2000).

❋ ***Les voies de dégradation : gènes impliqués***

Le devenir des hydrocarbures dans l'environnement dépend de processus biotiques et abiotiques tels que la photo-oxydation, l'oxydation chimique, et l'activité microbiologique. Les micro-organismes peuvent agir soit directement via le métabolisme cellulaire, soit de manière indirecte en modifiant les conditions physico-chimiques du milieu. De nombreuses voies de dégradation aérobie et anaérobie ont été étudiées permettant de connaître les gènes impliqués et de comprendre leurs régulations :

- Des hydroxylases (mono-oxygénases) réalisent les premières étapes de dégradation des alcanes en aérobie, puis les intermédiaires hydroxylés peuvent suivre les voies de la β-oxydation (Morgan and Watkinson, 1994; Rehm and Reiff, 1982). Les opérons de dégradation aérobie des alcanes regroupant les gènes *alk* ont été caractérisés chez de nombreuses souches bactériennes tel que les genres *Pseudomonas* (Canosa *et al.*, 2000; Panke *et al.*, 1999; van Beilen *et al.*, 2001; Yuste and Rojo, 2001), *Burkholderia* (Marín *et al.*, 2001), *Acinetobacter* (Geissdorfer *et al.*, 1999; Ratajczak *et al.*, 1998), *Nocardioides* (Hamamura *et al.*, 2001), *Rhodococcus* (Koike *et al.*, 1999) et *Alcanivorax* (Dutta and Harayama, 2001).

Bien que très peu d'études aient mis en évidence la dégradation des alcanes en anaérobiose, les bactéries sulfato-réductrices sont toutefois capables de dégrader des composés en C_{20} (Aeckersberg *et al.*, 1991).

- Les composés aromatiques sont transformés, en aérobiose, en intermédiaires hydroxylés grâce à l'action de mono-oxygénases et de di-oxygénases. L'ouverture du cycle est alors réalisée à partir des intermédiaires hydroxylés catechol, protocatechuate, et gentisate obtenus (Smith, 1994). De nombreux opérons de dégradation aérobie des Hydrocarbures Aromatiques Polycycliques (HAP) ont été caractérisés. Parmi ceux-ci citons ceux regroupant les gènes *nah* de dégradation du naphtalène chez *Pseudomonas* (Simon *et al.*, 1999; Simon *et al.*, 1993; Yen and Serdar, 1988), les gènes *ndo*, dox et *nag* codant pour des dioxygenases impliquées dans la dégradation du naphtalène chez *Pseudomonas* (Denome *et al.*, 1993; Fuenmayor *et al.*, 1998; Kurkela *et al.*, 1988), les gènes *phn* et *pah* de dégradation du phénathrène chez *Burkholderia* et *Pseudomonas* respectivement (Kiyohara *et al.*, 1994; Laurie and Lloyd-Jones, 1999), les gènes *phd* et *nid* chez les souches à gram positif *Nocardioides* et *Rhodococcus* (Saito *et al.*, 2000; Treadway *et al.*, 1999), les gènes *nid* et *pbh* impliqués dans la dégradation de l'anthracène, fluorenthène et pyrène chez *Mycobacterium* et *Sphingomonas* respectivement (Story *et al.*, 2000).

- Récemment, les opérons de dégradation anaérobie des HAP regroupant les gènes *bbs* impliqués dans la voie de la benzylsuccinate synthase chez *Thauera aromatica* (Leuthner and J., 1998) et les gènes *edb* chez *Azoarcus* (Johnson *et al.*, 2001; Kaine *et al.*, 1983; Kniemeyer and Heider, 2001) ont été étudiés et caractérisés.

I.2.3.2.2. Par les tapis microbiens

La structure polysaccharidique des tapis microbiens joue vraisemblablement un rôle important dans la dégradation des hydrocarbures, permettant leur adsorption et les rendant ainsi accessibles aux différentes communautés bactériennes présentes. Au sein des tapis microbiens (Figure 8), la dégradation des hydrocarbures est probablement réalisée par des groupes bactériens physiologiquement distincts utilisant des accepteurs d'électrons différents. Au niveau de la couche superficielle oxique, les bactéries aérobies réaliseraient les premières étapes de dégradation, tandis que dans la zone intermédiaire inférieure, où l'oxygène est moins disponible, des bactéries micro-aérophiles assureraient l'essentiel de la dégradation. Lorsque la lumière est présente dans ces zones, les bactéries photosynthétiques anoxygéniques également présentes participent à la dégradation des hydrocarbures. Au niveau des zones anoxiques riches en sulfates, les bactéries sulfato-réductrices sont les plus actives. La dégradation de composés aromatiques comme le toluène, le xylène, et le naphtalène par les BSR en culture pure a été mise en évidence (Rabus and Widdel, 1995).

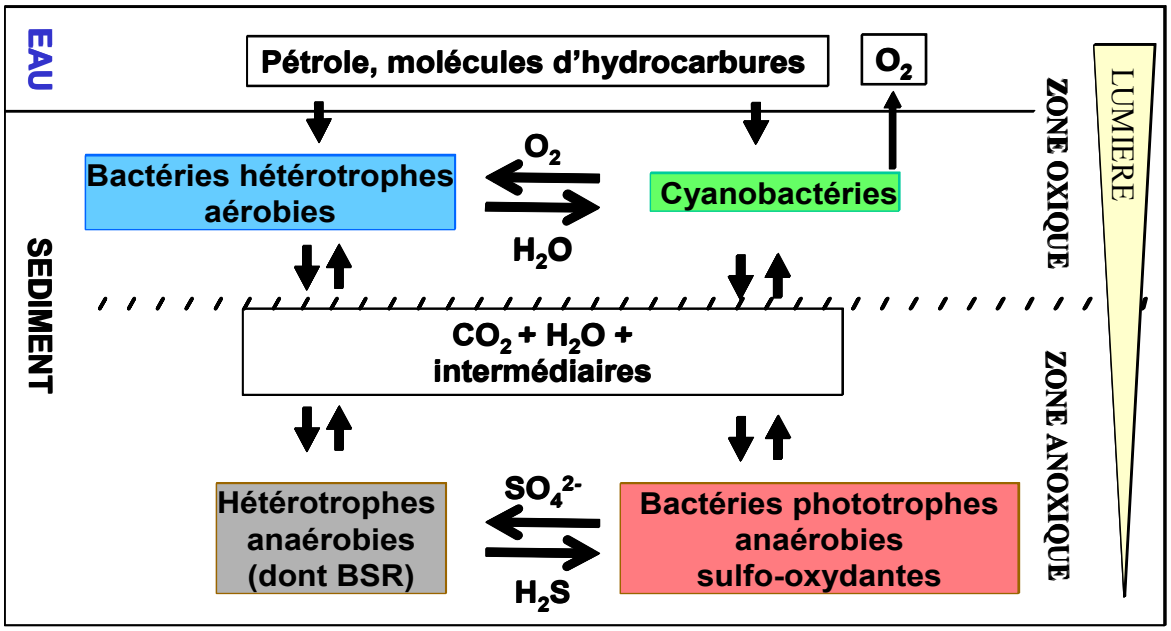

Figure 8 : Schéma de la biodégradation des hydrocarbures par les tapis microbiens.

De tels écosystèmes microbiens possèdent donc les capacités de dégradation de plusieurs espèces bactériennes associées. Des structures de ce type peuvent ainsi permettre de dégrader des hydrocarbures de façon séquentielle. Un groupe bactérien débuterait la

dégradation puis celle-ci serait poursuivie à partir des produits intermédiaires obtenus grâce à l'activité d'un autre groupe.

L'étude de différents tapis microbiens (Abed *et al.*, 2002; Cohen, 2002; Höpner *et al.*, 1996) a pu mettre en évidence une adaptation importante des populations bactériennes après une pollution aux hydrocarbures. En effet, les populations capables de métaboliser les hydrocarbures présents sont devenues dominantes au sein de l'écosystème. De plus, il en ressort une diversité plus faible de ces microorganismes hydrocarbonoclastes, en comparaison avec des systèmes microbiens non stressés. Les Bactéries à coloration Gram négative font parties des bactéries les plus représentées dans ces conditions de stress aux hydrocarbures.

Du point de vue de la dégradation, Abed *et al.* (2002) a pu montrer que les tapis microbiens étaient responsables d'environ 30 % de la dégradation des molécules modèle n-octadécane et de phénantrène. De même Grotzschel *et al.* (2002) ont pu observer la dégradation préférentielle des composés aromatiques phénanthrène et dibenzothiophène en comparaison aux alcanes pristane et n-octadécane. Cependant la dégradation de tous ces composés modèles sur 18 semaines n'est pas complète.

I.3. Les techniques moléculaires d'écologie microbienne

L'essor de la biologie moléculaire combinée à la phylogénie a permis un fort développement des connaissances lié à la diversité microbienne jusqu'alors sous-estimée. Celle-ci fut longtemps abordée uniquement par des méthodes microbiologiques reposant sur l'isolement de souches. Les techniques moléculaires, reposant principalement sur l'étude du gène *ADNr 16S*, ont donné un nouvel élan à l'écologie microbienne. L'analyse d'écosystèmes plus complexes semble désormais accessible à travers ces méthodes indirectes. En effet à partir de ces approches, il est possible de décrire la diversité microbienne *in situ* à un instant t, et dans un espace donné. Les paramètres définissant la diversité, à savoir la richesse en espèce (nombre d'espèce au sein d'une communauté), et la régularité (Evenness) sont désormais plus aisés à déterminer.

Parmi les nombreuses techniques moléculaires d'analyse de la biodiversité : la T-RFLP et la DGGE seront développées car elle représentent deux méthodes majeures pour aborder la biodiversité.

I.3.1. La T-RFLP (Terminal Restriction Fragment Length Polymorphism)

Cette technique développée par Liu *et al.* (1997) est une méthode rapide d'analyse des communautés microbiennes, basée sur le polymorphisme de restriction (Marsh, 1999). A partir de l'ADN génomique extraits d'échantillons, une PCR amplifiant le gène codant pour l'*ADNr 16S* est réalisée à l'aide d'amorces marquées en 5'par un fluorochrome. Le produit d'amplification est ensuite digéré par une ou plusieurs endonucléase de restriction. Les fragments digérés sont séparés par électrophorèse capillaire(Trotha *et al.*, 2002). Seuls les fragments de restriction terminaux fluorescents seront détectés. Les résultats obtenus constituent une empreinte de la communauté analysée.

Principalement réalisée sur le gène *ADNr 16S*, elle peut aussi l'être sur des gènes fonctionnels. Par exemple, les bactéries phototrophes pourpres phylogénétiquement très diverses, se répartissent en plusieurs sous-classes α-, β- et γ-protéobactéries. La forte conservation du gène *PufM,* codant pour une sous-unité du centre réactionnel de la photosynthèse permet d'utiliser ce gène, et d'être ainsi un marqueur de ce groupe phylogénétique (Achenbach *et al.*, 2001).

A l'heure actuelle, l'analyse des fragments de restrictions terminaux ou T-RFs est une étape limitante dans l'analyse des empreintes obtenues. Le site web RDP (Ribosomal Database Project) propose une base de données des séquences *ADNr 16S* et des programmes d'analyse des profils T-RFLP (Maidak *et al.*, 2001 ; Marsh *et al.*, 2000) et plus récemment MiCA (Microbial Community Analysis) et le T-RFLP PAT (phylogenetic assignment tool) (Kent *et al.*, 2003). De plus, il a été mis en évidence l'existence de pseudo T-RFs (Egert and Friedrich, 2003) et de variations possibles entre le T-RF observée et leur taille réelle (Kaplan and Kitts, 2003), pointant sur l'importance de l'analyse et de la justesse des résultats. Malgré cela, la sensibilité et la reproductibilité de cette technique ont été démontrés par Osborn *et al.* (2000) et Dunbar *et al.* (2001).

De part la rapidité de cette technique, la quantité d'informations et de résultats produits demandent désormais des analyses statistiques supplémentaires à l'analyse phylogénétique des profils T-RLFP (Blackwood *et al.*, 2003; Grant and Ogilvie, 2003). Ceci laisse entrevoir la possibilité d'intégrer des données additionnelles tels que les facteurs environnementaux afin d'appréhender leurs rôles dans la diversité observée.

Mengoni *et al.* (2002), comme Grant and Ogilvie (2004) ont développé des approches de clonage des T-RFs afin de compléter cette technique de la T-RFLP par une identification des communautés observées.

I.3.2. DGGE (Denaturing Gradient Gel Electrophoresis)

La technique de la DGGE permet de discriminer des fragments d'ADN de tailles identiques (200-700 bp), mais de compositions en bases différentes (substitution de bases) (Muyzer *et al.*, 1993). Son principe est basé sur la différence de mobilité électrophorétique des fragments d'ADN amplifié en fonction de leurs températures de fusion. La température de fusion d'un produit PCR, c'est-à-dire la température moyenne de dénaturation des deux brins est fonction de sa séquence. Une modification de séquence entraîne donc une modification de température de fusion. Cette modification est mise en évidence par électrophorèse sur gel de polyacrylamide en présence d'un gradient d'agent dénaturant (formamide, urée).

En écologie microbienne, les échantillons étudiés sont comparés sur leurs contenus en *ADNr 16S*, image des différentes communautés bactériennes présentes (Muyzer *et al.*, 1998). L'avantage de cette technique est de pouvoir déterminer les différentes séquences détectées par excision des bandes du gel, réamplification et séquençage. Cette méthode est donc fortement appropriée à l'étude d'écosystème microbien et à leur dynamique des populations (Benlloch *et al.*, 2002; Ferris *et al.*, 1996).

La DGGE présentent quelques variantes, au niveau du gradient mi en jeu :

- TGGE (Temperature Gradient Gel Electrophoresis) : la séparation des fragments amplifiés se fait sous l'effet d'un gradient de température (Muyzer, 1999; Muyzer and Smalla, 1998).
- TTGE (Temporal Temperature Gradient gel Electrophoresis) : La séparation se fait sur un gel sous l'effet d'un agent dénaturant en concentration uniforme, et d'une température graduellement croissante (Farnleitner *et al.*, 2000; Ogier *et al.*, 2002).

Chapitre II : Procédures expérimentales

II. Procédures expérimentales

II.1. Sites d'étude

II.1.1. Présentation

Cette thèse entre dans le cadre du programme européen MATBIOPOL* dans lequel quatre tapis microbiens ont été pris comme modèles d'étude, localisés sur les sites : de Camargue (Salins-de-Giraud - France), des Iles Orcades (Ecosse), de Solar Lake (Eilat - Israël) et du Delta de l'Ebre (Espagne). Elle s'intègre également au sein du programme national LIT'EAU dans lequel le tapis microbien de Guérande (Pradel - France) a été utilisé comme modèle au sein de notre laboratoire. Dans ce travail, seuls les tapis microbiens de Camargue, des Iles Orcades et de Guérande ont été analysés.

II.1.1.1. Les salins de Camargue (Salins-de-Giraud - France)

Les tapis microbiens étudiés se développent dans les environnements naturels appelés les salins de Salins-de-Giraud au sud du Delta du Rhône en Camargue (Figure 9). Cette zone est soumise au climat méditerranéen côtier, avec des températures douces s'étendant de 13°C à 25°C, et des précipitations annuelles moyennes de 750 à 1000 mm.

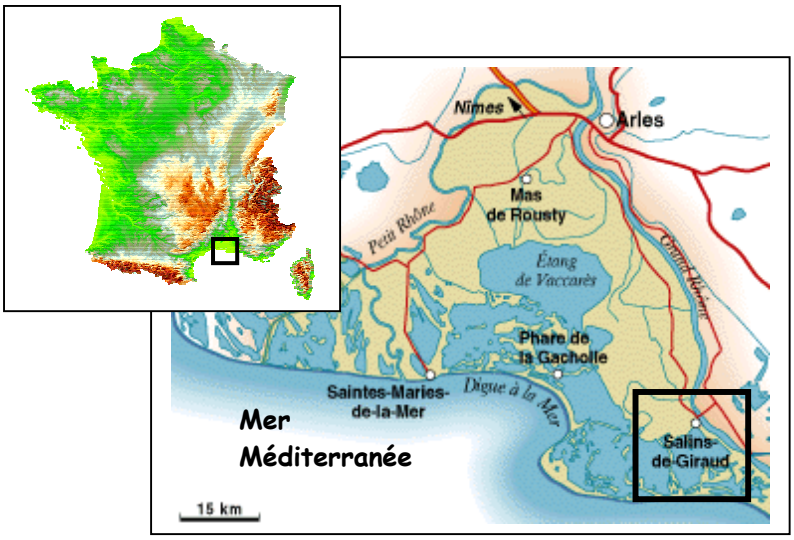

Figure 9 : Situation géographique des salins de Salins-de-Giraud.

* http://www.univ-pau.fr/RECHERCHE/MATBIOPOL

Les salins sont exploités par évaporation naturelle de l'eau de mer, pour produire du sel. Celle-ci circule dans de grands bassins lagunaires, les « partènements », où sous l'action conjuguée du soleil et du vent son volume est réduit de 20 % à 10 % et permet au carbonate de calcium ($CaCO_3$) et au gypse ($CaSO_4.2H_2O$) de précipiter. La saumure ainsi prête à cristalliser est ensuite dirigée vers des bassins soigneusement dimensionnés appelés « tables salantes », où a lieu la précipitation et la récolte de la halite (NaCl naturel). Les salins de Camargue présentent une surface de 10 000 hectares de partènements, et de 770 hectares consacrés aux tables salantes. La production de sel des Salins du Midi s'élève en moyenne à 1 000 000 de tonnes par an.

Le site de prélèvement est situé dans un partènement appelé la Baisse de Cinq Cents Francs (Figure 10). Ce bassin d'environ 10 km^2 est employé pour le stockage de l'eau, par la compagnie des Salins du Midi. L'eau n'y excède jamais la profondeur de 20 cm et se situe dans une échelle de salinité comprise entre 70 et 150 ‰ (m/v).

Figure 10 : Carte du site de prélèvement des salins de Salins-de-Giraud (échelle : 1/500 000).

Le tapis microbien étudié se développe à la surface de ce bassin de pré-concentration, alimentant les salins adjacents avec de l'eau de mer pré-concentrée en sels (Figure 11). En fonction des manœuvres effectuées, par la compagnie des Salins du Midi, (ouverture ou fermeture des vannes d'entrée d'eau) et des conditions climatiques existantes (soleil et vent), le niveau d'eau de ce bassin peut varier fortement. Ce site est exploité uniquement du mois d'avril au mois de septembre, les tapis microbiens sont donc soumis en période hivernale à de fréquentes dessiccations. En dépit de ces variations environnementales prononcées, un tapis microbien photosynthétique épais de plusieurs centimètres se développe au sein de ce bassin.

Figure 11 : Vue du site de prélèvement (Baisse de cinq cents francs)

Les tapis microbiens prenant place dans ces milieux hypersalés, sont dominés par les cyanobactéries des genres *Microcolleus* et *Phormidium*. Ces tapis photosynthétiques couvrent une très large partie de la Baisse de Cinq Cents Francs et d'autres étangs adjacents. Ils sont constitués de couches stratifiées de profondeur d'environ 5 à 10 mm (Figure 12).

D'autres tapis microbiens se développant au-dessous d'une croûte de gypse dans des bassins de salinités supérieures (130-200 ‰ (m/v)), ont été précédemment décrits (Caumette *et al.*, 1994 ; Mouné, 2000 ; Mouné *et al.*, 2003). A partir de ce tapis microbien, de nombreuses espèces bactériennes anaérobies ont été isolées (Caumette *et al.*, 1988 ; Caumette *et al.*, 1991 ; Mouné *et al.*, 1999 ; Mouné *et al.*, 2000; Ollivier *et al.*, 1994).

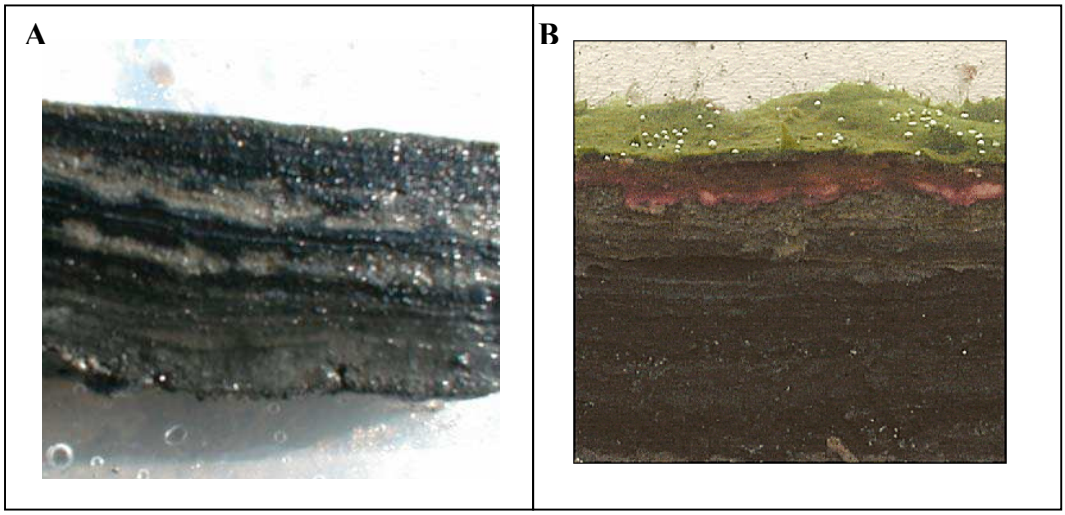

Figure 12 : Coupes transversales du tapis microbien de Camargue. Observation des couches successives de haut en bas : cyanobactéries brunes, bactéries phototrophes anoxygéniques pourpres, bactéries sulfato-réductrices. A/ tapis microbien lors du prélèvement. B/ Tapis microbien après stabilisation au laboratoire.

II.1.1.2. Les îles Orcades (Ecosse)

Les îles Orcades se trouvent à 25 kilomètres de la côte Nord-Est de l'Ecosse. La baie de Swanbister, où sont présents les tapis microbiens prélevés, se situe sur le rivage nordique de Scapa Flow (Figure 13).

Les plages de Scapa Flow sont localement enrichies en matière organique riche en azote, dû à la décomposition des microalgues sur les plages. Dans la baie de Swanbister, un apport supplémentaire en matière organique est amené par les rejets des distilleries locales de Whisky. La matière organique ainsi accumulée stimule l'activité respiratoire en surface du sédiment. Au-dessous d'une profondeur de 2 à 3 mm, les sédiments deviennent anoxiques, et présentent des taux de sulfato-réduction importants.

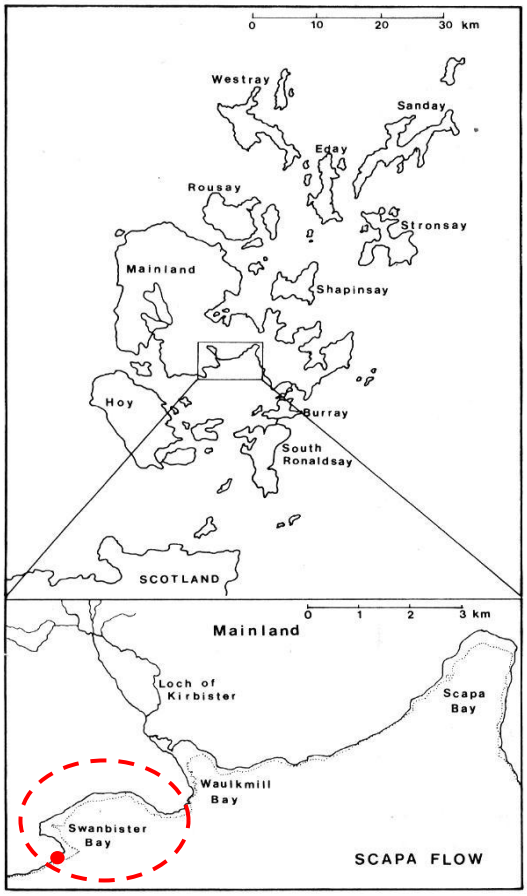

Figure 13 : Carte de Scapa Flow localisant le site de prélèvement dans la baie de Swanbister.

Figure 14 : Vue du site de prélèvement des plages de la baie de Swanbister.

Les tapis microbiens stratifiés se développant sur ces plages sablonneuses abritées (Figure 14), sont décrits comme des tapis microbiens marins dominés par les bactéries sulfureuses pourpres, principalement *Thiocapsa roseopersicina.* Les microcolonies distinctes formées par ces bactéries sulfureuses pourpres participent à la cohésion des grains du sédiment. Ces agrégats mènent à une réduction de l'érosion, ainsi qu'à une stabilisation du sédiment. Cependant ces agrégats ne sont pas aussi efficaces dans la stabilisation du sédiment sableux et dans la prévention de l'érosion que ne le sont des structures cohésives telles que les tapis cyanobactériens.

Trois tapis microbiens des Iles Orcades, se distinguant par la position de la couche de cyanobactéries, ont déjà été décrits. En effet, celle-ci peut se situer soit au-dessus, soit au-dessous de la couche de bactéries pourpres ou bien être totalement absente permettant ainsi le développement exclusif des bactéries pourpres à la surface du sédiment (Figure 15) (Herbert, 1985 ; van Gemerden *et al.*, 1989a; van Gemerden *et al.*, 1989b).

Figure 15 : Coupe transversale du tapis microbien se développant sur les plages de Swanbister.

II.1.1.3. Les marais salants de Guérande (Pradel – France)

Les marais salants de Guérande constituent le site de production de sels le plus septentrional d'Europe (Ouest de la Loire Atlantique - Bretagne) avec ses 2000 hectares de marais exploités depuis plus de 1000 ans. Les prélèvements ont été effectués sur les marais salants de la commune de Pradel (Figure 16).

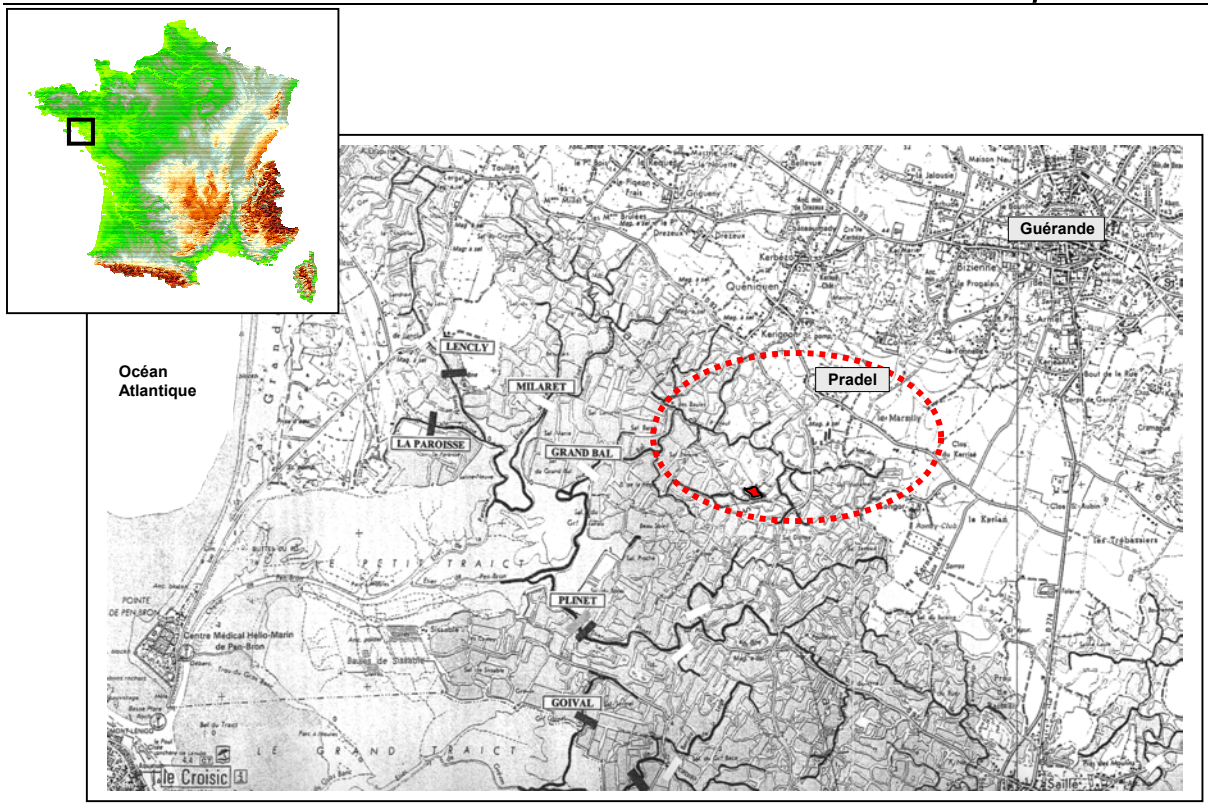

Figure 16 : Situation géographique des salines sur la commune de Pradel proche de Guérande. (échelle : 1/25 000)

Dans les marais salants de Guérande (Figure 17) la production du sel, réalisée de manière artisanale par les Salines de l'Ouest, s'élevait entre 1994 et 1998 à 12 000 tonnes par an. Malgré la pollution pétrolière du littoral atlantique due au naufrage de l'Erika en décembre 1999, les marais salants de Guérande n'ont pas été atteints par la marée noire.

Figure 17 : Vue du site des marais salants de Pradel (Guérande).

Chaque saline est une mosaïque de bassins aux formes géométriques variées permettant à l'eau de mer de circuler par des « Étiers » creusés dans l'argile, d'un premier bassin d'évaporation ou « Vasière » (salinité de 40 ‰) aux bassins de cristallisation appelés « Œillets » (salinité supérieure à 250 ‰). La salinité de l'eau augmente ainsi par évaporation en suivant un trajet en chicanes à travers une succession de bassins intermédiaires en commençant par le « Cobier » (50 ‰), les « Fares » (50 à 200 ‰), puis les « Adernes » (250 ‰) (Figure 18).

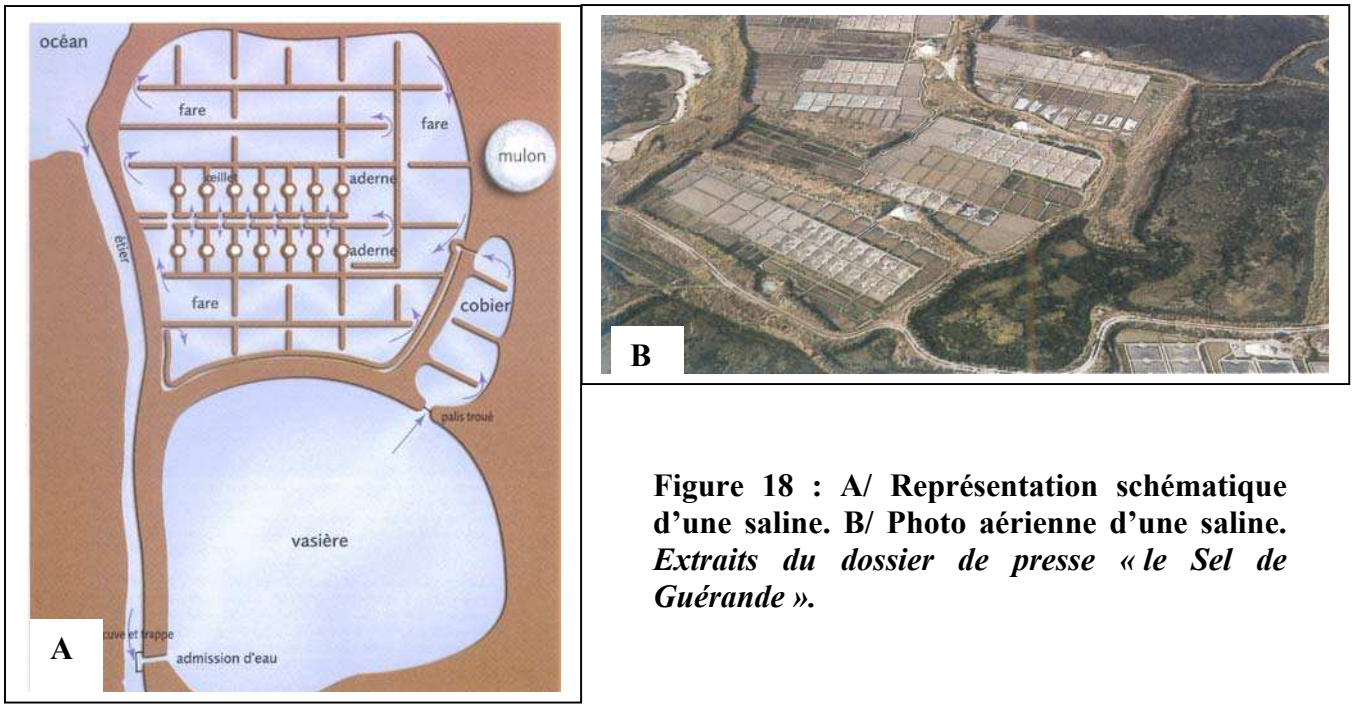

Figure 18 : A/ Représentation schématique d'une saline. B/ Photo aérienne d'une saline. ***Extraits du dossier de presse « le Sel de Guérande ».***

Différents tapis microbiens sont présents dans les bassins hypersalés des marais salants de Guérande, sous des températures d'environ 11-12°C et des précipitations annuelles moyennes de 800-900 mm. L'eau au sein des bassins n'excède jamais la profondeur de 10 cm.

Les tapis microbiens qui s'y développent sont très fins, entre 5 et 10 mm. Ils sont majoritairement composés d'algues, de diatomées et de bactéries oxy- et anoxyphototrophes. Lorsque la salinité est autour de 10 ‰ (m/v) (bassins de stockage), les principales populations microbiennes en sont les cyanobactéries des genres *Aphonothece, Microcoleus, Spirulina,* et *Oscillatoria*, mais aussi les *Chromatiacae*. Lorsque la salinité augmente, dans les bassins de récolte des salines, les genres *Halobacterium sp*. et *Dunaliella* sont prédominants (Giani *et al.*, 1989).

Le tapis microbien que nous avons analysé, a été prélevé dans un fare d'une salinité d'environ 70 ‰ (m/v).

II.2. Echantillonnages

Les tapis microbiens ont été prélevés et échantillonnés de différentes manières au cours de plusieurs campagnes.

1- **Carottage de tapis microbien (épaisseur 1 cm, diamètre 3 cm) à l'aide de seringues de 20 ml en plexiglas, enfoncées verticalement dans le tapis.**

Les carottes de tapis ont ensuite été congelées sur place dans de l'azote liquide et transportées dans une glaciaire de carboglace jusqu'au laboratoire. Ces carottes ont ensuite été coupées en tranches de quelques centaines de micromètres à l'aide du cryomicrotome *MICROM HM 500M* du laboratoire d'ingénierie agronomique de l'ENSAT (Ecole Nationale Supérieure Agronomique de Toulouse).

2- **Collecte de sections de tapis microbien (50 x 50 cm, épaisseur 3 cm).**

Ces tapis microbiens ont été conservés et transportés dans des glacières à 4°C jusqu'au laboratoire. Ils ont ensuite été stabilisés dans de l'eau de mer synthétique 70 ‰ (m/v) (cf II.1.3 *Maintien de tapis microbien en microcosme*) sous une lumière naturelle.

II.2.1. Le tapis microbien de Camargue

II.2.1.1. Campagne de mars/ juin 2000

Les carottes de tapis prélevées ont été coupées en 12 tranches très fines à l'aide d'un cryomicrotome. Les 10 premières coupes, avec une épaisseur de 200 µm, représentent les 2 premiers millimètres. Les deux dernières sections de 500 µm chacune correspondent au 3ème millimètre de la carotte. Ces différents échantillons ont ensuite été stockés à -20°C.

II.2.1.2. Campagne de juin 2001

Des prélèvements de 8 sections de 50 cm² de tapis ont été effectués. De même, des prélèvements de tapis, sous forme de carottes, ont été effectués du 11 au 12 juin 2001 à 6 moments différents au cours des 24h (9^H30, 15^H, 18^H, 22^H, 4^H, 7^H45). Ces carottes ont été coupées en 30 tranches très fines à l'aide d'un cryomicrotome (Figure 19).

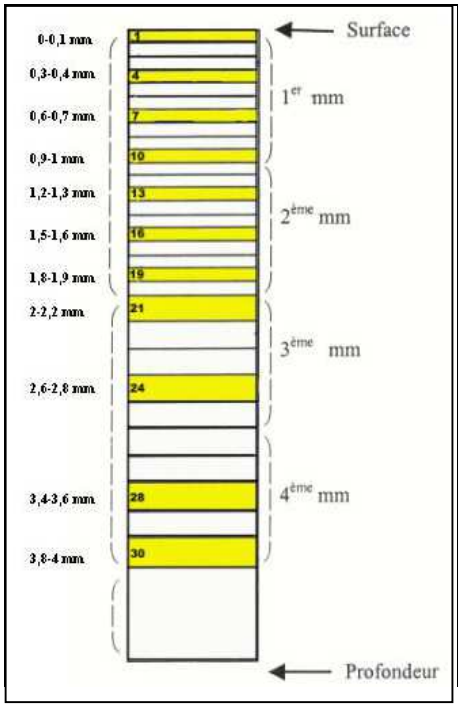

Figure 19 : Schéma des sections réalisées sur les carottes prélevées à Salins-de-Giraud. Seules les sections colorées en jaune ont été prises en compte dans l'étude présentée.

Les 20 premières coupes, d'une épaisseur de 100 µm chacune, représentent les 2 premiers millimètres du tapis. Les dix dernières sections de 200 µm chacune correspondent aux 3ème et 4ème millimètres du tapis. Ces différents échantillons ainsi coupés ont ensuite été stockés à -20°C.

II.2.2. Le tapis microbien des Iles Orcades

❋ ***Campagne de juillet 2000***

Les carottes prélevées ont été coupées en 12 tranches très fines à l'aide d'un cryomicrotome. Les 10 premières coupes, avec une épaisseur de 200 µm, représentent les 2 premiers millimètres. Les deux dernières sections, de 500 µm chacune, correspondent au 3ème millimètre de la carotte. Ces différents échantillons ont ensuite été stockés à -20°C.

II.2.3. Le tapis microbien de Guérande

❋ ***Campagne de mars 2001***

Des prélèvements de tapis, sous forme de sections de 50 cm^2, ont été réalisés en mars 2002. Ces parcelles ont été conservées dans des conditions similaires à celles de leur milieu naturel, sous lumière naturelle et dans des bacs d'eau de salinité adéquate (70 ‰ (m/v)).

II.3. Maintien de tapis microbien en microcosme

II.3.1. Eau de mer synthétique (Camargue et Guérande)

La préparation de l'eau de mer synthétique à 70 ‰ (m/v) utilisée pour maintenir les tapis microbiens en laboratoire, a été réalisée en préparant séparément 3 solutions, stérilisées séparément à l'autoclave :

Solution ①		**Solution ②**		**Solution ③**	
KCl	1.5 $g.l^{-1}$	$MgSo_4.7H_2O$	13.28 $g.l^{-1}$	Na_2Co_3	0.53 $g.l^{-1}$
$CaCl_2.2H_2O$	2.94 $g.l^{-1}$	$MgCl_2.6H_2O$	10.56 $g.l^{-1}$		
NH_4Cl	2.65 $mg.l^{-1}$				
NaCl	53 $g.l^{-1}$				
KBr	0.24 $g.l^{-1}$				
$SrCl_26H_2O$	0.048 $g.l^{-1}$				
NaF	0.003 $g.l^{-1}$				
Tampon phosphate 1M pH 7,4	5 µM				
SL12 sans EDTA	1 $ml.l^{-1}$				

L'eau de mer synthétique est obtenue en mélangeant 650 ml de la solution ①, 250 ml de la solution ②, et 100 ml de la solution ③.

La solution d'oligo-éléments **SL12** utilisée dans la solution ① est préparée en solution stock comme suit (modifiée d'après Overmann *et al.* (1992)) :
H_3BO_3, 300 $mg.l^{-1}$; $FeSO_4.7H_2O$, 1.1 $g.l^{-1}$; $CoCl_2.6H_2O$, 190 $mg.l^{-1}$; $MnCl_2.2H_2O$, 50 $mg.l^{-1}$; $ZnCl_2$, 42 $mg.l^{-1}$; $NiCl_2.6H_2O$, 24 $mg.l^{-1}$; $Na_2MoO_4.2H_2O$, 18 $mg.l^{-1}$; $CuCl_2.2H_2O$, 2 $mg.l^{-1}$.

II.3.2. Mise en place d'un microcosme : exemple du tapis de Guérande

A partir des parcelles de tapis prélevées, quatorze carottes de tapis microbiens (5 cm de diamètre et 1 cm d'épaisseur) ont été maintenues en microcosme au sein de carottiers de verre, dans de l'eau de mer synthétique à 70 ‰ (m/v). La moitié de ces carottes a été contaminée en surface avant leur mise en eau en ajoutant par pesée une quantité de pétrole brut de l'Erika (300 à 350 mg par carottier). Les carottes restantes ont été utilisées comme tapis témoin non contaminé par le pétrole. Deux des carottes restantes ont été stérilisées puis contaminées par du pétrole brut de l'Erika pour servir de témoins abiotiques (Figure 20).

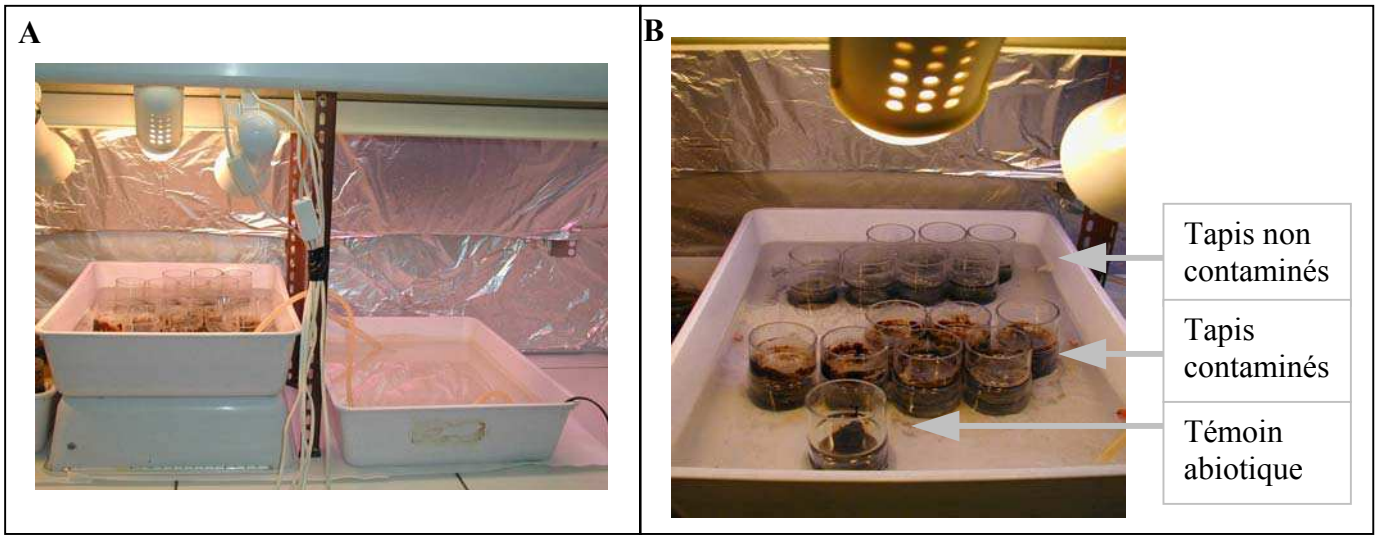

Figure 20 : A/ Photographie du dispositif de maintien des tapis microbiens de Guérande. B/ Photographie des tapis microbiens de Guérande en carottiers contaminés par du pétrole brut Erika.

Le témoin abiotique a été analysé uniquement pour les temps de prélèvement t_0 et t_{90} jours. Il consiste en une carotte de tapis stérilisée par 3 cycles d'autoclave successifs de 21 min à 110°C à la pression de 1 bar. Il a ensuite été contaminé en surface par du pétrole brut Erika. Sa mise en eau a été faite dans le même bac que les autres carottiers non stériles. Pour cela, le bas du carottier a été bouché hermétiquement à l'aide d'un dispositif équipé d'un filtre (0,45 µm) pour « stériliser » le flux d'eau synthétique entrant dans le carottier (Figure 21).

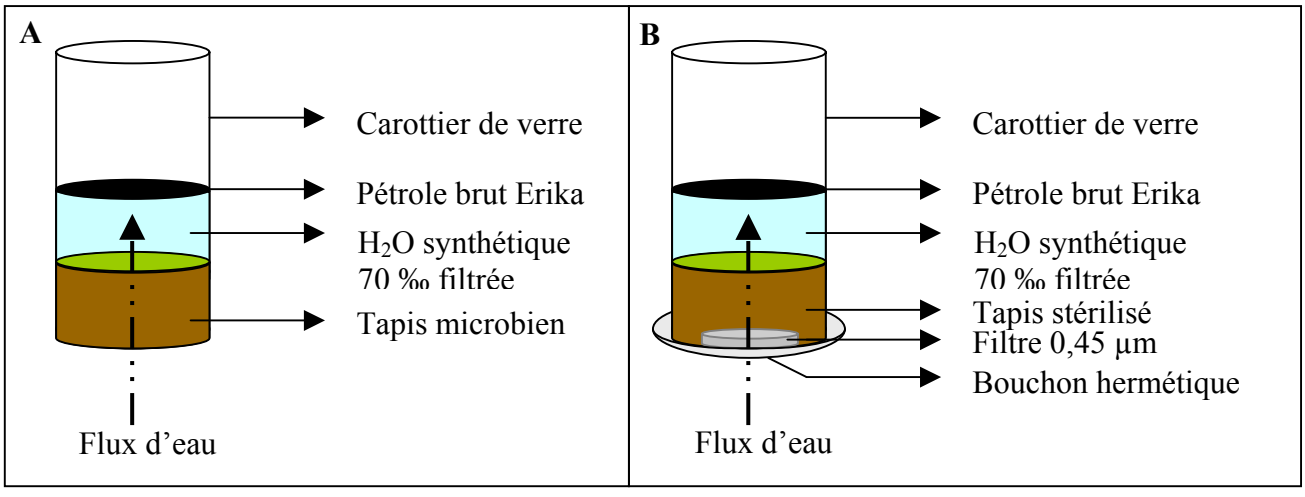

Figure 21 : Représentation schématique des tapis microbiens maintenus en microcosme dans des carottiers de verre. A/ Tapis microbien contaminé par du pétrole. B/ Témoin abiotique.

Par ailleurs, les paramètres du milieu ont été contrôlés tout au long de l'expérience, afin de pouvoir considérer la pollution pétrolière comme le facteur principal affectant la biodiversité des tapis :

- Maintien du niveau d'eau à l'aide d'un système de circulation d'eau (pompe péristaltique),
- Cycle 16h de lumière / 8h d'obscurité, à l'aide d'un éclairage de 8 ampoules à incandescence de 60W, 1 néon à fluorescence (émetteant à 450 nm, et 700-780 nm), et un néon lumière blanche (émettant à 600 nm).
- Maintien du pH ~ 8,
- Maintien de la salinité S ~ 70 ‰ (m/v),
- Température ambiante ~ 25°C.

A partir des microcosmes mis en place, des prélèvements ont été réalisés tous les quinze jours et ce durant les trois mois d'incubation (de t_0 à t_{90} jours). Pour chaque prélèvement, un carottier témoin et un contaminé ont été échantillonnés. A partir de ces carottiers prélevés, une vingtaine de micro-carottages (5 mm de diamètre et 1 cm d'épaisseur) ont été effectués à la surface du tapis, à l'aide de pipettes Pasteur en verre. Les échantillons ainsi prélevés ont été immédiatement stockés à -80°C.

II.4. Souches bactériennes, milieux de culture et conservation

II.4.1. Souches bactériennes utilisées

Toutes les souches types et *Escherichia coli* décrites ci-dessous ont été utilisées comme souches témoins positifs lors des PCR sur des gènes d'intérêt. *Escherichia coli* a aussi été utilisée comme cellule hôte de clonage. Leurs caractéristiques génotypiques sont présentées dans le tableau 7.

Tableau 7 : Récapitulatif des souches bactériennes et de leurs caractéristiques génotypiques.

Souches	Génotypes	Références
Escherishia coli (TOP 10)	F^-, *mcrA,* △(*mrr-hsd*RMS-*mcr*BC), ϕ80*lacZ*△M15, △*lac*X74, *deo*R, *rec*A1, *ara*D139, △(*ara-leu*)7697 *gal*U, *gal*K, *rps*L (Str^R), *end*A1, *nup*G	Invitrogen
Desulfobacter postgatei	Sauvage	DSM 2034
Desulfosarcina variabilis	Sauvage	DSM 2060
Desulfovibrio desulfuricans subsp. *Desulfuricans*	Sauvage	DSM 642
Desulfotomaculum nigrificans	Sauvage	DSM 574
AR2107 *Rhodospirillum centenum*-like	Sauvage	AR 2107 *Souche isolée au laboratoire*

II.4.2. Milieux et conditions de cultures

II.4.2.1. Culture d'Escherichia coli

La souche de *E. coli* (TOP 10) a été cultivée sous agitation en milieu liquide riche Luria Bertani (LB : Tryptone 10 $g.l^{-1}$, NaCl 5 $g.l^{-1}$, extrait de levure 10 $g.l^{-1}$) à 37°C. Les isolements de colonies, après transformation, ont été réalisés sur des boites de Pétri en milieu LB additionné d'agar à 15 $g.l^{-1}$. L'ampicilline (Sigma) à 100 $\mu g.l^{-1}$ de concentration finale, a été utilisée comme agent de sélection du plasmide pCR2.1, le X-Gal (30 $\mu g.l^{-1}$) comme substrat de la β-galactosidase, et l'IPTG (isopropylthio-β-D-galactoside 30 $\mu g.ml^{-1}$) comme inducteur du promoteur Plac.

Au cours du clonage, l'expression phénotypique du gène de résistance à l'ampicilline au sein de *E. coli* transformé, est effectuée en milieu riche liquide agité SOC (2 % Tryptone ; 0,5 % extrait de levure ; 10 mM NaCl ; 2,5 mM KCl ; 10 mM $MgCl_2$; 10 mM $MgSO_4$; 20 mM glucose) à 37°C.

II.4.2.2. Culture des bactéries anaérobies

Les bases minérales sont préparées dans une fiole conique (Figure 22) et stérilisées à l'autoclave pendant 20 min à 121°C sous une pression de 1 bar. Après stérilisation, la fiole est refroidie sous atmosphère N_2/CO_2 (90/100, v/v) jusqu'à température ambiante.

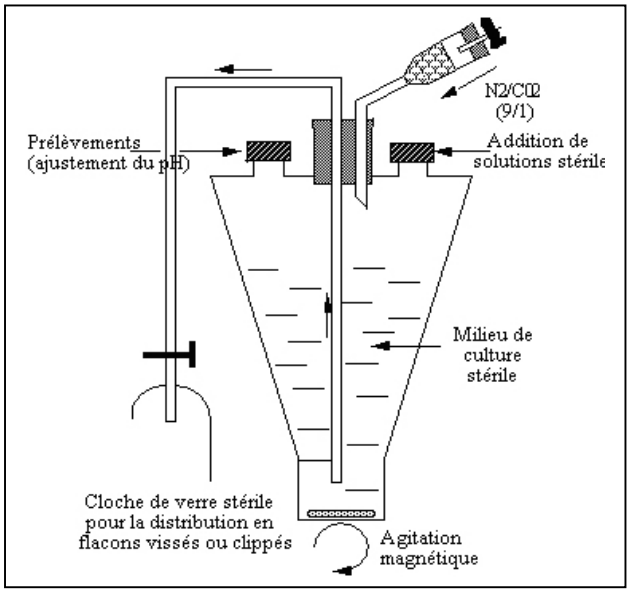

Figure 22 : Fiole conique utilisée pour la préparation des milieux de culture, d'après Widdel (1980).

❋ ***Bactéries anoxygéniques phototrophes***

Le milieu de culture utilisé est préparé à partir d'un milieu de base synthétique dont la composition est la suivante :

KH_2PO_4	0.25 $g.l^{-1}$			
NH_4Cl	0.50 $g.l^{-1}$			
$CaCl_2.2H_2O$	0.05 $g.l^{-1}$			
Solution SL12 sans EDTA*	1 $ml.l^{-1}$			
NaCl**	0 $g.l^{-1}$	20 $g.l^{-1}$	50 $g.l^{-1}$	100 $g.l^{-1}$
$MgSO_4.7H_2O$**	0.4 $g.l^{-1}$	0.8 $g.l^{-1}$	1.5 $g.l^{-1}$	3 $g.l^{-1}$
$MgCl_2.6H_2O$**	1 $g.l^{-1}$	2 $g.l^{-1}$	3 $g.l^{-1}$	6 $g.l^{-1}$

La base minérale est stérilisée, puis refroidie comme précédemment décrit. Les solutions suivantes sont alors additionnées stérilement :

* cf II.1.3.1 Maintien de tapis microbien en microcosme / Eau de mer synthétique (Camargue et Guérande)
** selon la salinité désirée

- Solution de $NaHCO_3$: 1,5 g de $NaHCO_3$ dans 30 ml d'eau distillée, préparée dans un tube fermé hermétiquement par un bouchon en butyl sous atmosphère de N_2/CO_2 (9/1 en volume) et stérilisée à l'autoclave (20 min, 121°C).
- Solution de $Na_2S.9H_2O$: 0,5 g (2 mM) de $Na_2S.9H_2O$ dans 10 ml d'eau distillée, préparée dans un tube fermé hermétiquement par un bouchon en butyl sous atmosphère d'argon ou d'azote et stérilisée à l'autoclave (20 min, 121°C).
- Solution de vitamine V7 stérilisée par filtration (0,2 µm) : 1 ml.

Le milieu est ensuite ajusté à pH 7,0 – 7,4 à l'aide de solutions stériles de H_2SO_4 et/ou NaOH (2 M). Le milieu est distribué dans des flacons stériles munis de capsules en aluminium vissées avec un joint en caoutchouc. Les flacons sont complètement remplis afin d'éviter la contamination par l'oxygène de l'air et stockés à l'obscurité. Un léger précipité noir de sulfure de fer doit apparaître dans les 24 heures suivant la préparation du milieu.

Remarque : Dans le cas des bactéries photohétérotrophes, 5mM de succinate de sodium et 0,5 $g.l^{-1}$ d'extrait de levure sont ajoutés à la base minérale avant stérilisation à l'autoclave.

La composition de la solution de vitamines **V7** est réalisée selon (Pfennig and Trüper, 1992) : biotine, 2 $mg.l^{-1}$; p-aminobenzoate, 10 $mg.l^{-1}$; thiamine, 10 $mg.l^{-1}$; pantothénate, 5 $mg.l^{-1}$; pyridoxamine, 50 $mg.l^{-1}$; vitamine B12, 20 $mg.l^{-1}$; nicotinate, 20 $mg.l^{-1}$.

❋ *Bactéries sulfato-réductrices (BSR)*

Un milieu riche synthétique pour les BSR a été utilisé, adapté d'après (Widdel and Bak, 1992), dont la base minérale est décrite ci-dessous.

La base minérale est ensuite stérilisée, et refroidie comme précédemment décrit. La solution suivante est alors additionnées stérilement :

- Solution de vitamine V7 stérilisée par filtration (0.2 µm) : 1 ml.

Le milieu est ensuite ajusté à pH 7,4 à l'aide de solutions stériles de Na_2CO_3 (2 M) ou H_2SO_4 (1 M). Le milieu est distribué dans des flacons pénicilline de 60 ou 100 ml, fermés par des bouchons en butyl, sous atmosphère N_2/CO_2 (90/100, v/v), et stockés à l'obscurité.

	Eau saumâtre	Eau de mer
NaCl	7 $g.l^{-1}$	20 $g.l^{-1}$
$MgCl_2.6H_2O$	1,2 $g.l^{-1}$	3 $g.l^{-1}$
$CaCl_2.2H_2O$	0,1 $g.l^{-1}$	0,15 $g.l^{-1}$
Na_2SO_4	4 $g.l^{-1}$	4 $g.l^{-1}$
NH_4Cl	0,25 $g.l^{-1}$	0,25 $g.l^{-1}$
KH_2PO_4	0,2 $g.l^{-1}$	0,2 $g.l^{-1}$
KCl	0,5 $g.l^{-1}$	0,2 $g.l^{-1}$
CH_3 COO Na.$3H_2O$	10 mM	10 mM
$CH_3CHOHCOOH$	10 mM	10 mM
Extrait de levure	0,5 $g.l^{-1}$	0,5 $g.l^{-1}$
Na_2 S.$9H_2O$	0,1 $g.l^{-1}$	0,1 $g.l^{-1}$
$NaHCO_3$	2,5 $g.l^{-1}$	2,5 $g.l^{-1}$
Solution d'oligo-éléments SL12	1 $ml.l^{-1}$	1 $ml.l^{-1}$

II.4.3. Conservation des souches

Les souches d'*E. coli* et sulfato-réductrices sont conservées à -80°C, à partir d'une culture dense en phase exponentielle, avec ajout de glycérol stérile à une concentration finale de 20 % (v/v).

Pour la conservation des bactéries sulfato-réductrices, le glycérol stérile employé a été au préalable dégazé sous atmosphère N_2/CO_2 (90/100, v/v). De même, les flacons de culture (tubes Ungate) sont de nouveau dégazés, après addition de glycérol, sous atmosphère N_2/CO_2 (90/100, v/v) avant stockage à -80°C.

Les Bactéries phototrophes anoxygéniques (BPA) sont conservées au froid (4°C) et à l'obscurité dans les flacons de leurs cultures liquides en phase exponentielle de croissance. Les souches peuvent ainsi être gardées plusieurs mois, après quoi, il est nécessaire de les repiquer. Pour cela un flacon est replacé à température ambiante, et exposé à une faible intensité lumineuse (100 lux) pendant 2 à 3 h. Une solution neutre de sulfure et de carbonate (Siefert and Pfennig, 1984) est ensuite additionnée à la culture. La culture peut alors être replacée à une intensité lumineuse plus forte (500 à 1000 lux) puis servir de base pour l'ensemencement d'autres flacons, qui seront de nouveau stockés au froid.

II.5. Techniques de biologie moléculaire

II.5.1. Extraction d'ADN génomique

II.5.1.1. A partir de cultures pures

L'extraction de l'ADN génomique de souches pures a été réalisée à partir de cultures denses en phase stationnaire. 1 ml de culture est centrifugé entre 10 000 à 15 000 rpm pendant 10 à 15 min. (si le culot est instable, la centrifugation peut être réalisée à 4°C). Le culot bien sec peut être stocké à – 20°C.

Afin d'effectuer la lyse cellulaire, le culot est mis en suspension dans du TGE (Tris 25 mM, Glucose 50 mM, EDTA 10 mM) avec du lysozyme (1 $mg.ml^{-1}$) puis incubé pendant 10 minutes à 37°C. Les protéines sont ensuite dégradées par action de la protéinase K (100 $\mu g.ml^{-1}$) au cours d'une incubation de 30 minutes à 37°C en présence de SDS (0,5%). Une seconde incubation après ajout de SDS (0,5%), est effectuée pendant 10 minutes à 60°C.

Les molécules insolubles (débris cellulaires, protéines, polysaccharides, lipides) sont ensuite éliminées par dénaturation au cours de différentes extractions au phénol. La première étape s'effectue en additionnant à l'extrait cellulaire un volume de phénol saturé et équilibré avec du TE [pH 8] contenant des antioxydants (0,1 % hydroxyquinoline, 0,2 % β-mercaptoéthanol). Les deux phases sont mélangées quelques secondes au vortex puis séparées par une centrifugation de 5 min à 10 000 rpm. La phase aqueuse est soigneusement prélevée en évitant de récupérer les protéines dénaturées situées à l'interface phase aqueuse/phénol. La phase organique peut être de nouveau extraite par ajout de TE (Tris HCl 10 mM, EDTA 1 mM, [pH 8]) volume à volume en procédant comme précédemment décrit. Une seconde extraction au PCIH (phénol/chloroforme/alcool isoamilique/hydroxyquinoléine : 48/48/4/0.1 ; v/v/v/p) est réalisée volume à volume sur les phases aqueuses réunies. Le phénol résiduel de la phase aqueuse est éliminé par une extraction au CI (chloroforme/alcool isoamilique : 96/4 ; v/v) volume à volume.

Les acides nucléiques obtenus en solution sont alors précipités à l'éthanol, en ajoutant à la phase aqueuse $1/10^{e}$ de volume d'acétate de sodium 3 M [pH 5,2] et deux volumes d'éthanol absolu à froid (conservé à –20°C). Le mélange est incubé soit 1 h à -80°C, soit toute une nuit à -20°C.

Les acides nucléiques sont ensuite récupérés par centrifugation pendant 15 à 30 min à 14 000 rpm à une température de 4°C. Le culot est lavé de ses sels par un volume d'éthanol 70% à froid, suivi d'une centrifugation de 15 à 30 min à 14 000 rpm à 4°C. Puis il est séché

au Speed-Vac (*Dna 120*, SAVANT) pendant 5 min à chaleur moyenne. Le culot d'acides nucléiques est remis doucement en suspension dans 50 µl d'H_2O distillée stérile ou de TE [pH 8]. Au cours d'une incubation de 30 min à 37°C, un traitement enzymatique à la Rnase pancréatique (Rnase A 1 $mg.ml^{-1}$) est appliqué aux acides nucléiques en solution, afin de dégrader les ARNs présents dans l'extrait. L'ADN génomique ainsi extrait et traité peut alors être stocké à -20°C.

II.5.1.2. A partir d'échantillons de tapis microbien

L'extraction d'ADN génomique des différents échantillons de tapis est réalisée à l'aide d'un kit (*UltraClean™ Soil DNA isolation kit*, MoBio Laboratories) selon les recommandations du fournisseur. Toutefois, l'addition d'EDTA (10 mM) est nécessaire lors de la première étape de lyse cellulaire, permettant ainsi d'inactiver les nucléases présentes au cours de l'extraction. Ce kit combine deux types différents de lyses cellulaires, une lyse mécanique par broyage et une lyse enzymatique. L'ADN génomique d'un large spectre de bactéries peut ainsi être extrait.

Les échantillons de granulosité plus importante, ont plutôt subit la lyse alternative du kit commercial, proposée par le fournisseur. Cette méthode de lyse utilise le choc thermique pour effectuer la lyse cellulaire plutôt que le broyage. Les ADNs génomiques ainsi extraits peuvent alors être stockés à -20°C.

II.5.2. Réactions de polymérisation en chaîne (PCR)

La technique de PCR permet d'amplifier un fragment d'ADN à partir de deux amorces oligonucléotidiques spécifiques (Mullis *et al.*, 1986; Saiki *et al.*, 1985). Elle repose sur la synthèse enzymatique d'ADN par une Taq polymérase thermostable (*Hot Start Taq polymerase*, Qiagen) à partir de deux amorces de polarités opposées et dont la séquence est complémentaire de chacune des bornes du fragment à amplifier.

Uniquement dans le cas de la T-RFLP, des amorces fluorescentes portant en 5' un fluorochrome (phosphoramidites telles que TET : 5-tétra-chloro-fluorescéine ; HEX : 5-hexa-chloro-fluorescéine ; FAM : 5-carboxy-fluorescéine) ont été utilisées.

II.5.2.1. PCR classique

❋ Conditions de réaction

Le choix d'utiliser un mélange réactionnel commercial (*Hot Start Taq master mix*, Qiagen) contenant au préalable, l'enzyme, le tampon de réaction, le $MgCl_2$, et les 4 désoxyribonucléotides (dNTPs), permet d'éviter de nombreuses étapes de transferts de produits et donc de diminuer les risques de contamination. L'utilisation a néanmoins été optimisée à partir des recommandations du fournisseur (dilution au ¼), la Taq polymérase et les dNTPs en excès entraînant des amplifications aspécifiques.

Chaque amplification est réalisée dans un volume final de 50 µl où sont réunis les composants suivants : *Hot Start Taq Master Mix* dilué au ¼ (Taq polymérase 0,625 U ; $MgCl_2$ 0,375 mM ; Tampon réactionnel 1X ; dNTPs 50 µM) ; Oligonucléotides 1 & 2 (0,5 µM chacun) ; $MgCl_2$ (1,125 mM) ; 10 ng matrice d'ADN (ADNgénomique ou plasmide).

❋ Conditions d'amplification

Un cycle de PCR est constitué de 3 étapes successives réalisées sur un thermocycler automatisé (*PTC-100 ou 200*, MJ Research). Le programme d'amplification utilisé est le suivant :

- Hot Start (dénaturation de l'ADN et activation de l'enzyme) : 95°C pendant 15 min.
- 35 cycles d'amplification :
    a) dénaturation de la matrice d'ADN à 95°C pendant 1 min.
    b) hybridation des amorces à la température d'hybridation appropriée (50°C<Tm<60°C) pendant 30 s.
    c) élongation des amorces par l'ADN polymérase à 72°C pendant 1 min.
- élongation finale à 72°C pendant 10 min.

L'analyse du rendement et de la spécificité des produits PCR est ensuite réalisée par une électrophorèse sur gel d'agarose de 1 à 2 % en fonction de la taille des fragments attendus.

❋ *Amorces utilisées pour l'étude*

Différents couples d'oligonucléotides ont été sélectionnés (Tableaux 8 et 9), dans le but de caractériser différentes populations bactériennes au sein du tapis microbien : les eubactéries, les bactéries sulfato-réductrices (BSR) et les bactéries phototrophes anoxygéniques (BPA).

Tableau 8 : Séquences des amorces ciblant le gène *ADNr 16s* ou le gène *PufM* des Eubactéries, BSR et BPA.

Amorces	Séquences (5'→3')	Gènes ciblés	Spécificité	Références
8f*	AGA GTT TGA TCC TGG CTC AG	*ADNr 16S*	Eubactérie	(Lane, 1991)
926r*	CCG TTC AAT TCC TTT RAG TTT	*ADNr 16S*	Eubactérie	(Muyzer *et al.*, 1995)
1489r*	TAC CTT GTT ACG ACT TCA	*ADNr 16S*	Eubactérie	(Weisburg *et al.*, 1991)
BSR 385r*	CGG CGT CGC TGC GTC AGG	*ADNr 16S*	BSR	(Amann *et al.*, 1990)
PB 557f**	CGC ACC TGG ACT GGA C	*PufM*	BPA	(Achenbach *et al.*, 2001)
PB 750r**	CCC ATG GTC CAG CGC CAG AA	*PufM*	BPA	(Achenbach *et al.*, 2001)

*Les noms de ces amorces sont basés sur les positions du gène codant pour l'ARNr 16S de *E. coli*.
** Les noms de ces amorces sont basés sur les positions du gène *PufM* de *Rh. sphaeroides*

Tableau 9 : Taille des amplicons en paire de base (pb) des couples d'amorces du tableau 8.

Couples d'amorces	Taille des fragments (pb)
8f-926r	918
8f-1489r	1481
8f-BSR385r	377
PB557f-PB750r	229

II.5.2.2. « Nested » PCR

Il s'agit d'une seconde PCR effectuée sur le produit d'amplification d'une 1ère PCR, en utilisant un couple d'amorces internes au domaine défini par les amorces de la 1ère PCR. Cette technique de PCR apporte ainsi une plus grande sensibilité et spécificité d'amplification. La « nested » PCR a été employée dans cette étude pour amplifier une partie du gène *ADNr16S*, issu spécifiquement de genres particuliers de la communauté des BSR, en utilisant comme matrice le gène *ADNr16S* préalablement amplifié avec le couple d'amorces 8f-1489r. Elle permet ainsi de mettre en évidence des communautés bactériennes minoritaires au sein du tapis.

❋ *Conditions de réaction et d'amplification*

Les conditions de réactions et d'amplifications de la « nested » PCR sont identiques à celles d'une PCR classique, décrites ci-dessus.

❋ *Amorces choisies pour l'étude*

Le tableau 10 ci-dessous regroupe les différents couples d'amorces utilisés pour mettre en évidence des genres bactériens particuliers :

Tableau 10 : Couples d'amorces ciblant le gène *ADNr 16S* des bactéries sulfato-réductrices en fonction des genres.

Amorces*	Séquences (5'→3')	Spécificité	Références
Dfm140f	TAG MCY GGG ATA ACR SYK G	*Desulfotomaculum*	(Daly *et al.*, 2000)
Dfm842r	ATA CCC SCW WCW CCT AGC AC		
Dsb127f	GAT AAT CTG CCT TCA AGC CTG G	*Desulfobacter*	
Dsb1273r	CYY YYY GCR RAG TCG STG CCC T		
Dcc305f	GAT CAG CCA CAC TGG RAC TGA CA	*Desulfococcus* *Desulfonema* *Desulfosarcina*	
Dcc1165r	GGG GCA GTA TCT TYA GAG TYC		
Dsv230f	GRG YCY GCG TYY CAT TAG C	*Desulfovibrio* *Desulfomicrobium*	
Dsv838r	SYC CGR CAY CTA GYR TYC ATC		

*Les noms de ces amorces sont basés sur les positions du gène codant pour l'ARNr 16S des espèces types correspondantes.

II.5.3. Purification des produits PCR

Les produits PCR en solution sont purifiés à l'aide du kit commercial *GFX™ DNA and Gel Band Purification Kit* (Amersham Pharmacia Biotech). Cette purification a pour but de séparer le fragment d'ADN amplifié du reste des composants du milieu de réaction (protéines, sels, etc.…) et notamment des autres acides nucléiques (amorces non utilisées, amplification de séquences non désirées inférieures à 100 paires de bases, etc.…).

II.5.4. Dosage de l'ADN par la méthode des « dots »

Cette technique de dosage de l'ADN est utilisée lorsqu'on ne dispose que de petites quantités d'acides nucléiques. Un gel fin d'agarose à 1 % contenant du bromure d'éthidium (0.5 $\mu g.ml^{-1}$) est coulé dans une boîte de Pétri. Pour chaque échantillon, 1 µl du produit PCR purifié y est déposé. Après avoir réalisé une gamme de dilution en déposant, en parallèle des échantillons à doser, de l'ADNg de sperme de saumon à différentes concentrations connues (5 $ng.\mu l^{-1}$ à 1 $\mu g.\mu l^{-1}$) les gels sont visualisés sous lumière UV. Les intensités des spots pour chaque échantillon dosé sont comparées avec celles de la gamme de dilution, ce qui permet d'estimer les quantités d'ADN.

II.5.5. Digestion enzymatique

La digestion enzymatique est ici utilisée afin d'étudier le polymorphisme de longueur au sein de différents échantillons. Les enzymes de restriction utilisées reconnaissent des sites spécifiques de clivages à 4 paires de bases (Tableau 11) et présentent ainsi une fréquence de coupure importante (4^4=256 paires de bases).

Les différents produits PCR purifiés sont soumis à des digestions enzymatiques par différentes endonucléases de restriction selon les recommandations du fournisseur (New England BioLabs).

Tableau 11: site de coupures des enzymes de restriction utilisées.

Enzyme	Site de coupure
Hae III	$^{5'}$ GG / CC $_{3'}$
HinP1I	$^{5'}$ GCG / C $_{3'}$
RsaI	$^{5'}$ GT / AC $_{3'}$

L'hydrolyse a été réalisée dans le tampon réactionnel préconisé par le fournisseur avec 10 unités d'enzymes pour digérer environ 1 µg d'ADN amplifié. L'incubation est effectuée à la température optimale d'activité de l'enzyme utilisée, pendant 3h.

II.5.6. Electrophorèse

Après extraction, la séparation des ADN génomiques a été réalisée par migration électrophorétique sur gel d'agarose (*QA-Agarose*, Q-Biogène) à 1 % (m/v) dans un tampon TAE 1X (Tris-acétate 40 mM, EDTA 1 mM). La séparation des fragments d'ADN digérés a été réalisée sur gel d'agarose haute résolution optimisé pour les petits fragments d'ADN (*Metaphor*, Tebu-bio), à une concentration entre 2 et 4 % (m/v) en fonction de la taille des fragments à séparer, dans un tampon TBE 1X (Tris-borate 89 mM, acide borique 89 mM, EDTA 2 mM). Les ADNs sont visualisés par fluorescence au UV après avoir baigné les gels d'agarose dans un bain de BET (bromure d'éthidium 0,5 $\mu g.ml^{-1}$).
La migration des différents échantillons se fait en parallèle d'un marqueur de poids moléculaire (*Smart ladder* échelle de 200 à 10000 pb ou *Smart ladder low 20 bp* échelle de 20 à 1000 pb, Eurogentec).

II.5.7. T-RFLP

II.5.7.1. Principe

La méthode de la T-RFLP (Terminal Restriction Fragment Length Polymorphism) a été développée par (Liu *et al.*, 1997). Après extraction des ADNs génomiques de chaque échantillon et amplification par PCR avec des amorces fluorescentes spécifiques, les communautés bactériennes ne sont plus représentées que par un mélange de gènes d'intérêts amplifiés (les gènes *ADNr 16S* par exemple). La T-RFLP permet de mettre en évidence le polymorphisme de taille des fragments terminaux de restriction (T-RFs), obtenus après hydrolyse des produits PCR marqués avec des endonucléases de restriction. La longueur de ces T-RFs varie d'une espèce à l'autre selon la position de la séquence nucléotidique reconnue par l'enzyme. Les populations bactériennes peuvent ainsi être représentées par la taille en paires de bases (pb) de leurs fragments de restriction terminaux respectifs.

II.5.7.2. Protocole expérimental

Pour chaque échantillon, les produits PCR sont obtenus par amplification à partir d'environ 10 ng de matrice d'ADN génomique et à l'aide d'amorces fluorescentes. Après purification et quantification des produits PCR, environ 700 ng d'ADN sont digérés par différentes enzymes de restriction. Uniquement 100 ng de chaque digestion sont ensuite dénaturés pendant 2 min à 94°C, en présence de 0,5 µl de marqueur de poids moléculaire (*TAMRA 500*, Applied Biosystems) et de 20 µl de formamide. Les produits de digestion sont séparés par électrophorèse capillaire sur un séquenceur automatique (*ABI PRISM™ 310 Genetic Analyzer*, Applied Biosystems). Après une injection électrocinétique de l'échantillon pendant 30 secondes dans un capillaire contenant un gel polymère adapté (gel de polyacrylamide *Pop4*, Applied Biosystems), la migration est effectuée sous une tension de 15 kV pendant 30 minutes à 60°C. Cette migration entraîne alors la séparation des différents fragments de restriction selon leur taille. Seuls les fragments de restriction en position terminale (T-RFs) vont être détectés, car ils contiennent l'amorce fluorescente (Figure 23).

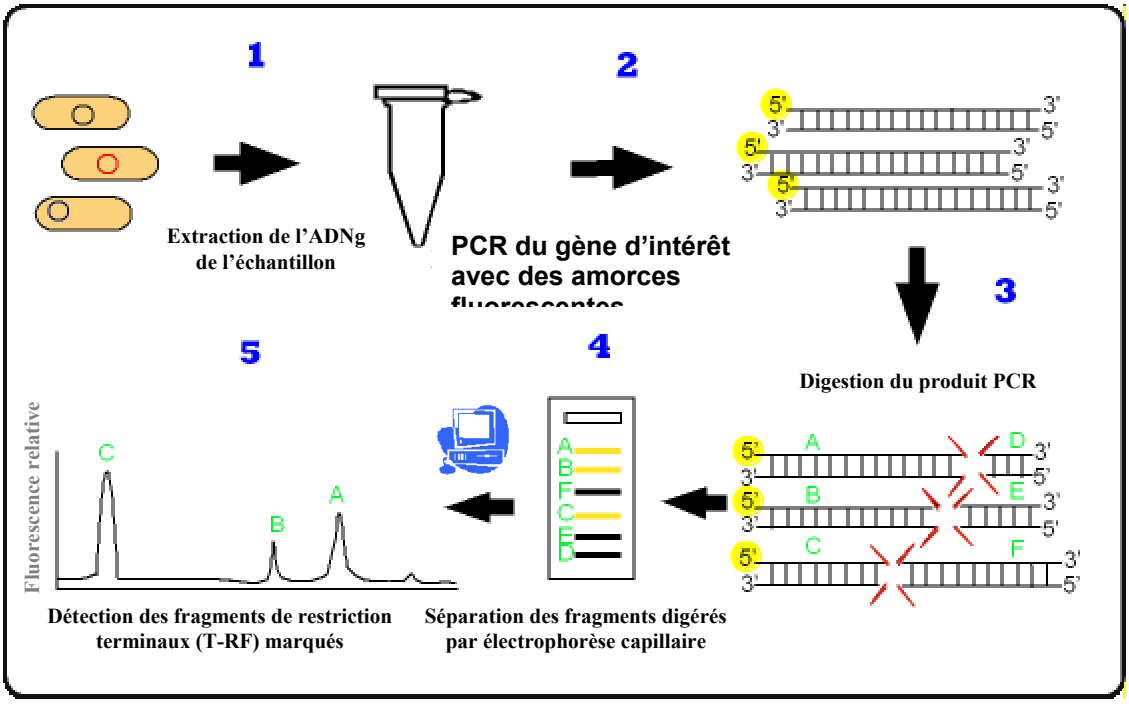

Figure 23 : Schéma récapitulatif de l'approche T-RFLP. ***Extrait du site web RDP II.***

Une analyse préliminaire des électrophorégrammes est réalisée grâce au logiciel Genescan v3.0 (Applied Biosystems) permettant de déterminer les tailles des différents fragments détectés.

Des digestions prédictives peuvent être réalisées sur le programme TAP-TRFLP du site web *Ribosomal Database Project II* (RDP II : http://rdp.cme.msu.edu/html/analyses.html) afin, si possible, d'associer une espèce bactérienne à une taille de T-RF observée (Maidak *et al.*, 1996 ; Maidak *et al.*, 1997 ; Maidak *et al.*, 1994 ; Maidak *et al.*, 2001; Maidak *et al.*, 2000 ; Maidak *et al.*, 1999).

II.5.7.3. Analyses statistiques

L'analyse des données de manière statistique vise à répartir, en un certain nombre de groupes, les différents profils T-RFLP en fonction de leurs caractéristiques respectives mesurées (T-RFs définis par la taille en pb, aire ou hauteur de l'intensité de fluorescence en UF, etc.…). Le choix des groupes, aussi homogènes que possible, résulte d'un compromis entre une description simple et suffisamment détaillée.

1) Traitement des données brutes correspondant à une série de transformation des valeurs numériques pour chaque caractéristique mesurée. Cette standardisation s'effectue en plusieurs étapes :

- **Elimination du bruit de fond des profils T-RFLP**, en délétant tous les T-RFs ayant une hauteur d'intensité de fluorescence inférieure à 100 UF. La suppression de ces données présente un faible taux d'erreurs sur l'analyse effectuée (Blackwood *et al.*, 2003).

- **Normalisation des quantités de fluorescence** afin de permettre une comparaison des différents profils T-RFLP entre eux. Cela consiste à ramener les hauteurs totales d'intensités de fluorescence (IF) de chaque profil T-RFLP, à la plus petite somme d'IF observée. Les hauteurs d'IF de chaque T-RF sont donc recalculées de manière proportionnelle à cette somme minimale d'IF. Certaines valeurs (hauteurs d'IF), une fois normalisées, sont alors de nouveau inférieures au seuil de détection de l'appareil (30 UF). Il convient donc de les éliminer de l'analyse avant toute comparaison.

- **Regroupement des T-RFs** restants, pour un même profil, sur la base de leur taille en pb. Les tailles en paire de base étant calculées par le logiciel Genescan v3.0 d'après la méthode du « Local Southern » (relation entre la taille des fragments et leur mobilité), les valeurs numériques obtenues sont des valeurs décimales. Il s'agit donc de regrouper les tailles

de T-RFs ayant des valeurs similaires (+ ou – 0,5 pb) et de définir une valeur moyenne entière en pb. Les intensités de fluorescence correspondantes sont alors cumulées.

- **Constitution d'une table variables / échantillons** contenant les valeurs relatives des intensités de fluorescence, pour chaque T-RF observé (variable) en fonction de tous les profils T-RFLP (échantillons) à comparer. Ce tableau à deux entrées est ensuite soumis aux analyses statistiques du logiciel MVSP v3.1 (Multi-Variate Statistical Package v3.1, Kovach Computing Services) (Kovach, 1999).

2) Analyses statistiques des données grâce au logiciel MVSP v3.1

- **Calcul de l'indice de similarité** (S_{ij}) entre tous les échantillons (sur la base de leurs profils T-RFLP). Cet indice sera d'autant plus élevé que les caractéristiques (T-RFs) de ces derniers seront éloignées. Nos données sont constituées de différentes variables qualitatives (intensités de fluorescence relatives de chaque T-RF). Ces données peuvent être regroupées par la méthode de la distance de Jaccard. Les effets des biais de la PCR peuvent être réduits lors de l'analyse statistique par l'utilisation de cette méthode métrique qui prend en compte uniquement la présence ou l'absence des T-RFs (Blackwood *et al.*, 2003).

Soit : $S_{ij} = a_{ij} / (a_{ij}+b_{ij}+c_{ij})$

a_{ij} le nombre de T-RFs présents entre 2 échantillons *i* et *j* à comparer,

b_{ij} le nombre de T-RFs absents entre 2 échantillons *i* et *j* à comparer,

c_{ij} le nombre de T-RFs absents dans l'échantillon *i* et présent dans l'échantillon *j*.

- **Classification hiérarchique ascendante par la méthode UPGMA (Unweighted Pair Group Method with Arithmetic Mean).** C'est une méthode de construction de dendrogrammes obtenus à partir d'une distance ou dissimilarité entre 2 échantillons. Son algorithme consiste à regrouper de manière séquentielle les 2 échantillons les plus proches (sur la base de leur indice de Jaccard), et à réitérer ce processus jusqu'au regroupement complet des échantillons comparés. Le profil en branche du dendrogramme obtenu illustre les dissimilarités entre les différents échantillons regroupés.

- **Statistique descriptive par des méthodes multifactorielles : AFC (Analyse Factorielle des Correspondances) et ACC (Analyse Canonique des Correspondances).** Ces méthodes ont pour but de décrire des données consignées dans un tableau (matrice) croisant des

échantillons (lignes) et des variables ou T-RFs (colonnes) mesurés sur ces échantillons. L'étude s'effectue par réduction du nombre de variables en construisant de nouvelles variables synthétiques obtenues en combinant les variables initiales (méthode factorielle).

AFC, méthode proposée par Benzécri (1976), elle permet l'analyse des données qualitatives (tableaux de contingence, de présence-absence, etc…). Très brièvement, l'AFC va permettre de réduire à un espace à deux ou trois dimensions, l'espace de représentation des éléments des ensembles des échantillons (profils T-RFLP) et des variables (T-RFs), initialement à n et m dimensions. Cette réduction sera opérée en fonction des proximités (similarité) entre les éléments « profils T-RFLP » et « T-RFs ». Son algorithme est calculé à la manière d'une ACP (Analyse des Composantes Principales), cependant la matrice de similarité produite est basée sur le χ^2. Le résultat graphique est un diagramme de dispersion montrant un nuage de points (échantillons) sur un plan de deux ou trois dimensions défini par des axes (composantes principales) représentant les variables synthétiques et leurs importances (en pourcentages) dans la distribution observée des échantillons.

ACC, méthode dérivée d'une analyse des correspondances, permettant d'incorporer des données écologiques à l'analyse des correspondances (Ter Braak, 1986). Celle-ci consiste à étudier les relations linéaires existant entre 2 groupes de caractères quantitatifs observés sur un même ensemble d'individus. Le résultat graphique est un diagramme de dispersion contenant : les variables environnementales dessinées sous forme de vecteurs émanant du centre du graphe et un nuage de points (échantillons) sur un plan défini par des axes représentant une combinaison linéaire entre les variables environnementales et les T-RFs. La longueur et l'orientation de ces vecteurs sont proportionnelles à leurs influences dans la distribution des échantillons.

II.5.8. RFLP

II.5.8.1. Principe

Le polymorphisme des gènes *ADNr16S* peut aussi être étudié, au sein d'une population microbienne, en analysant les variations de leurs profils de restriction. Cette méthode est connue sous le nom de RFLP (Restriction Fragment Length Polymorphism) (Kiko *et al.*, 1979). Préalablement, une banque de gène *ADNr 16S*, est réalisée sur les

échantillons étudiés. Les fragments amplifiés *ADNr 16S* avec des amorces eubactéries non marquées, sont clonés au plasmide pCR2.1-TOPO puis transformés dans la souche hôte *Escherichia coli* TOP10. L'insert est amplifié à nouveau à l'aide d'amorces flanquantes situées sur le plasmide, puis digéré par des enzymes de restriction. Les différents clones sont par la suite classés en fonction de leurs profils de restriction respectifs, mettant en évidence différentes populations. Pour chacune de ces populations, la séquence des inserts *ADNr16S* clonés, a été déterminée.

II.5.9. Banque de gènes amplifiés

II.5.9.1. Principe

La banque de gène ADNr 16S a été réalisée à l'aide du vecteur de clonage pCR-2.1 (*TopoTA Cloning kit*^{TM}, Invitrogen) commercialisé sous forme linéaire (Figure 24).

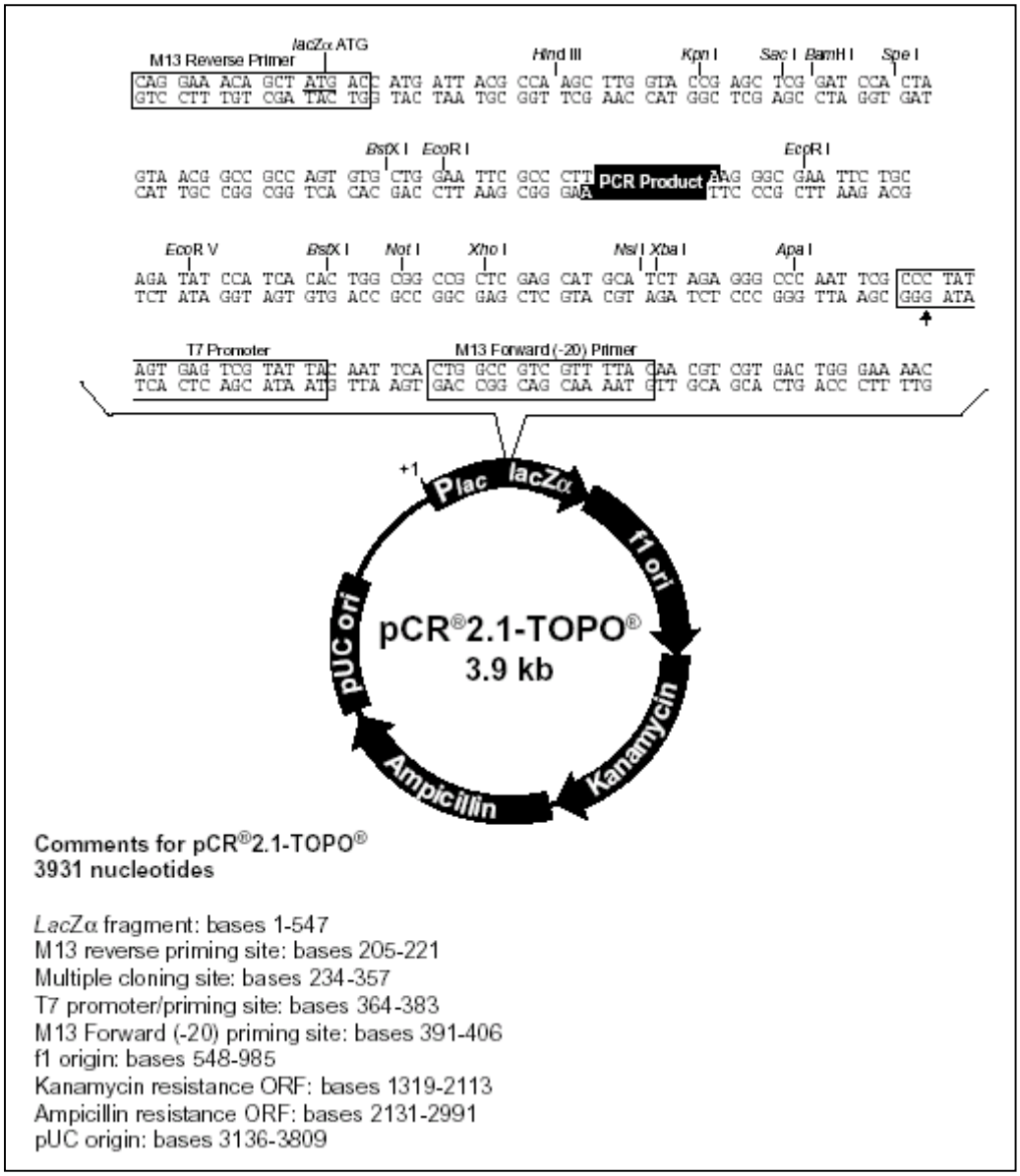

Figure 24 : Carte de restriction du vecteur pCR2.1-TOPO, *d'après Invitrogen*.

Il comprend, entre autres, deux gènes de résistance à des antibiotiques (kanamycine et ampicilline), et *lacZα* qui est une partie du gène *lacZ* d'*Escherichia coli* codant pour la β-galactosidase déficiente, sous contrôle du promoteur Plac inductible à l'IPTG.

Après transformation avec le plasmide recombinant d'une souche hôte (voir II.3 Souches bactériennes utilisées) produisant une β-galactosidase déficiente, il y aura une α-complémentation. La β-galactosidase résultante va alors dégrader le substrat X-Gal, présent dans le milieu, et donner une coloration bleue aux clones non recombinants. Lorsque l'insert est intégré au plasmide, la bactérie ne produira plus l'enzyme active, les clones positifs seront blancs.

II.5.9.2. Ligation

Ce vecteur présente à chaque extrémité un résidu thymidine (T) supplémentaire en 3', et une enzyme Topoisomérase I liée de manière covalente au vecteur. Ceci permet une ligation efficace entre le vecteur et les inserts provenant uniquement de produits PCR obtenus avec la Taq polymérase, celle-ci ajoutant un résidu adénosine (A) en 3' des fragments amplifiés. La ligation se fait selon les recommandations du fournisseur.

II.5.9.3. Transformation

La transformation est effectuée par la méthode du choc thermique sur des cellules *E. coli* TOP 10 (voir II.3 Souches bactériennes utilisées) chimiocompétentes, selon les recommandations du fournisseur.

II.5.10. Séquençage

II.5.10.1. Séquençage automatique

Les réactions de séquençage d'ADN ont été réalisées selon la méthode de Sanger, à l'aide du kit *BigDye® Terminator v3.1 Cycle Sequencing Kit* (Applied Biosystems) selon les

recommandations du fournisseur. Les produits des réactions de séquences sont ensuite purifiés sur des colonnes Sephadex *AutoSeq G-50* (Amersham Pharmacia Biotech). L'électrophorèse capillaire a été effectuée sur un séquenceur automatique *ABI PRISM™ 310 Genetic Analyzer* (Applied Biosystems).

Une partie des déterminations de séquences a été effectuée chez un prestataire de service de séquençage (Biofidal) à partir de clones étalés sur une boite de Pétri ou de produits PCR non purifiés.

❋ *Méthode de Sanger*

D'après Sanger *et al.* (1992), la réaction de séquençage est basée sur le principe d'une réaction cyclique (dénaturation, hybridation, élongation). Le fragment à séquencer est utilisé comme matrice d'une synthèse nucléotidique réalisée par une ADN polymérase. Cette réaction est établie, dans un même tube, en présence des quatre précurseurs dNTP (désoxyribonucléotides tri-phosphates) et d'une faible quantité des quatre analogues portant quatre fluorochromes différents, les ddNTP (didésoxyribonucléotides tri-phosphates). Lors de la polymérisation, ces derniers s'incorporent au hasard, ce qui arrête la synthèse. Les fragments néosynthétisés, de longueurs variées, sont ensuite séparés en fonction de leur taille par électrophorèse capillaire (séquenceur *ABI PRISM™ 310 Genetic Analyzer*, Applied Biosystems). Il devient alors possible de déterminer pour chacun des quatre fluorochromes utilisés la taille des fragments obtenus et d'en déduire la séquence nucléotidique du fragment analysé.

II.5.10.2. Analyse des séquences

Les traitements des séquences brutes ont été réalisés à l'aide du logiciel Séquencher v4.1.4. Les séquences nucléotidiques ont ensuite été comparées aux séquences contenues dans les banques de données à l'aide du logiciel Blast (Basic Local Alignment Search Tool, www.ncbi.nlm.gov/blast). Le logiciel Clustal W (www.infobiogen.fr) a permis l'alignement des séquences. La construction d'arbres phylogénétiques à partir de ces séquences traitées a été réalisée à l'aide du logiciel MEGA v2.1 (Kumar *et al.*, 2001).

Une partie des séquences déterminées lors de cette étude a été déposée dans une banque de données (Genbank).

Chapitre III : Description de tapis microbiens

III. Description de tapis microbiens

III.1. Introduction

Depuis une vingtaine d'années, les tapis microbiens photosynthétiques ont fait l'objet de nombreuses études d'écologie descriptive afin de permettre une meilleure compréhension de ces écosystèmes côtiers (Krumbein *et al.*, 1977 ; Stal, 1994 ; Stal *et al.*, 1985 ; van Gemerden, 1993). A cette époque, les méthodes classiques comme la microbiologie et la biogéochimie ont permis d'entrevoir la complexité de tels écosystèmes.

Ce chapitre vise à décrire deux tapis microbiens photosynthétiques différents : l'un hypersalé, l'autre marin. Déjà présentés dans la littérature, l'analyse des tapis microbiens de Camargue (Salins-de-Giraud) et des Iles Orcades (Ecosse) a été appréhendée de manière intégrée, afin de mettre en lien les communautés bactériennes présentes et leurs rôles écologiques au sein de ces écosystèmes complexes. Ainsi, les différents aspects de la biodiversité et de l'écologie, ont été abordés par la combinaison d'approches variées (moléculaire, microscopique, chimique et biogéochimique) permettant de caractériser à l'échelle du micromètre la distribution des groupes fonctionnels majoritaires composant la partie métaboliquement active de ces tapis.

Les tapis microbiens hypersalés représentent des écosystèmes particulièrement bien adaptés aux habitats ayant des conditions de salinité fluctuantes. Les marais salants de Salins-de-Giraud en Camargue abritent le développement de tapis microbiens au sein de ses nombreux partènements. Les travaux de Caumette *et al.* (1994) ont pu décrire ces tapis issus de bassins de très fortes salinités (entre 150 ‰ et 300 ‰) en abordant l'étude d'un point de vue microbiologique et écologique. Ainsi, les cyanobactéries du genre *Phormidium* dominent la surface de ce tapis, et recouvrent une couche de bactéries pourpres principalement composée des genres *Halochromatium* et *Halothiocapsa*. Par la suite, plusieurs études moléculaires ont permis d'approfondir cette première description des tapis de Camargue (Mouné, 2000 ; Mouné *et al.*, 2003; Mouné *et al.*, 1999 ; Mouné *et al.*, 2000), révélant une diversité bactérienne bien plus importante qu'attendue.

En première partie de ce chapitre, les travaux présentés dans l'article "Characterization of functional bacterial groups in a hypersaline microbial mat community (Salins-de-Giraud, Camargue, France)", concerne cette fois un tapis microbien issu de bassins de salinités inférieures (de 70 ‰ à 110 ‰). La biodiversité des communautés bactériennes de ce tapis

s'organise en une structure très fine, constituée verticalement de couches distinctes de quelques micromètres, où s'agencent les populations bactériennes en fonction de leurs caractéristiques physiologiques et des conditions environnementales. Les cyanobactéries filamenteuses dominent la surface de ce tapis, essentiellement par la présence de *Microcoleus chthonoplastes.* Les bactéries phototrophes pourpres et sulfato-réductrices présentent une forte diversité qui s'organise le long des microgradients d'oxygène, de lumière et de sulfure.

Les tapis microbiens sont capables de se développer dans des habitats très divers, ainsi ils ont été observés dans des zones intertidales tels que les plages des îles Orcades (Herbert, 1985). Cet écosystème stratifié, se développant annuellement sur ces sédiments, est dominé par la bactérie sulfureuse pourpre *Thiocapsa roseopersicina*. Cette bactérie forme des microcolonies distinctes solidement fixées aux grains de sable, permettant ainsi un maintien et une cohésion du sédiment. Ce tapis microbien est pauvre en cyanobactéries, et exclut totalement le développement de *Microcoleus chtonoplastes* en son sein (van Gemerden *et al.*, 1989a; van Gemerden *et al.*, 1989b).

La seconde partie de ce chapitre, exposée dans l'article "Microbial mats on the Orkney Islands revisited: microenvironment and microbial community composition", a permis une caractérisation plus complète des tapis photosynthétiques marins présents sur deux sites différents, Waulkmill et Swanbister. L'analyse de biomarqueurs caractéristiques a ainsi révélé la présence de micro-algues, diatomées, cyanobactéries et bactéries sulfato-réductrices. Les méthanogènes majoritairement présentes sur les plages de Swanbister indiquent le rôle probable de la méthanogénèse dans le cycle du carbone au sein de ces sédiments. L'analyse microscopique par CLSM (Confocal Laser Scanning Microscopy) a montré une faible diversité des cyanobactéries, filamenteuses et unicellulaires, au sein de ces tapis. Le tapis de Swanbister a révélé par l'analyse des spectres d'irradiances scalaires une hétérogénéité importante des bactéries phototrophes anoxygéniques, en terme de distribution verticale et de densité. La T-RFLP et les mesures physico-chimiques ont montré une importante diversité des bactéries pourpres et sulfato-réductrices, ainsi qu'une organisation verticale très fine liée aux conditions environnementales. Les principaux facteurs qui influencent la structure des communautés bactériennes sont l'oxygène et le sulfure ou d'autres composés sulfurés.

III.2. Le tapis microbien hypersalé de Camargue (Salins-de-Giraud)

Ce travail a été soumis au journal FEMS Microbiology Ecology sous le titre :

Characterization of functional bacterial groups in a hypersaline microbial mat community (Salins-de-Giraud, Camargue, France)

Par: Aude Fourçans[1], Tirso García de Oteyza[2], Andrea Wieland[3], Antoni Solé[4], Elia Diestra[4], Judith van Bleijswijk[5], Joan O. Grimalt[2], Michael Kühl[3], Isabel Esteve[4], Gerard Muyzer[6], Pierre Caumette[1] et Robert Duran[1]

ABSTRACT

A photosynthetic microbial mat was investigated in large pond of a Mediterranean saltern (Salins-de-Giraud, Camargue, France) of water salinity from 70 ‰ to 110 ‰ (w/v). Analysis of characteristic biomarkers (e.g., major microbial fatty acids, hydrocarbons, alcohols and alkenones) revealed the presence of cyanobacteria as major components, in addition to diatoms and other algae. Functional bacterial groups involved in the sulfur cycle could be correlated to these biomarkers, i.e. sulfate-reducing, sulfur-oxidizing and anoxygenic phototrophic bacteria. In the first 0.5 millimeters of the mat, a high rate of photosynthesis showed the activity of oxygenic phototrophs in the surface layer. Ten different cyanobacterial populations were detected with Confocal Laser Scanning Microscopy (CLSM): six filamentous species, with *Microcoleus chthonoplastes* and *Halomicronema excentricum* as dominant ones (73% of total counts); and four unicellular types affiliated to *Microcystis*, *Chroococcus*, *Gloeocapsa*, and *Synechocystis* (27% of total counts). Denaturing Gradient Gel Electrophoresis (DGGE) of PCR-amplified 16S rRNA gene fragments showed some differences with the dominance of *Microcoleus*, *Oscillatoria*, and *Leptolyngbya* strains (*Halomicronema* was not found here) and additional presence of *Phormidium*, *Pleurocaps*a and *Calotrix* types. Spectral scalar irradiance measurements did not reveal a particular zonation of cyanobacteria, purple or green bacteria in the first millimeter of the mat. Terminal-Restriction Fragment Length Polymorphism (T-RFLP) analysis of PCR-amplified 16S rRNA gene fragments of bacteria depicted a high diversity and a fine-scale depth-distribution of at least five different populations of anoxygenic phototrophs and at least three ones of sulfate-reducing bacteria along the microgradients of oxygen and light inside the microbial mat.

[1]Laboratoire d'Ecologie Moléculaire EA 3525, Université de Pau et des Pays de l'Adour, avenue de l'Université, BP 1155, F-64013 Pau Cedex, France.
[2]Department of Environmental Chemistry (ICER-CSIC), E-08034 Barcelona, Spain.
[3]Marine Biological Laboratory, University of Copenhagen, DK-3000 Helsingør, Denmark.
[4]Department of Genetics and Microbiology, Autonomous University of Barcelona, E-08193 Bellaterra, Spain
[5]Royal Netherlands Institute of Sea Research, Texel, The Netherlands.
[6]Department of Biotechnology, Delft University of Technology, NL-2628 BC Delft, The Netherlands

INTRODUCTION

Photosynthetic microbial mats develop at the water-sediment interface in shallow environments such as estuaries [1,2], sheltered sandy beaches [3,4], or hypersaline salterns [5,6]. Most of these microbial mats are formed of horizontally stratified, multicolored and cohesive thin layers, of several functional groups of microorganisms, such as cyanobacteria, colorless sulfur bacteria, purple sulfur bacteria, or sulfate-reducing bacteria, distributed along vertical microgradients of oxygen, sulfide and light [7,8].

Hypersaline mats from salterns represent interesting ecosystems adapted to fluctuating salinity conditions. Microbial mats existing in the most hypersaline ponds of the salterns of Salins-de-Giraud (Camargue, French Mediterranean coast) were described in ecological, microbiological and recently molecular studies since more than ten years [6,9-11]. These saline ponds with water salinity between 150 ‰ and 300 ‰ (w/v) contain microbial mats similar to those previously described in other hypersaline habitats [5,12]. They are formed of an upper layer of cyanobacteria belonging to the genus *Phormidium*, covering a purple layer of phototrophic bacteria mainly composed of members of the genera *Halochromatium* [13] and *Halothiocapsa* [14], well adapted to such high salinities. The molecular studies [11] showed that the bacterial composition of these mats was more diverse as expected both in Bacterial and in Archaeal groups.

In the present study, we investigated another mat from the same salterns growing in ponds of lower salinity (70 ‰ to 110 ‰ (w/v)). This mat developed over several decades in large areas used by the Saltern Company as water reservoirs for salt production. The simultaneous use of different methods in terms of bacterial composition and microenvironment, allowed a precise *in situ* analysis of the Camargue mat. In the mat, the major bacterial groups were investigated by characteristic biomarkers, Confocal Laser Scanning Microscopy (CLSM), by Denaturing Gradient Gel Electrophoresis (DGGE) and Terminal Restriction Fragment Length Polymorphism (T-RFLP) analysis of PCR amplified 16S rRNA or functional gene fragments. In order to understand the bacterial occurrence and distribution at the microscale level, all the microbiological results were related to microenvironmental gradients determined by *in situ* microsensor measurements.

MATERIALS AND METHODS

Sampling site description

The sampling site was located in a very large shallow pond at the saltern of Salins-de-Giraud, close to the sand barrier and the sea coast (Camargue, France). This pond was used for the storage of pre-concentrated seawater. In this pond of about 10 km^2 area, the water column never exceeded 20 cm depth and its salinity ranged from 70 ‰ to 110 ‰ (w/v). The photosynthetic microbial mat covered a very large area of this pond and also of other adjacent ponds, and was constituted of thin laminated cohesive layers of about 5 to 10 mm thick. Due to its development over several decades, the whole mat was about 5 to 10 cm in total thickness. The underlying sediment is mostly composed of a mixture of sand and clay.

Sampling procedure

All mat samples analyzed were collected in May 2000, by mean of plexiglas cores. For biomarkers analysis, mat cores of 26 mm i.d. were immediately frozen until further analysis. For Confocal Laser Scanning Microscopy, two cores (18 mm i.d.) were transferred into small plastic tubes containing 2.5 % (v/v) glutaraldehyde in a phosphate buffer (0.2 M adjusted to the appropriate salinity with NaCl), and stored at 4ºC awaiting further processing. For DGGE and T-RFLP methods, the upper 10 mm of the mat cores (35 mm i.d.) were sliced off aseptically, transferred to sterile Petri dishes, frozen in liquid nitrogen, and then stored at -80°C.

Microsensor measurements of O_2 and oxygenic photosynthesis profiles

Depth profiles of O_2 and gross oxygenic photosynthesis distribution were measured in May 2000. Microsensor measurements were done *in situ* from a small measuring platform placed above the mat. A Clark-type O_2 microsensor [15] connected to a picoammeter (UniSense A/S, Denmark) was manually operated with a micromanipulator (Märzhäuser, Germany) mounted on a heavy solid stand. Microsensor signals were recorded with a strip chart recorder (Servogor, U.K.) operated via batteries. The O_2 microsensor had a tip diameter of 6 µm, a stirring sensitivity of ~0 % and a response time, t_{90}, of 0.2 s. The O_2 microsensor was linearly calibrated on site from readings of microsensor current in the overlying water and in the anoxic part of the mat (0 % O_2). Dissolved O_2 concentrations in the overlying water were determined by Winkler titration [16]. Experimental light-dark shifts for *in situ* measurements of oxygenic gross photosynthesis [17] were performed with a custom-made, light-impermeable box, which was approached to the sensor avoiding physical contact and thus disturbance of microsensor readings.

Spectral scalar irradiance measurements with fiber-optic microprobes

Mat samples were collected in February 2001 for spectral scalar irradiance measurements under controlled conditions. For this, a fiber-optic scalar irradiance microprobe [18] was connected to a sensitive fiber-optic diode array spectrometer with a spectral range of 250-950 nm (PMA-11, Hamamatsu Photonics, Japan). Profiles of spectral scalar irradiance were measured in the mat by stepwise inserting the microprobe with a motor-driven micromanipulator (Märzhäuser, Germany; Oriel, USA) at a zenith angle of 140° relative to the incident light beam. The downwelling spectral scalar irradiance at the mat surface was measured by positioning the scalar irradiance microprobe over a black light trap at the same position relative to the light field as the mat surface. Scalar irradiance spectra in the mat were normalized to the downwelling spectral scalar irradiance at the mat surface. The attenuation spectrum of scalar irradiance was calculated over discrete depth intervals from the scalar irradiance profiles according to Kühl and Fenchel [19].

Analysis of fatty acids, hydrocarbons, alcohols and alkenones

The microbial mat samples were extracted after homogenization with methanol, dichloromethane and *n*-hexane. Fatty acids were separated from the extracts after saponification. Afterwards the neutral lipids were fractionated by column chromatography with silica and alumina into different compound classes. Hydrocarbons and polar fractions were analyzed by Gas Chromatography (GC) and Gas Chromatography Mass Spectrometry (GC-MS) after derivatisation. The methodology was described in detail recently by Wieland et *al.* [4].

Confocal laser scanning microscopy

The mat samples were analyzed with a microscope (Olympus BH2, Japan) and a confocal laser microscope (Leica TCS 4d, Germany) equipped with an argon-krypton laser. For confocal analysis, horizontal slices of defined dimensions were placed on cavity slides, covered and sealed with cover slips and observed under an excitation beam of 568 nm. Pigment fluorescence emission was detected with a 590 nm long pass filter. Different 512 × 512 pixel confocal images in two (optical sections) and three-dimensions (summa projections and stereoscopic images) were obtained from these samples. The cyanobacteria were identified using different morphological criteria according to Castenholz [20], i.e. diameter (µm), cell division patterns, and the presence or absence of a sheath for unicellular morphotypes. Presence of septation and gas vacuoles were also considered for

filamentous cyanobacteria. In addition, the abundance of each cyanobacterial morphotype was indicated.

DGGE analysis

Genomic DNA was extracted from the mat samples using the UltraClean Soil DNA Isolation Kit (Mobio Laboratories) according to manufacturer's protocol. Serial dilutions of genomic DNA up to 10^{-4} were made in sterile water and stored at –20 °C. To specifically amplify the 16S rRNA encoding gene fragments of oxygenic phototrophs, 1 or 2 µl of the DNA dilutions were used as template in 50 or 100 µl PCR reactions using primer pair CYA359F+GC/CYA781R and PCR conditions as described by Nübel et *al*. [21]. The two different reverse primers CYA781RA and CYA781RC were added in separate PCR reactions. DGGE was applied according to Schäfer and Muyzer [22] with conditions optimized for the oxygenic phototrophs specific PCR fragments [21]. We used 1 mm thick 6% acrylamide/bisacrylamide gels and an urea-formamide (UF) gradient of 20-80%. On top of the gradient gel, an acrylamide gel without UF was cast to obtain good slots. Gels were run in TAE buffer for 3.5 h at 200 V and at a constant temperature of 60°C. Subsequently, the gels were stained in an ethidium bromide solution and inspected under UV illumination using a Fluor-S Multi Imager (Bio-Rad). Contrast and brightness of the photographs were optimized using Adobe PhotoShop software. DNA fragments separated by DGGE were excised from the gel [23], re-amplified, purified using the Qiaquick Gel Extraction Kit (Qiagen), and then sequenced. Purified bands were sequenced in two directions according to the Sanger reaction using the Bigdye Terminator Cycle Sequencing Kit (Applied Biosystem) on an ABI PRISM 310 Genetic Analyzer. Close relatives of consensus sequences were searched in the GenBank Nucleotide Database using BLAST search. Subsequently, new sequences and their closest relatives (if not yet present in ARB) were added to ARB database and aligned using the automatic alignment tool. Phylogenetic analysis was performed in ARB using several different algorithms (e.g., maximum parsimony, neighbour-joining, maximum likelyhood). The GeneBank accession numbers of each partial 16S rRNA sequencing clones (SdG1 to SdG7) are AY393850 to AY393856, respectively.

T-RFLP analysis

The upper 2 mm of the mat cores were sliced with a cryomicrotome (MICROM GmbH, Germany) at around 200 µm, and the third mm at around 500 µm vertical depth resolution. These mat slices were grinded with liquid nitrogen in a mortar with a pestle and genomic

DNA was extracted using the UltraClean Soil DNA Isolation Kit (MoBio Laboratories Inc., USA) according to the manufacturer. All extracted genomic DNA samples were stored at -20°C until further processing. T-RFLP analysis was performed with different primer sets, 8f-926r [24,25], 8f-SRB385 [26], and pb557f-pb750r [27], according to the experimental conditions described in Wieland et *al.* [4]. Respectively, these primer sets allowed targeting the whole bacterial community, the sulfate-reducing bacteria (SRB), and the phototrophic anoxygenic bacteria (PAB). Restriction enzymes used in T-RFLP analysis were HaeIII and RsaI (New England Biolabs, UK), for analysis of the entire bacterial diversity, and HaeIII and Hin6I for the SRB and PAB. Dominant T-RFs (terminal restriction fragments) were selected by comparison of numerical values and electropherograms. From T-RF values, predicted digestions were realized on the TAP-TRFLP program of the RDP (Ribosomal Database Project) web site (http://rdp.cme.msu.edu/) [28] in order to assign the different T-RFs to a certain genus or species. All depth T-RFLP profiles were compared, from tables assembling T-RFs relatives values of each restriction enzyme by a Correspondence Factorial Analysis (CFA). The CFA were realized with MVSP v3.12d software (Rockware Inc., UK) [29].

RESULTS

Description and environmental conditions of the microbial mat

Structure of the microbial mat

The mat of several centimeters in thickness was composed of three distinct colored layers. An upper brown-green colored layer was constituted of filamentous cyanobacteria morphologically related to the genus *Microcoleus*, and of unicellular cyanobacteria similar to the form-genus *Synechocystis*. Under this dense cyanobacterial layer, a thin purple layer was visible, composed of purple non-sulfur bacteria morphologically resembling members of the family *Rhodospirillaceae* and of *Chromatiaceae*-like purple sulfur bacteria (R. Guyoneaud, personal communication). Beneath these two layers a black zone occurred with iron sulfide precipitates, indicating intense sulfate-reduction activity. The physical and chemical parameters measured in the sampling site (Table 1) were in general constant, although rapid variations of the water salinity and the redox values within two days during the sampling campaign could be observed. This was probably due to water exchanges managed by the saltern company exposing the mat to environmental changes.

Depth profiles of O_2, gross photosynthesis, and spectral scalar irradiance

High O_2 consumption in the mat led to a low O_2 concentration and O_2 penetration *in situ* during the night (5:32 h, 17°C, 94 ‰ (v/w)), confining the oxic zone to the top 0.2 mm of

the mat (Fig. 1). In the afternoon (15:50 h, 30°C, 100 ‰ (v/w)), high rates of oxygenic photosynthesis led to a strong increase of O_2 concentration both in the overlying water and within the mat. The O_2 penetration depth in the mat increased to 2 mm. Gross oxygenic photosynthesis was measurable in the top 0.6 mm of the mat. An important photosynthetic activity at 0.3-0.6 mm depth indicated the presence and/or activities of oxygenic phototrophs in the upper mat layers.

From measured spectral scalar irradiance profiles, distinct spectral regions of pronounced absorption could be ascribed to the presence of different pigments (Fig. 2, upper graph). The presence of cyanobacteria led to pronounced scalar irradiance minima at around 630 and 680 nm, corresponding to phycocyanin and chlorophyll *a* (Chl *a*) absorption. The scalar irradiance minima in the region between 800 and 900 nm correspond to bacteriochlorophyll *a* (Bchl *a*) absorption, indicating the presence of purple bacteria. A shoulder at 740-750 nm indicated some absorption by Bchl *c* present in green photosynthetic bacteria. In the spectral region of 400-550 nm, scalar irradiance was strongly attenuated due to Chl *a* and carotenoid absorption. Absorption by Chl *a*, phycocyanin, Bchl *a*, and Bchl *c* occurred in all mat layers within the top 0.8 mm of the mat, indicating a homogeneous distribution of these photosynthetic groups. However, the spectral scalar irradiance in the wavelength regions of Chl *a*, phycocyanin and carotenoid absorption were stronger attenuated than wavelengths corresponding to Bchl *a* and Bchl *c* absorption (Fig. 2, lower graph), indicating as expected a dominance of cyanobacteria in the surface layer of the mat.

Bacterial diversity in the top active layers of the microbial mat

Bacterial diversity estimated by biomarkers

Fatty acids were the major lipid compounds found in the microbial mat. Their distribution essentially encompassed C_{14}-C_{22} homologues, namely *n*-hexadec-9(Z)-enoic, *n*-hexadecanoic, *n*-octadec-9(Z)-enoic, *n*-octadec-11(Z)-enoic, *iso*-pentadecanoic and *anteiso*-pentadecanoic acids (Fig. 3a), typically representative of algal and bacterial communities.

C_{37}-C_{38} di-, tri- and tetra-unsaturated alkenones were also found in this mat (Fig. 3b). These compounds are specific of *Hapthophyceae* [30,31]. However, their occurrence cannot be attributed to species typically found in pelagic environments and are probably related to unknown species.

The sterol distribution of this mat showed minor proportions of sterols having the unsaturated positions at Δ^5, Δ^{22} and $\Delta^{5,22}$ (Fig. 3b), which could originate from cyanobacteria [32-34], Chlorophyta [35,36], or diatoms [36-38]. The common diatom marker

24-methylcholesta-5,24(28)-dien-3β-ol [36-38] was found in minor proportion, suggesting the presence of diatoms probably in the surface layer of the mat.

However, the major feature of the sterol distribution from this mat was the high relative abundance of 5α(H)-stanols. These compounds may originate from direct biogenic inputs [30,33], including cyanobacteria [39], or from *in situ* hydrogenation processes [33,40]. The dominance of Δ^5-stenols and 5α(H)-stanols is indicative of the prevalence of hydrogenation processes. Cholestan-5β(H)-ol was also present in significant proportion. The transformation of Δ^5-stenols into 5α(H)- and 5β(H)-stanol mixtures generally occurs via Δ^4-sten-3-ones [41,42] or, in highly reducing environments, by direct conversion [43]. The concentrations of stanones and stenones were below their detection limit, which points to a direct conversion between both compounds as the most likely mechanism.

n-Heptadecane and *n*-heptadecenes were the main hydrocarbons (Fig. 3c). These compounds are generally found in cyanobacteria [34,44] or in phototrophic eukaryota [45]. Other hydrocarbons specific of cyanobacterial inputs, such as 9-methylhexadecane, were also found in major proportion, indicating the dominance of cyanobacteria in this mat.

Phyt-1-ene, which occurred together with other phytene homologues, also constituted one of the major hydrocarbon groups. These hydrocarbons are characteristic for methanogenic bacteria [46] and may also be produced in the decomposition of phytol [47].

In addition to these hydrocarbons, a distribution of C_{23}-C_{35} *n*-alkanes predominated by the odd carbon numbered homologues, namely C_{29}, C_{31} and C_{33}, was found. This distribution is representative for inputs from higher plants [48] and is currently found in microbial sediments from coastal environments [49], probably reflecting the influence of wind transported materials from nearby higher plants.

Diversity of oxygenic phototrophs

Confocal Laser Scanning Microscopy (CLSM) and molecular techniques were used to identify the cyanobacteria of the Camargue microbial mat. Using CSLM, both filamentous and unicellular cyanobacteria were found in the mat (Table 2; Fig. 4). Filamentous types were the most abundant, accounting for 73 % of the total cyanobacteria present (Table 2a). *Microcoleus chthonoplastes* (Fig. 4b) was dominating the filamentous cyanobacterial community, as typically found in hypersaline mats [1,50,51]. *Halomicronema excentricum* characterized by thin filaments and cylindrical shape (less than 1 μm wide trichomes) (Fig. 4c), was the second most frequent filamentous cyanobacterium, also typical of microbial mats from man-made Solar ponds [52]. Another abundant (18 %) filamentous cyanobacterium (Fig.

4e) with thin filaments and short trichomes could not be identified. *Leptolyngbya* sp., *Limnothrix* sp. and *Pseudanabaena* sp. filaments were also present like in other mats as well, e.g. from the Ebro delta [1,50,51] and the Orkney Islands [4]. Unicellular cyanobacteria *Chroococcus* sp., *Microcystis* sp. and members of *Synechocystis* and *Gloeocaspsa* groups represented 27 % of the total cyanobacteria in the Camargue mat (Table 2b).

In addition to CLSM analysis, a molecular approach was used to describe the oxygenic phototroph diversity. 16S *rDNA* PCR products, specific for cyanobacteria, were separated by DGGE. Fifteen different bands were counted, of which the strongest fluorescent were excised from the gel (bands 1 to 7 in Fig. 5a) and retrieved for DNA sequencing. Phylogenetic analysis of these sequences (SdG1 to SdG7 in Fig. 5b) showed, that the pristine hypersaline Camargue mat was dominated by the filamentous cyanobacteria genera *Microcoleus* (SdG5 and 6 in Fig. 5b), *Oscillatoria* (SdG3 in Fig. 5b) and *Leptolyngbya* (SdG7 in Fig. 5b). Other cyanobacteria composing this mat were related to the unicellular *Pleurocapsa* sp. (SdG1 in Fig. 5b), *Calotrix sp*. (SdG4 in Fig. 5b), and *Phormidium* sp. (SdG2 in Fig. 5b). In addition, a *16S rDNA* sequence affiliated to the prymnesiophyte alga *Isochrysis* was also obtained with the same cyanobacterial primers.

Diversity and community structure at a microscale level

The organization and composition of the bacterial community in the mat was investigated by T-RFLP using an eubacterial primer set (8f-926r) [24,25], targeting a partial sequence of the *16S rDNA* gene. T-RFLP profiles so obtained, with around 35 T-RFs with the HaeIII digestion (data not shown), corresponding to diverse phylogenetics groups or OTUs (Operational Taxonomic Unit) were characteristic of each microlayer within the top three millimeters of the mat, and of the underlying layer. A correspondance factorial analysis (CFA) of each T-RFLP profiles for the restriction enzymes HaeIII and RsaI revealed a particular distribution in three zones: a surface layer (0-0.2 mm), a large mid layer (0.2-3 mm), and a deeper region (underlying layer) (Fig. 6a). This distribution was mostly influenced by the first axis, which explains 27.8% of the variance particularly in the deep third millimeter. Among the most influencing variables, (T-RFs or OTUs) of this deeper zone, T-RFs 58 bp with RsaI enzyme could be related *to Desulfomicrobium baculatum*; and also T-RFs 205 and 244 pb with HaeIII could be correlated to *Desulfobulbus* and *Streptomyces* genera (Fig. 6b). In contrast, the second axis influenced particularly the structure of the surface mat (0-0.2 mm) with 11.8% of the variance by the T-RFs of 125 bp (Rsa digest), and of 200 bp and 297 bp (HaeIII digest), related to the genera *Neisseria, Chloroflexus* and

Mycoplasma. All these OTUs seemed to play an important role in the observed vertical organization of this mat.

In addition, the distribution of the bacterial communities involved in the sulfur cycle of the mat was also investigated. In order to understand more precisely their putative role in the structure of this mat, a T-RFLP approach was applied by targeting diverse functional groups.

Sulfate-reducing bacteria (SRB) were accessed by their *16S rDNA* encoding gene with the primer pair 8f-385r [26], and combination of the results with the two restriction enzymes HaeIII and Hin6I. In the same way, the CFA of this data set showed a specific distribution of the SRB. Particularly two distinct SRB communities were characteristic of the third deeper millimeter layer and of the layer at 1.6 millimeter (Fig. 7a). This later layer seemed to be really independent, since the first axis with a high percentage of 40.7% explained alone the distinct structure of the mid layer, characterized by many T-RFs, including mainly 200 and 270 bp (HaeIII). These T-RFs could be related to genera *Desulfovibrio* and *Desulfobacter,* respectively (Fig. 7b). The second axis explained essentially with 14.8% the composition of the third millimeter, mainly with T-RFs of 72 and 197 bp (HaeIII) and of 55 bp (Hin6I). The first T-RF cited may possibly assimilate to some *Desulfovibrio* species.

Therefore, the SRB community was organized in a depth-dependent distribution in the mat and was composed of at least three distinctive populations. The observed stratification is probably influenced by the high oxygen penetration depth down to 2 millimeters, and by the high oxygen concentration detected during the day more than 900 µM in the surface layer of the mat (Fig. 1). The upper population developed in the uppermost 1.6 mm of the mat, could therefore represent SRB highly tolerant to oxygen (Fig. 1). Beneath this depth, the oxygen concentration strongly decreased, due to the absence of photosynthetic activity and high oxygen consumption in this layer. Therefore, another populations of SRB could be detected in this layer, probably adapted to such low oxygen conditions. Below in the totally anoxic mat, a third SRB population probably more sensitive to the oxygen was present.

In addition to SRB communities, the phototrophic anoxygenic bacteria (PAB) were also investigated in the same layers. Their presence in the mat was detected with the primer pair pb557f-pb750r [27], targeting on the *pufM* gene, which encodes a subunit of the photosynthetic center of purple sulfur and non-sulfur bacteria.

CFA on T-RFLP patterns of these PAB communities revealed the presence of five distinct clusters in the mat organized in five layers through the top three millimeters (Fig. 8a). The layers from 0.2 to 0.4 mm and from 0.4 to 1.8 mm were explained by the first axis,

showing a high percentage (38.4%) of the variance and corresponding to some T-RFs (199 pb, HaeIII) related to *Halochromatium salexigens* (Fig. 8b). The three other layers, from 0 to 0.2 mm, from 1.8 to 2 mm, and from 2.5 to 3 mm, were mostly influenced by the second axis (12%). This included T-RFs (Hin6I) of 137 bp, corresponding to *Roseospira marina,* and also 146 bp.

Measurements of the spectral scalar irradiance revealed the presence of purple bacteria in surface layer of the mat, especially in the zone at 0.5-0.8 mm depth (Fig. 2). This confirms the observation with T-RFLP, showing the presence of distinct populations at 0.4 to 1.8 mm. In contrary, only few PAB were observed in the upper layer (0-0.4 mm) by these methods, explaining maybe their particular position revealed through the CFA scatter plot (Fig. 8a). So, the PAB developing at greater depths in the mat could be adapted to lower light intensities, as compared to the PAB community of the surface layer, since light is strongly attenuated in the mat (Fig. 2). Moreover, oxygen could also play a role in the stratification of the PAB, discriminating populations of different tolerance to the presence of oxygen, especially in the surface layer of the mat with high oxygen concentrations (Fig. 1).

DISCUSSION

The investigated photosynthetic microbial mat showed a nice spatial distribution of different functional groups at the microscale level. As revealed by spectral scalar irradiance (Fig. 2), by CLSM (Table 2), and by DGGE (Fig. 5), the cyanobacteria were the dominant rather diverse photosynthetic microorganisms very active in the first millimeter of the mat. Analyses of biomarkers (Fig. 3) corroborated these observations of a dominance of oxygenic phototrophs, since major fatty acids (*N*-octadec-9(Z)-enoic acid) , alcohols (5α(H)-stanols), and hydrocarbons (*n*-Heptadecane, *n*-heptadecenes, and 9-methylhexadecane) found in this mat corresponded to cyanobacteria [53].

Identification of oxygenic phototrophs down to the genus or even species level was done by Confocal Laser Scanning Microscopy (CLSM) and sequencing analysis (PCR-DGGE-sequencing). Two dominant filamentous cyanobacteria *Microcoleus* sp. and *Leptolyngbya* sp. were identified by both techniques. Other oxygenic phototrophs were either identified by CLSM (*Halomicronema*, *Limnothrix*, *Pseudanabaena*, *Synechocystis* – group, *Gloeocapsa* – group, *Chroococcus, and Microcystis*) or by sequencing analysis (*Phormidium*, *Calotrix*, *Pleurocapsa*, *Oscillatoria*, and presumably a Prymnesiophyte alga).

As described previously [54-56], bacterial biodiversity depends on gradient salinity, with a decreasing bacterial diversity when salinity increases. However, in this investigated

halophilic microbial mat, the diversity of oxygenic phototrophs is quite important with the dominance of *Microcoleus chthonoplastes,* a typical inhabitant of halophilic microbial mats [57-59]. At higher salinity, other cyanobacterial morphotypes could be like *Phormidium* dominant [6].

Within the mat, analysis of biomarkers revealed the presence of purple bacteria like *Rhodobacter* and *Ectothiorhodospira* , and also of sulfate-reducing bacteria. *Iso*- and *anteiso*-pentadecanoic acids are abundant in sulfate-reducing bacteria and sulfur-oxidizing bacteria such as *Thiomicrospira* [60]. Cyclopropylnonadecanoic acid was also a major compound in the distribution of fatty acids. This compound is abundant in purple phototrophic bacteria such as *Rhodobacter* and *Ectothiorhodospira* where it occurs together with significant amounts of *n*-octadec-11(Z)-enoic acid [60]. The ratio between these two acids (0.5) could be related to the growth status of the microbial mat, with a high relative proportion of the cyclopropyl acid being indicative of stationary growth [61]. The high abundance of *iso*- and *anteiso*-pentadecanoic acids, as well as of cyclopropylnonadecanoic and *n*-octadec-11(Z)-enoic acids likely reflects the dominance of two different populations exchanging hydrogen sulfide, which could be sulfate-reducing and purple phototrophic bacteria, respectively.

By the use of specific primer sets, the T-RFLP allowed to distinguish photosynthetic anoxygenic bacteria and sulfate-reducing bacteria organized in five and three distinct populations among the first three millimeters of this mat, respectively (Fig. 7-8).

We could demonstrate the presence of *Desulfobacter*-like and *Desulfovibrio*-like SRB, in the mid layer of the mat, corresponding to the fluctuating oxic and anoxic zone during the diel cycle (Fig. 1). Many *Desulfovibrio* species were isolated from the oxic zone of microbial mats, and were found to be able to tolerate and even to use lower extent oxygen [62,63]. The 1.6 mm top layer, completely oxic during the day, was inhabited by an oxygen tolerant SRB community, which could not be correlated by T-RFLP to any known SRB. Previous molecular studies have described the presence of *Desulfonema*-like species in the oxic surface layer of several microbial mats. They were found to be metabolically versatile with a high affinity to oxygen [64,65]. In the deeper 3 mm layer, our study showed that one SRB population was specific of the anoxic layer, indicating probably a high sensitivity to oxygen. Thus, T-RFLP analysis illustrated a specific vertical stratification of the SRB populations within the top 3 mm layers of the mat, that could be explained by their behavioral responses to oxygen including aggregation, migration to anoxic zones, and aerotaxis [62].

The microscale zonation of these populations is partly controlled by the microgradient of oxygen, sulfide and light. In the investigated mat, no free sulfide was measurable with microsensors (Fig. 2), but iron sulfide precipitates, and measurements of sulfate reduction rates (SRR) (Rod Herbert, unpublished results) indicated high bacterial sulfate reduction activity and subsequent precipitation of the produced sulfide by iron. Investigation of the biogeochemistry of the mat in year 2001 confirmed that this Camargue mat is characterized by high sulfate reduction rates and a high iron and FeS content [66]. Additionally, in this mat *Chloroflexus*-like bacteria, detected by T-RFLP, were found as important members in the surface layer community (Fig. 6). Their presence was also indicated by the BChl *c* absorption detected in the top layer of the mat (Fig. 2). These microorganisms could play an important role in hypersaline and iron-rich microbial mats [67].

These results demonstrated a clear stratification of the main photosynthetic and sulfur bacterial populations in distinct and specific vertical microlayers according to their physiological characteristics. In man-made artificial salterns, where such a type of mat develops, environmental conditions can change dramatically on a short-term [66]. Since several years, the structure of the bacterial communities in the microbial mats was often described globally at the macroscale level. In contrast, this study on the hypersaline Camargue microbial mat represents the first exhaustive investigation, which clearly shows the structure and the distribution of the main bacterial communities at the microscale level according to the microgradients of oxygen, sulfide and light.

ACKNOWLEDGEMENTS

We acknowledge the financial support by the EC (MATBIOPOL project, grant EVK3-CT-1999-00010). The authors are grateful to the company of Salins-du-midi at Salins-de-Giraud for facilitating access to the salterns, sampling and field experiments. AF is partly supported by a doctoral grant from the general council of Atlantic Pyrenees. MK was supported by the Danish Natural Science Council (contract no. 9700549). Anni Glud is gratefully acknowledged for microsensor construction and assistance during the field experiment.

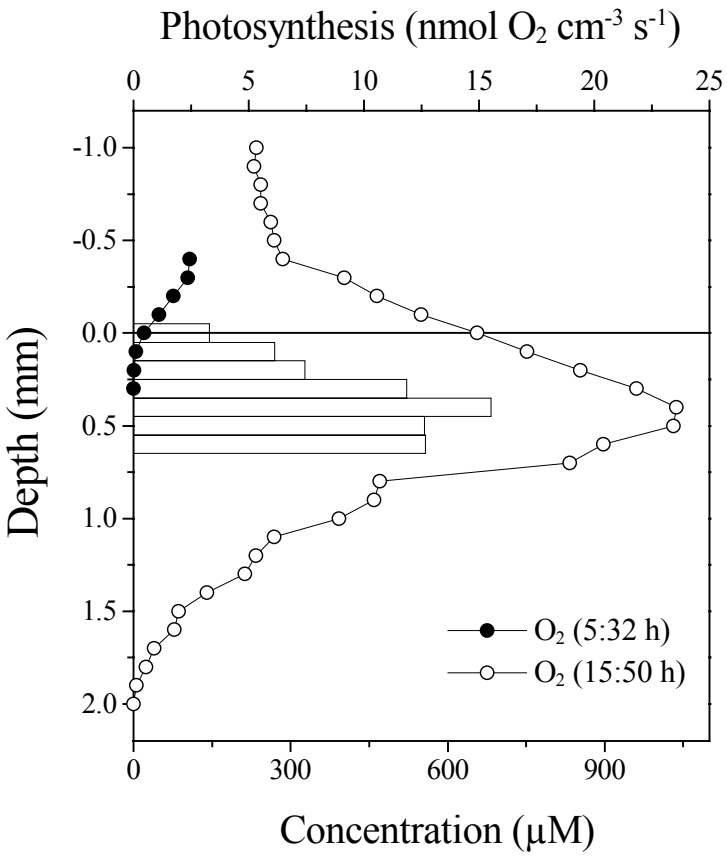

Figure 1. *In situ* depth profiles of O_2 and gross photosynthesis (bars) measured during the afternoon (15:50 h) and night (5:32 h) in mats from a pre-concentration pond of the Salins-de-Giraud saltern.

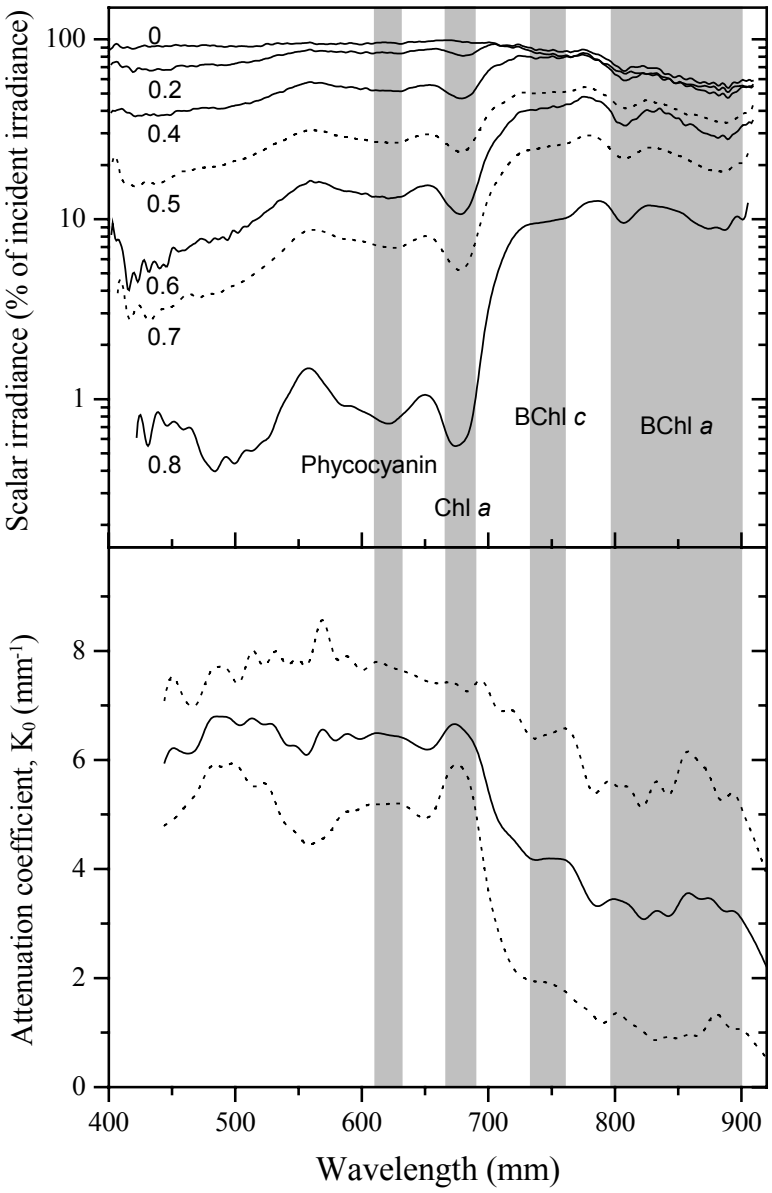

Figure 2. Depth profiles of spectral scalar irradiance in the Camargue mat normalized to the downwelling spectral scalar irradiance at the mat surface (upper graph). Numbers indicate depth (mm). Average attenuation spectrum of scalar irradiance over the depth interval of 0-0.8 mm (lower graph), calculated from the profile shown in the upper graph. Broken lines indicate the standard deviations of the attenuation coefficients, K_0.

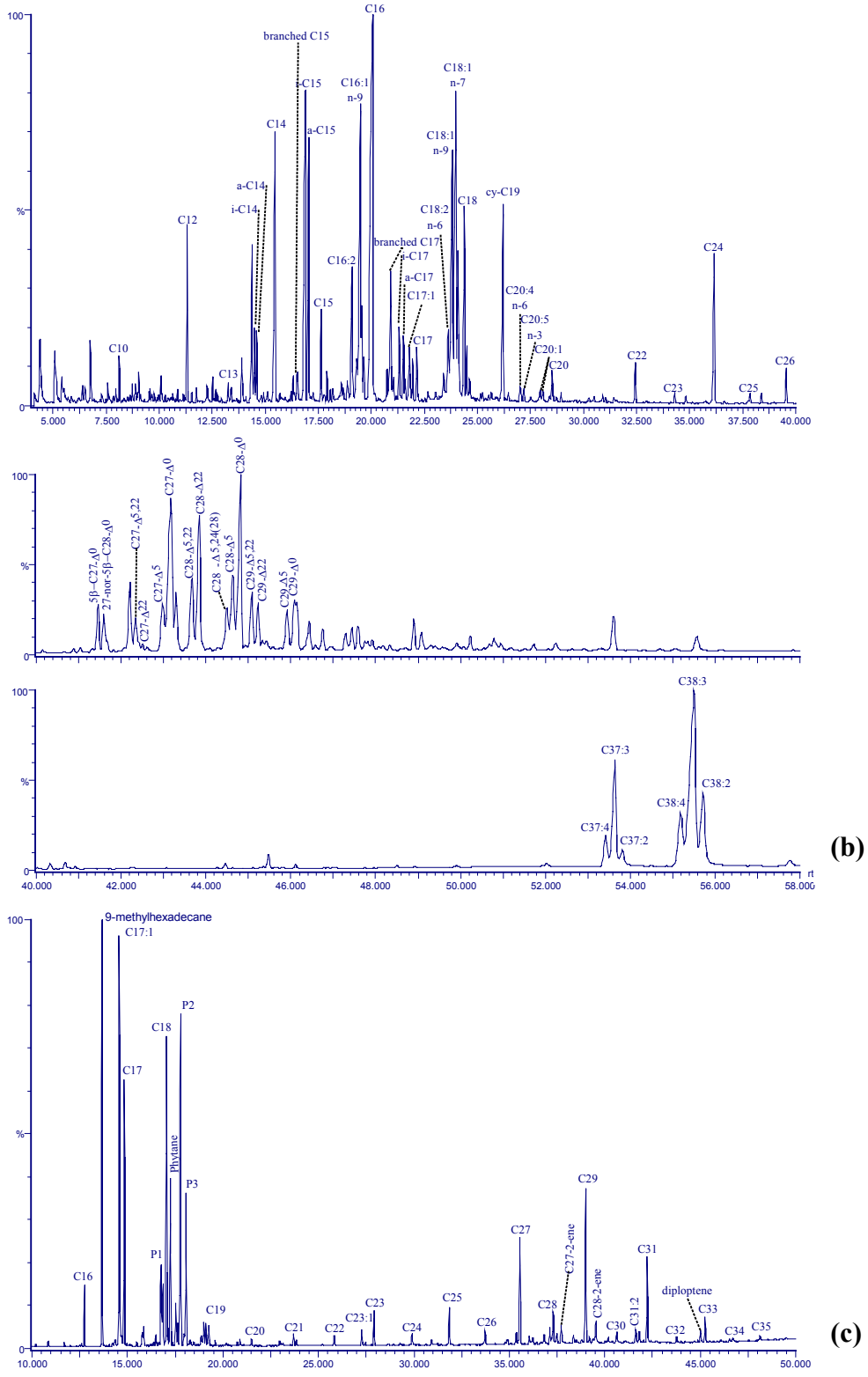

Figure 3. Gas chromatographic profiles showing the major (a) fatty acids, (b) alcohol and alkenone fractions, (c) hydrocarbons (P1, P2, P3 phytenes) from Salins-de-Giraud microbial mat.

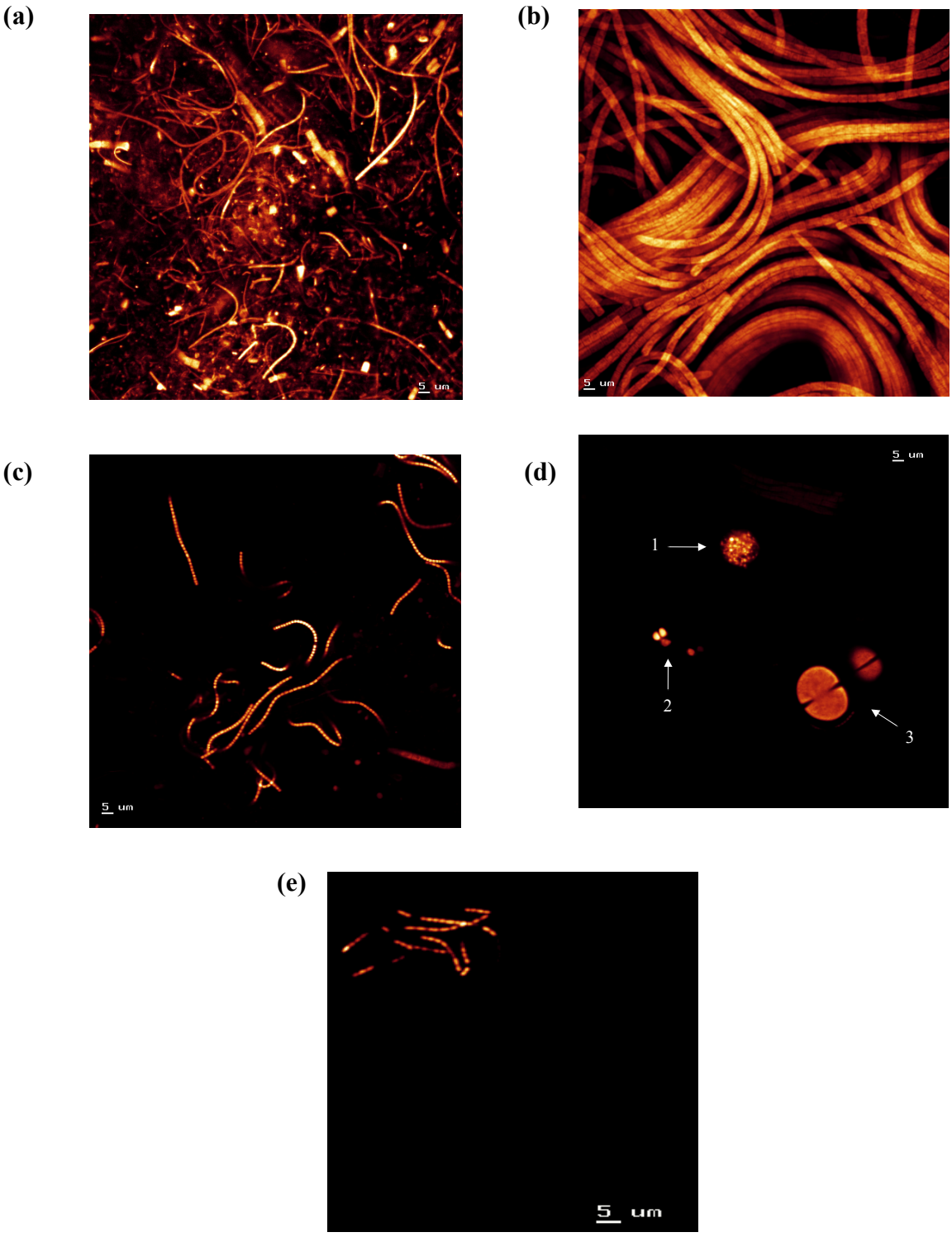

Figure 4. CLSM images in Salins-de-Giraud microbial mat. (a) *Leptolyngbya* sp. (b) *Microcoleus chthonoplastes* (c) *Halomicronema excentricum* (d) 1. *Microcystis* sp., 2. *Synechocystis*-group., 3. *Chroococcus* sp. (e) Unidentified filaments. (c), (d) and (e) images are photographic compositions.

Figure 5. (a) DGGE analysis of 16S rRNA gene fragments of oxygenic phototrophs. The PCR products were obtained with 2 different primer sets and genomic DNA from the microbial mat of Salins-de-Giraud (SdG). Lane 1 and 6, marker fragments; lane 2 and 3, PCR products obtained with primers CYA359F and GC/CYA781Rb; lane 4 and 5 PCR products obtained with primers CYA359F + GC/CYA781Ra. The numbers in figures refer to bands that were excised from the gel, sequenced and used for phylogenetic analysis. (b) Phylogenetic tree based on 16S rRNA sequence data showing the affiliation of predominant oxygenic phototrophs (i.e., cyanobacteria and diatoms) in the microbial mat of Salins-de-Giraud. Sequences determined in this study are shown in bold. The sequences of *Thermus aquaticus* and *Chloroflexus aurantiacus* were used as an outgroup, but were pruned from the tree. The scale bar represents 10% estimated sequence divergence.

(a)

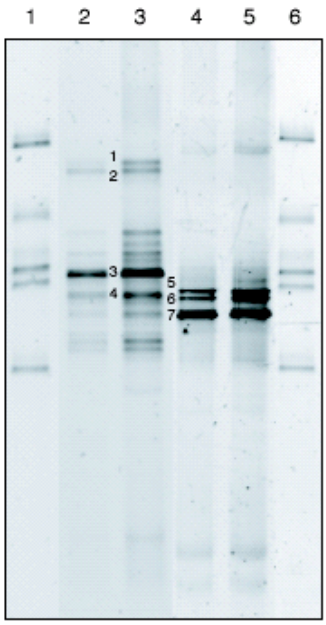

(b)

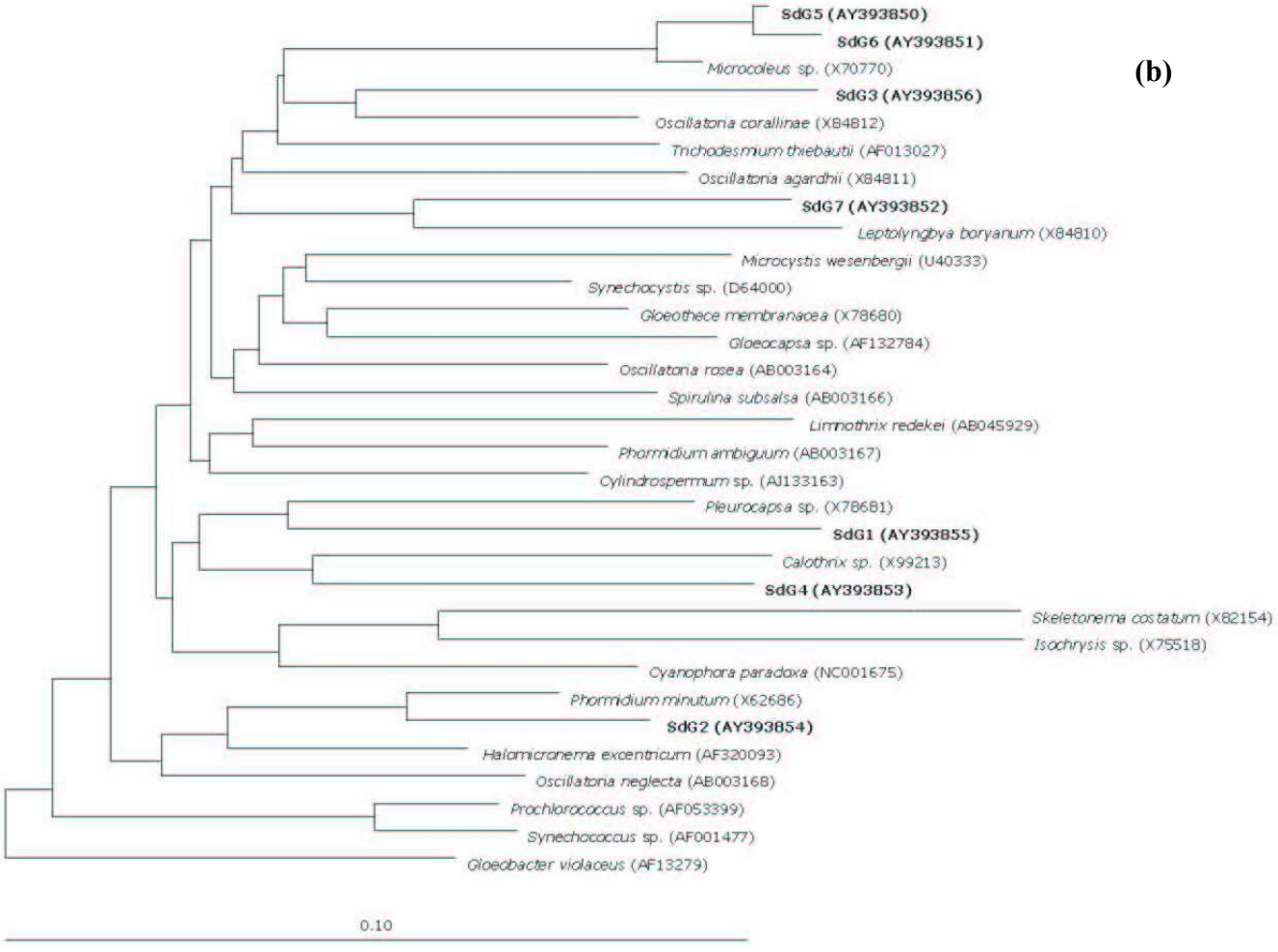

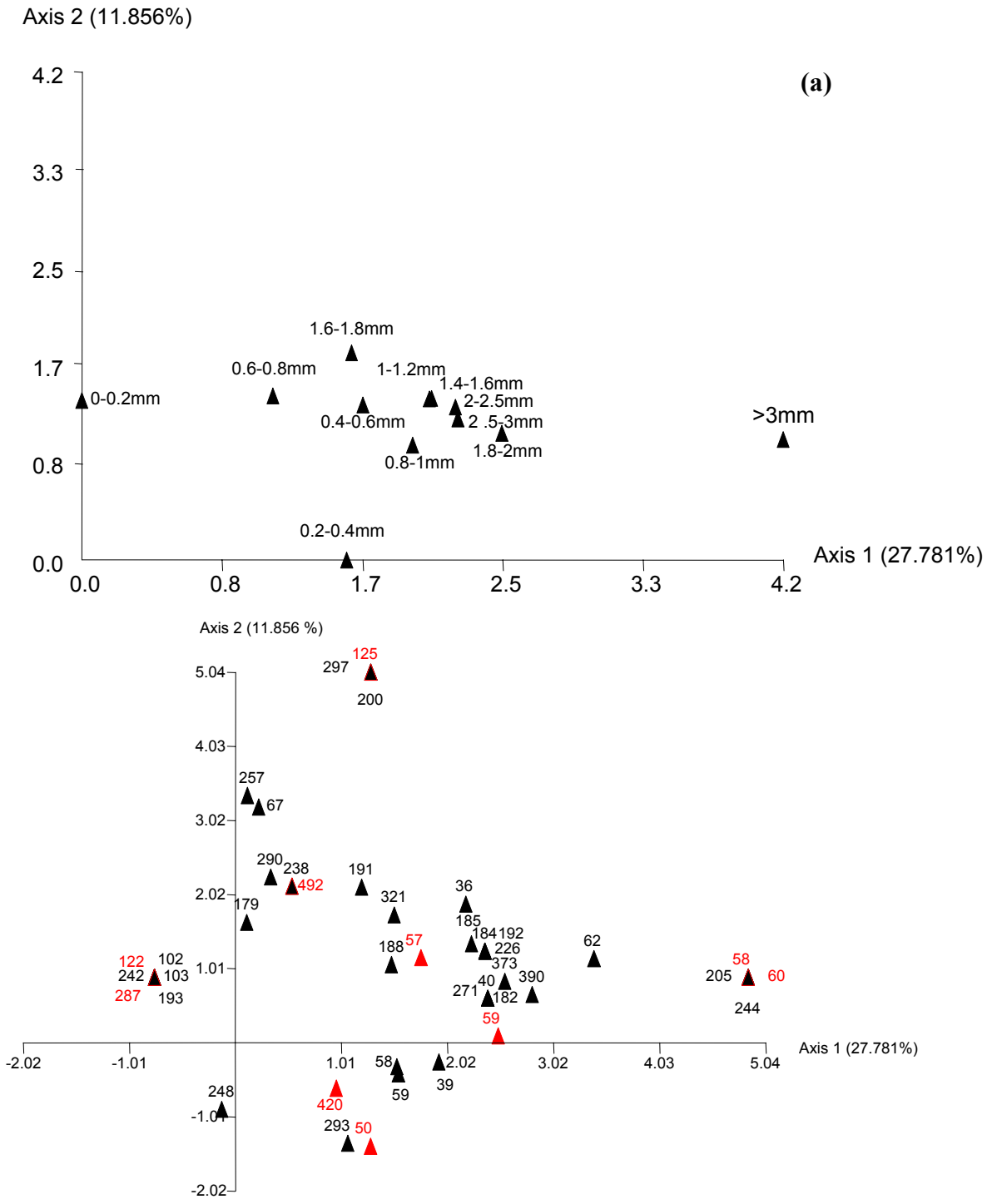

Figure 6. Correspondence Factorial Analysis (CFA) of the whole bacterial communities. (a) CFA of each layer of the three millimeters of Salins-de-Giraud microbial mat. Each black triangle was represented by a 5' end T-RFLP pattern corresponding to the combining digests HaeIII and RsaI of the *16s rDNA* encoding gene. **(b)** CFA of variables, i.e., T-RFs derived from the CFA in panel (a). Each number corresponds to the T-RF length in base pairs. Red and black triangles correspond to HaeIII and RsaI T-RFs, respectively. Red/black triangles correspond to common T-RFs between two enzymes.

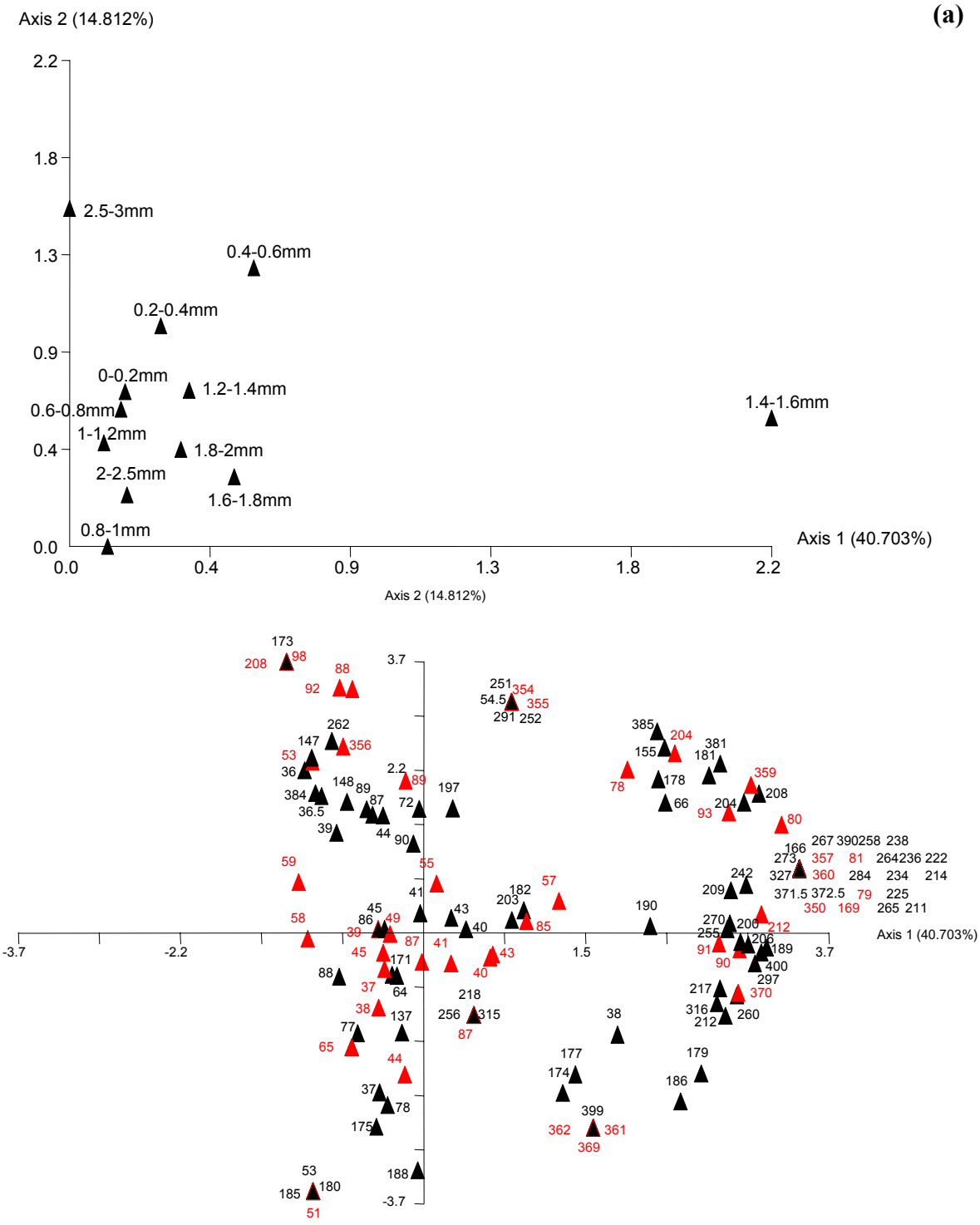

Figure 7. Correspondence Factorial Analysis (CFA) of the sulfate-reducing communities. CFA of each layer of the three millimeters of Salins-de-Giraud microbial mat. Each black triangle was represented by a 5' end T-RFLP pattern corresponding to the combining digests HaeIII and Hin6I of the *16s rDNA* encoding gene. (b) CFA of variables, i.e., T-RFs derived from the CFA in panel (a). Each number corresponds to the T-RF length in base pairs. Red and black triangles correspond to HaeIII and Hin6I T-RFs, respectively. Red/black triangles correspond to common T-RFs between two enzymes.

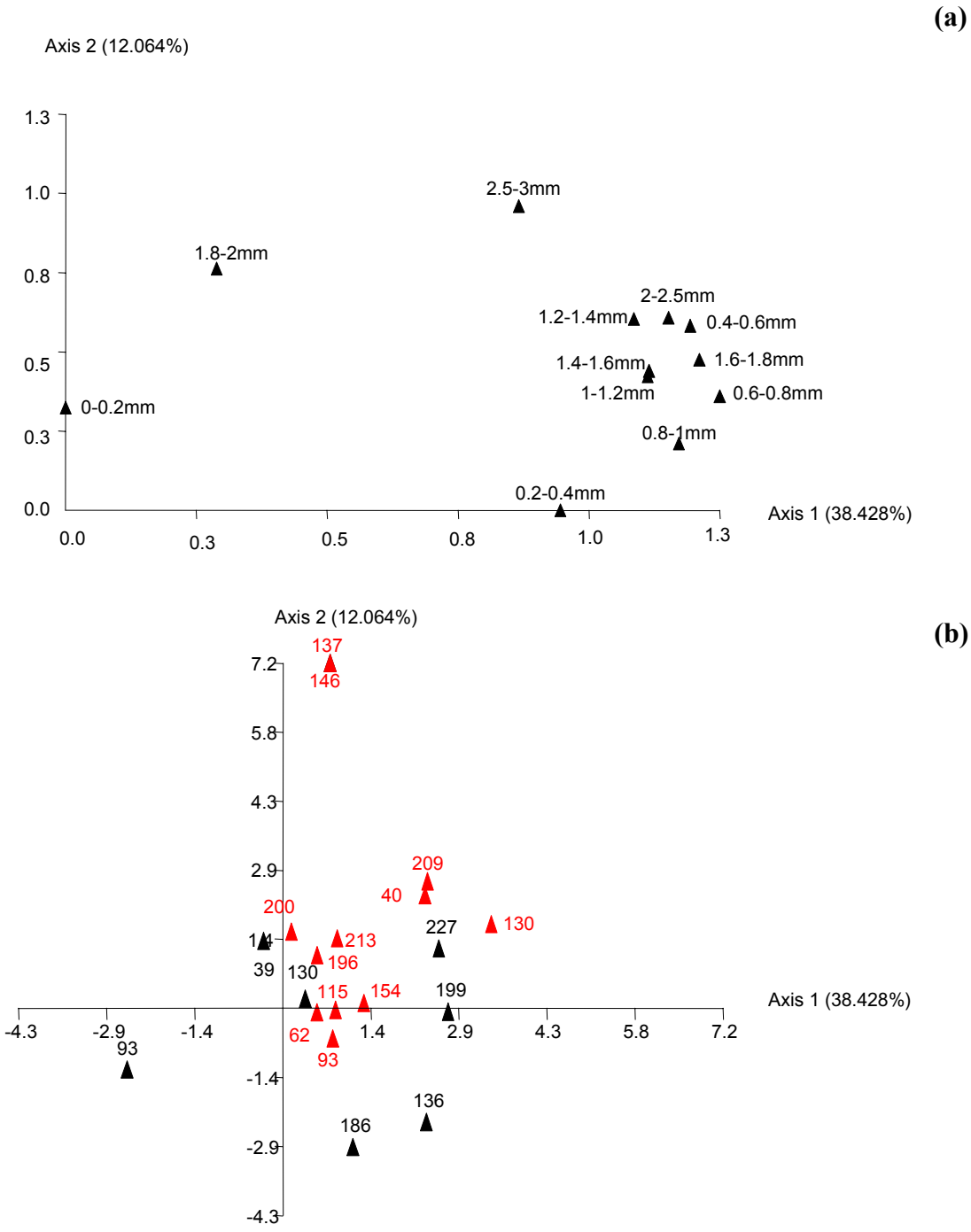

Figure 8. Correspondence Factorial Analysis (CFA) of the phototrophic anoxygenic communities. (a) CFA of each layer of the three millimeters of Salins-de-Giraud microbial mat. Each black triangle was represented by a 5' end T-RFLP pattern corresponding to the combining digests HaeIII and Hin6I of the *PufM* encoding gene. (b) CFA of variables, i.e., T-RFs derived from the CFA in panel (a). Each number corresponds to the T-RF length in base pairs. Red and black triangles correspond to HaeIII and Hin6I T-RFs, respectively. Red/black triangles correspond to common T-RFs between two enzymes.

Table 1: Comparison of physicals and chemicals parameters in the water column of the pre-concentrated ponds of Camargue saltern.

Dates	**T (°C)**	**O_2 (mg/L)**	**Rh* (mV)**	**pH**	**S (g/L)**
14.03.00	21.8	19	-34* 112**	8.11	105
23.05.00	20	17	+3* -4**	8.39	103
25.05.00	23	-	+90* -	8.5	75

***surface, **10mm depth**

Table 2: Morphological identification of cyanobacteria in microbial mats of Salins-de-Giraud by CLSM according to Castenholz 2001 [21], and relative abundance fore each one. **(a)** Filamentous cyanobacteria. **(b)** Unicellular cyanobacteria.

(a)

	Genera	**Diameter (μm)**	**Septation**	**Gas vacuoles**	**Sheath**	**Relative abundance (%)**
FILAMENTOUS CYANOBACTERIA	*Microcoleus chthonoplastes*	3.13 – 3.75	+	-	+	27
	Halomicronema excentricum	0.96	+	-	+	18
	Unidentified	< 1.25 (short filaments)	+	-	+	18
	Leptolyngbya sp.	< 1 (large filaments)	+	-	+	14
	Limnothrix sp.	1.25	+	-	+	14
	Pseudanabaena sp.	2.5	+	+	+	9

(b)

	Genera	**Diameter (μm)**	**Cell division**	**Sheath**	**Relative abundance (%)**
UNICELLULAR CYANOBACTERIA	*Synechocystis* - group (marine cluster)	3.5 x 3.5	2 or 3 planes	+ (thin)	25
	Gloeocapsa - group	4 x 14	2 or 3 planes	+	25
	Chroococcus sp.	19 x 28	2 planes	+	25
	Microcystis sp.	1.9 x 1.9	Binary fissions in different planes	+	25

REFERENCES

[1] Esteve, I., Martínez, M., Mir, J. and Guerrero, R. (1992) Typology and structure of microbial mats communities in Spain: A preliminary study. Limnetica 8, 185-195.

[2] Mir, J., Martínez-Alonso, M., Esteve, I. and Guerrero, R. (1991) Vertical stratification and microbial assemblage of a microbial mat in the Ebro Delta (Spain). FEMS Microbiol. Ecol. 86, 59-68.

[3] Van Gemerden, H., Tughan, C.S., De Witt, R. and Herbert, R.A. (1989) Laminated microbial ecosystems on sheltered beaches in Scapa Flow, Orkney Islands. FEMS Microbiol. Ecol. 62, 87-102.

[4] Wieland, A., Kuhl, M., McGowan, L., Fourçans, A., Duran, R., Caumette, P., Garcia De Oteyza, T., Grimalt, J.O., Solé, A., Diestra, E., Esteve, I. and Herbert, R.A. (2003) Microbial mats on the Orkney islands revisited: microenvironment and microbial community composition. Microb. Ecol. sous presse.

[5] Giani, D., Seeler, J., Giani, L. and Krumbein, W.E. (1989) Microbial mats and physicochemistry in a saltern in the Bretagne (France) and in a laboratory scale saltern model. FEMS Microbiol. Ecol. 62, 151-162.

[6] Caumette, P., Matheron, R., Raymond, N. and Relexans, J.C. (1994) Microbial mats in the hypersaline ponds of Mediterranean salterns (Salins-de-Giraud, France). FEMS Microbiol. Ecol. 13, 273-286.

[7] Van Gemerden, H. (1993) Microbial mats : A joint venture. Mar. Geol. 113, 3-25.

[8] Revsbech, N.P., Jorgensen, B.B., Blackburn, T.H. and Cohen, Y. (1983) Microelectrode studies of the photosynthesis and O2, H2S and pH profiles of a microbial mat. Limnol. Oceanogr. 28, 1062-1074.

[9] Mouné, S., Caumette, P., Matheron, R. and Willison, J.C. (2003) Molecular sequence analysis of prokaryotic diversity in the anoxic sediments underlying cyanobacterial mats of two hypersaline ponds in Mediterranean salterns. FEMS Microbiol. Ecol. 44, 117-130.

[10] Mouné, S., Eatock, C., Matheron, R., Willison, J.C., Hirschler, A., Herbert, R. and Caumette, P. (2000) *Orenia salinaria* sp. nov., a fermentative bacterium isolated from anaerobic sediments of Mediterranean salterns. Int. J. Syst. Evol. Microbiol. 50 Pt 2, 721-729.

[11] Mouné, S., Manac'h, N., Hirschler, A., Caumette, P., Willison, J.C. and Matheron, R. (1999) *Haloanaerobacter salinarius* sp. nov., a novel halophilic fermentative bacterium that reduces glycine-betaine to trimethylamine with hydrogen or serine as

electron donors; emendation of the genus *Haloanaerobacter*. Int. J. Syst. Bacteriol. 49 Pt 1, 103-112.

[12] Jørgensen, B.B. and Des Marais, D.J. (1988) Optical properties of benthic photosynthetic communities: Fiber-optic studies of cyanobacterial mats. Limnol. Oceanogr. 33, 99-113.

[13] Caumette, P., Baulaigue, R. and Matheron, R. (1988) Characterization of *Chromatium salexigens* sp. nov., a halophilic *Chromatiaceae* isolated from Mediterranean salinas. System. Appl. Microbiol. 10, 284-292.

[14] Caumette, P., Baulaigue, R. and Matheron, R. (1991) *Thiocapsa halophila* sp. nov., a new halophilic phototrophic purple sulfur bacterium. Arch. Microbiol. 155, 170-176.

[15] Revsbech, N.P. (1989) An oxygen microelectrode with a guard cathode. Limnol. Oceanogr. 34, 474-478.

[16] Grasshoff, K., Ehrhardt, M. and Kremling, K. (1983) Methods of seawater analysis, Verlag Chemie, Weinheim.

[17] Revsbech, N.P. and Jørgensen, B.B. (1983) Photosynthesis of benthic microflora measured with high spatial resolution by the oxygen microprofile method: Capabilities and limitations of the method. Limnol. Oceanogr. 28, 749-756.

[18] Lassen, C., Ploug, H. and Jørgensen, B.B. (1992) A fibre-optic scalar irradiance microsensor: application for spectral light measurements in sediments. FEMS Microbiol. Ecol. 86, 247-254.

[19] Kuhl, M. and Fenchel, T. (2000) Bio-optical Characteristics and the Vertical Distribution of Photosynthetic Pigments and Photosynthesis in an Artificial Cyanobacterial Mat. Microb. Ecol. 40, 94-103.

[20] Castenholz, R.W. (2001) Phylum Bx. Cyanobacteria. Oxygenic Photosynthetic Bacteria. In: Bergey's Manual of Systematic Bacteriology. The Archeae and the Deeply Branching and Phototrophic Bacteria (2nd ed.). (Boone DR, C.R., Garrity GM, ed.), pp. 473-599, Springer Verlag, New York.

[21] Nübel, U., Garcia-Pichel, F. and Muyzer, G. (1997) PCR primers to amplify 16S rRNA genes from cyanobacteria. Appl. Environ. Microbiol. 63, 3327-3332.

[22] Schäfer, H. and Muyzer, G. (2001) Denaturing gradient gel electrophoresis in marine microbial ecology. In: Methods in Microbiology (Paul, J.H., ed.), pp. 425-468, Academic Press, London.

[23] Muyzer, G., Brinkhoff, T., Nübel, U., Santegoeds, C., Schäfer, H. and Wawer, C. (1998) Denaturing gradient gel electrophoresis (DGGE) in microbial ecology. In:

Molecular microbial ecology manual (Akkermans ADL, v.E.J., de Bruijn FJ (9eds), ed.), pp. 1-27, Kluwer, Dordrecht.

[24] Lane, D.J. (1991) rRNA sequencing. In: Nucleic acid techniques in bacterial systematics. (Stachenbradt E., G.M., (Eds), ed.), pp. 115-175, Wiley, Chichester.

[25] Weisburg, W.G., Barns, S.M., Pelletier, D.A. and Lane, D.J. (1991) 16S ribosomal DNA amplification for phylogenetic study. J. Bacteriol. 173, 697-703.

[26] Amann, R., Binder, B., Olson, R., Chisholm, S., Devereux, R. and Stahl, D. (1990) Combination of 16S rRNA-targeted oligonucleotide probes with flow cytometry for analyzing mixed microbial populations. Appl. Environ. Microbiol. 56, 1919-1925.

[27] Achenbach, L.A., Carey, J. and Madigan, M.T. (2001) Photosynthetic and phylogenetic primers for detection of anoxygenic phototrophs in natural environments. Appl. Environ. Microbiol. 67, 2922-2926.

[28] Maidak, B.L., Cole, J.R., Lilburn, T.G., Parker, C.T., Jr., Saxman, P.R., Farris, R.J., Garrity, G.M., Olsen, G.J., Schmidt, T.M. and Tiedje, J.M. (2001) The RDP-II (Ribosomal Database Project). Nucl. Acids. Res. 29, 173-4.

[29] Kovach, W.L. (1999) MVSP - a Multivariate Statistical Package for Windows. Kovack Computing Services, Wales U.K.

[30] Volkman, J.R., Guillan, F.T., Johns, R.B. and Eglinton, G. (1981) Sources of neutral lipids in a temperate intertidal sediment. Geochim. Cosmochim. Acta. 45, 1817-1828.

[31] Marlowe, I.T., Brassell, S.C., Eglinton, G. and Green, J.C. (1984) Long chain unsaturated ketones and esters in living algae and marine sediments. Org. Geochem. 6, 135-141.

[32] Nes, W.R. and McKean, M.L. (1977) Biogeochemistry of Steroids and Other Isoprenoids, University Park Press, Baltimore, MD.

[33] Nishimura, M. (1977) Origin of stanols in young lacustrine sediments. Nature 270, 711-712.

[34] Paoletti, C., Pushparaj, B., Florenzano, G., Capella, P. and Lercker, G. (1976) Unsaponifiable matter of green and blue-green algal lipids as a factor of biochemical differentiation of their biomasses: II. Terpenic alcohol and sterol fractions. Lipids 11, 266-271.

[35] Patterson, G.W. (1974) Sterols of some green algae. Comp. Biochem. Physiol. 47B, 453-457.

[36] Ballantine, J.A., Lavis, A. and Morris, R.J. (1979) Sterols of the phytoplankton - effects of illumination and growth stage. Phytochem. 18, 1459-1466.

[37] Orcutt, D.M. and Paterson, G.W. (1975) Sterol, fatty acid and elemental composition of diatoms grown in chemically defined media. Comp. Biochem. Physiol. 50B, 579-583.

[38] Kates, M., Tremblay, P., Anderson, R. and Volcani, B.E. (1978) Identification of the free and conjugated sterol in a non-photosynthetic diatom, *Nitzschia alba* as 24-methylene cholesterol. Lipids 13, 34-41.

[39] Kohlhase, M. and Pohl, P. (1988) Saturated and unsaturated sterols of nitrogen fixing blue-green algae (Cyanobacteria). Phytochem. 27, 1735-1740.

[40] Gaskell, S.J. and Eglinton, G. (1975) Rapid hydrogenation of sterols in a contemporary lacustrine sediment. Nature 254, 209-212.

[41] Edmunds, K.l.H., Brassell, S.C. and Eglinton, G. (1980) The short-term diagenetic fate of 5a-cholestan-3b-ol: in situ radiolabelled incubation in algal mats. In: Advances in Organic Geochemistry (Douglas, A.G. and J.R., M., eds.), pp. 427-434, Pergamon Press, Oxford.

[42] Robinson, N., Eglinton, G., Brassell, S.C. and Cranwell, P.A. (1984) Dinoflagellate origin for sedimentary 4a-methyl-steroids and 4a(H)-stanols. Nature 232, 327-330.

[43] Mermoud, F., Wunsche, L., Clerc, O., Gulaçar, F.O. and Buchs, A. (1984) Steroidal ketones in the early diagenetic transformations of sterols in different types of sediments. Org. Geochem. 6, 25-29.

[44] Han, J., McCarthy, E.D., Calvin, M. and Benn, M.H. (1968) Hydrocarbon constituents of the blue-green algae *Nostoc muscorum, Anacystis nudulans, Phormidium luridum* and *Chlorogloea fritschii*. J. Chem. Soc., 2785-2791.

[45] Blumer, M., Guillard, R.R.L. and Chase, T. (1971) Hydrocarbons of marine phytoplankton. Mar. Biol. 8, 183-189.

[46] Tornabene, T.G., Langworthy, T.A., Holzer, G. and Oro, J. (1979) Squalenes, phytanes and other isoprenoids as major neutral lipids of methanogenic and thermoacidophilic "archaebacteria". J. Molec. Evol. 13, 73-83.

[47] Didyk, B.M., Simoneit, B.R.T., Brassell, S.C. and Eglinton, G. (1978) Organic geochemical indicators of palaeoenvironmental conditions of sedimentation. Nature 272, 216-222.

[48] Eglinton, G. and Hamilton, R.J. (1967) Leaf epicuticular waxes. Science 156, 1322.

[49] Barbe, A., Grimalt, J.O., Pueyo, J.J. and Albaigés, J. (1990) Characterization of model evaporitic environments through the study of lipid components. Org. Geochem. 16, 815-828.

[50] Solé, A., Gaju, N. and Esteve, I. (2003) The Biomass Dynamics of Cyanobacteria in an Annual Cycle Determined by Confocal Laser Scanning Microscopy. Scanning 25, 1-7.

[51] Solé, A., Gaju, N., Guerrero, R. and Esteve, I. (1998) Confocal laser scanning microscopy of Ebro Delta microbial mats. Microsc. Anal. 29, 13-15.

[52] Abed, R.M., Garcia-Pichel, F. and Hernández-Mariné, M. (2002) Polyphasic characterization of benthic, moderately halophilic, moderately thermophilic cyanobacteria with very thin trichomes and the proposal of Halomicronema excentricum gen. nov., sp. nov. Arch. Microbiol. 177, 361-370.

[53] Chuecas, L. and Riley, J.P. (1969) Component fatty acids of the total lipids of some marine phytoplankton. J. Mar. Biol. Ass. U.K. 49, 97-116.

[54] Nubel, U., Garcia-Pichel, F., Clavero, E. and Muyzer, G. (2000) Matching molecular diversity and ecophysiology of benthic cyanobacteria and diatoms in communities along a salinity gradient. Environ. Microbiol. 2, 217-226.

[55] Benlloch, S., López-López, A., Casamayor, E.O., Ovreas, L., Goddard, V., Daae, F.L., Smerdon, G., Massana, R., Joint, I., Thingstad, F., Pedros-Alio, C. and Rodriguez-Valera, F. (2002) Prokaryotic genetic diversity throughout the salinity gradient of a coastal solar saltern. Environ. Microbiol. 4, 349-360.

[56] Casamayor, E.O., Massana, R., Benlloch, S., Ovreas, L., Diez, B., Goddard, V.J., Gasol, J.M., Joint, I., Rodríguez-Valera, F. and Pedrós-Alió, C. (2002) Changes in archaeal, bacterial and eukaryal assemblages along a salinity gradient by comparison of genetic fingerprinting methods in a multipond solar saltern. Environ. Microbiol. 4, 338-348.

[57] Karsten, U. (1996) Growth and organic osmolytes of geographically different isolates of *Microcoleus chthonoplastes* (cyanobacteria) from benthic microbial mats : Response to salinity change . J. Phycol. 32, 501-506.

[58] Guerrero, R., Urmeneta, J. and Rampone, G. (1993) Distribution of types of microbial mats at the Ebro Delta, Spain. Biosystems 31, 135-44.

[59] Jonkers, H.M., Ludwig, R., De Wit, R., Pringault, O., Muyzer, G., Niemann, H., Finke, N. and De Beer, D. (2003) Structural and functional analysis of a microbial mat ecosystem from a unique permanent hypersaline inland lake: 'La Salada de Chiprana' (NE Spain). FEMS Microbiol. Ecol. 44, 175-189.

[60] Grimalt, J.O., de Witt, R., Teixidor, P. and Albaiges, J. (1992) Lipid biogeochemistry of *Phormidium* and *Microcoleus* mats. Org. Geochem. 19, 509-530.

[61] Navarrete, A., Urmeneta, J. and Guerrero, R. (2001) Physiological status and community composition of microbial mats by signature lipid biomarkers. In: MATBIOPOL. First Scientific Progress Report, pp. 111-116., Caumette, P. (coord).

[62] Cypionka, H. (2000) Oxygen respiration by *Desulfovibrio* species. Annu. Rev. Microbiol. 54, 827-848.

[63] Cypionka, H., Widdel, F. and Pfennig, N. (1985) Survival of sulfate-reducing bacteria after oxygen stress, and growth in sulfate-free oxygen-sulfide gradients. FEMS Microbiol. Lett. 31, 39-45.

[64] Minz, D., Fishbain, S., Green, S.J., Muyzer, G., Cohen, Y., Rittmann, B.E. and Stahl, D.A. (1999) Unexpected population distribution in a microbial mat community: sulfate-reducing bacteria localized to the highly oxic chemocline in contrast to a eukaryotic preference for anoxia. Appl. Environ. Microbiol. 65, 4659-4665.

[65] Minz, D., Flax, J.L., Green, S.J., Muyzer, G., Cohen, Y., Wagner, M., Rittmann, B.E. and Stahl, D.A. (1999) Diversity of sulfate-reducing bacteria in oxic and anoxic regions of a microbial mat characterized by comparative analysis of dissimilatory sulfite reductase genes. Appl. Environ. Microbiol. 65, 4666-4671.

[66] Wieland, A., Zopfi, J., Benthien, M. and Kühl, M. (2003) Biogeochemistry of an iron-rich hypersaline microbial mat (Camargue, France). Microb. Ecol. Submitted for publication.

[67] Pierson, B.K. and Parenteau, M.N. (2000) Phototrophs in high iron microbial mats : microstructure of mats in iron-depositing hot springs. FEMS Microbiol. Ecol. 32, 181-196.

III.3. Le tapis microbien marin des Iles Orcades (Ecosse)

Ce travail a été publié dans le journal Microbial Ecology 2003 46(4): 371-390 sous le titre:

Microbial mats on the Orkney Islands revisited: microenvironment and microbial community composition

Par : Andrea Wieland[1], Michael Kühl[1], Laura McGowan[2], Aude Fourçans[3], Robert Duran[3], Pierre Caumette[3], Tirso García de Oteyza[4], Joan O. Grimalt[4], Antoni Solé[5], Elia Diestra[5], Isabel Esteve[5], et Ron A. Herbert[2]

ABSTRACT

The microenvironment and community composition of microbial mats developing on beaches in Scapa Flow (Orkney Islands) were investigated. Analysis of characteristic biomarkers (major fatty acids, hydrocarbons, alcohols and alkenones) revealed the presence of different groups of bacteria and microalgae in mats from Waulkmill and Swanbister beach, including diatoms, Haptophyceae, cyanobacteria and sulfate-reducing bacteria. These analyses also indicated the presence of methanogens, especially in Swanbister beach mats, and therefore a possible role of methanogenesis for the carbon cycle of these sediments. High amounts of algal lipids and slightly higher numbers (genera, abundances) of cyanobacteria were found in Waulkmill Bay mats. However, overall only a few genera and low numbers of unicellular and filamentous cyanobacteria were present in mats from Waulkmill and Swanbister beach, as deduced from CLSM (confocal laser scanning microscopy) analysis. Spectral scalar irradiance measurements with fiber-optic microprobes indicated a pronounced heterogeneity concerning zonation and density of mainly anoxygenic phototrophs in Swanbister Bay mats. By microsensor and T-RFLP (terminal restriction fragment length polymorphism) analysis in Swanbister beach mats, the depth-distribution of different populations of purple and sulfate-reducing bacteria could be related to the microenvironmental conditions. Oxygen, but also sulfide and other (inorganic and organic) sulfur compounds, seem to play an important role in the stratification and diversity of these two major bacterial groups involved in sulfur cycling in Swanbister beach mats.

[1]Marine Biological Laboratory, University of Copenhagen, Strandpromenaden 5, DK-3000 Helsingør, Denmark,
[2] Division of Environmental and Applied Biology, School of Life Sciences, University of Dundee, Dundee DD1 4HN, UK,
[3]Laboratoire d`Ecologie Moléculaire-Microbiologie, Université de Pau et des Pays de l`Adour, Avenue de l`Université, IBEAS, F-64000 Pau, France,
[4]Department of Environmental Chemistry (ICER-CSIC), Jordi Girona 18, E-08034 Barcelona, Spain,
[5]Department of Genetics and Microbiology, Autonomous University of Barcelona, E-08193 Bellaterra, Spain

INTRODUCTION

Laminated microbial communities frequently develop in the upper intertidal zone of sandy beaches and tidal flats (e.g., [79, 16, 87, 49]). After initial colonization and succession of cyanobacteria [79], the mature states of these stratified phototrophic communities develop into microbial mats, consisting of a thin top layer of sand and/or diatoms covering a dense layer of filamentous cyanobacteria. Below the cyanobacteria, a distinct layer of purple sulfur bacteria is often present with a reduced black layer of precipitated iron sulfides underneath due to intensive sulfate reduction [84]. Sulfate-reducing bacteria are also present at high numbers in the upper millimeters of the mats [88, 98]. Because of the macroscopically visible lamination such coastal microbial mats were named colored sands or 'Farbstreifensandwatt' [33]. Both cyanobacteria and anoxygenic phototrophs contribute to sediment binding and stabilization of the sediment [28]. The dominant cyanobacterium is generally *Microcoleus chthonoplastes* [79, 16, 84, 89], whereas the immotile *Thiocapsa roseopersicina* is often the dominant purple sulfur bacterium [16, 87, 84].

Mass blooms of purple sulfur bacteria, mainly *T. roseopersicina*, have been observed during summer in the intertidal zone of sheltered sandy beaches in Scapa Flow on the Orkney Islands [31, 85, 86]. Three different laminated microbial mats were described [86], distinguished by the position of the cyanobacterial layer, above or beneath the purple sulfur bacterial layer or its complete absence and therefore exclusive development of purple sulfur bacteria in the top layer of the sediment. Mats with a typical lamination pattern (see above) were most common [86]. However, cyanobacteria were only present at relatively low population densities and *M. chthonoplastes* was absent in all investigated mats [86].

The beaches of Scapa Flow are locally enriched in nitrogen-containing organic matter due to decomposition of accumulated macro-algal debris [31, 86]. In Scapa Bay, additional organic matter was supplied by discharges from local whiskey distilleries [86]. The high organic carbon content of the sediments leads to availability of low molecular weight organic substrates for sulfate-reducing bacteria, and the produced sulfide serves as an electron donor for anoxygenic photosynthesis by purple sulfur bacteria [31]. Distinct micro-colonies formed by the purple sulfur bacteria (mainly *T. roseopersicina*) can effectively bind sediment grains. This aggregation leads to a reduction of erosion and, therefore, to a stabilization of the sediment [85]. Although these aggregates may not be as effective as the cohesive structures of cyanobacterial mats in stabilizing sandy sediments and preventing erosion, purple sulfur bacteria and mainly *T. roseopersicina* were capable of rapidly recolonizing eroded sites on beaches in Scapa Flow [85].

Further characteristics of these sediment ecosystems dominated by purple sulfur bacteria are the absence of chemolithotrophic sulfur bacteria, normally present in marine microbial mats [88], and the almost permanent exposure of purple sulfur bacteria to O_2 at the sediment surface [85, 86].

In this study, the composition of the microbial community and the microenvironmental conditions in microbial mats from Orkney Islands beaches was investigated. This included determination of phototrophic populations with confocal laser scanning microscopy (CLSM) and fiber-optic microprobe-based spectrometry in microbial mats from Waulkmill and Swanbister beaches. Dominant groups of mat-inhabiting microorganisms were determined by their characteristic biomarkers. Furthermore, the stratification of major bacterial groups in relation to microenvironmental gradients was investigated in Swanbister beach mats. For this, O_2 and sulfur cycling was quantified by controlled microsensor experiments in the laboratory and by sulfate reduction rate measurements. The depth-zonation and diversity of the entire microbial community and of the major bacterial groups involved in sulfur cycling in Swanbister beach mats was analyzed with terminal restriction fragment length polymorphism (T-RFLP).

MATERIALS AND METHODS

Sampling

Sediment samples were taken in July 2000 at low tide with Plexiglas core tubes (53 mm i.d.) on beaches of Waulkmill and Swanbister Bay located in Scapa Flow, Orkney Islands (a map with locations can be found in [86]). *In situ* temperature and salinity of remaining stagnant seawater were 12-13°C and 40‰ at the time of sampling. Downwelling irradiance around noon on clear and sunny days was >1100 µmol photons m^{-2} s^{-1}. Sampled sediment cores were transported to the laboratory of the Orkney County Council Marine Unit on Orkney Island (Mainland), where microsensor measurements were performed under controlled conditions.

Microsensor measurements

Clark-type O_2 [72] and H_2S [36, 50] microsensors connected to a picoammeter (Unisense A/S, Denmark), and glass pH microelectrodes [74] connected to a high-impedance mV-meter (WPI Inc., USA) were used for fine-scale measurements of O_2 and sulfide distribution in Swanbister beach mats. Oxygenic gross photosynthesis was quantified with the light-dark shift method [73]. The O_2 microsensor had a tip diameter of 10 µm, a stirring sensitivity of ~1% and a response time, t_{90}, of ~0.4 s. The H_2S microsensor had a tip diameter

of 40 µm and was coated with a black enamel paint to avoid light interference [50]. The length and the tip diameter of the pH-sensitive glass of the pH microelectrode were 250 and 10 µm, respectively.

The O_2 microsensor was linearly calibrated in the experimental set-up (see below) by a two-point calibration using readings of microsensor current in the air saturated overlying water (100% air saturation) and in the anoxic part of the mats (0% O_2). Dissolved O_2 concentrations of air saturated seawater at experimental temperatures and salinities were calculated according to García and Gordon [27]. The pH microelectrode was calibrated in standard buffer solutions (Radiometer, Denmark). The pH of the overlying water in the experimental set-up was determined with a commercial pH meter calibrated in standard buffer solutions (Radiometer, Denmark). The readings of the pH microelectrode in the overlying water were adjusted to the measured pH of the seawater. The H_2S microsensor was calibrated in anoxic buffer solutions (0.2 M phosphate buffer, pH 7.5) of increasing sulfide concentrations. A sample of each sulfide buffer solution was fixed in zinc acetate (5% w/v) for subsequent spectrophotometric analysis of sulfide concentration after Fonselius [23] with modifications, i.e. acidification of the samples to pH <1 with 6M HCl and determination of the absorption of the formed complex at the second peak (750 nm) in the spectrum (C. Steuckart, unpublished). Calculation of H_2S and total sulfide (S_{tot}) concentration profiles from H_2S and pH microsensor data was as described in Wieland and Kühl [97], using pK_1 values calculated from experimental temperatures according to Hershey et al. [32].

Experimental microsensor set-up

Sediment cores were mounted in a flow chamber modified for insertion of whole sediment cores [21]. A constant flow over the mat surface of aerated seawater from the sampling site was generated with a submersible water pump (Aqua Clear, Germany) connected to the flow chamber. Measurements were performed at room temperature (21°C ± 1°C). The mat was illuminated with a fiber-optic halogen light source (KL 2500, Schott, Germany) and the downwelling irradiance at the mat surface was quantified with an underwater quantum irradiance meter (QSL-101, Biospherical Instruments, USA). The microsensors were fixed together with the measuring tips in the same horizontal plane within an area of ca. 0.5-1 cm^2 of the mat surface in a motor-driven micromanipulator (Märzhäuser, Germany; Oriel, USA) mounted on a heavy solid stand. Microsensor signals were recorded with strip chart recorders (Servogor, U.K.; Kipp&Zonen, Netherlands) and with a computer data acquisition system (LabView, National Instruments, USA) that also controlled the

micromanipulator. Gross photosynthesis measurements in steps of 100 or 200 µm vertical depth intervals were performed as described in Wieland and Kühl [97].

Spectral scalar irradiance measurements with fiber-optic microprobes

A fiber-optic scalar irradiance microprobe [52] was connected to a sensitive fiber-optic diode array spectrometer with a spectral range of 250-950 nm (PMA-11, Hamamatsu Photonics, Japan). Profiles of spectral scalar irradiance in the mats were measured by stepwise inserting the microprobe with a motor-driven micromanipulator (Märzhäuser, Germany; MICOS GmbH, Germany; Jenny Electronics AG, Switzerland) at a zenith angle of 135° relative to the incident light beam. The mats were illuminated vertically with a fiber-optic halogen light source (KL 2500, Schott, Germany). Measurements were performed at vertical depth intervals of 200 µm. The downwelling spectral scalar irradiance at the mat surface was measured by positioning the scalar irradiance microprobe over a black light trap at the same position relative to the light field as the mat surface. Scalar irradiance spectra at various depths in the mats were normalized to the downwelling scalar irradiance at the mat surface. Attenuation spectra of scalar irradiance were calculated over discrete depth intervals from the depth profiles of spectral scalar irradiance by

$$K_0 = \ln(E_1/E_2)/(z_2-z_1) \quad (1)$$

where K_0 is the vertical spectral attenuation coefficient for scalar irradiance, E_1 and E_2 are the spectral scalar irradiance measured at depths z_1 and z_2 in the mat, where $z_2 > z_1$ [48].

Calculations

Diffusive O_2 fluxes across the mat-water interface were calculated from O_2 profiles using Fick's first law of diffusion as described in Wieland and Kühl [96]. Areal rates of O_2 consumption in the aphotic zone, R_{aphot}, were calculated as the downward O_2 flux, J_s, at the lower boundary of the photic zone:

$$J_s = -\phi\, D_s\, dC/dz \quad (2)$$

where dC/dz is the linear concentration gradient, ϕ is the sediment porosity and D_s is the sediment diffusion coefficient, which was calculated from the porosity and D_0 according to Ullman and Aller [83]. The D_0 of O_2 was taken from Broecker and Peng [8] and corrected for experimental temperatures and salinities [53]. Fluxes of H_2S were calculated according to Eq. 2 from the linear part of the profiles. The diffusion coefficient of H_2S was estimated as D_0 (H_2S) = 0.7573 D_0 (O_2) (Tables for seawater and gases, Unisense A/S, Denmark).

Determination of sediment porosity

Sediment porosity (ml water cm^{-3}) was determined (n = 5) on samples collected from Swanbister Bay in July 2001 using a 2.5 cm diameter stainless steel corer. The cores were sectioned using a sediment slicer to give the following four consecutive depth horizons: 0-5 mm, 5-10 mm, 10-20 mm and 20-30 mm. Porosity was measured as weight loss after drying at 110°C for 24 hours.

Determination of sulfate reduction rates

Triplicate sediment cores (13 mm i.d.) were collected from Swanbister Bay in truncated 5 ml disposable syringes and sealed with Suba seals (W. Freeman Ltd., U.K.). Carrier-free $^{35}SO_4^{2-}$ (10 µl; Amersham Pharmacia Biotech, U.K.) was injected through the Suba seal using a microliter syringe into each sediment core, giving an average activity of 50 kBq per cm^3. To ensure even distribution of the isotope throughout the cores the isotope was added progressively as the syringe needle was withdrawn. At the end of the 12 h incubation period at ambient temperature (16°C) in the dark, the cores were sectioned to give the following depth horizons: 0-10 mm, 10-20 mm and 20-30 mm. Each sediment section was transferred to plastic bottles containing 5 ml of a 20% w/v zinc acetate solution to stop biological activity and preserve sulfide. The samples were then frozen and stored until required for analysis. Production of $H_2^{35}S$ was determined using the one-step distillation method of Fossing and Jørgensen [24]. Sulfate reduction rates were calculated according to the method of Isaksen and Finster [35]. Pore-water sulfate was determined according to the method of Tabatabai [80].

Confocal laser scanning microscopy

Sediment cores (18 mm i.d.) were taken from Waulkmill and Swanbister Bay using truncated 20 ml disposable syringes. The samples were transferred into small plastic containers containing 2.5% glutaraldehyde in a phosphate buffer (0.2 M) adjusted to the appropriate salinity with NaCl. The samples were fixed for 3 hours and then washed 2-3 times with phosphate buffer. The samples were stored at 4°C until further analysis.

The samples were investigated with a compound microscope (Olympus BH2, Japan) and a laser confocal microscope (Leica TCS 4d, Germany) equipped with an argon-krypton laser. For confocal analysis, subsamples (slices) of defined dimension were placed in cavity slides, covered and sealed with cover slips and observed under an excitation beam of 568 nm. Pigment fluorescence emission was detected with a 590 nm long pass filter. Optical sections

(every focal plane), optical series (all focal planes from each imaged area), summa images (all optical series projected to one image), and stereoscopic images (one image in three dimensions from every optical series) were obtained from these analyses. A volume data set was generated by combining all optical sections.

After screening of the different cyanobacteria present in all images from each sampling site, each type of cyanobacterium was identified after morphological criteria according to Castenholz [10].

Analysis of fatty acids, hydrocarbons, alcohols and alkenones

Sediment cores (26 mm i.d.) were collected on Waulkmill and Swanbister beach and stored frozen until further analysis. The upper 4 cm of the mat samples (approximately 10 g) were homogenized with a mortar and extracted three times with methanol, dichloromethane and *n*-hexane. Extracts were saponified with 30 ml of KOH (6% w/v) in methanol and the neutral components were recovered by extraction with 3 × 30 ml of *n*-hexane. The alkaline mixture was then acidified to pH 2 with 5 ml of HCl and the acidic compounds were recovered by extraction with 3 × 30 ml of *n*-hexane. The neutral compounds were fractionated in a column filled with silica (8 g, bottom) and alumina (8 g, top). These packings were prepared previously by heating at 120°C and 350°C for 12 h, respectively. Milli-Q-water was added to both adsorbents for deactivation (5%). Six fractions were obtained by successive elution with 20 ml of *n*-hexane, 20 ml of *n*-hexane/dichloromethane (9:1), 40 ml of *n*-hexane/dichloromethane (8:2), 40 ml of *n*-hexane/dichloromethane 75% (1:3), 20 ml of dichloromethane/methanol (95:5) and 40 ml of dichloromethane/methanol (9:1). The two most polar fractions were silylated after redissolution in 100 µl of dichloromethane and addition of 100 µl bis-(trimethylsilyl)trifluoroacetamide (heating 1h at 60°C). The fatty acid fractions were methylated before instrumental analysis using diazomethane, which was synthesized as described elsewhere [91]. These fractions were dissolved in 100 µl of *n*-hexane and diazomethane was added until the yellowish color remained.

Samples were analyzed by gas chromatography and flame ionization detection in a Varian Star 3400 (Varian Inc., USA). A 30 m capillary column (0.25 mm i.d.) coated with DB-5 (25 µm film thickness) was used with hydrogen as carrier gas. The oven was kept at 70°C for 1 min, heated to 140°C at 10°C/min, then to 310°C at 4°C/min and finally held at 310°C for 30 min. The temperature of the detector was 330°C. Analyses by gas chromatography and mass spectrometric detection were performed with a Fisons MD-800 quadrupole mass analyzer (Thermo Instruments, U.K.). Samples were injected in splitless

mode at 300°C into a 30 m capillary column (0.25 mm i.d.) coated with DB-5 (25 µm film thickness). Helium was used as carrier gas and the temperature program was as described above. Mass spectra were recorded in electron impact mode at 70 eV by scanning between m/z 50-650 every second. Ion source and transfer line were kept at 300°C.

T-RFLP analysis

Sediment cores (35 mm i.d.) were taken with falcon tubes from Swanbister Bay. The upper 10 mm of the sediment core was sliced off aseptically, transferred to sterile Petri-dishes, frozen in liquid nitrogen, transported on dry ice and finally stored at –80°C until further analysis.

The upper 2 mm of the mat cores were sliced with a cryomicrotome (MICROM GmbH, Germany) at around 200 µm, and the third mm at around 500 µm vertical depth resolution. From these mat slices, DNA was extracted with the UltraClean Soil DNA Isolation Kit using the alternative lysis method (MoBio Laboratories Inc., USA). All extracted genomic DNA samples were stored at -20°C until further processing.

The different primers used for T-RFLP analysis to assess the bacterial community structure are listed in Table 1. For T-RFLP analysis, forward (f) and reverse (r) primers were fluorescently labeled with TET and HEX (E.S.G.S. Cybergene group, France), respectively. The PCR amplification mixture contained 12.5 µl hot start Taq polymerase mix (Qiagen, Netherlands), 0.5 µl of each primer (20 µM) and 1 µl of DNA template. A final volume of 50 µl was adjusted with distilled water. Reactions were cycled in a PTC200 thermocycler (MJ Research, USA) at 94°C for 15 min, followed by 35 cycles of 94°C for 1 min, T_m for 1.5 min, with T_m denoting the corresponding melting temperature for hybridization between primers and template DNA, and 72°C for 1 min, with a final extension step at 72°C for 10 min. The amount of PCR product was determined by comparison to known concentrations of standards (Smartlader, Eurogentec, Belgium). PCR products were purified with the GFX PCR DNA purification kit (Amersham, U.K.).

Purified PCR products (600 to 700 ng) were digested with 12 units of enzyme HaeIII or Hin6I (New England Biolabs, USA). The precise length of T-RFs from the digested PCR products was determined by capillary electrophoresis (ABI prism 310, Applied Biosystems, USA). About 50 ng of the digested DNA from each sample was mixed with 10 µl of deionized formamide and 0.25 µl of TAMRA size standard and then denatured at 94°C for 2 min and immediately chilled on ice prior to electrophoresis. After an injection step of 10 s,

electrophoresis was carried out for up to 30 min applying a voltage of 15 KV. T-RFLP profiles were performed using GeneScan software (ABI).

Dominant T-RFs were selected by comparison of numerical values and electropherograms. The clustering values were analyzed with the T-RFLP similarity matrix on the RDP (Ribosomal Database Project) web site (http://rdp.cme.msu.edu/) [56]. The obtained distance matrix was used to construct a dendrogram with MEGA version 2.1 [51] using the UPGMA method (Unweighted Pair Group Method with Arithmetic Mean).

T-RFLP profiles were also compared by Canonical Correspondence Analysis (CCA) according to Fromin et al. [25]. This test is based on the linear correlation between community data (abundance of each T-RF) and environmental parameters in the mat at light conditions (scalar irradiance at wavelengths of Chl *a*-(676 nm) and BChl *a*-(845 nm) absorption, depth, and O_2 concentration). The CCA were realized with MVSP v3.13d software (Rockware Inc., U.K.).

RESULTS

Biomarkers in Waulkmill and Swanbister Bay mats

The major lipid compounds in both Waulkmill and Swanbister beach mats were fatty acids, encompassing essentially C_{14}-C_{22} homologues dominated by *n*-hexadec-9(Z)-enoic and *n*-hexadecanoic acids (Fig. 1A, B). Other major compounds were *n*-octadec-9(Z)-enoic, *n*-eicosapentenoic, *n*-tetradecanoic and *n*-pentadecanoic acids, which are generally representative of algal and microbial contributions. *N*-octadec-9(Z)-enoic acid is abundant in photosynthetic algae and cyanobacteria [11]. *N*-eicosapentenoic acid and other polyunsaturated *n*-eicosane and *n*-docosane acids are specific of inputs from diatom species [93]. *Iso*- and *anteiso*-pentadecanoic acids were the two main branched fatty acids present in significant proportions. These compounds are abundant in sulfate-reducing bacteria and sulfur-oxidizing bacteria such as *Thiomicrospira* [29].

The aliphatic hydrocarbon phyt-1-ene together with other phytene homologues occurred in both mats, but their presence was more pronounced in the Swanbister mat (Fig. 1C, D). These hydrocarbons are characteristic for methanogens [82] and may also be produced during the decomposition of phytol [18]. The presence of an isoprenoid compound specific of methanogenic origin, 2,6,10,15,19-pentamethylicosane [34, 75], in the Swanbister mat (Fig. 1C) suggests that at least in this mat the occurrence of the phytanes is due to inputs from these microorganisms. *N*-heptadecane and *n*-heptadecenes were major compounds in both mats and especially abundant in the Waulkmill mat (Fig. 1D). These compounds are

generally found in cyanobacteria [30, 67] or in phototrophic eukaryotes [7]. Other hydrocarbons specific for algal inputs such as C_{25} highly branched isoprenoid alkenes synthesized by diatoms [62] were also present in the Waulkmill mat. In addition to these hydrocarbons, a distribution of C_{23}-C_{35} *n*-alkanes predominated by the odd carbon numbered homologues, namely C_{29}, C_{31} and C_{33}, representative for inputs from higher plants [20], were found in both mats. This distribution can also be found in other sediments in coastal environments [5], probably reflecting the influence of wind transported materials from nearby higher plants.

A significant amount of phytol was found in the Waulkmill mat, representing contributions from algae (Fig. 2). Other lipids of algal origin, like C_{37}-C_{38} di-, tri- and tetra-unsaturated alkenones specific for Haptophyceae [92, 57] and sterols were also present. The sterol distribution in the Waulkmill mat was dominated by cholest-5-en-3β-ol and contains minor proportions of 24-ethyl cholest-5-en-3β-ol, cholesta-5,24-dien-3β-ol, 24-methyl cholesta-5,24(28)-dien-3β-ol and their homologues saturated at Δ^5 (Fig. 2, upper graph). Sterols unsaturated at positions Δ^5, Δ^{22} and $\Delta^{5,22}$ can originate from cyanobacteria [67, 61, 63], green algae [68, 4] or diatoms [64, 41, 4]. 24-Methyl cholesta-5,24(28)-dien-3β-ol is a common diatom marker [64, 41, 4] and its occurrence is consistent with the presence of highly branched isoprenoid hydrocarbons.

Spectral scalar irradiance and cyanobacteria in Waulkmill Bay mats

From spectral scalar irradiance profiles the zonation of phototrophs in the mats could be inferred due to the absorption characteristics of their pigments at specific wavelengths. In the Waulkmill mat, three main wavelength regions of pronounced absorption could be identified (Fig. 3). The pronounced minimum of scalar irradiance in the narrow region around 675 nm corresponds to Chl *a*-absorption, indicating the presence of cyanobacteria and/or microalgae. A shoulder in the spectra measured over the upper 2 mm indicated some absorption at ~625 nm due to the presence of phycocyanin. The presence of purple bacteria throughout the upper millimeters of the mat was indicated by the pronounced minima in the region from 760 to 900 nm and at around 590 nm corresponding to BChl *a*-absorption. The scalar irradiance in these wavelength regions was already at 1 mm depth less than 50% of the downwelling scalar irradiance at the mat surface and at 2.6 mm depth less than 1-2%. The strong absorption by Chl *a* and BChl *a* indicates the presence of dense populations of oxygenic and anoxygenic phototrophs in the upper 2.6 mm of the mat.

Several different genera of filamentous and unicellular cyanobacteria were identified (Table 2), with cyanobacteria of the genera *Lyngbya* and *Oscillatoria*, and of the *Pleurocapsa*- and *Gloeocapsa*-group being the most abundant in the Waulkmill Bay mat as observed with CLSM and light microscopy. Some cyanobacteria occurred only at certain depths of the mat, whereas others were found in several or all mat slices investigated.

Spectral scalar irradiance and cyanobacteria in Swanbister Bay mats

In a Swanbister Bay mat, spectral scalar irradiance minima at characteristic Chl *a*- and BChl *a*-absorption wavelengths were found (Fig. 4). Pronounced light scattering was detected at the mat surface and in the uppermost mat layers. Wavelengths corresponding to Chl *a*-absorption were more strongly attenuated in the Swanbister mat than wavelengths corresponding to BChl *a*-absorption (Fig. 4), whereas in the Waulkmill mat both wavelength regions were almost equally attenuated throughout the mat (Fig. 3).

Spectral scalar irradiance profiles in another mat sample from Swanbister Bay, which was densely covered by purple bacteria and characterized by a pink-colored surface, showed a much more pronounced BChl *a*-absorption (Fig. 5, upper graph). The spectral irradiance in the wavelength regions of Chl *a*- and BChl *a*-absorption was already at a depth of 0.8 mm <10% of the downwelling spectral scalar irradiance. From these profiles, the average attenuation spectrum of scalar irradiance over the depth interval of 0-0.8 mm was calculated (Fig. 5, lower graph). The vertical spectral attenuation coefficient (K_0) was highest in the wavelength region between 400 and 550 nm, the region of carotenoid and Chl *a*-absorption. The attenuation coefficient of BChl *a*-absorption wavelengths was higher than the attenuation coefficient of Chl *a*-absorption, indicating higher densities of purple bacteria in this mat. Thus, mats from Swanbister Bay were very heterogeneous and patchy concerning zonation and population densities of oxygenic and especially anoxygenic phototrophs.

In Swanbister Bay mats covered by purple bacteria (pink surface), only a few genera of cyanobacteria, i.e. mainly unicellular morphotypes of the *Pleurocapsa*-group and one filamentous type, were found in low numbers (Table 3).

Microbial community structure of Swanbister Bay mats

To assess the microbial community structure of a Swanbister Bay mat the universal primer pair 8f-926r targeting a partial sequence of the 16S rDNA gene of eubacteria was applied. After digestion with two different restriction enzymes (HaeIII, Hin6I), the diversity of the amplified 16S fragments was analyzed by T-RFLP. The structure of the T-RFLP

profiles, as characterized by the number and distribution of major bands (peaks of highest relative fluorescence intensity), varied from top to bottom of the mat (data not shown). Depending on the restriction enzyme used, different dominant T-RFs were observed. Degrees of similarity among the microbial communities of the different mat layers were quantified with the T-RFLP profile matrix program (RDP). The resulting similarity dendrogram (not shown) did not reveal any specific distribution of microbial communities in the analyzed mat layers, most probably due to the fact that several bacterial species may have terminal fragments of identical size.

More specific primers were used to analyze the sulfate-reducing and anoxygenic phototrophic microbial community. The biodiversity of the sulfate-reducing bacteria (SRB) was analyzed using the primers 8f-SRB385 and the combination of both restriction enzymes (HaeIII, Hin6I). The resulting T-RFLP profiles contained almost 60 different peaks. In almost all mat layers fragments of 64, 189, 190, 191, 193, 200, 204 bp were found after digestion with HaeIII, as well as dominant fragments of 64, 87, 89, 92, 337, 348, 350, 352, 371 bp using Hin6I (data not shown). Some T-RFs, however, showed a depth-dependent distribution, as T-RFs obtained with HaeIII of 178, 181, 182, 209, 267, 314 and 317 bp were predominating only in the upper mat layers, whereas T-RFs of 268, 312, 315 bp were dominant in layers below 1 mm depth (data not shown). A similarity dendrogram was obtained by comparing all T-RFs observed with the two different restriction enzymes in each mat layer (Fig. 6A), which indicated a stratification of the SRB communities. The SRB communities in the upper mat layer (0-1 mm) seemed to be related and formed a distinct cluster, clearly differing from the ones at increasing depths. Two other closely related groups were located between 1-1.6 mm and 2-3 mm depth, suggesting two different communities of SRB in these depth horizons. Furthermore, populations of SRB in the layer at 1.6-2 mm depth seem to form a really divergent cluster.

The T-RFLP patterns were analyzed by Canonical Correspondence Analysis to reveal the variables, which influenced the organization of each SRB population. Using the averaged microsensor O_2 profile at 1312 µmol photons m^{-2} s^{-1} and scalar irradiance profiles at Chl *a*-(676 nm) and BChl *a*-(845 nm) absorption wavelengths in the top 3 mm of the mat (Figs. 4, 7C), this analysis showed that their dispersion was influenced mostly by irradiance and O_2 concentration (Fig. 6C). Two distinct groups appeared, one in the anaerobic zone and one in the aerobic zone exposed to light. This analysis showed a distribution of different SRB species with depth and thus that SRB were displayed according to depth.

The biodiversity of purple anoxygenic phototrophic bacteria (PAB) was assessed by using primers designed to target the *pufM* gene, which is encoding for a subunit of the photosynthetic reaction center in purple sulfur and purple non-sulfur bacteria. T-RFLP analysis of the amplified *pufM* fragments resulted in complex profiles containing about 30 peaks. Major T-RFs were observed, which allowed a comparison and distinction between the different mat layers. In the upper mat layers fragment peaks of 129, 187, 201, and 203 bp were found (HaeIII), whereas the bottom layers were characterized by fragment peaks of 215 and 225 bp (data not shown).

Similarity dendrograms showed delineation of the profiles into clusters, indicating a stratification of purple phototrophic bacteria within the mat (Fig. 6B). Purple phototrophic communities from 1.4-2 mm, and from 1-1.4/2-3 mm depth were closely related. These two community clusters were less closely related to the community in the upper mat layers than to the community below 3 mm depth. Furthermore, the similarity dendrogram also suggests that there were significant differences between the anoxygenic phototrophic communities in the uppermost mm of the mat.

Canonical correspondence analysis obtained from T-RFLP profiles showed that the phototrophic communities of the upper layers were clearly influenced by irradiance. In contrast, communities of the deep layers were negatively influenced by O_2 penetration (Fig. 6D). Surprisingly, predicted patterns of T-RFs from *pufM* sequences digested with HaeIII or Hin6I obtained from the NCBI bank (data not shown) showed that the T-RFs specific of the upper layers could correspond to aerobic heterotrophic alpha-proteobacteria, like e.g. the genus *Sphingomonas*. Indeed, it has been recently demonstrated that this genus possesses the *pufM* gene [6]. T-RFs from deep layers of the mat could correspond to predicted T-RF patterns of purple sulfur bacteria from the genus *Thiocystis* and of purple non-sulfur bacteria from the genus *Rhodomicrobium*. The general T-RF fingerprints observed within the mat could be equivalent to predicted T-RF patterns of gamma-proteobacteria such as members of the genera *Rhodobacter* or *Allochromatium*.

Microenvironment of Swanbister Bay mats

Profiles of O_2, gross photosynthesis, pH and H_2S were measured at different positions in a Swanbister Bay mat incubated in darkness and at an irradiance of 1312 µmol photons m^{-2} s^{-1} (Fig. 7). During dark incubation, the average O_2 penetration was 0.8 mm and steep gradients of both H_2S and S_{tot} developed below this depth (Fig. 7A). A gradual decrease of pH was found in the dark incubated mat, accounting for a decrease of

approximately 1 pH unit between the water and the mat at around 4 mm depth (Fig. 7B). Sulfate reduction rates were lowest in the upper centimeter of dark incubated Swanbister Bay mats and highest in the 1-2 cm depth interval (Table 4).

At an irradiance of 1312 µmol photons m^{-2} s^{-1}, gross oxygenic photosynthesis occurred in the upper 2.8 mm of the mat, leading to an increased O_2 penetration of 4 mm and a peak of O_2 concentration at 1.6 mm depth (Fig. 7C). As calculated from the profiles of spectral scalar irradiance measured in the same mat sample (Fig. 4), this O_2 maximum occurred in the depth layer of highest Chl *a*-absorption, as indicated by the depth profile of the vertical attenuation coefficient, K_0, at 676 nm. Below that zone, both O_2 concentration and K_0 (676 nm) decreased, whereas the attenuation coefficient at 845 nm, indicative for BChl *a*-absorption, increased. This indicates an increasing population density of BChl *a*-containing anoxygenic phototrophic bacteria in the anoxic mat layer. The presence of a population of anoxygenic phototrophs in the zone of highest O_2 concentration and Chl *a*-absorption was indicated by a peak of K_0 (845 nm) in that zone, which was, however, less pronounced than the peak of K_0 (676 nm).

In the upper 5 mm of the light incubated mat, H_2S was undetectable, only in one position very low concentrations of H_2S and sulfide were detected below 3 mm depth (data not shown). Photosynthetic CO_2 fixation led to an increase of pH in the upper 2 mm of the mat by more than 0.5 pH unit, with the peak of pH located approximately in the layer of maximal O_2 concentration and K_0 (676 nm). At increasing depths the pH decreased to pH 7.5 (Fig. 7D).

Oxygen and sulfide cycling as a function of irradiance in Swanbister Bay mats

In the same sediment core, O_2, gross photosynthesis, H_2S and pH profiles were measured at a fixed position at increasing downwelling irradiances (Fig. 8). Oxygen penetration increased in the mat with increasing irradiance from 0.8 mm during darkness to 1.4, 1.6, 2.2 and 2.6 mm at 43, 96, 183, and 349 µmol.photons.m^{-2}.s^{-1}, respectively. At an irradiance of 96 µmol.photons.m^{-2}.s^{-1}, a net production of O_2 was detected. The thickness of the photic zone increased gradually from 0.5 mm at 43 µmol.photons.m^{-2}.s^{-1} to 1.8 mm at 349 µmol photons m^{-2} s^{-1} (Fig. 8, upper panel). The increase of gross oxygenic photosynthesis and of the photic zone thickness with irradiance led to a gradual increase of pH in the upper mat layers (Fig. 8, lower panel). The pronounced pH maximum in the upper mat layer at irradiances >43 µmol photons m^{-2} s^{-1} affected the corresponding S_{tot} profiles (Fig. 8, upper panel). Profiles of S_{tot} were calculated from measured H_2S and pH profiles. The S_{tot} profiles at

these irradiances showed a pronounced shoulder of S_{tot} concentration, which was not present in the corresponding H_2S profiles and was probably caused by the curvature of the pH profiles. Since H_2S and pH profiles could not be measured at exactly the same position, the unusual shape of the S_{tot} profiles was most probably caused by a pronounced microheterogeneity of the mat. These shoulders in the S_{tot} profiles thus represent overestimations of sulfide concentration and will not be discussed further. Compared to the H_2S profile in the dark incubated mat, the upper H_2S boundary moved downwards in the mat at irradiances >96 μmol.photons.m^{-2}.s^{-1} (Fig. 8, upper panel).

A real rates of net oxygenic photosynthesis (P_n), calculated as the O_2 flux across the mat-water interface, rates of O_2 consumption in the aphotic zone (R_{aphot}) and of H_2S oxidation/production (H_2S fluxes) increased with irradiance and saturated at higher irradiances (Fig. 9). The determined H_2S fluxes, however, strongly underestimate sulfide fluxes, since pH tends to increase also in deeper layers at higher irradiance, which results in calculation of higher sulfide concentrations from H_2S data. Increasing H_2S fluxes will therefore translate to much stronger increases of sulfide fluxes.

DISCUSSION

Microbial community composition of Waulkmill and Swanbister Bay mats

In mats from both Waulkmill and Swanbister Bay, the presence of oxygenic phototrophs was evident (Figs. 1-4, Table 2, 3). Biomarker and CLSM analysis revealed a more pronounced abundance of cyanobacteria and high amounts of algal lipids (phytol, sterols, alkenones, highly branched isoprenoid hydrocarbons, heptadecane and heptadecenes) in Waulkmill Bay mats. This indicates high contributions of oxygenic phototrophs in Waulkmill Bay mats, with specific contributions from diatoms and Haptophyceae. The latter were most probably of planktonic origin, buried in the sediment after settling on the sediment surface.

The bio-optical properties of two different Swanbister Bay mat samples revealed a strong heterogeneity concerning the phototrophic community (Figs. 4, 5), indicating a pronounced patchiness of the distribution of purple bacteria on Swanbister beach. A factor influencing the distribution and population densities of purple sulfur bacteria can be the availability of sulfide. The amount of sulfide present in the mat will limit the presence of oxygenic phototrophs to species able to cope with temporary exposure to sulfide. Environmental conditions on beaches in Scapa Flow are restrictive for the development of cyanobacteria, as indicated by the low abundances and few genera found (Table 2, 3). The

production of sulfide by sulfate-reducing bacteria is, among other environmental parameters, controlled by the amount and quality of organic matter in the sediment (e.g., [78]). The main sources of organic matter are decomposing macro-algae buried in the sediment [31], resulting in a heterogeneous distribution of low molecular weight organic substrates for sulfate-reducing bacterial activity.

A pronounced microheterogeneity of sulfate reduction and sulfide distribution was found in Swanbister beach mats, as indicated by the standard deviations of measured sulfate reduction rates and sulfide microprofiles (Table 4, Fig. 7A). Thus, a heterogeneous distribution of sulfide could affect the distribution of the different phototrophs. A patchy distribution of sites virtually covered by purple bacteria (pink surface) was observed on Swanbister beach during sampling in July 2000, as well as a patchy distribution of macro-algae growing on the beach or deposited on the sediment surface. Additional to organic matter supply after decomposition, organic sulfur compounds like dimethylsulfide (DMS) and dimethylsulfoniopropionate (DMSP) might be released from degrading macro-algae. Both compounds are potential substrates for purple bacteria [39], including *Thiocapsa roseopersicina* [90, 37, 38]. By providing such organic sulfur substrates, degrading macro-algae could also directly enhance growth of purple sulfur bacteria in their nearby surroundings, further contributing to their patchy distribution on these beaches.

Biomarker analysis showed that lipids reflecting the presence of methanogens (phytenes and 2,6,10,15,19-pentamethylicosane), as well as fatty acids characteristic of sulfate-reducing bacteria (*iso*- and *anteiso*-pentadecanoic acids) were abundant especially in Swanbister Bay mats (Fig. 1). With our data we can, however, only speculate on the biogeochemical importance of methanogens in the mat. As has been shown in salt marsh sediments (e.g., [66, 76]), methane production in marine sediments is most probably due to utilization of noncompetitive substrates like methylamines and DMS [43, 65]. Glycine betaine, one of the most widespread compatible solutes [94], and the osmoregulatory compound of marine algae, DMSP [42], present at high concentrations in microbial mats [39, 89], are precursors of trimethylamine and DMS [65]. Thus, these compounds could potentially play a role as substrates for methanogenesis in these mats.

Oxygen and sulfur cycling in Swanbister Bay mats

Microsensor data showed a gradual increase of both O_2 concentration and penetration with irradiance due to increasing oxygenic photosynthesis by cyanobacteria and microalgae in Swanbister Bay mats (Fig. 8, 9). Furthermore, H_2S fluxes tended to increase with irradiance

(Fig. 9), indicating higher sulfide turnover rates in light conditions. These include both higher production rates by sulfate reduction and higher sulfide consumption rates. Although (aerobic) chemolithotrophic sulfide oxidation by *T. roseopersicina* may occur in light conditions [70, 71], phototrophic oxidation (in the presence of O_2) seem to be preferred due to higher energetic yields by phototrophy than by chemotrophy [17, 84, 85]. The light-dependency of the H_2S fluxes (Fig. 9) further suggests that anoxygenic photosynthesis by purple sulfur bacteria strongly affected net H_2S consumption in light incubated Swanbister beach mats.

Microsensor data on sulfide cycling underestimate sulfur cycling in microbial mats, since fluxes calculated from microprofiles represent only net rates of sulfide turnover. As has been shown in light-incubated cyanobacterial mats [9, 88, 77], sulfate reduction can occur in the highly oxygenated surface layer. This activity, however, is not detectable with H_2S microsensors due to immediate reoxidation of the produced sulfide. Furthermore, other reduced sulfur compounds, like polysulfides, elemental sulfur and thiosulfate, which are present in Swanbister mats [86], may play a significant role in the sulfur cycle of these mats. The dominant purple sulfur bacterium in these mats, *T. roseopersicina*, is characterized by a high metabolic versatility [69, 84] and can use polysulfide [87], thiosulfate [17], and intracellular elemental sulfur [70, 71].

Oxygen consumption rates in the aphotic zone (R_{aphot}) increased with irradiance (Fig. 9). Although H_2S fluxes underestimate sulfide fluxes especially in light conditions (see Results), aerobic/oxic sulfide oxidation seemed not to have significantly contributed to R_{aphot} at higher irradiances. This points to a more important role of other O_2-consuming processes, like aerobic respiration. T-RFLP analysis together with predicted patterns of T-RFs supplied from the NCBI Bank indicated the presence of aerobic, heterotrophic alpha-proteobacteria in the upper layers of the mat, which could have contributed to O_2 consumption in that zone. As mentioned by Nagashima et al. [60], the detection of these non-phototrophic bacteria with the primer set targeting specifically the *pufM* gene conserved among purple phototrophic bacteria could be due to horizontal gene transfer. T-RFLP analysis also revealed the presence of different communities of SRB in the uppermost layers of Swanbister Bay mats (Fig. 6A). Sulfate-reducing bacteria are also characterized by their capacity for aerobic respiration [47, 81] and could have directly contributed to O_2 consumption in these mat layers.

Communities of sulfate-reducing and purple bacteria in Swanbister Bay mats

The populations of purple bacteria within the upper millimeters of the Swanbister mat (Figs. 4, 6B, 7C) experienced pronounced variations of microenvironmental conditions between dark-light transitions (Fig. 8). A minor population in the surface layer experienced highly oxic conditions during light periods and micro-oxic conditions during the night, with sulfide being available only during the night at low concentrations (Figs. 7A, 8). Populations in the depth interval between the surface layer and the permanently anoxic zone (Figs. 7C, 8) were only exposed to sulfide during darkness. In light, these populations experience, at least temporarily, simultaneously low O_2 and sulfide concentrations, since the depth of the oxygen-sulfide interface increased with increasing irradiance (Fig. 8). This condition is subsequently followed by exposure to either solely O_2 or sulfide at further increasing or decreasing irradiances. Populations present below this transition zone always experienced sulfide, but may have been light limited (Fig. 4). Thus, the full spectrum of metabolic versatility may be used by different populations of *T. roseopersicina* zonated in the mats. This includes chemolithotrophy during darkness using O_2 and sulfide as substrates, degradation of storage carbohydrates (glycogen) under anoxic dark conditions, photolithotrophy in the light in the presence of only sulfide, both sulfide and O_2, or in the presence of only O_2 using intracellular elemental sulfur or other external reduced sulfur compounds [69, 84].

A pronounced diversity and a depth-dependent distribution of purple bacteria was found by T-RFLP analysis (Fig. 6B). From *pufM* T-RFLP profiles, a T-RF of 93 bp (restriction enzyme HaeIII) was detected in all mat layers within the top 3 mm of the mat. The sequences of the *pufL* and *pufM* genes of *T. roseopersicina* strain T. ork were recently determined (A. Fourçans, R. Duran, P. Caumette (unpublished), accession number AJ544223) and a predictive T-RF of 92 bp was found for the *pufM* gene of *T. roseopersicina* digested with this restriction enzyme. So, the observed T-RF could correspond to the predominant purple sulfur bacterium *T. roseopersicina*. The results also show that in Swanbister mats different communities of anoxygenic phototrophs are zonated within the mat in response to the microenvironmental conditions (Fig. 6D). The predominant T-RF of 214 bp obtained with restriction enzyme Hin6I represents the dominating anoxygenic phototrophic community in Swanbister beach mats, as deduced from the sequences and T-RFs of purple bacteria presently available. Although predictive digestions made *in silico* on the RDP website (TAP: T-RFLP Analysis Program) cannot be used for phylogenetic identification of communities based on their T-RFs [58], this T-RF could be related to the species *Allochromatium vinosum*. The presence of this major species seemed to be independent of depth, O_2 and irradiance (Fig. 6D)

and was distributed all over the mat (data not shown). This species was also found by van Gemerden et al. [86]. Further determination of *pufM* gene sequences from isolated purple bacteria will be useful to obtain more information about the dominant members.

Two closely related community clusters of purple bacteria were found in the depth layer from 1-3 mm (Fig. 6B), i.e. in the transition layer of the mat. Communities present in this layer experienced pronounced variations, ranging from highly oxic during high light conditions to sulfidic conditions during darkness. These pronounced variations seem to select for versatile species of purple bacteria (also others than *T. roseopersicina*) able to thrive under these conditions. As indicated by T-RFLP analysis, these could include species of the genus *Allochromatium*, which are characterized by a pronounced metabolic versatility [40, 69].

Since microsensor and T-RFLP analyses were not performed in exactly the same Swanbister mat sample, some deviations concerning the localization of this transition layer might have occurred between both samples. Furthermore, the O_2 and sulfide microgradients measured in a lab under controlled conditions similar to the conditions during immersion periods might change during emersion periods as occurring *in situ* during low tide. However, our laboratory microsensor data compare relatively well to microsensor profiles measured *in situ* at low tide by van Gemerden et al. [86]. Furthermore, the fact that these two community clusters were less related to the community in the upper mat layers than to the community below 3 mm depth, points to an O_2-dependent distribution of purple bacteria in Swanbister Bay mats. This is consistent with the CCA showing that O_2 is the most important variable influencing the distribution of purple bacteria. Thus, despite the predominance of *T. roseopersicina* in these mats, a variety of different purple bacteria may have stratified in response to O_2 and sulfide gradients.

Also the distribution and diversity of sulfate-reducing bacteria seemed to be partly influenced by O_2. A distinct and related SRB community cluster was found in the uppermost mat layer, clearly differing from the communities found at increasing depths (Fig. 6A). Thus, the almost permanent oxic conditions in the uppermost mat layer (Figs. 7, 8) may select for especially O_2-tolerant SRB species. Communities of SRB below this layer are exposed to anaerobic conditions at least during low light and dark periods (Figs. 7, 8). Several SRB, e.g., *Desulfovibrio* species and *Desulfonema*-related bacteria, possess adaptive strategies for survival under oxic conditions, enabling them to thrive in microbial mats. These strategies include aggregation, migration, aerotaxis and O_2 respiration [46, 47, 81, 22, 59, 77, 14].

The CCA demonstrated that factors other than the presence of O_2 also influenced the depth-distribution and diversity of SRB. The influence of irradiance at Chl *a*- and BChl *a*-

absorption wavelengths (Fig. 6C) could be the result of interactions between phototrophs and SRB and might be considered as an indirect irradiance effect. The finding of some groups at different depths was not directly correlated with O_2 or sulfide gradients. Sulfate-reducing bacteria are characterized by a pronounced metabolic versatility and are apparently able to catalyze all reactions of a complete sulfur cycle [13, 14]. This includes the use of a variety of electron acceptors like sulfite, sulfur, thiosulfate, nitrate, nitrite, O_2, Fe(III), as well as their ability to perform disproportionation and oxidation of diverse sulfur compounds (sulfur, thiosulfate, sulfite), and aerobic respiration [3, 44, 19, 15, 12, 55, 45, 26, 95]. Thus, not only the presence of O_2 and the availability of organic substrates, but also the distribution of sulfur compounds like thiosulfate, sulfur, and sulfite could influence the distribution of SRB in this mat.

Microbial communities of coastal microbial mats on the Orkney Islands are apparently more diverse than previously described. Furthermore, although mats on Swanbister beach could be distinguished concerning population density and localization of the purple layer on or below the mat surface (Figs. 4, 5), a clear differentiation between different microbial mats as found and described earlier [86] was not possible in July 2000. In particular, sediments populated only by purple bacteria and characterized by an absence of Chl *a*-containing oxygenic phototrophs could not be found. This type of mat was previously described as one of the three types of mat systems developing especially on Swanbister beach [86]. The enforcement of strict waste discharge regulations has lead to improved waste water treatment in the area over the last decade, which has significantly reduced the amount of organic matter discharged onto the beaches. These changes have created environmental conditions less favorable for the exclusive development of purple sulfur bacteria, which would also account for the increased microbial diversity in these mat sediments.

ACKNOWLEDGEMENTS

We acknowledge the financial support by the EC (MATBIOPOL project, grant EVK3-CT-1999-00010) and the Danish Natural Science Research Council (M.K., contract no. 9700549). The staff and especially Alex Simpson, Director of the Orkney County Council Marine Unit laboratory, are gratefully acknowledged for providing excellent laboratory facilities. Anni Glud is acknowledged for the construction of the microsensors.

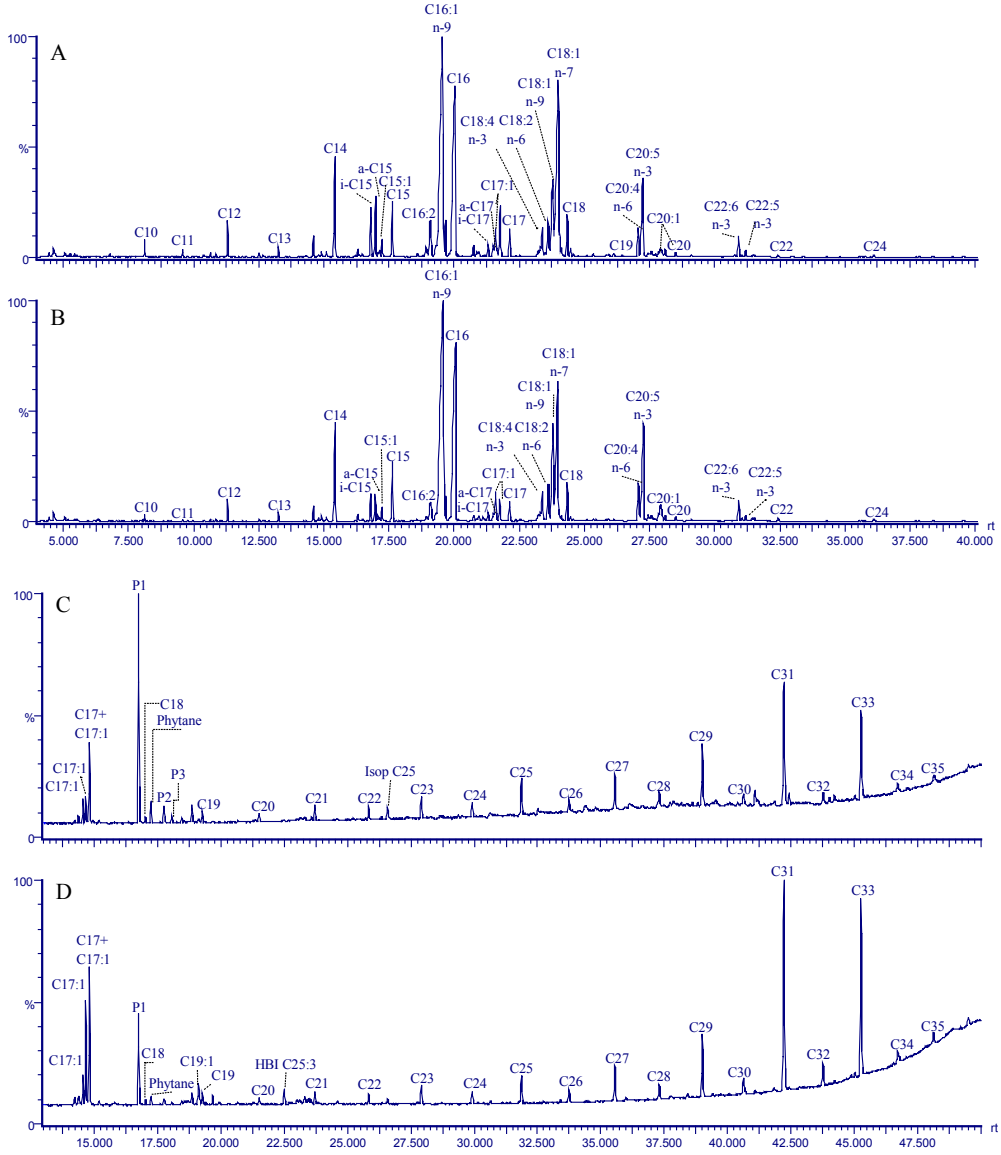

Figure 1. Gas chromatographic profiles showing the major fatty acids (A, B) and the major hydrocarbons (C, D) in microbial mats from Swanbister (A, C) and Waulkmill (B, D) Bay. P1 denotes phyt-1-ene and P2 and P3 are phytenes. HBI C25, highly branched isoprenoid hydrocarbon. Isop C_{25}, 2,6,10,15,19-pentamethylicosane.

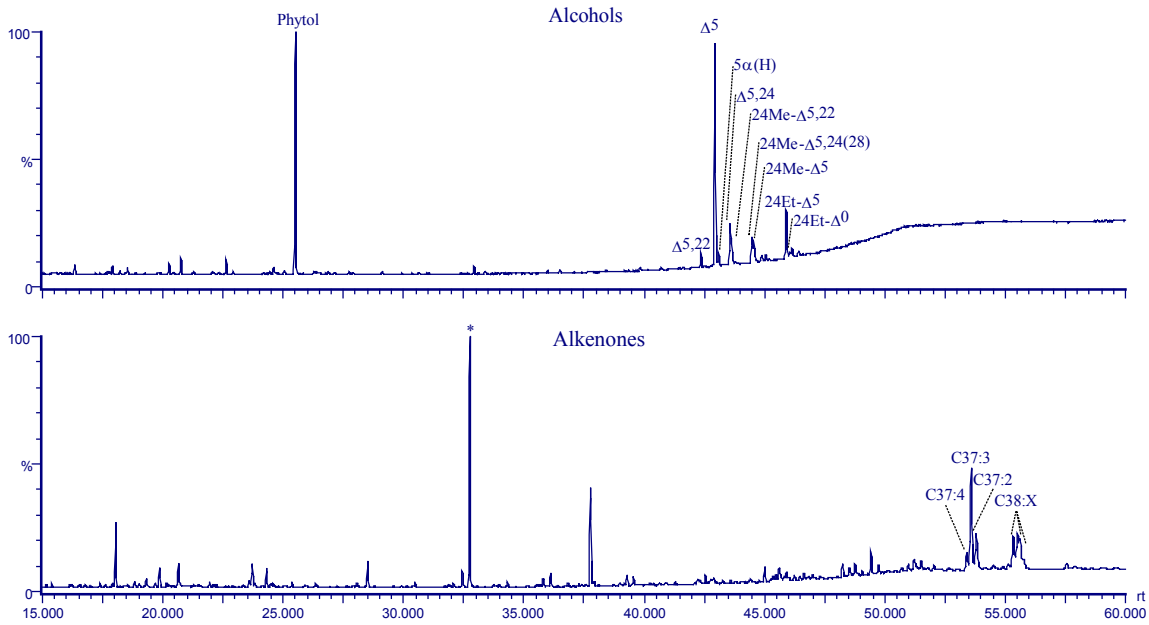

Figure 2. Gas chromatographic profiles showing the major alcohols (upper graph) and alkenones (lower graph) in Waulkmill Bay mats.

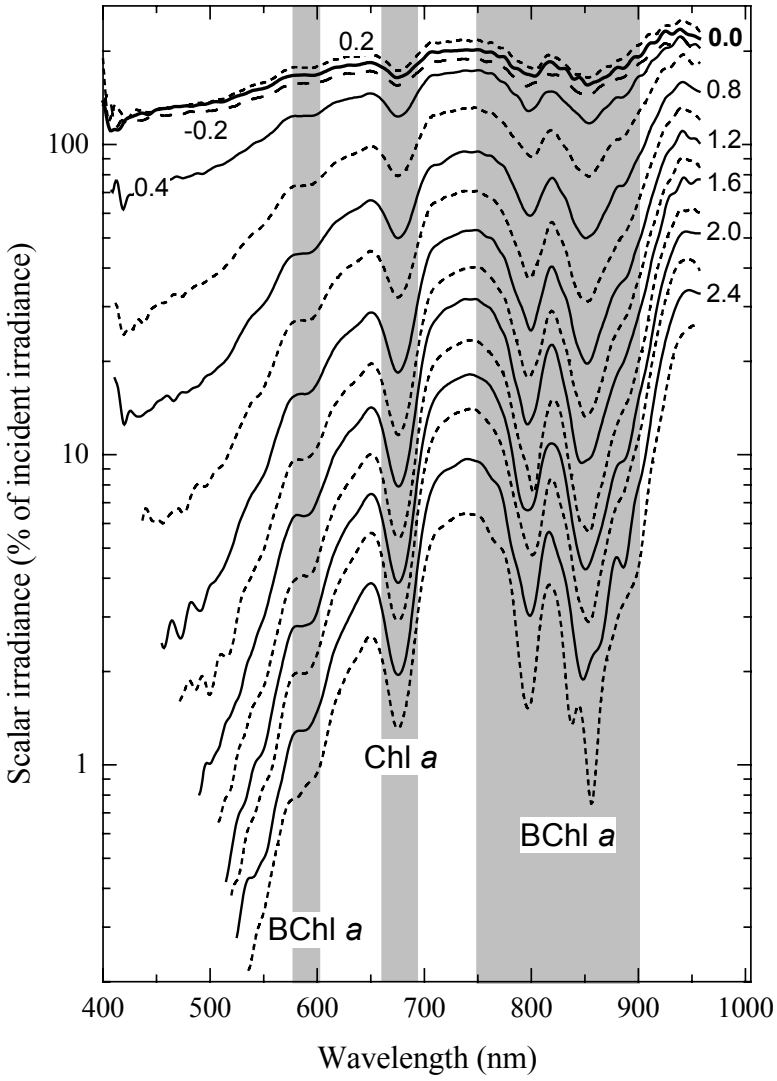

Figure 3. Depth profile of spectral scalar irradiance in a Waulkmill Bay mat normalized to the downwelling spectral scalar irradiance at the mat surface. Numbers on curves indicate depth (mm). Depth 0 indicates the mat surface and increasing positive numbers indicate increasing depths in the mat.

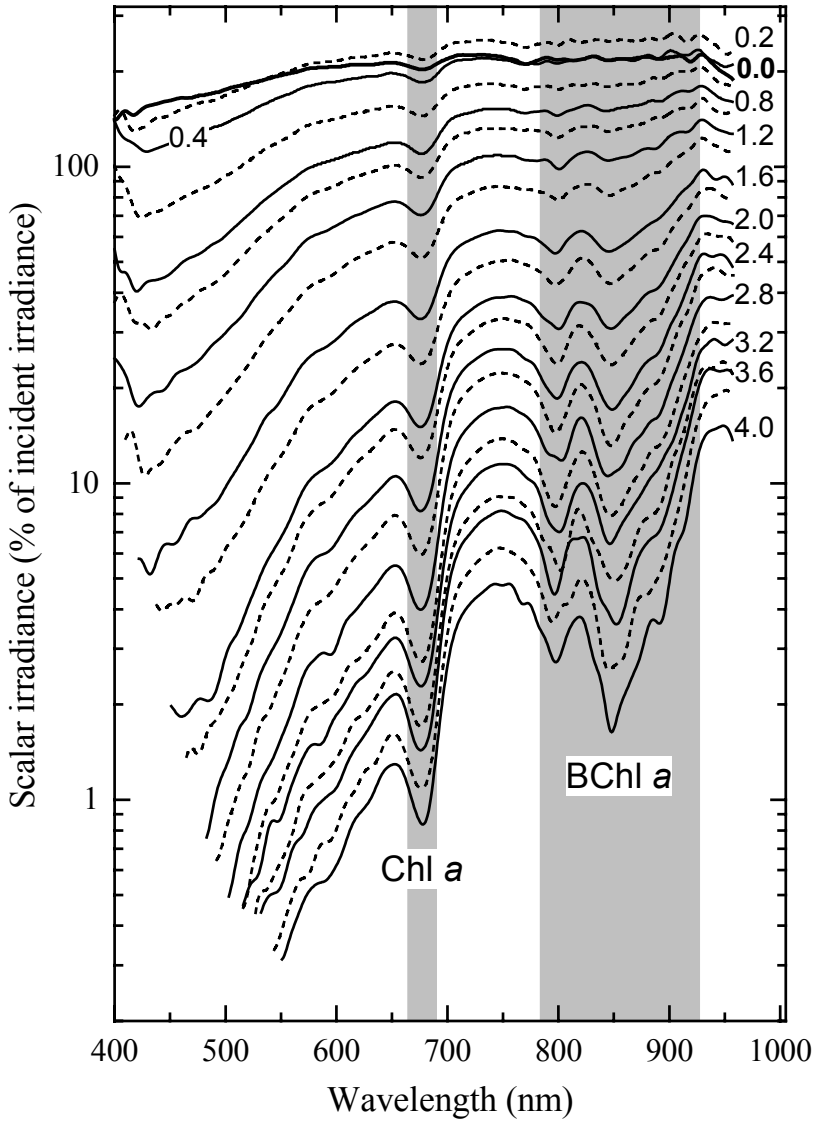

Figure 4. Depth profile of spectral scalar irradiance in a Swanbister Bay mat normalized to the downwelling spectral scalar irradiance at the mat surface. Numbers indicate depth (mm).

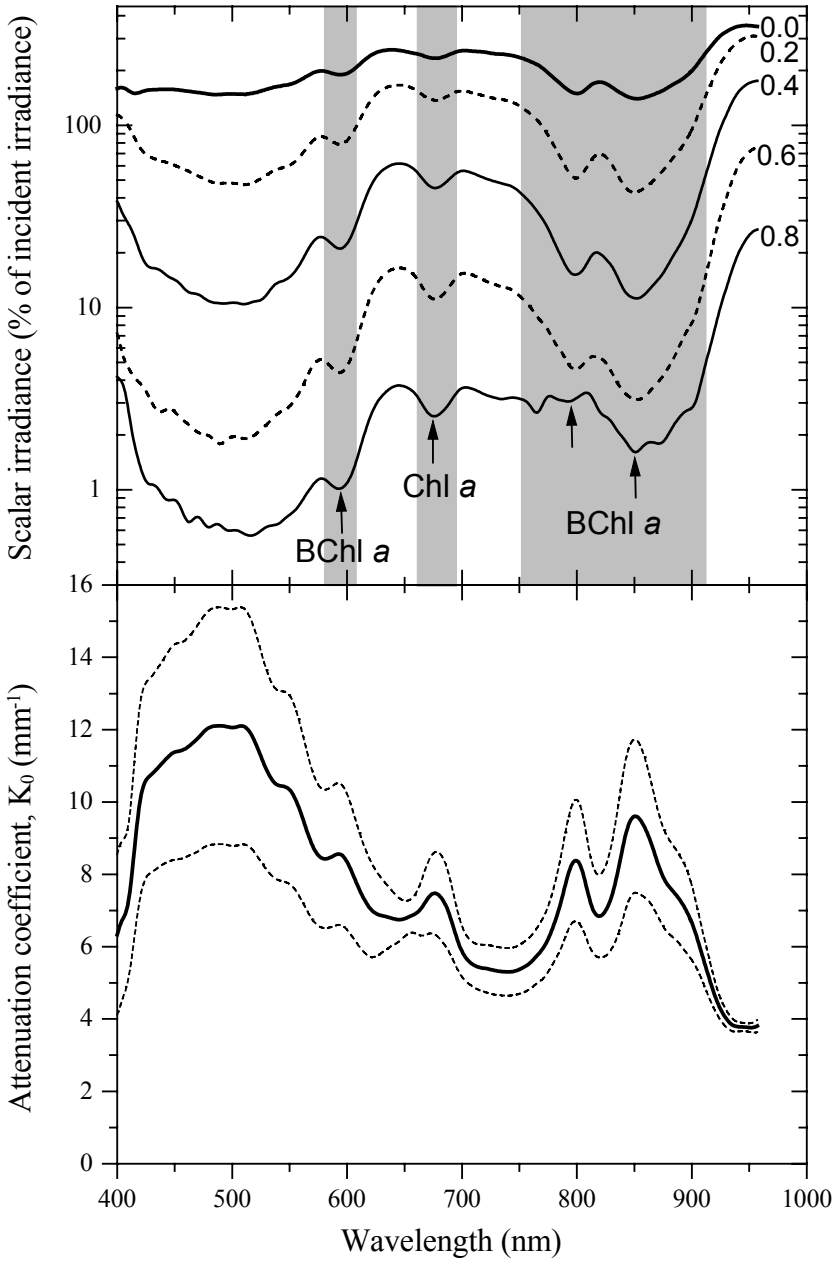

Figure 5. Depth profile of spectral scalar irradiance (upper graph) in a Swanbister Bay mat densely covered by purple bacteria. The profiles of spectral scalar irradiance were normalized to the downwelling spectral scalar irradiance at the mat surface. Numbers indicate depth (mm). Average attenuation spectrum of scalar irradiance over the depth interval of 0-0.8 mm (lower graph), calculated from the spectral scalar irradiance profiles shown in the upper graph. Broken lines in the lower graph indicate the standard deviations of the attenuation coefficients, K_0.

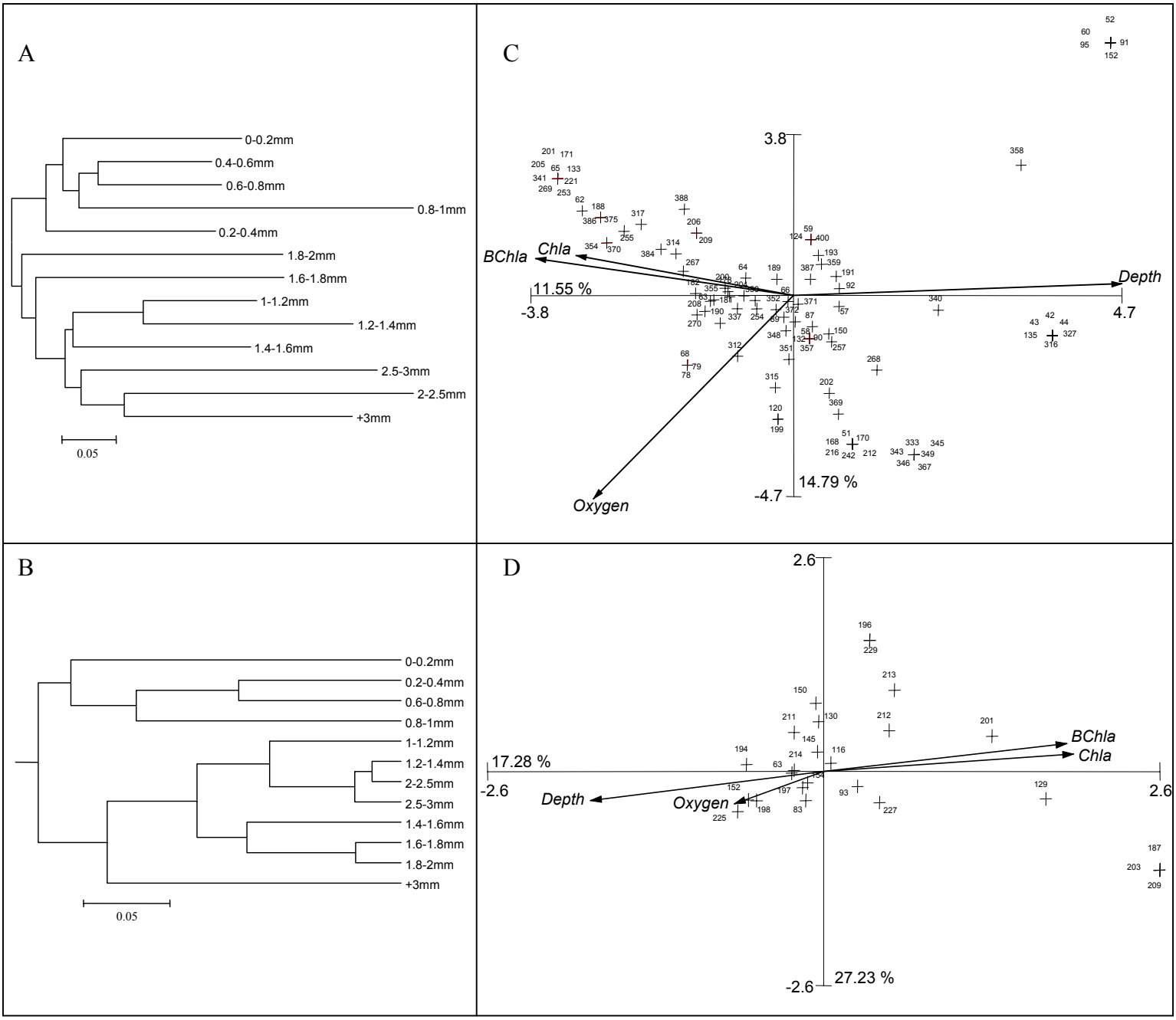

Figure 6. The sulfate-reducing (SRB) (A) and the purple anoxygenic bacterial (PAB) (B) community relatedness of each layer of a Swanbister Bay mat based on the Jaccard coefficient. Each community was represented by a phylogenetic signature constructed by stacking two individual 5' T-RFLP patterns corresponding to the HaeIII and Hin6I digests of the 16S rRNA encoding gene for the SRB and the *pufM* gene for the PAB. Canonical correspondence analysis (CCA) between SRB (C) or PAB (D) (T-RF in base pairs) and environmental variables: scalar irradiance at characteristic Chl *a*- (676 nm) and BChl *a*- (845 nm) absorption wavelengths, O_2 concentration, and depth.

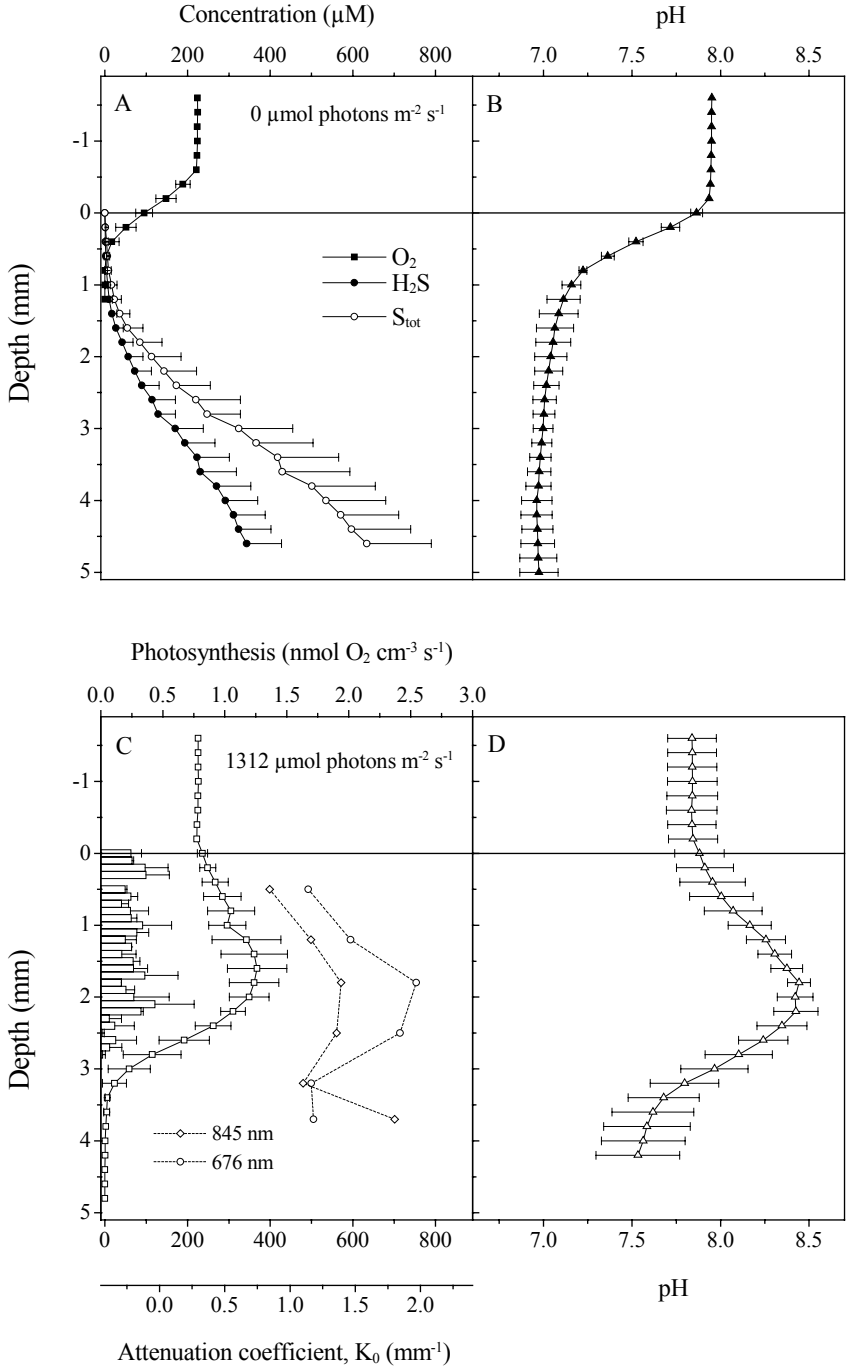

Figure 7. Average profiles (n = 2-3) of gross photosynthesis (bars), O_2, H_2S, sulfide (S_{tot}) (A, C) and pH (B, D) measured at different positions in a Swanbister Bay mat at 0 (A, B) and 1312 µmol photons m^{-2} s^{-1} (C, D). Error bars indicate standard deviation. Depth profiles of the vertical attenuation coefficient, K_0, at characteristic Chl *a*- (676 nm) and BChl *a*- (845 nm) absorption wavelengths as calculated from the depth profiles of spectral scalar irradiance measured in the same mat sample (profiles shown in Fig. 4).

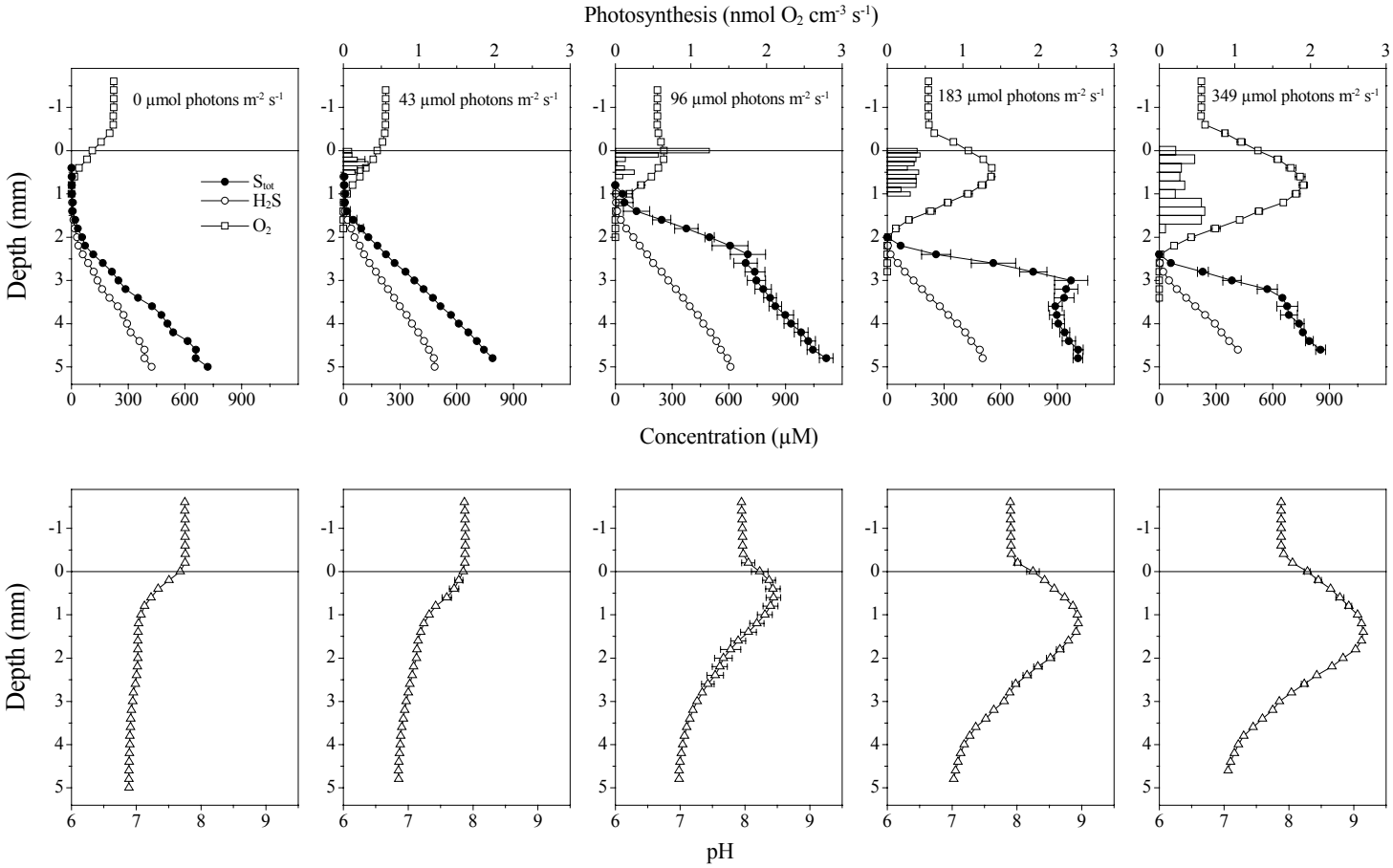

Figure 8. Average profiles (n = 1-3) of gross photosynthesis (bars), O_2, H_2S, sulfide (S_{tot}) (upper panel) and pH (lower panel) measured at a fixed position in the same mat from Swanbister Bay at increasing downwelling irradiances. Error bars indicate standard deviation.

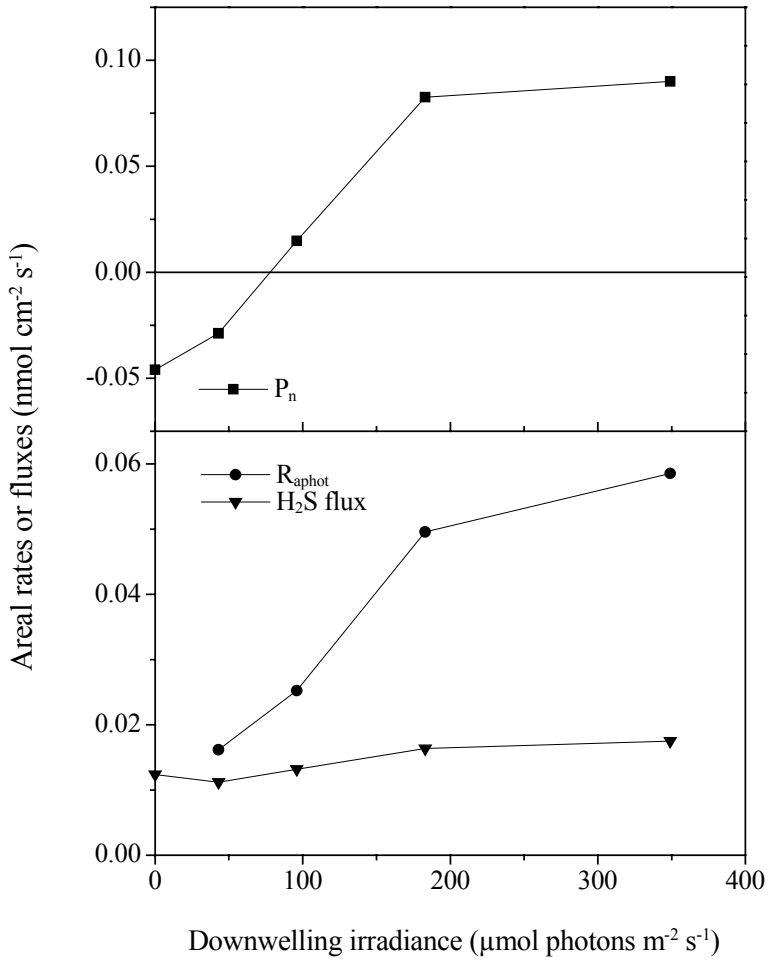

Figure 9. Areal rates of net photosynthesis (P_n), O_2 consumption in the aphotic zone (R_{aphot}) and of net H_2S production/consumption (H_2S flux) versus irradiance in the Swanbister Bay mat.

Table 1: Phylogenetic and photosynthetic primers used in T-RFLP analysis. Amplimer sizes for the different primer sets: *16S rDNA* eubacteria, 918 bp; *16S rDNA* sulfate-reducing bacteria, 377 bp; *pufM*, 229 bp. All 16S rDNA primer names are based on *E. coli* numbering. SRB denotes sulfate-reducing bacteria and PAB purple anoxygenic bacteria.

Primer	**Sequence (5'→3')**	**Target gene**	**Target group**	**Reference**
8F	AGA GTT TGA TCC TGG CTC AG	*ssu 16S rDNA*	Eubacteria	[54]
926R	CCG TTC AAT TCC TTT RAG TTT	*ssu 16S rDNA*	Eubacteria	[54]
BSR 385R	CGG CGT CGC TGC GTC AGG	*ssu 16S rDNA*	SRB	[2]
PB 557F	CGCACCTGGACTGGAC	*PufM*	PAB	[1]
PB 750R	CCCATGGTCCAGCGCCAGAA	*PufM*	PAB	[1]

Table 2: Filamentous and unicellular cyanobacteria in Waulkmill Bay mats tentatively identified according to Castenholz [10] and their characteristics and depth distribution as determined by CLSM and light microscopy.

Filamentous cyanobacteria						
Genera (tentatively)	**Diameter (μm)**	**Septation**	**Gas vacuoles**	**Sheath**	**Abundance**	**Depth (mm)**
Lyngbya sp.	6.25-10.30	+	-	+	(+++)	0; 1.85
Oscillatoria sp.	12.5-14	+	-	+	(+++)	0; 1.85
Leptolyngbya sp.	0.94	+	-	+ (thin)	(++)	3.2
Pseudoanabena sp.	2.5	+	+	+ (thin)	(+)	1.85

Unicellular cyanobacteria					
Genera (tentatively)	**Diameter (μm)**	**Cell division**	**Sheath**	**Abundance**	**Depth (mm)**
Pleurocapsa-group	2 × 3	Binary fissions in many different planes	+	(+++)	3.2
Gloeocapsa-group	4 - 8	2 or 3 planes	+	(+++)	0; 1.85; 3.2
Microcystis sp.	1.9 × 1.9	Binary fissions in many different planes	+	(++)	0; 1.85; 3.2; 5.1
Aphanothece sp.	5 × 7	1 plane	+ (thin)	(++)	0
Pleurocapsa-group	Diverse size and form	Binary fissions in several planes (pseudofilaments)	-	(+)	1.85

Table 3: Filamentous and unicellular cyanobacteria in Swanbister Bay mats tentatively identified according to Castenholz [10] and their characteristics and depth distribution as determined by CLSM and light microscopy.

Filamentous cyanobacteria						
Genera (tentatively)	**Diameter (μm)**	**Septation**	**Gas vacuoles**	**Sheath**	**Abundance**	**Depth (mm)**
Borzia *sp.*	1.88 (short filaments)	+	-	+ (thin)	(+)	1.55

Unicellular cyanobacteria					
Genera (tentatively)	**Diameter (μm)**	**Cell division**	**Sheath**	**Abundance**	**Depth (mm)**
Pleurocapsa-group (*Microcystis* sp.)	1.9 × 1.9	Binary fissions in many different planes	+	(+++)	0; 1.55; 3.35
Pleurocapsa-group	Diverse size and form	Binary fissions in several planes (pseudofilaments)	-	(+++)	0; 1.55; 3.35
Pleurocapsa-group (*Stanieria* sp.)	2 × 3	Multiple fissions or in combination with limited (1-3) binary fissions	-	(+)	3.35

Table 4: Depth distribution of average sulfate reduction rates (n = 2-3) in Swanbister Bay mats.

Depth (cm)	Sulfate reduction rate (nmol cm^{-3} d^{-1})
0-1	234 ± 58
1-2	297 ± 33
2-3	245 ± 56

REFERENCES

1. Achenbach LA, Carey J, Madigan MT (2001) Photosynthetic and phylogenetic primers for detection of anoxygenic phototrophs in natural environments. Appl Environ Microbiol 67:2922-2926
2. Amann RI, Binder BJ, Olson RJ, Chisholm SW, Devereux R, Stahl DA (1990) Combination of 16S rRNA-targeted oligonucleotide probes with flow cytometry for analyzing mixed microbial populations. Appl Environ Microbiol 56:1919-1925
3. Bak F, Cypionka H (1987) A novel type of energy metabolism involving fermentation of inorganic sulphur compounds. Nature 326:891-892
4. Ballantine JA, Lavis A, Morris RJ (1979) Sterols of the phytoplankton - effects of illumination and growth stage. Phytochemistry 18:1459-1466
5. Barbe A, Grimalt JO, Pueyo JJ, Albaigés J (1990) Characterization of model evaporitic environments through the study of lipid components. Org Geochem 16:815-828
6. Béjà O, Suzuki MT, Heidelberg JF, Nelson WC, Preston CM, Hamada T, Eisen JA, Fraser CM, DeLong EF (2002) Unsuspected diversity among marine aerobic anoxygenic phototrophs. Nature 415:630-633
7. Blumer M, Guillard RRL, Chase T (1971) Hydrocarbons of marine phytoplankton. Mar Biol 8:183-189
8. Broecker WS, Peng T-H (1974) Gas exchange rates between air and sea. Tellus 26:21-35
9. Canfield DE, Des Marais DJ (1991) Aerobic sulfate reduction in microbial mats. Science 251:1471-1473
10. Castenholz RW (2001) Phylum BX. Cyanobacteria. Oxygenic photosynthetic bacteria. In: Boone DR, Castenholz RW (eds) Bergey´s manual of systematic bacteriology. The Archea and the deeply branching and phototrophic bacteria, vol. 1, Springer, Berlin, pp 473-599
11. Chuecas L, Riley JP (1969) Component fatty acids of the total lipids of some marine phytoplankton. J Mar Biol Ass UK 49(97-116)
12. Coleman ML, Hedrick DB, Lovley DR, White DC, Pye K (1993) Reduction of Fe(III) in sediments by sulphate-reducing bacteria. Nature 361:436-438
13. Cypionka H (1994) Novel metabolic capacities of sulfate-reducing bacteria, and their activities in microbial mats. In: Stal LJ, Caumette P (eds.) Microbial Mats: Structure, Development and Environmental Significance, NATO ASI Series G vol. 35, Springer, Berlin, pp 367-376

14. Cypionka H (2000) Oxygen respiration by *Desulfovibrio* species. Annu Rev Microbiol 54:827-848
15. Dannenberg S, Kroder M, Dilling W, Cypionka H (1992) Oxidation of H_2, organic compounds and inorganic sulfur compounds coupled to reduction of O_2 or nitrate by sulfate-reducing bacteria. Arch Microbiol 158:93-99
16. de Wit R, Jonkers HM, van den Ende FP, van Gemerden H (1989) *In situ* fluctuations of oxygen and sulphide in marine microbial sediment ecosystems. Neth J Sea Res 23:271-281
17. de Wit R, van Gemerden H (1987) Chemolithotrophic growth of the phototrophic sulfur bacterium *Thiocapsa roseopersicina*. FEMS Microbiol Ecol 45:117-126
18. Didyk BM, Simoneit BRT, Brassell SC, Eglinton G (1978) Organic geochemical indicators of palaeoenvironmental conditions of sedimentation. Nature 272:216-222
19. Dilling W, Cypionka H (1990) Aerobic respiration in sulfate-reducing bacteria. FEMS Microbiol Lett 71:123-128
20. Eglinton G, Hamilton RJ (1967) Leaf epicuticular waxes. Science 156:1322
21. Epping EHG, Khalili A, Thar R (1999) Photosynthesis and the dynamics of oxygen consumption in a microbial mat as calculated from transient oxygen microprofiles. Limnol Oceanogr 44:1936-1948
22. Eschemann A, Kühl M, Cypionka H (1999) Aerotaxis in *Desulfovibrio*. Environ Microbiol 1:489-495
23. Fonselius SH (1983) Determination of hydrogen sulphide. In: Grasshoff K, Ehrhardt M, Kremling K (eds) Methods of seawater analysis, Verlag Chemie, Weinheim, pp 73-80
24. Fossing H, Jørgensen BB (1989) Measurement of bacterial sulfate reduction in sediments: evaluation of a single-step chromium reduction method. Biogeochemistry 8:205-222
25. Fromin N, Hamelin J, Tarnawski S, Roesti D, Jourdain-Miserez K, Forestier N, Teyssier-Cuvelle S, Gillet F, Aragno M, Rossi P (2002) Statistical analysis of denaturing gel electrophoresis (DGE) fingerprinting patterns. Environ Microbiol 4:634-643
26. Fuseler K, Krekeler D, Sydow U, Cypionka H (1996) A common pathway of sulfide oxidation by sulfate-reducing bacteria. FEMS Microbiol Lett 144:129-134
27. García HE, Gordon LI (1992) Oxygen solubility in seawater: Better fitting equations. Limnol Oceanogr 37:1307-1312
28. Grant J, Gust G (1987) Prediction of coastal sediment stability from photopigment content of mats of purple sulphur bacteria. Nature 330:244-246

29. Grimalt JO, de Wit R, Teixidor P, Albaiges J (1992) Lipid biogeochemistry of *Phormidium* and *Microcoleus* mats. Org Geochem 19:509-530
30. Han J, McCarthy ED, Calvin M, Benn MH (1968) Hydrocarbon constituents of the blue-green algae *Nostoc muscorum*, *Anacystis nidulans*, *Phormidium luridum* and *Chlorogloea fritschii*. J Chem Soc C:2785-2791
31. Herbert RA (1985) Development of mass blooms of photosynthetic bacteria on sheltered beaches in Scapa Flow, Orkney Islands. Proc Roy Soc Edinburgh 87B:15-25
32. Hershey JP, Plese T, Millero FJ (1988) The pK_{1*} for the dissociation of H_2S in various ionic media. Geochim Cosmochim Acta 52:2047-2051
33. Hoffmann C (1942) Beiträge zur Vegetation des Farbstreifen-Sandwattes. Kieler Meeresforschungen Sonderheft 4:85-108
34. Holzer G, Oro J, Tornabene TG (1979) Gas chromatographic-mass spectrometric analysis of neutral lipids from methanogenic and thermoacidophilic bacteria. J Chromatogr 186:795-809
35. Isaksen M, Finster K (1996) Sulfate reduction in the root zone of the sea grass *Zostera noltii* on the intertidal flats of a coastal lagoon (Arcachon, France). Mar Ecol Prog Ser 137:187-194
36. Jeroschewski P, Steuckart C, Kühl M (1996) An amperometric microsensor for the determination of H_2S in aquatic environments. Anal Chem 68:4351-4357
37. Jonkers HM, de Bruin S, van Gemerden H (1998a) Turnover of dimethylsulfoniopropionate (DMSP) by the purple sulfur bacterium *Thiocapsa roseopersicina* M11: ecological implications. FEMS Microbiol. Ecol 27:281-290
38. Jonkers HM, Jansen M, Van der Maarel MJEC, van Gemerden H (1999) Aerobic turnover of dimethyl sulfide by the anoxygenic phototrophic bacterium *Thiocapsa roseopersicina*. Arch Microbiol 172:150-156
39. Jonkers HM, Koopmans GF, van Gemerden H (1998b) Dynamics of dimethyl sulfide in a marine microbial mat. Microb Ecol 36:93-100
40. Kämpf C, Pfennig N (1980) Capacity of Chromatiaceae for chemotrophic growth. Specific respiration rates of *Thiocystis violacea* and *Chromatium vinosum*. Arch Microbiol 127:125-135
41. Kates M, Tremblay P, Anderson R, Volcani BE (1978) Identification of the free and conjugated sterol in a non-photosynthetic diatom, *Nitzschia alba*, as 24-methylene cholesterol. Lipids 13:34-41

42. Kelly DP, Smith NA (1990) Organic sulfur compounds in the environment. Adv Microb Ecol. 11:345-385
43. King GM (1984) Utilisation of hydrogen, acetate and "noncompetitive" substrates by methanogenic bacteria in marine sediments. Geomicrobiol J 3:275-306
44. Krämer M, Cypionka H (1989) Sulfate formation via ATP sulfurylase in thiosulfate- and sulfite-disproportionating bacteria. Arch Microbiol 151:232-237
45. Krekeler D, Cypionka H (1995) The preferred electron acceptor of *Desulfovibrio desulfuricans* CSN. FEMS Microbiol Ecol 17:271-278
46. Krekeler D, Sigalevich P, Teske A, Cypionka H, Cohen Y (1997) A sulfate-reducing bacterium from the oxic layer of a microbial mat from Solar Lake (Sinai), *Desulfovibrio oxyclinae* sp. nov. Arch Microbiol 167:369-375
47. Krekeler D, Teske A, Cypionka H (1998) Strategies of sulfate-reducing bacteria to escape oxygen stress in a cyanobacterial mat. FEMS Microbiol Ecol 25:89-96
48. Kühl M, Fenchel T (2000) Bio-optical characteristics and the vertical distribution of photosynthetic pigments and photosynthesis in an artificial cyanobacterial mat. Microb Ecol 40:85-93
49. Kühl M, Jørgensen BB (1992) Spectral light measurements in microbenthic phototrophic communities with a fiber-optic microprobe coupled to a sensitive diode array detector. Limnol Oceanogr 37:1813-1823
50. Kühl M, Steuckart C, Eickert G, Jeroschewski P (1998) A H_2S microsensor for profiling biofilms and sediments: application in an acidic lake sediment. Aquat Microb Ecol 15:201-209
51. Kumar S, Tamura K, Jakobsen IB, Nei M (2001) MEGA2: Molecular evolutionary genetics analysis software, Bioinformatics
52. Lassen C, Ploug H, Jørgensen BB (1992) A fibre-optic scalar irradiance microsensor: Application for spectral light measurements in sediments. FEMS Microbiol Ecol 86:247-254
53. Li Y-H, Gregory S (1974) Diffusion of ions in sea water and in deep-sea sediments. Geochim Cosmochim Acta 38:703-714
54. Liu WT, Marsh TL, Cheng H, Forney LJ (1997) Characterization of microbial diversity by determining terminal restriction fragment length polymorphisms of genes encoding 16S rRNA. Appl Environ Microbiol 63:4516-4522
55. Lovley DR, Phillips EJP (1994) Novel processes for anaerobic sulfate production from elemental sulfur by sulfate-reducing bacteria. Appl Environ Microbiol 60:2394-2399

56. Maidak BL, Cole JR, Lilburn TG, Parker CTJ, Saxman PR, Farris RJ, Garrity GM, Olsen GJ, Schmidt TM, Tiedje JM (2001) The RDP-II (Ribosomal Database Project). Nucleic Acids Res 29:173-174
57. Marlowe IT, Brassell SC, Eglinton G, Green JC (1984) Long chain unsaturated ketones and esters in living algae and marine sediments. Org Geochem 6:135-141
58. Marsh TL, Saxman P, Cole J, Tiedje J (2000) Terminal restriction fragment length polymorphism analysis program, a web-based research tool for microbial community analysis. Appl Environ Microbiol 66:3616-3620
59. Minz D, Flax JL, Green SJ, Muyzer G, Cohen Y, Wagner M, Rittmann BE, Stahl DA (1999) Diversity of sulfate-reducing bacteria in oxic and anoxic regions of a microbial mat characterized by comparative analysis of dissimilatory sulfite reductase genes. Appl Environ Microbiol 65:4666-4671
60. Nagashima KVP, Hiraishi A, Shimada K, Matsuura K (1997) Horizontal transfer of genes coding for the photosynthetic reaction centers of purple bacteria. J Mol Evol 45:131-136
61. Nes WR, McKean ML (1977) Biogeochemistry of steroids and other isoprenoids. University Park Press, Baltimore.
62. Nichols PD, Volkman JK, Palmisano AC, Smith GA, White DC (1988) Occurrence of an isoprenoid C_{25} diunsaturated alkene and high neutral lipid content in Antarctic sea-ice diatom communities. J Phycol 24:90-96
63. Nishimura M, Koyama T (1977) The occurrence of stanols in various living organisms and the behaviour of sterols in contemporary sediments. Geochim Cosmochim Acta 41:379-385
64. Orcutt DM, Paterson GW (1975) Sterol, fatty acid and elemental composition of diatoms grown in chemically defined media. Comp Biochem Physiol 50B:579-583
65. Oremland RS, King GM (1989) Methanogenesis in hypersaline environments. In: Cohen Y, Rosenberg E (eds) Microbial mats: Physiological ecology of benthic microbial communities, American Society for Microbiology, Washington D.C., pp 180-190
66. Oremland RS, Marsh LM, Polcin S (1982) Methane production and simultaneous sulfate reduction in anoxic, salt marsh sediments. Nature 296:143-145
67. Paoletti C, Pushparaj B, Florenzano G, Capella P, Lercker G (1976) Unsaponifiable matter of green and blue-green algal lipids as a factor of biochemical differentiation of their biomass: II. Terpenic alcohol and sterol fractions. Lipids 11:266-271
68. Patterson GW (1974) Sterols of some green algae. Comp Biochem Physiol 47B:453-457

69. Pfennig N, Trüper HG (1992) The family Chromatiaceae. In: Balows A, Trüper HG, Dworkin M, Harder W, Schleifer K-H (eds) The Prokaryotes, Springer, Berlin, pp 3200-3221
70. Pringault O, de Wit R, Caumette P (1996) A benthic gradient chamber for culturing phototrophic sulfur bacteria on reconstituted sediments. FEMS Microbiol Ecol 20:237-250
71. Pringault O, de Wit R, Kühl M (1999) A microsensor study of the interaction between purple sulfur and green sulfur bacteria in experimental benthic gradients. Microb Ecol 37:173-184
72. Revsbech NP (1989) An oxygen microelectrode with a guard cathode. Limnol Oceanogr 34:474-478
73. Revsbech NP, Jørgensen BB (1983) Photosynthesis of benthic microflora measured with high spatial resolution by the oxygen microprofile method: Capabilities and limitations of the method. Limnol Oceanogr 28:749-756
74. Revsbech NP, Jørgensen BB (1986) Microelectrodes: Their use in microbial ecology. Adv. Microb Ecol 9:293-352
75. Schouten S, van der Maarel MEJ, Huber R, Sinninghe Damsté JS (1997) 2,6,10,15,19-Pentamethylicosenes in *Methanolobus bombayensis*, a marine methanogenic archaeon and *Methanosarcina mazei*. Org Geochem 26:409-414
76. Senior E, Lindstrom EB, Banat I, Nedwell DB (1982) Sulfate reduction and methanogenesis in the sediment of a saltmarsh on the east coast of the United Kingdom. Appl Environ Microbiol 43:987-996
77. Sigalevich P, Meshorer E, Helman Y, Cohen Y (2000) Transition from anaerobic to aerobic growth conditions for the sulfate-reducing bacterium *Desulfovibrio oxyclinae* results in flocculation. Appl Environ Microbiol 66:5005-5012
78. Skyring GW (1987) Sulfate reduction in coastal ecosystems. Geomicrobiol J 5:295-374
79. Stal LJ, van Gemerden H, Krumbein WE (1985) Structure and development of a benthic marine microbial mat. FEMS Microbiol Ecol 31:111-125
80. Tabatabai MA (1974) Determination of sulfate in water samples. Sulfur Institute Journal 10:11-14
81. Teske A, Ramsing NB, Habicht K, Fukui M, Küver J, Jørgensen BB, Cohen Y (1998) Sulfate-reducing bacteria and their activities in cyanobacterial mats of Solar Lake (Sinai, Egypt). Appl Environ Microbiol 64:2943-2951

82. Tornabene TG, Langworthy TA, Holzer G, Oro J (1979) Squalenes, phytanes and other isoprenoids as major neutral lipids of methanogenic and thermoacidophilic "archaebacteria". J Molec Evol 13:73-83
83. Ullman WJ, Aller RC (1982) Diffusion coefficients in nearshore marine sediments. Limnol Oceanogr 27:552-556
84. van Gemerden H (1993) Microbial mats: a joint venture. Mar Geol 113:3-25
85. van Gemerden H, de Wit R, Tughan CS, Herbert RA (1989a) Development of mass blooms of *Thiocapsa roseopersicina* on sheltered beaches on the Orkney Islands. FEMS Microbiol Ecol 62:111-118
86. van Gemerden H, Tughan CS, de Wit R, Herbert RA (1989b) Laminated microbial ecosystems on sheltered beaches in Scapa Flow, Orkney Islands. FEMS Microbiol Ecol 62:87-102
87. Visscher PT, Nijburg JW, van Gemerden H (1990) Polysulfide utilization by *Thiocapsa roseopersicina*. Arch Microbiol 155:75-81
88. Visscher PT, Prins RA, van Gemerden H (1992) Rates of sulfate reduction and thiosulfate consumption in a marine microbial mat. FEMS Microbiol Ecol 86:283-294
89. Visscher PT, Quist P, van Gemerden H (1991) Methylated sulfur compounds in microbial mats: in situ concentrations and metabolism by a colorless sulfur bacterium. Appl Environ Microbiol 57(6):1758-1763
90. Visscher PT, van Gemerden H (1991) Photo-autotrophic growth of *Thiocapsa roseopersicina* on dimethyl sulfide. FEMS Microbiol Lett 81:247-250
91. Vogel AI (1978) Textbook of practical organic chemistry, Longman, New York
92. Volkman JK, Eglinton G, Corner EDS, Sargent JR (1980) Novel unsaturated straight-chain C_{37}-C_{39} methyl and ethyl ketones in marine sediments and a coccolithophore *Emiliania huxleyi*. Adv Org Geochem 1979:219-227
93. Volkman JK, Jeffrey SW, Nichols PD, Rogers GI, Garland CD (1989) Fatty acids and lipid composition of 10 species of microalgae used in mariculture. J Exp Mar Biol Ecol 128:219-240
94. Welsh DT (2000) Ecological significance of compatible solute accumulation by micro-organisms: from single cells to global climate. FEMS Microbiol Rev 24:263-290
95. Widdel F (1988) Microbiology and ecology of sulfate- and sulfur-reducing bacteria. In: Zehnder AJB (ed) Biology of anaerobic microorganisms, John Wiley, New York, pp 469-585

96. Wieland A, Kühl M (2000a) Irradiance and temperature regulation of oxygenic photosynthesis and O_2 consumption in a hypersaline cyanobacterial mat (Solar Lake, Egypt). Mar Biol 137:71-85
97. Wieland A, Kühl M (2000b) Short-term temperature effects on oxygen and sulfide cycling in a hypersaline cyanobacterial mat (Solar Lake, Egypt). Mar Ecol Prog Ser 196:87-102
98. Wieringa EBA, Overmann J, Cypionka H (2000) Detection of abundant sulphate-reducing bacteria in marine oxic sediment layers by a combined cultivation and molecular approach. Environ Microbiol 2:417-427

Chapitre IV : Dynamique verticale des populations bactériennes en fonction des fluctuations physico-chimiques d'un cycle nycthéméral

IV. Dynamique verticale des populations en fonction des fluctuations physico-chimiques d'un cycle nycthéméral

IV.1. Introduction

Les tapis microbiens correspondent à une stratification verticale fine de différents microorganismes. Cette structure est le résultat à la fois de microgradients verticaux de lumière, d'oxygène, et de sulfure, mais aussi des groupes bactériens fonctionnels qui la composent. De nombreux métabolismes bactériens cohabitent donc sur ces quelques millimètres de tapis, tels que les photosynthèses oxygénique ou anoxygénique, la fermentation et la sulfato-réduction (van Gemerden, 1993).

Quotidiennement, les gradients physico-chimiques fluctuent au sein du tapis en terme de distribution et de concentration (Revsbech *et al.*, 1983). Ainsi les variations de pH, de lumière, de salinité, de concentrations en oxygène et en sulfures imposent aux bactéries présentes des stress réguliers auxquels elles doivent s'adapter. Différentes stratégies sont alors utilisées par celles-ci afin d'échapper à ces fortes variations répétées. Ainsi, certaines bactéries présentent des métabolismes versatiles capables de passer de la sulfato-réduction à la respiration aérobie ou bien de la photosynthèse oxygénique à la photosynthèse anoxygénique (Moezelaar *et al.*, 1996). D'autres bactéries se protègent en formant des agrégats ou en s'associant à des particules. Des bactéries physiologiquement différentes peuvent aussi s'associer en formant des consortiums stables par un recyclage mutuel de leurs intermédiaires métaboliques respectifs (Bield and Pfennig, 1978; Cypionka *et al.*, 1985 ; Fukui *et al.*, 1999).

La migration reste un processus majeur d'adaptation des bactéries leurs permettant de fuir les conditions défavorables ou bien de rechercher les conditions environnementales optimales à leurs croissances (Bebout and Garcia-Pichel, 1995 ; García-Pichel *et al.*, 1994 ; Krekeler *et al.*, 1998 ; Pringault and Garcia-Pichel, 2003 ; Teske *et al.*, 1998; Thar and Kuhl, 2001). Les bactéries mobiles contrôlent leurs déplacements en réponse à différents stimuli tels que les composés chimiques, la lumière ou le potentiel redox. Ces différents comportements entrent en jeu dans les phénomènes dits d'énergie-tactisme, incluant l'aéro-tactisme, le photo-tactisme, le redox-tactisme, le chimio-tactisme vers les sources de carbone et le tactisme vers les accepteurs d'électrons (Alexandre and Zhulin, 2001; Alexandre *et al.*, 2004; Taylor *et al.*, 1999).

Ce chapitre propose l'étude de la distribution spatio-temporelle de différents groupes fonctionnels des tapis microbiens, au cours d'un cycle nycthéméral, afin d'appréhender leurs comportements.

Le premier article "Vertical shift of phototrophic bacterial communities during a diel cycle in a cyanobacterial microbial mat (Salins-de-Giraud, Camargue, France) s'est focalisé sur l'étude des microorganismes phototrophes du tapis microbien, à savoir les cyanobactéries et les bactéries phototrophes anoxygéniques pourpres. Deux méthodes différentes, mais adaptées aux microorganismes étudiés, ont été utilisées. Ainsi la CLSM (Confocal Laser Scanning Microscopy) a mis en évidence la diversité modérée en cyanobactéries du tapis de Camargue (six types différents) mais surtout la dominance de l'espèce filamenteuse *Microcoleus chthonoplastes*. Cette dernière montre une distribution en fonction du cycle nycthéméral suggérant son déplacement dans le tapis au cours des 24h. La T-RFLP a permis de décrire la forte diversité, l'organisation très fine des bactéries pourpres anoxygéniques et leurs réarrangements existants au sein du tapis, en fonction du cycle nycthéméral et des gradients physico-chimiques. La dynamique de ces bactéries phototrophes ainsi mise en évidence montre aussi la complexité de leurs comportements, l'existence de compétitions spatiales ou métaboliques et le rôle écologique important de l'énergie tactisme dans l'organisation verticale du tapis microbien.

La seconde partie de ce chapitre intitulée "Hypersaline microbial mat: Vertical migration of sulfate reducing bacteria along a diel cycle" décrit le comportement du groupe fonctionnel des bactéries sulfato-réductrices. La T-RFLP combinée au criblage d'une banque de gènes *ADNr 16S* par RFLP et au séquençage des clones intéressant a permis de mettre en évidence la dynamique importante des sulfato-réducteurs et tout particulièrement des genres *Desulfonema*, *Desulfosarcina* et *Desulfococcus*. De plus, cette étude décrit la présence de bactéries appartenant au genre *Desulfotignum*, présentant un profil de migration vertical net fuyant la lumière et l'oxygène du jour pour les profondeurs anoxiques du tapis.

IV.2. Bactéries photosynthétiques

Ce travail a été soumis au journal "Environmental Microbiology" sous le titre :

Vertical shift of phototrophic bacterial communities during a diel cycle in a cyanobacterial microbial mat (Salins-de-Giraud, Camargue, France).

Par : Aude Fourçans[1], Antoni Solé[2], Elia Diestra[2], Isabel Esteve[2], Pierre Caumette[1] et Robert Duran[1]

SUMMARY

The spatio-temporal distribution of oxygenic and anoxygenic phototrophic communities from a photosynthetic microbial mat (Salins-de-Giraud, Camargue, France) were investigated during a diel cycle. This study was performed in order to appreciate the impact of fluctuating environmental parameters (light, temperature, pH, H_2S and oxygen) on the structure of this hypersaline mat. Confocal Laser Scanning Microscopy (CLSM) revealed the dominance of *Microcoleus chthonoplastes* and moderate cyanobacterial diversity in comparison to others already described hypersaline mats. Five others cyanobacterial phylotypes were observed, which are, considering their decreasing abundance, *Halomicronema excentricum,* an unidentified filamentous bacterium, *Pseudanabaena* sp., and two unicellular cyanobacteria from the *Gloeocapsa* and *Pleurocapsa*-groups. All these microorganisms showed a specific spatio-temporal distribution in the mat. Furthermore, the biomass determination of *Microcoleus chthonoplastes* allowed investigating its dynamic revealing its vertical migration during the diel cycle. T-RFLP was applied to investigate anoxygenic phototrophic communities by analyzing their specific *PufM* gene encoding for a photosynthetic center subunit. By this approach, we depicted a highly anoxyphototroph diversity, a fine depth scaling structure of the microbial mat, and important dynamic behaviors of all these phototrophic communities.

[1] Laboratoire d'Ecologie Moléculaire EA 3525, Université de Pau et des Pays de l'Adour, avenue de l'Université, BP 1155, F-64013 Pau Cedex, France
[2] Department of Genetics and Microbiology, Autonomous University of Barcelona, E-08193 Bellaterra, Spain

INTRODUCTION

Microbial mats are cohesive microbial communities growing at solid-aqueous interfaces, in environments as diverse as intertidal coastal sediments (Esteve et al., 1992; Guerrero et al., 1993), hypersaline ponds (Giani et al., 1989; Caumette et al., 1994; Fourçans et al., 2004), or thermal springs (Ferris et al., 1996). Mainly dominated by phototrophic, oxygenic and anoxygenic, microorganisms, they are composed of laminated microbial communities in few scale where sharp gradients of electron acceptors are established near the surface layers. These chemical gradients are influenced by the mutual activities of benthic microorganisms that are strongly light dependent.

Cyanobacteria, located at the surface layer, have been described as main primary producers in microbial mats. They are very important in the stabilization as their filaments, on intercrossing, form a complex network throughout the mat (D'Amelio et al., 1987). Among cyanobacteria, the gliding bacterium *Microcoleus chthonoplastes* was described as dominant in hypersaline environments (García-Pichel et al., 1994; Fourçans et al., 2004), marine intertidal microbial mats (Stal and Krumbein, 1985; Stal, 1994), and in hot deserts (Campbell, 1979). On the other hand, phototrophic sulfur bacteria of the anoxic zone take part in the energy flow of the mat as "secondary" primary producers. They perform - simultaneously to the detoxification of H_2S provided by sulfate-reducers - a photoassimilation of CO_2 produced by the cyanobacteria (Pfennig, 1975).

Daily, the chemical gradients dramatically change exposing bacteria to extremely variable environmental conditions including light, temperature, pH, sulfur concentration and oxygen availability (Revsbech et al., 1983; van Gemerden, 1993). By migration, bacteria escape from extreme conditions and therefore can benefit of optimal habitats for their development (Taylor et al., 1999; Alexandre et al., 2004). This migration process has been reported in some mats for several microorganisms such as sulfur-oxidizing bacteria (García-Pichel et al., 1994), sulfate-reducing bacteria (Teske et al., 1998) and especially for cyanobacteria (Whale and Walsby, 1984; Nelson et al., 1986a; Richardson and Castenholz, 1987; Richardson, 1996; Teske et al., 1998).

Motile bacteria are able to control their spatial position with respect to various stimuli such as chemicals, light, and redox potential by variety of mechanisms. In microbial mats aerotaxis, chemotactic behavior in response to oxygen has been found to be the main mechanism guiding *Beggiatoa* spp. to the sulfide oxygen interface (Nelson et al., 1986b). In contrast, aerotaxis also contributes by a negative effect to the deal of sulfate reducing bacteria (Krekeler et al., 1998). Phototaxis is often described as the main tactic response in

cyanobacteria (García-Pichel et al., 1994; Bebout and Garcia-Pichel, 1995), but others sensing mechanisms have been proposed to participate to the overall behavior of cyanobacteria in the mat. Recently the phenomenon of hydrotaxis was described as a new energy-dependent reaction for cyanobacteria (Garcia-Pichel and Pringault, 2001; Pringault and Garcia-Pichel, 2003). Similarly, complex behavior of purple sulfur bacteria could be explained by chemotaxis and photoresponses as described for *Marichromatium gracile* (Thar and Kuhl, 2001).

The spatio-temporal distribution of anoxygenic and oxygenic phototrophic communities was investigated in the Camargue microbial mat from Salins-de Giraud along a diel cycle. Different approaches based on pigment properties of these phototrophic communities allowed their precise *in situ* distribution. Cyanobacteria were identified and quantified with Confocal Laser Scanning Microscopy (CLSM), while anoxyphototrophs were investigated by a Terminal Restriction Fragment Length Polymorphism (T-RFLP) analysis of PCR amplified *pufM* gene.

EXPERIMENTAL PROCEDURES

General information

This analysis was realized on the microbial mat of the Salins-de Giraud saltern during June of the year 2001, in parallel of *in situ* microsensor measurements (O_2, H_2S, pH) over a diel cycle (Wieland et al., 2003). This mat presents range salinity between 70 ‰ to 110 ‰ (w/v) (Fourçans et al., 2004).

Sampling procedure

Microbial mats were sampled from a very large shallow pond at the saltern of Salins-de-Giraud, close to the sand barrier and seacoast in the Camargue area, France. Several samples were collected at different times (9:40, 15:00h, 18:00h, 22:00h, 4:00h, and 7:30h) over a diel cycle from 11 to 12 June 2001.

For T-RFLP analysis, at time 15:00h, 4:00h, and 22:00h triplicates samples of mat cores (35 mm i.d.) were sampled with falcon tubes. The upper 10 mm of the mat core was sliced off aseptically, transferred into sterile Petri dishes, frozen in liquid nitrogen, transported on dry ice and finally stored at –80°C until further analysis. This froze samples mat were sliced, with a cryomicrotome, at about 100 µm thick for the 2 first millimeters, and 200 µm thick for the 2 next millimeters. Genomic DNA was extracted from these different slices and vertical distribution of microbial communities for each depth was first performed using the

T-RFLP method, and secondly by cloning and sequencing terminal restriction fragments (T-RFs). According to the results of microsensor measurements (Wieland et al., 2003) we choose to analyze samples for only 11 slices along the fourth millimeters, to characterize bacterial communities.

For CLSM analysis, one core (18 mm) from each time in the diel cycle was transferred into small plastic tubes containing 2,5 % (v/v) glutaraldehyde in a phosphate buffer (0,2 M adjusted to the appropriate salinity with NaCl), and stored at 4ºC waiting further processing. The different mat samples were analyzed by means of a Leica True Confocal Scanner TCS 4d (Leica Laser-Technik GmbH, Heidelberg, Germany) equipped with an argon-krypton laser. This study used the main features of this microscope facilitating observation of cyanobacteria in microbial mats (Solé et al., 2001a). Subsamples were cut in vertical slices of defined dimensions taking to account the need to preserve the vertical stratification of the mat. Confocal images from three replicates, optical series and summa projections, were taken at every 250 μm depth in each subsample.

Cyanobacteria characterization

Characterization of the cyanobacteria diversity in every mat subsample by CLSM was realized directly on-screen in continuous mode and from the confocal images obtained. Cyanobacteria identification in the Salins-de-Giraud microbial mats by CLSM has been described in a general sense in (Fourçans et al., 2004). After cyanobacteria identification, the profiles of abundance for each of these were determined.

Biomass estimation of Microcoleus chthonoplastes

CLSM suma projection images corresponding to the different time profiles (three replicates each 250 μm depth) were transformed to binary images (black/white) using Adobe Photoshop 6.0 for Windows. In these images *M. chthonoplastes* black contours were selected from among cyanobacteria, which were erased from them. A black line, one pixel line has also been erased to avoid white areas between the black contours being subsequently considered as a *M. chthonoplastes*. Morphological data of the perimeter and area for every *M. chthonoplastes* outline were obtained through the UTHSCSA Image Tool 3.0, an image processing and analysis program, and exported to a Microsoft Excel 97 book. Values for length, width and biovolume were calculated in accordance with the expressions described in (Solé et al., 2001a). The quotient between the biovolume of *M. chthonoplastes* and the volume of sediment analyzed was multiplied by a factor of 310 fg C / μm^3 to convert these

data to biomass. Average biomass data from every depth and for each profile studied was calculated. Results were expressed in μg C / cm^2 sediment. Finally, the dynamics of the *M. chthonoplastes* biomass, including space and time, were determined.

T-RFLP (Terminal Restriction Fragment Length Polymorphism) analysis

From each mat slice, genomic DNA was extracted with the UltraClean Soil DNA Isolation Kit (MoBio Laboratories,USA), according to the recommended of the supplier; except in the first step where 10mM EDTA were added to avoid degradation of genomic DNA. All extracted genomic DNA samples were stored at -20°C until further processing. For T-RFLP analysis (Liu et al., 1997), we target specifically the purple anoxygenic phototrophs with the primers set pb557f-pb750r, which amplifies a pufM DNA gene fragment (Achenbach et al., 2001). For T-RFLP analysis, Forward (f) and reverse (r) primers were fluorescently labeled with TET and HEX respectively. Restriction enzyme used in T-RFLP analysis was HaeIII (New England Biolabs, UK). T-RFs (terminal restriction fragments) superior to 100 fluorescent units and present in each triplicate were selected. Predicted digestions were realized on all PufM sequences known in order to assign the different T-RFs to a certain genus or species. A Correspondence Factorial Analysis (CFA) compared all depth T-RFLP profiles, from tables assembling T-RFs relative values. The CFA were realized with MVSP v3.12d software (Rockware Inc., UK; (Kovach, 1999).

Statistical analysis

All depth T-RFLP profiles were next compared, from tables assembling T-RF relative values of each restriction enzyme, by a Correspondence Factorial Analysis (CFA). The CFA were realized with MVSP v3.12d software (Rockware Inc., UK; (Kovach, 1999).

Canonical Correspondence Analysis (CCA), performed with MVSP v3.12d software (Rockware Inc., UK), were realized from data of T-RFLP profiles, biomass of *Microcoleus chthonoplastes* estimated by CLSM, and environmental parameters (oxygen, pH, H_2S, Stot) measured in a previous study on the diel cycle (Wieland et al., 2003).

RESULTS

Communities of oxygenic phototrophic bacteria in Camargue mat

Through CLSM, three filamentous cyanobacteria were essentially observed (Figure 1): *Microcoleus chthonoplastes*, *Halomicronema excentricum,* together with an unidentified bacterium forming filaments of 0.96 μm diameter. Confocal image of the most abundant cyanobacteria showed bundles with several trichomes oriented in parallel with cells longer

than wide characteristic of *Microcoleus chthonoplastes* (Figure 2). This bacterial species was widely distributed in the mat independently of the daytime.

Halomicronema excentricum, a filamentous cyanobacterium described in high salinity environments, was found broadly distributed overall the mat during the day while it was found at the surface during the night. The unidentified filamentous cyanobacteria showed an ubiquitous distribution with a favorite location on the deep zone around the 2 last mm. Additionally, *Pseudanabaena* sp. filaments have been located only in the morning (9:40 h) at the depth 3.25 mm. Unicellular cyanobacteria of the *Gloeocapsa*-group have been observed at different location, 0.5 and 2 mm (15:00 h), 0.25 mm (22:00 h) and 0.75 mm (4:00 h). Finally, the *Pleurocapsa*-group has only been found at 4:00 h at different depths throughout the 4 mm analyzed.

Since *M. chthonoplastes* was found to be the most abundant cyanobacteria, its spatio-temporal distribution within the mat was determined by biomass analysis during a diel cycle (Figure 3). At 9:40h, it was distributed mainly in three areas with the maximum biomass (0.99 mgC/cm^2 sediment) observed around the first mm. Two others zones, at 1.75 mm depth presenting a biomass of 0.61 mgC/cm^2 sediment, and at 2.5 mm (0.74 mgC/cm^2 sediment) were observed. At 15:00h, the filaments were principally distributed in two areas at the upper layer (0.25 mm) with a concentration of 0.78 mgC/cm^2 sediment, and at 1.75 mm depth (0.72 mgC/cm^2 sediment). At 18:00h the distribution was found completely different, *M. chthonoplastes* reached its maximum concentration at 0.5 mm (1.32 mgC/cm^2 sediment), while it was absent elsewhere. At 22:00h, after sunset *M. chthonoplastes* filaments were mainly localized between 0 and 1.5 mm, and decreased under this depth and was practically undetected from 2.25 mm. At 4:00h, *M. chthonoplastes* filaments were well distributed throughout the 3 mm of the microbial mat. Finally at 7:30h, the distribution of *M. chthonoplastes* was similar to that described at 9:40h, i.e. a maximum biomass (0.88 mgC/cm^2 sediment – 0.83 mgC/cm^2 sediment) between 0.75 mm and 1 mm, a concentration of 0.65 mgC/cm^2 sediment at 1.75 mm depth, and 0.28 mgC/cm^2 sediment at 2.5 mm.

Communities of anoxygenic phototrophic bacteria in Camargue mat

The distribution of the anoxygenic phototrophic bacteria (PAB) within the mat was analyzed along a diel cycle by the T-RFLP method targeting the functional *pufM* gene encoding for a subunit of the photosynthetic center of purple bacteria (Achenbach et al., 2001). (Wieland et

al., 2003) described an opposite physico-chemical gradient on two hours (15:00h and 4:00h) of a diel cycle that it was interesting to investigate in terms of PAB diversity.

T-RFLP profiles revealed an important diversity of the PAB communities within the mat, with 24 different OTUs (Operational Taxonomic Unit) detected only for the digestion HaeIII. From T-RFLP profiles obtained at each depth, all relative abundances of each T-RF were summarized in the histograms presented in Figure 4. The observed bacterial communities of the mat stratification were completely distinct, between the day afternoon and the night. Specific T-RFs were observed in function of the nycthemeral cycle, i.e., at 15:00h the fragments of 93, 119, 167, 202, 225 bp (Figure 4a); and at 4:00h fragments of 36, 46, 90, 125, 132, 156, 177, 197, 212 bp (Figure 4b). Moreover, we could remark some common OTUs at both hours, but located differently within the 4 millimeters of the mat. Indeed, T-RFs 104 bp settled the oxic zone (0-0.4 mm) at 15:00h, although always abundant (about 75 % of the layer) in the top layer (0.3-0.4 mm) at 4:00h, it was found in anoxic zones 1.2-1.3 mm and 3.4-4 mm. Interestingly, at an intermediate hour (22:00h), its zonation was also seen in an intermediate state at 0 to 1.6 mm representing 8 % of the population in each layer (data not shown). In the same way, the OTUs 137 and 192 bp showed a clustering inside the mat during the night. Since T-RF 137 bp, largely present in the 4 mm of the mat during the day, was only observed in a mid anoxic layer (1.2-1.3 mm) at 4:00h. Identically, at 15:00h the T-RF 192 bp was present in an oxic zonation between 0.9-1.6 mm, and at 4:00h it was just confined in the anoxic 1.5-1.6 mm. HaeIII predictive digestion of all *pufM* sequences available correlated the OTU 137 bp to the purple non sulfur bacteria *Roseospira marina*. In contrary, the OTUs 114, 148, 187 bp were detected only in anoxic area during the day, while they were located into the surface or spread overall the mat in the night. Finally, terminal fragments 117, 129, 199, and 228 bp were homogeneously developed within the 4 mm, independently of the diel cycle. The OTU 129 bp could be related to the chemotrophic bacteria *Erythrobacter litoralis.*

Factorial correspondence analysis (CFA) done on T-RFLP data showed clearly a different spatial distribution of the PAB communities in the mat depending on the nycthemeral cycle (Figure 5) emphasizing three distinct clusters. Communities from each layer of the 4:00h mat were grouped, except those from the two layers 0.3-0.4 mm and 1.2-1.3 mm. These PAB communities were contrariwise close to a second cluster formed by almost communities from the layers of the 15:00h mat. The communities of the deep layer (3.4-3.6 mm) of the day mat appeared to be really independent from the others two groups,

mainly influenced by the axis 2 showing a variance of 11.82 %. Among T-RFs corresponding to the axis 2, the T-RF 199 bp (HaeIII) could be related to the purple sulfur bacteria *Halochromatium salexigens* and to a purple non sulfur bacterium recently isolated from this marsh (data not shown).

The mat of 4:00h is most influenced by OTUs 114, 129 and 132 bp composing inter alia the axis 1, and OTU 148 bp composing the axis 2. The mat of 15:00h is contrariwise impacted by others OTUs composing axis 1 and 2, corresponding to the fragments 129, 137, 202, 228 bp and 117, 199 bp respectively, that could not be correlated to known PAB species.

DISCUSSION

Organization of phototrophic communities in the mat during the diel cycle

Dominance of Microcoleus chthonoplastes

The Salins-de-Giraud microbial mat presented restrained cyanobacteria diversity in comparison to other studied mats, probably due to the fact that salinity favors lower diversity (Fourçans et al., 2004). *M. chthonoplastes, Halomicronema excentricum* and a still unidentified bacterium were detected as majority forms within the cyanobacteria community. *M. chthonoplastes* presents great metabolic diversity, and is able to live in hypersaline environments (Caumette et al., 1994). *Halomicronema excentricum* develops in hypersaline environments since it was described in the Solar Lake (Eilat, Israel) microbial mats (Abed et al., 2002). Further studies are needed to understand the ecophysiology of the still unidentified filaments. Figure 3 illustrates the tendency of *M. chthonoplastes* to locate in the first few millimeters of the mat during the day, as it carries out an oxygenic photosynthesis. *M. chthonoplastes* was also detected in anoxic zones during the day that is consistent with its ability to develop through anoxygenic photosynthesis (De Wit and Van Gemerden, 1987). Previous studies have proved that low concentration of sulfide (974 μM) is growth-inhibiting for *M. chthonoplastes* (De Wit and Van Gemerden, 1987), notwithstanding that this bacterium has the ability to protect itself from a potentially toxic environment using sheaths (Decho, 1990). In the night, mainly at 4.00h, *M. chthonoplastes* was found uniformly distributed in the mat enriched in sulfur (Wieland et al., 2003), probably because of its capacity to carry out alternative metabolisms. Indeed, (Moezelaar et al., 1996) have demonstrated its aptitude to ferment carbohydrates in the dark, using sulfur as an electron acceptor, and producing sulfide. Similarly, studies on the pigmented zone of the Ebro Delta (Spain) microbial mats during an annual cycle revealed that *M. chthonoplastes* was the dominant cyanobacterium of the first few millimeters (oxic zone) with maximum biomass in May 1997 (6,55 mgC/cm^2 sediment),

although its spatial distribution demonstrated its considerable metabolic versatility (Solé et al., 2003).

Anoxyphototrophs communities changes during the diel cycle

T-RFLP fingerprints of the PAB communities based on the analysis of their own *pufM* gene allowed to estimate their biodiversity inside the mat in a spatial way at a microscale level (Fourçans et al., 2004). Considering the active four millimeters of the mat, the PAB showed strong changes in diversity at different period of the nycthemeral cycle. Indeed, the Evenness index calculated from T-RFLP profiles revealed diversity in PAB lower in night (4:00h) than in day (15:00h) with respective values of 0.789 and 0.907. This visible impact on the bacterial diversity could be explained by the existence of variable physico-chemical gradients. (Wieland et al., 2003) have characterized the biogeochemistry of the Camargue mat over a diel cycle, describing two opposite periods. Firstly, in the afternoon a clearly defined upper oxic zone of 1.5 mm was followed by an anoxic part from the 2nd to the 4th millimeter. Secondly, in the night the oxic upper 0.5 mm of the mat was overlapped with sulfide while the deeper zone (0.5 mm-4 mm) became completely anoxic. Comparison of T-RFLP fingerprints revealed common and specific populations of PAB between night and afternoon. The predominance of specific OTUs in each hour, 93, 119, 167, 202, 225 bp (15:00h) and 36, 46, 90, 125, 132, 156, 177, 197, 212 bp (4:00h), suggested an adaptation of the bacterial metabolic type in function of the diel environmental conditions. Moreover, some common PAB differently located in each hour (104, 114, 137, 148, 187, 192 bp) indicated their vertical migration to optimal or tolerable conditions of growth. Thus, when sulfide reaches the mat in night, bacteria able to versatile metabolism such as purple non sulfur bacteria supporting few concentration of sulfide (less than 3mM) (Pfennig, 1975) could be favored. For, example, the motile purple non sulfur bacteria *Roseospira marina* (HaeIII T-RF of 137 bp), able to tolerate the sulfide concentration found in this mat, could be preserved. In contrast, the fact that others OTUs (117, 129, 199, 228 bp) keeping constant zonation in the 4 mm of the mat suggested a metabolic switch. Close to the oxygen-sulfide interface, the development of some purple sulfur bacteria as small-size *Chromatiaceae* tolerating microoxic conditions could be promoted. Furthermore, comparison of the PAB mat structure with previous studies (Fourçans et al., 2004) revealed little differences suggesting a real dynamic of the populations in function of seasonal conditions.

Dynamic of the microbial mat along a diel cycle

A canonical correspondence analysis (CCA) was realized including biogeochemical data (O_2, pH, H_2S, S_{tot}, measured in parallel of sampling) from (Wieland et al., 2003), biomass of *M. chthonoplastes*, and T-RFLP data on PAB, in order to evaluate parameters influencing the spatial distribution of PAB over a diel cycle (Figure 6). CCA revealed a PAB community structure in the afternoon (15:00h) mainly influenced by the sulfide rather in depth than in surface. Indeed, in contrast to the night oxygen and sulfide gradients were well defined in the afternoon showing an oxygen-sulfide interface. Oxygen, pH, and biomass of *M. chthonoplastes* influenced negatively the structure of the PAB rather in depth than in surface. Active photosynthesis of cyanobacteria in mat surface in day promotes an increase of the pH up to 9.4 along the first 1.5 mm (Wieland et al., 2003). The decreasing of pH to 6.8 during the night due to lack of photosynthesis (Wieland et al., 2003) could favor the presence of phototrophic bacteria such as green sulfur bacteria like *Chlorobiaceae* (van Gemerden and Beeftink, 1981). The predominance of *M. chthonoplastes* in different zones of this mat could also act as a PAB competitor. During the night, the influence of sulfide on PAB structure was less strong than in the noon since it only reached the mat surface but kept regular concentration. Similarly in day, the biomass of *M. chthonoplastes* influenced strongly the PAB diversity independently of their spatial distribution, suggesting either a spatial or a metabolic competition with PAB since it is able to perform anoxygenic photosynthesis. The absence of oxygenic photosynthesis during the night will explain the poor concentration of oxygen in the mat and the decrease of pH, and consequently their impact on PAB structure and diversity was less strong in night than in day.

The very steep and diel fluctuating gradient of electrons donors and acceptors across this microbial mat seems to induce a large change on the distribution of oxyphototrophic bacteria. (García-Pichel et al., 1994) already described the behavior of some cyanobacteria gliding to optimal conditions in hypersaline microbial mat mainly in response to light. From early morning to dusk, blue-green cyanobacteria such as *Oscillatoria* and *Spirulina* spp. have shown downward migration into the mat to avoid photodamage and photosynthesis inhibition by high level of irradiance. Similar studies showed the orientation abilities of *M. chthonoplastes* in a diel cycle in natural habitats such as Ebro Delta microbial mats (Solé et al., 2001b). However, others taxis mechanisms such as aero- or sulfide-taxis probably in association with phototaxis may contribute to the overall cyanobacteria distribution across the mat. *Microcoleus* cultures grown in oxic and anoxic conditions in the laboratory illustrated their capacity to use alternative metabolisms (data not shown). Sulfide toxicity is also well

known to inhibit oxygenic photosynthesis (Oren et al., 1979), although cyanobacteria can vary in sulfide tolerance (Cohen et al., 1986). Recently, (Miller and Bebout, 2004) described a *Microcoleus* strain (from a Baja California Sur microbial mat) able to perform oxygenic photosynthesis (reduced by 50 %) in presence of 29 µM total soluble sulfide. In Camargue mats, the distribution of *M. chthonoplastes* biomass suggests that two populations may coexist emphasizing its metabolic versatility. A population highly sensitive to sulfide located in mat area without sulfide and a second population tolerant to high sulfide concentration (around 200 µM) observed around the second millimeters.

Throughout the diel cycle, T-RFLP brought out different behavior of anoxyphototrophs. Several phototrophic bacteria, referred to detected T-RF, were observed in different mat location during the studied period. T-RF 104 bp, downward migrating from oxic non-sulfur zone in day to sulfur anoxic zone when night occurred, acted as versatile metabolic bacteria. In the same way T-RFs 117, 129, 199, and 228 bp, homogeneously existing across the mat independently of the diel cycle period, could be related to such flexible metabolism. They could be associated to microorganisms able of chemotrophy, or fermentation in dark oxic or microoxic conditions, like some purple non sulfur bacteria, small-size *Chromatiaceae*, *Ectothiorhodospiraceae,* or aerobic anoxygenic phototrophic bacteria (Pfennig and Truper, 1983; Yurkov and Beatty, 1998). Another phenomenon was observed for some bacterial OTUs (T-RF 137 and 192 bp) performing a spatial clustering from oxic to a precise anoxic zone of the mat at night, suggesting an aggregation of the population in a narrow zone. The marine purple non sulfur bacteria *Roseospira marina* (T-RF 137 bp) was described by (Guyoneaud et al., 2002) as highly motile and unable to respire or ferment under dark anoxic conditions. The aggregation could be considered as a behavior to protect the cell integrity. Oxygen is toxic for obligate anoxyphototrophic bacteria; therefore these bacteria react by a negative chemotactic response (Armitage et al., 1979). This could be the behavior of T-RFs 114, 148 and 187 bp keeping only anoxic zonation in the mat whatever the diel cycle period.

In conclusion, the phototrophic bacterial structure within the Camargue mat showed a great dynamic during a diel cycle induced by several fluctuating environmental stimuli. Energy taxis seems to have an important ecological role on the vertical stratification of bacterial communities through the microbial mat.

ACKNOWLEDGMENTS

We acknowledge the financial support by the EC (MATBIOPOL project, grant EVK3-CT-1999-00010). The authors are grateful to the Company of Salins-du-midi at Salins-de-Giraud for facilitating access to the salterns, sampling and field experiments. AF is partly supported by a doctoral grant from the general council of Atlantic Pyrenees. Hervé REMIGNON from ENSAT (Toulouse- France) is gratefully thanked for the technical support.

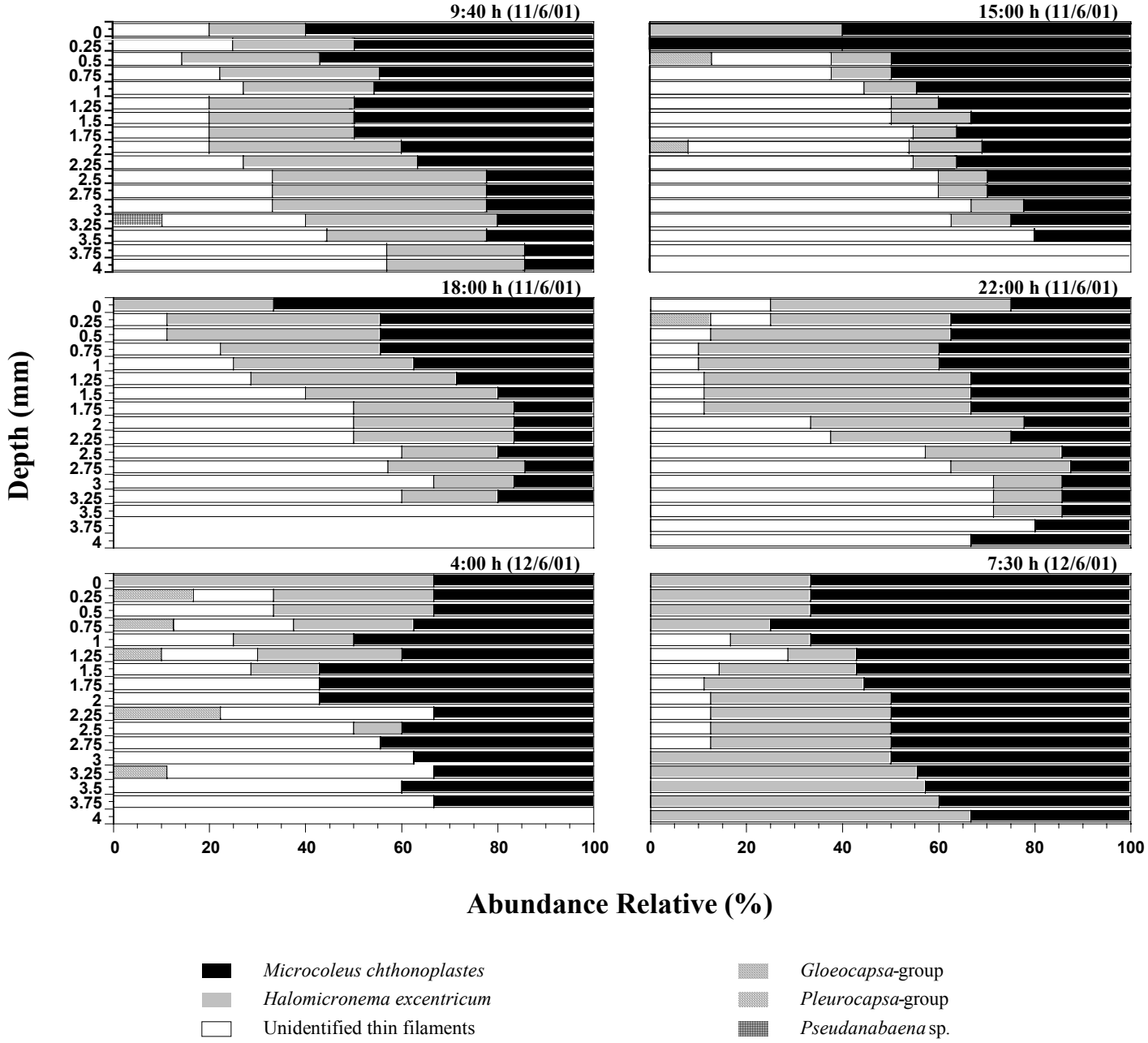

Figure 1. Abundance relative in depth of the different cyanobacteria characterized by CLSM during the diel cycle in Camargue mat. The abundance relative is expressed in %.

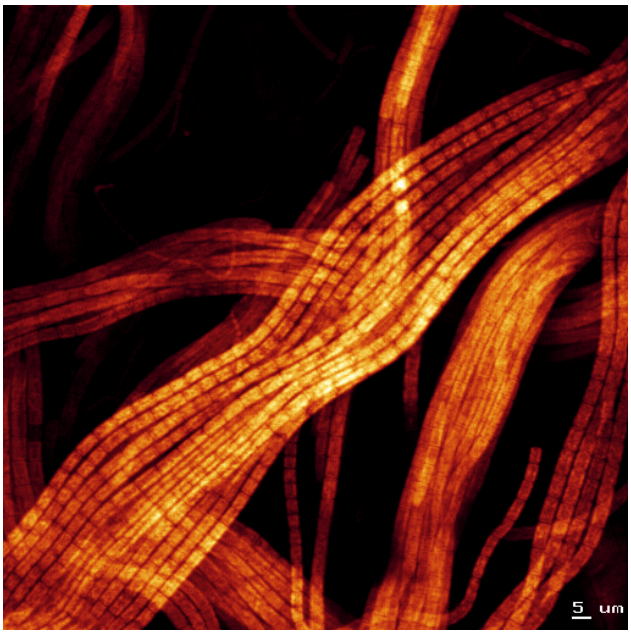

Figure 2. Confocal image of *Microcoleus chthonoplastes* forming bundles of filaments.

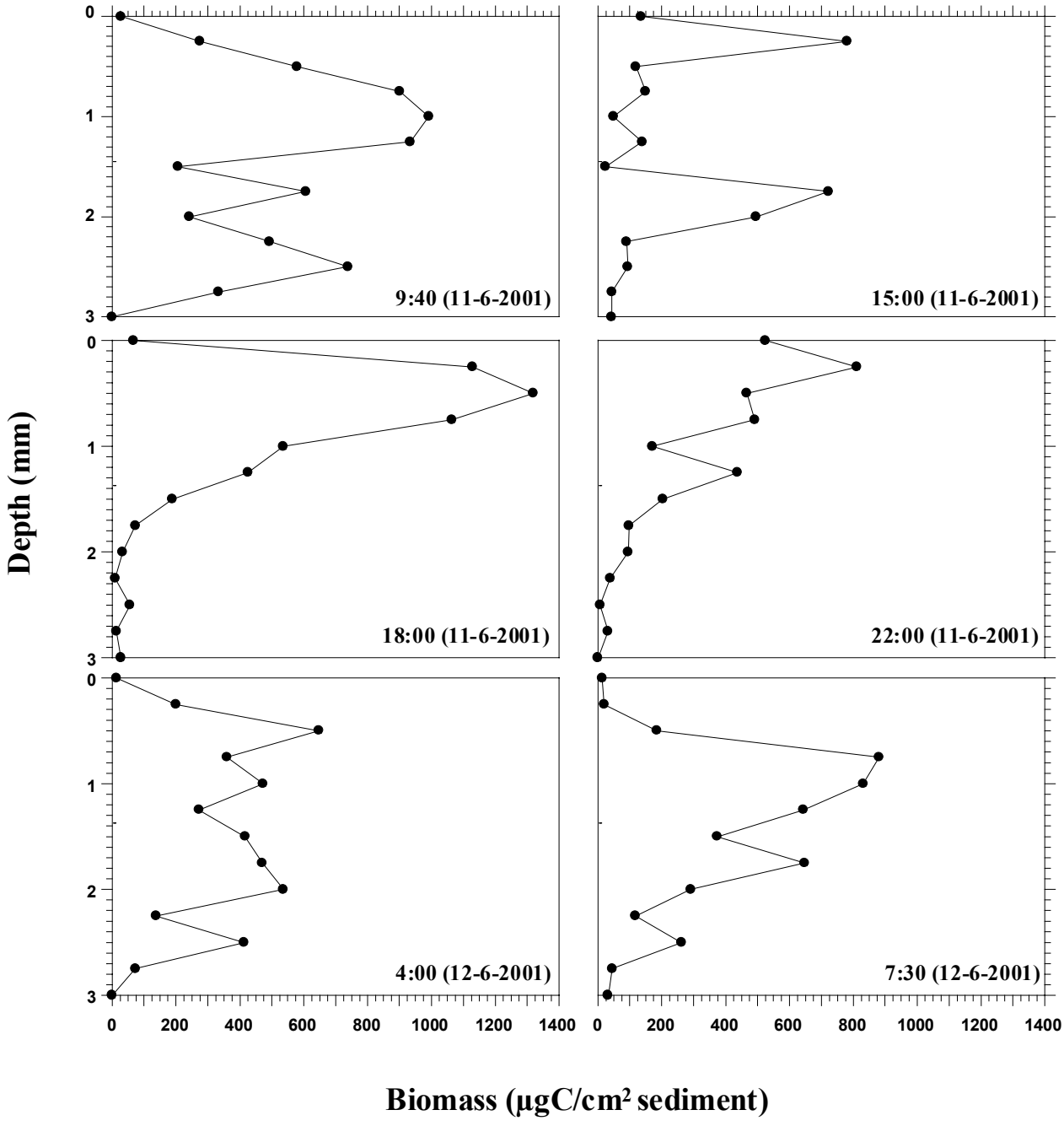

Figure 3. Biomass profiles of *Microcoleus chthonoplastes* during the diel cycle. The biomass is expressed in µgC / cm^2 sediment.

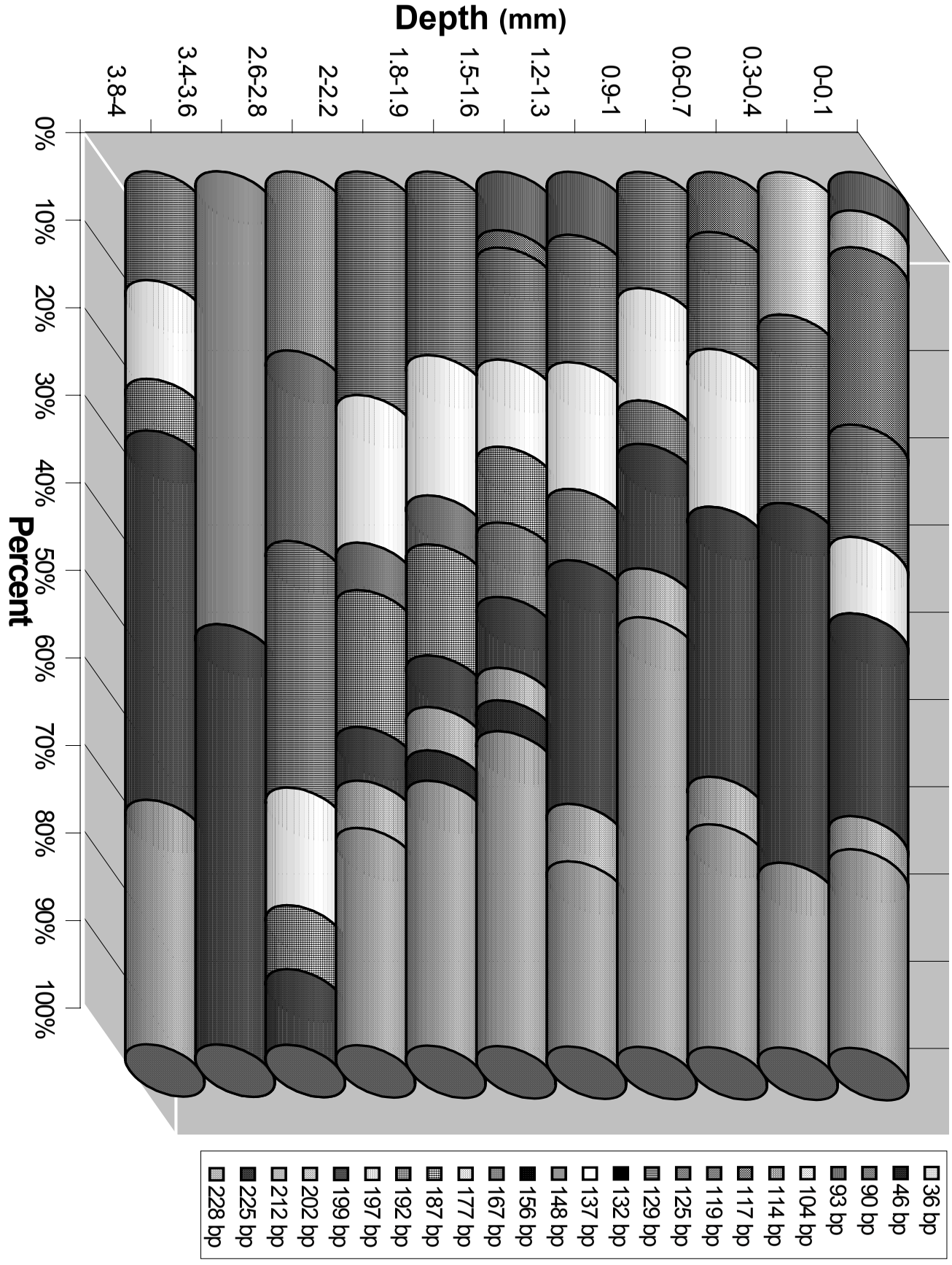

Figure 4a. Histograms of the relative abundance of 5' end of HaeIII digested *pufM* amplified fragments for each layer of the mat at 15:00h , obtained from T-RFLP profiles.

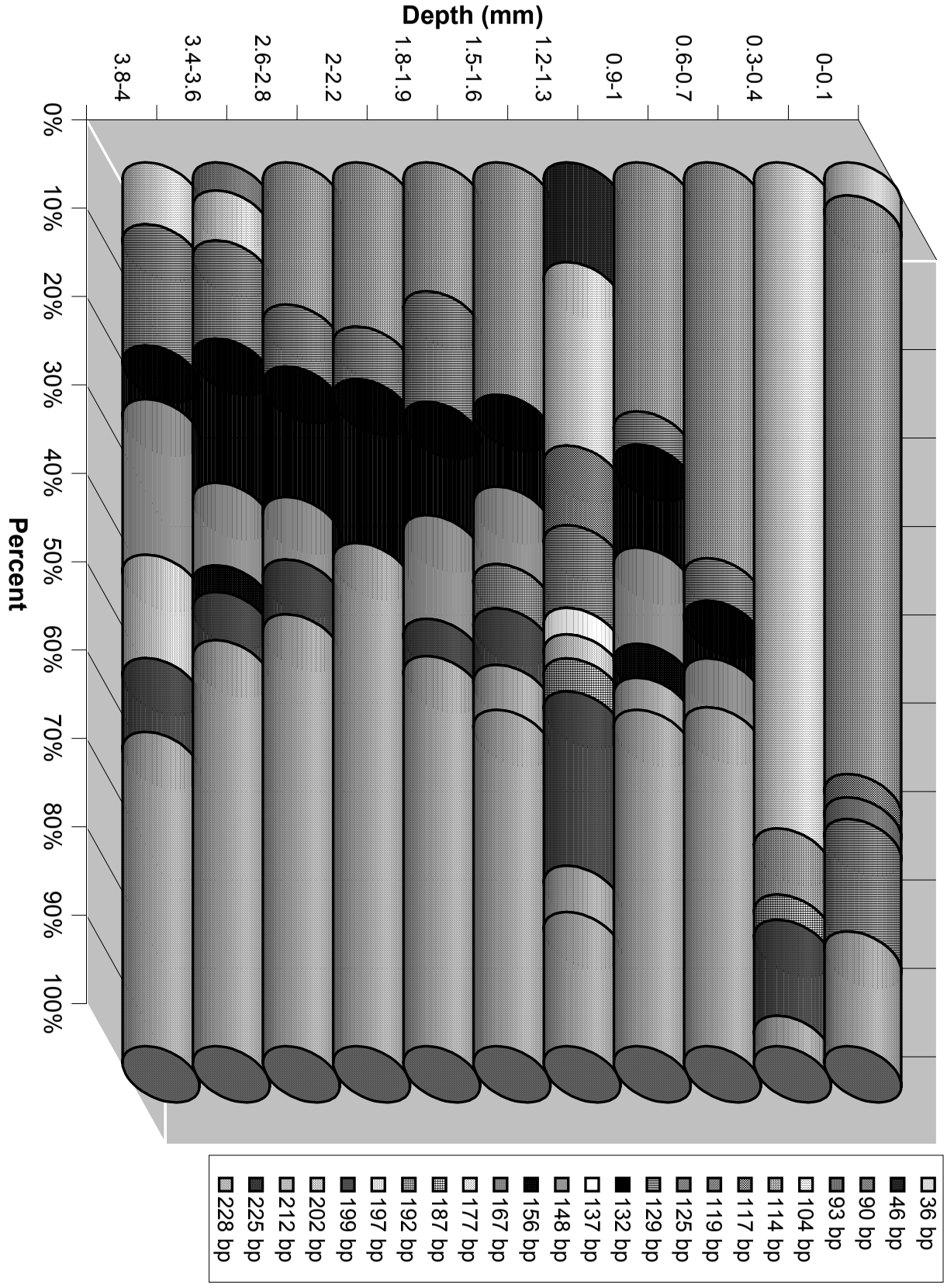

Figure 4b. Histograms of the relative abundance of 5' end of HaeIII digested *pufM* amplified fragments for each layer of the mat 4:00h, obtained from T-RFLP profiles.

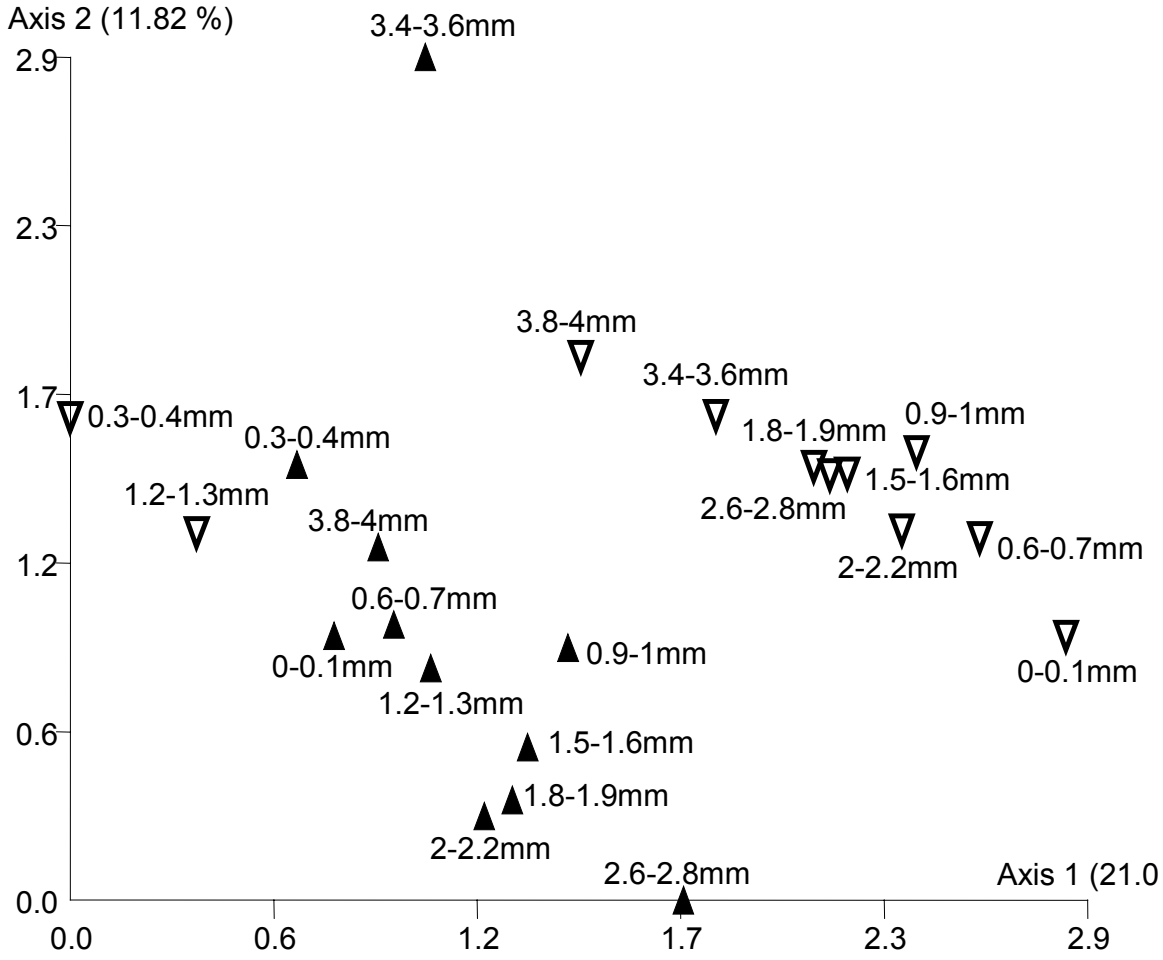

Figure 5. Correspondence Factorial Analysis (CFA) of the purple anoxygenic bacterial communities (PAB) of each layer of the mat at 15:00h (black symbol) and 4:00h (white symbol). Each community was represented by a 5'end T-RFLP pattern corresponding to the HaeIII digest of the *pufM* encoding gene.

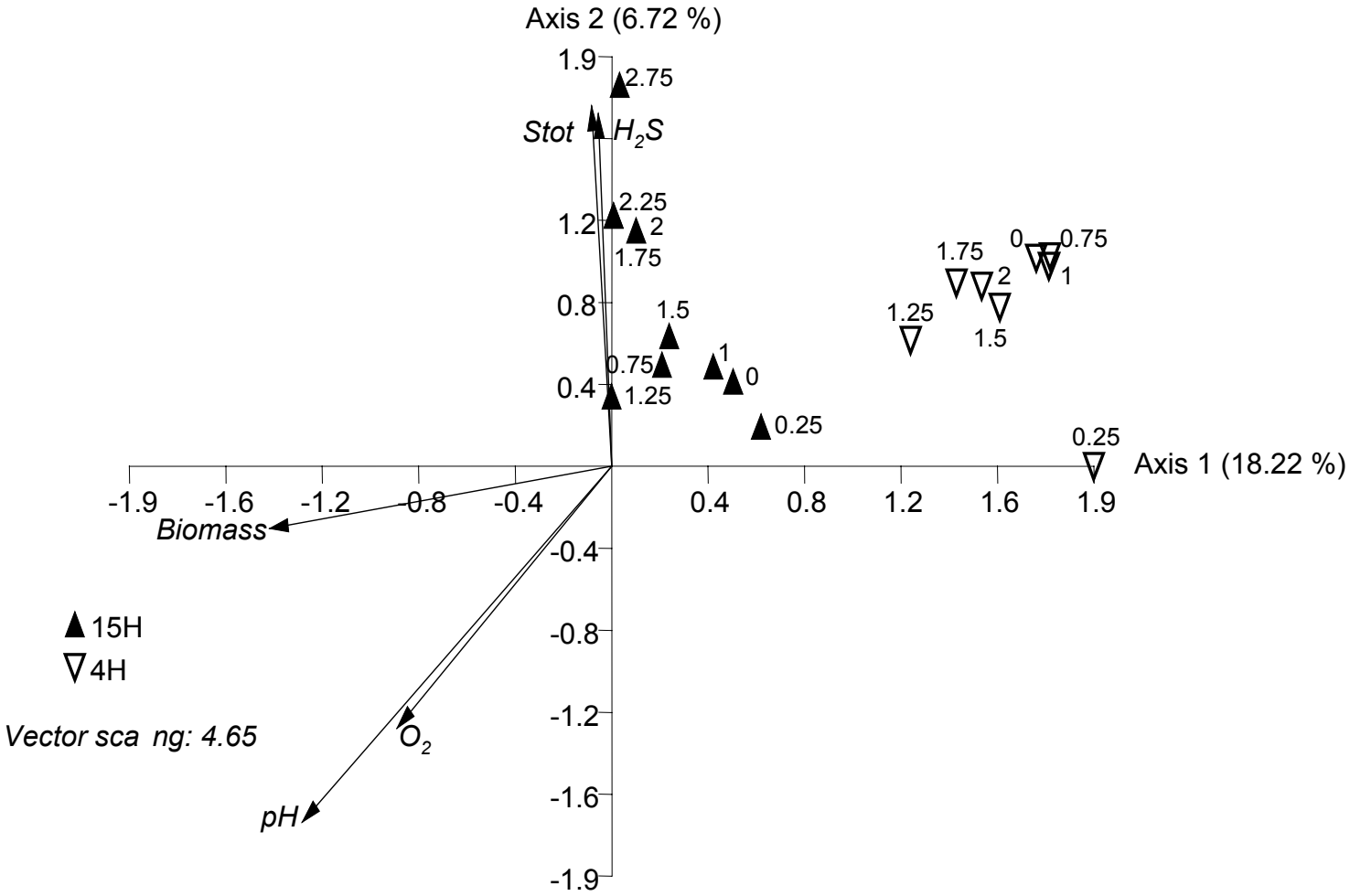

Figure 6. Canonical Correspondence Analysis (CCA) between the PAB communities, of each layer of the mat at 15:00h (black symbol) and 4:00h (white symbol), and environmental variables measured at this two hours: biomass of *Microcoleus chthonoplastes*, pH, concentration of O_2, H_2S and Stot.

REFERENCES

Abed, R.M., García-Pichel, F., and Hernández-Mariné, M. (2002) Polyphasic characterization of benthic, moderately halophilic, moderately thermophilic cyanobacteria with very thin trichomes and the proposal of *Halomicronema excentricum* gen. nov., sp. nov. *Arch. Microbiol.* **177**: 361-370.

Achenbach, L.A., Carey, J., and Madigan, M.T. (2001) Photosynthetic and phylogenetic primers for detection of anoxygenic phototrophs in natural environments. *Appl. Environ. Microbiol.* **67**: 2922-2926.

Alexandre, G., Greer-Phillips, S., and Zhulin, I.B. (2004) Ecological role of energy taxis in microorganisms. *FEMS Microbiol. Rev.* **28**: 113-126.

Armitage, J.P., Keighley, P., and Evans, M.C.W. (1979) Chemotaxis in photosynthetic bacteria. *FEMS Microbiol. Lett.* **6**: 99-102.

Bebout, B., and Garcia-Pichel, F. (1995) UV B-induced vertical migrations of cyanobacteria in a microbial mat. *Appl. Environ. Microbiol.* **61**: 4215-4222.

Campbell, S.E. (1979) Soil stabilization by a prokaryotic desert crust: implications for Precambrian land biota. *Orig. Life* **9**: 335-348.

Caumette, P., Matheron, R., Raymond, N., and Relexans, J.C. (1994) Microbial mats in the hypersaline ponds of Mediterranean salterns (Salins-de-Giraud, France). *FEMS Microbiol. Ecol.* **13**: 273-286.

Cohen, Y., Jorgensen, B.B., Padan, E., and Shilo, M. (1986) Adaptation to hydrogen sulfide of oxygenic and anoxygenic photosynthesis among cyanobacteria. *Appl. Environ. Microbiol.* **51**: 398-407.

D'Amelio, E.D., Cohen, Y., and Des Marais, D.J. (1987) Association of a new type of gliding, filamentous, purple phototrophic bacterium inside bundles of *Microcoleus chthonoplastes* in hypersaline cyanobacterial mats. *Arch. Microbiol.* **147**: 213-220.

De Wit, R., and Van Gemerden, H. (1987) Oxidation of sulfide to thiosulfate by *Microcoleus chtonoplastes*. *FEMS Microbiol. Lett.* **45**: 7-13.

Decho, A.W. (1990) Microbial exopolymer secretions in ocean environments: their role(s) in food webs and marine process. *Oceanogr. Mar. Biol. Ann. Rev.* **28**: 73-153.

Esteve, I., Martínez, M., Mir, J., and Guerrero, R. (1992) Typology and structure of microbial mats communities in Spain: A preliminary study. *Limnetica* **8**: 185-195.

Ferris, M.J., Muyzer, G., and Ward, D.M. (1996) Denaturing gradient gel electrophoresis profiles of 16S rRNA-defined populations inhabiting a hot spring microbial mat community. *Appl. Environ. Microbiol.* **62**: 340-346.

Fourçans, A., García de Oteyza, T., Wieland, A., Solé, A., Diestra, E., van Bleijswijk, J. et al. (2004) Characterization of functional bacterial groups in a hypersaline microbial mat community (Salins-de-Giraud, Camargue, France). *FEMS Microbiol. Ecol.* **in press**.

Garcia-Pichel, F., and Pringault, O. (2001) Microbiology. Cyanobacteria track water in desert soils. *Nature* **413**: 380-381.

García-Pichel, F., Mechling, M., and Castenholz, R.W. (1994) Diel migrations of microorganisms within a benthic, hypersaline mat community. *Appl. Environ. Microbiol.* **60**: 1500-1511.

Giani, D., Seeler, J., Giani, L., and Krumbein, W.E. (1989) Microbial mats and physicochemistry in a saltern in the Bretagne (France) and in a laboratory scale saltern model. *FEMS Microbiol. Ecol.* **62**: 151-162.

Guerrero, R., Urmeneta, J., and Rampone, G. (1993) Distribution of types of microbial mats at the Ebro Delta, Spain. *Biosystems* **31**: 135-144.

Guyoneaud, R., Moune, S., Eatock, C., Bothorel, V., Hirschler-Rea, A., Willison, J. et al. (2002) Characterization of three spiral-shaped purple nonsulfur bacteria isolated from coastal lagoon sediments, saline sulfur springs, and microbial mats: emended description of the genus Roseospira and description of Roseospira marina sp. nov., Roseospira navarrensis sp. nov., and Roseospira thiosulfatophila sp. nov. *Arch. Microbiol.* **178**: 315-324.

Kovach, W.L. (1999) MVSP - a Multivariate Statistical Package for Windows. In. Wales U.K.: Kovack Computing Services.

Krekeler, D., Teske, A., and Cypionka, H. (1998) Strategies of sulfate-reducing bacteria to escape oxygen stress in a cyanobacterial mat. *FEMS Microbiol. Ecol.* **25**: 89-96.

Liu, W.T., Marsh, T.L., Cheng, H., and Forney, L.J. (1997) Characterization of microbial diversity by determining terminal restriction fragment length polymorphisms of genes encoding 16S rRNA. *Appl. Environ. Microbiol.* **63**: 4516-4522.

Miller, S.R., and Bebout, B.M. (2004) Variation in Sulfide Tolerance of Photosystem II in Phylogenetically Diverse Cyanobacteria from Sulfidic Habitats. *Appl. Environ. Microbiol.* **70**: 736-744.

Moezelaar, R., Bijvank, S.M., and Stal, L. (1996) Fermentation and sulfur reduction in the mat-building cyanobacterium *Microcoleus chthonoplastes*. *Appl. Environ. Microbiol.*: 1752-1758.

Nelson, D.C., Revsbech, N.P., and Jorgensen, B.B. (1986a) Microoxic-anoxic niche of Beggiatoa spp. : microelectrode survey of marine and freshwater strains. *Appl. Environ. Microbiol.* **52**: 161-168.

Nelson, D.C., Jorgensen, B.B., and Revsbech, N.P. (1986b) Growth pattern and yield of a chemoautotrophic *Beggiatoa* sp. in oxygen-sulfide microgradients. *Appl. Environ. Microbiol.* **52**: 225-233.

Oren, A., Padan, E., and Malkin, S. (1979) Sulfide inhibition of Photosystem II in cyanobacteria (blue-green algae) and tobacco chloroplasts. *Biochimica et Biophysica Acta (BBA) - Bioenergetics* **546**: 270-279.

Pfennig, N. (1975) The phototrophic bacteria and their role in the sulfur cycle. *Plant and Soil* **43**: 1-16.

Pfennig, N., and Truper, H.G. (1983) Taxonomy of phototrophic green and purple bacteria: a review. *Ann Microbiol (Paris)* **134B**: 9-20.

Pringault, O., and Garcia-Pichel, F. (2003) Hydrotaxis of cyanobacteria in desert crusts. *Microb. Ecol.* **12**: 12.

Revsbech, N.P., Jorgensen, B.B., Blackburn, T.H., and Cohen, Y. (1983) Microelectrode studies of the photosynthesis and O2, H2S and pH profiles of a microbial mat. *Limnol. Oceanogr.* **28**: 1062-1074.

Richardson, L.L. (1996) Horizontal and vertical migration patterns of *Phormidium corallyticum* and *Beggiatoa* spp. associated with black-band disease of corals. *Microb. Ecol.* **32**: 323-335.

Richardson, L.L., and Castenholz, R.W. (1987) Diel vertical movements of the cyanobacterium *Oscillatoria terebriformis* in a sulfide-rich microbial mat. *Appl. Environ. Microbiol.* **53**: 2142-2150.

Solé, A., Gaju, N., and Esteve, I. (2003) The biomass dynamics of cyanobacteria in an annual cycle determined by confocal laser scanning microscopy. *Scanning* **25**: 1-7.

Solé, A., Gaju, N., Mendez-Alvarez, S., and Esteve, I. (2001a) Confocal laser scanning microscopy as a tool to determine cyanobacteria biomass in microbial mats. *J. Microscopy* **204**: 258-261.

Solé, A., Munill, X., Llirós, M., Diestra, E., and Esteve, I. (2001b) Migration studies of Microcoleus chthonoplastes filaments in Ebro delta microbial mats by means of CLSM. *Biology of the Cell* **93**: 348.

Stal, L.J. (1994) Microbial mats in coastal environments. In *Microbial Mats*. Stal, L.J., and Caumette, P. (eds). Berlin Heidelberg: Springer-Verlag, pp. 21-32.

Stal, L.J., and Krumbein, W.E. (1985) Isolation and characterization of cyanobacteria from a marine microbial mat. *Bot. Mar.* **28**: 351-365.

Taylor, B.L., Zhulin, I.B., and Johnson, M.S. (1999) Aerotaxis and other energy-sensing behavior in bacteria. *Annu. Rev. Microbiol.* **53**: 103-128.

Teske, A., Ramsing, N.B., Habicht, K., Fukui, M., Kuver, J., Jørgensen, B.B., and Cohen, Y. (1998) Sulfate-reducing bacteria and their activities in cyanobacterial mats of solar lake (Sinai, Egypt). *Appl. Environ. Microbiol.* **64**: 2943-2951.

Thar, R., and Kuhl, M. (2001) Motility of *Marichromatium gracile* in response to light, oxygen, and sulfide. *Appl. Environ. Microbiol.* **67**: 5410-5419.

van Gemerden, H. (1993) Microbial mats : A joint venture. *Mar. Geol.* **113**: 3-25.

van Gemerden, H., and Beeftink, H.H. (1981) Coexistence of Chlorobium and Chromatium in a sulfide-limited continuous culture. *Arch. Microbiol.* **129**: 32-34.

Whale, G.F., and Walsby, A.E. (1984) Motility of the cyanobacterium *Microcoleus chthonoplastes* in mud. *Phycol. J.* **19**: 117-123.

Wieland, A., Zopfi, J., Benthien, M., and Kühl, M. (2003) Biogeochemistry of an iron-rich hypersaline microbial mat (Camargue, France). *Microb. Ecol.* **in press**.

Yurkov, V.V., and Beatty, J.T. (1998) Aerobic anoxygenic phototrophic bacteria. *Microbiol Mol Biol Rev* **62**: 695-724.

IV.3. Bactéries sulfato-réductrices

Cet article est en préparation sous le titre :

Hypersaline microbial mat: vertical migration of sulfate reducing bacteria along a diel cycle.

Par : Aude Fourçans[1], Anthony Ranchou-Peyruse[1], Pierre Caumette[1] et Robert Duran[1]

ABSTRACT

The spatio-temporal distribution of sulfate-reducing bacteria was investigated in the microbial mat of Camargue (Salins-de-Giraud) over a diel cycle. This study was performed in order to appreciate the impact of fluctuating environmental parameters (light, temperature, pH, H_2S and oxygen) on the bacterial communities structure of this hypersaline mat. T-RFLP analysis on the *16S rDNA* gene revealed an important dynamic of all eubacteria developing inside the four millimeters of the microbial mat. The combination of T-RFLP and *16S rDNA* libraries analysis revealed similar conclusions concerning diel behavior of sulfate-reducing bacteria. Three genera *Desulfococcus*, *Desulfonema*, and *Desulfosarcina* showed two major movements in the mat. Three distinct OTUs migrated downward in the mat at daytime, while eight others OTUs moved upward. Particularly, *Desulfonema* sp. (T-RF 110 bp) and *Desulfosarcina variabilis* (T-RF 286 bp) were among the species migrating upward. In the same way, when we focused on the genus *Desulfobacter* two OTUs showed different behaviors. The OTU (157 bp) affiliated to new species of *Desulfobacter* stayed immobile independently of the diel microgradients. While the OTU (306 bp) related to the recently described *Desulfotignum* genus, showed a vertical downward migration to sulfidic zone when light and oxygen penetrate the first millimeter. Thus the results suggest that the migration is probably controlled by aero- and chemotaxis mechanisms.

[1]Laboratoire d`Ecologie Moléculaire EA 3525, Université de Pau et des Pays de l`Adour, avenue de l`Université, BP 1155, F-64013 Pau Cedex, France

INTRODUCTION

Microbial mats are described as fine vertically laminated structures where sharp environmental micro-gradients influence the distribution of few functional groups of microorganisms (van Gemerden, 1993). This kind of ecosystems develops under habitats as diverse as hot springs (Ferris *et al.*, 1997; Ramsing *et al.*, 2000; Ruff-Roberts *et al.*, 1994), salterns (Caumette *et al.*, 1994; Fourçans *et al.*, 2004b; Giani *et al.*, 1989), intertidal sediments (Wieland *et al.*, 2003b) or alkaline lake (Namsaraev *et al.*, 2003; Sorokin *et al.*, 2000). The development of a microbial mat is a result of bacterial growth and its corresponding activities. Among diverse metabolic processes coexisting in hypersaline microbial mats, dissimilatory sulfate reduction is the dominant process of anaerobic carbon mineralization independently of depth and oxygen presence (Canfield & Des Marais, 1991; Fründ & Cohen, 1992; Jørgensen, 1994).

Due to the compact nature of a microbial mat, coexistence of all biological activities generate microgradients inside the mat (Revsbech *et al.*, 1983). During the diel cycle, these gradients dramatically change, exposing bacteria to extremely variable conditions. Migration into the mat is one of the strategies developed by some microorganisms to fight against perpetual variations of environmental conditions (light, temperature, pH, sulfur concentration, and oxygen availability). By this mechanism bacteria escape from extreme conditions and therefore can benefit of optimal conditions for their development. This migration process has been described for several bacteria (Nelson *et al.*, 1986; Richardson, 1996; Richardson & Castenholz, 1987; Teske *et al.*, 1998; Whale & Walsby, 1984).

Camargue microbial mat of Salins-de-Giraud have been fully described since ten years (Caumette *et al.*, 1994; Fourçans *et al.*, 2004a; Fourçans *et al.*, 2004b; Mouné *et al.*, 2003; Wieland *et al.*, 2003a). This mat is characterized by high iron content (Wieland *et al.*, 2003a) and a high bacterial diversity, where purple and sulfate-reducing bacteria are organized in fine scale depth vertical distribution along microgradients (Fourçans *et al.*, 2004b). Phototrophic communities, oxygenic and anoxygenic, of this mat exhibited dynamic behavior in response to diel microgradients changes (Fourçans *et al.*, 2004a). Furthermore during the same diel cycle, Wieland *et al.* (2003a) established that inside this studied mat sulfate reduction rates were significantly higher in day than in night. With all these informations, the analysis of the bacterial communities structures would be of special interest to describe bacterial behavior in response to diel fluctuation of different physico-chemical parameters. The main objective of

this study is to characterize the spatial distribution of sulfate-reducing communities within Camargue microbial mat along the diel cycle. As preliminary approach, using T-RFLP (Terminal Restriction Fragment Length Polymorphism) method we investigated the whole eubacterial population. Then, we constructed *16S rDNA* libraries, and in combination with T-RFLP analysis we fully described the behavior of SRB communities. Few genera of these communities including *Desulfococcus*, *Desulfonema*, *Desulfosarcina* and *Desulfobacter* involved in the sulfur cycle, were especially considered.

MATERIAL AND METHODS

General informations

This analysis was realized on the microbial mat of the Salins-de-Giraud saltern over a diel cycle in June of the year 2001. In parallel, *in situ* microsensor measurements (O_2, H_2S, pH) were realized ((Wieland *et al.*, 2003a). This mat presents salinity between 70 ‰ to 110 ‰ (w/v) (Fourçans *et al.*, 2004b).

Sampling procedure

Microbial mats were sampled from a very large shallow pond at the saltern of Salins-de-Giraud, close to the sand barrier and seacoast in the Camargue area, France. Several samples were collected at different times (9:40, 15:00h, 18:00h, 22:00h, 4:00h, and 7:30h) over a diel cycle from 11 to 12 June 2001.

For T-RFLP analysis, at time 15:00h, 4:00h, and 22:00h triplicates samples of mat cores (35 mm i.d.) were sampled with falcon tubes. The upper 10 mm of the mat core was sliced off aseptically, transferred into sterile Petri dishes, frozen in liquid nitrogen, transported on dry ice and finally stored at –80°C until further analysis. These frozen mat samples were sliced, with a cryomicrotome, at about 100 µm thick for the 2 first millimeters, and 200 µm thick for the 2 next millimeters. Genomic DNA was extracted from these different slices and vertical distribution of microbial communities for each depth was first performed using the T-RFLP method, and secondly by cloning and sequencing. According to the results of microsensor measurements (Wieland *et al.*, 2003a), samples for only 11 slices within the fourth millimeters were analyzed to characterize bacterial communities.

T-RFLP analysis (terminal restriction fragment length polymorphism)

From each mat slice, genomic DNA was extracted with the UltraClean Soil DNA Isolation Kit *(MoBio Laboratories,USA*), according to the recommendations of the supplier; except for the first step where 10mM EDTA were added to avoid degradation of genomic DNA. All extracted genomic DNA samples were stored at -20°C until further processing. For T-RFLP analysis (Liu *et al.*, 1997), the 16S rRNA encoding genes of bacterial population were amplified using fluorescent-labeled primers.

Different primers were used to assess the eubacterial community structure of the mat (Table 1). To target the whole eubacterial community, a "direct" PCR reaction with the eubacterial primer pair 8f-1489r (Lane, 1991; Weisburg *et al.*, 1991) was performed, amplifying a large part of the 16S rRNA encoding gene (*16S rDNA* gene). In the same way, to obtain fingerprints of sulfate-reducing bacterial populations, different couples of primers (Table1) targeting few genera of sulfate-reducing bacteria were used (Daly *et al.*, 2000). A "nested" PCR amplification was performed using amplified DNA of the "direct" PCR (obtained with eubacterial primers) as template to detect SRB (Sulfate-Reducing Bacteria) present in lower numbers in the four millimeters of the mat. The first set (DCC305F-DCC1165R) targets specifically the *16S rDNA* gene of the three genera *Desulfococcus*, *Desulfonema*, *Desulfosarcina.* And the second pair (DSB127F- DSB1273R) was described to target only the genus *Desulfobacter*. Forward (f) primers were fluorescently labeled with TET fluorochrome. Restriction enzymes used in T-RFLP analysis were HaeIII or Hin6I (New England Biolabs, UK). T-RFs (Terminal Restriction Fragments) superior to 100 fluorescent units and present in each triplicate were selected. The clustering values were analyzed with the T-RFLP similarity matrix on the RDP (Ribosomal Database Project) web site (http://rdp.cme.msu.edu/; Maidak *et al.*, 2001). The obtained distance matrix was used to construct a dendrogram with MEGA version 2.1 (Kumar *et al.*, 2001) by the Neighbour Joining (NJ) method. Predicted digestions were realized on *16S rDNA* database of RDP web site using the program TAP-TRFLP.

16S rDNA library construction and analysis

Genomic DNA from mat slices was used to amplify the *16S rDNA* gene with the *Desulfobacter spp.* primers (unlabeled) presented in Table1. These PCR products were cloned in *E. coli* with the Topo TA cloning kit (Invitrogen). For each slice analyzed, *de novo* PCR product of the insert from one hundred clones were digested with HaeIII or Hin6I enzymes. Restriction profiles were analyzed on a 2.5% agarose gel electrophoresis with a high-

resolution agarose (Metaphor, Tebu-bio). The comparison of all these restriction profiles allows the evaluation of major populations in each slice.

16S rDNA Sequences

Topo PCR2.1 vector (Invitrogen) containing *16S rDNA* PCR products were extracted from clones. From these plasmids, whole sequences of the *16S rDNA* genes were determined by primer walking (Biofidal, France). All *16S rDNA* sequences were aligned on clustalX software (Thompson *et al.*, 1997) with *16S rDNA* sequences of type strains. From this alignment, phylogenetic tree was constructed by the NJ method with Mega v2.1 software (Kumar *et al.*, 2001).

RESULTS

Eubacterial distribution in the mat over a diel cycle

The distribution of mat eubacterial communities is represented by a similarity dendrogram (Figure 1) obtained from complex T-RFLP profiles performed on each slice of night (4:00h) and day (15:00h) conditions. T-RFLP profiles (data not shown) revealed high numbers of OTUs (Operational Taxonomic Units), lower at 4:00h (38 T-RFs) than at 15:00h (50 T-RFs). This dendrogram shows clearly a different distribution of eubacterial communities in the mat when environmental physico-chemical conditions are opposite. Communities of the deep layer (3.8–4 mm) were completely different between the considered times since they presented 85 % of divergence. On the other hand, eubacterial communities of the night layers from 2.6 to 4 mm were closely related to day layers from 1.5 to 2.2mm. Likewise, eubacteria structure of night layers from 1.5-2.2 mm was close to that of the day layers of 0.3-0.7 mm.

Sulfate-reducing bacteria distribution over a diel cycle

Distribution of Desulfococcus, Desulfonema and Desulfosarcina genera

In order to observe precisely the spatio-temporal distribution of sulfate-reducing bacteria over a diel cycle, we performed the T-RFLP analysis targeting only the genera *Desulfococcus*, *Desulfonema*, and *Desulfosarcina,* with specific primers (Table 1). From these less complex T-RFLP patterns, we have summarized in Figure 2 only the common HaeIII T-RFs (same OTUs obtained at each hour) in order to compare their localization in each layer. Three OTUs (101, 122, and 127 bp) of these genera were observed in deepest layers at 15:00h than at 4:00h. However, SRB OTUs of 101 and 127 bp kept in anoxic zones inside the mat

while the SRB OTU of 122 bp was observed in oxic surface layer during the night and in deepest anoxic layer when day occurred. Inversely, eight SRB OTUs (108, 109, 110, 121, 194, 280, and 286 bp) were present in upper layers during the afternoon than during the night. For several of them they often presented a zonation in oxic layer at 15:00h and anoxic at 4:00h. Predictive digestions of *16S rDNA* sequences available indicated that OTU of 110 bp could correspond to *Desulfonema*, and OTU of 286 bp to *Desulfosarcina variabilis.*

Distribution of Desulfobacter genus

Another primer set targeting only species of the genus *Desulfobacter* (Daly *et al.*, 2000) was used to investigate their spatio-temporal distribution in the mat over a diel cycle. T-RFLP fingerprints revealed two major interesting SRB populations (Figure 3). Indeed, OTU of 157 bp (HaeIII digestion) was localized along the 4 mm of the mat in both night and day conditions, independently of the presence of oxygen. Contrariwise, a second OTU of 306 bp (HaeIII digestion) was observed precisely in the 0-1.6 mm of the mat during the night at 4:00h, and at noon only on the 1.2-4 mm of the mat, i.e., in the anoxic zone. Predictive HaeIII T-RFLP patterns of SRB *16S rDNA* sequences showed that the OTU of 157 bp could correspond to all *Desulfobacter* species so far described. Moreover, the OTU of T-RF 306 bp could correspond to another genus recently described, *Desulfotignum* (Kuever *et al.*, 2001), close to *Desulfobacter* genus.

To confirm these results and further characterize these two populations, *16S rDNA* libraries were constructed allowing the inventory of the SRB inhabiting the first and last slices of the mat at 4:00h and 15:00h. Clones of the libraries were grouped in function of their HaeIII and Hin6I RFLP patterns. The comparison of all the restriction profiles obtained is summarized on a histogram representing share of each diverse population (Figure 4). At 4:00h in the surface of the mat, the major SRB population was present at 37 %, and was related by predictive HaeIII digestion to the previously observed OTU of 306 bp. The SRB population related to the OTU of 157 bp was also present in this layer but less abundant (11%). In the same layer at noon (15:00h), proportions of these populations were inverted, since major SRB population corresponded to OTU of 157 bp (49.5%), while SRB OTU of 306 bp was minor (4.5%). The same observation was done for the deep layer (3.8-4 mm) in the night, showing OTU of 157 bp also dominant in comparison to the OTU of 306 bp. In this same layer at day, restriction profiles revealed that SRB OTU of 306 bp was again the most important population.

To further characterize the *Desulfobacter* communities observed in these layers, *16S rDNA* sequences of clones corresponding to these 2 communities were determined. As expected all the clones sequenced were affiliated to the genus *Desulfobacter* (Figure 5). However, in accordance with T-RFLP results, clones A4-1-70 and A15-30-10 corresponding to the OTU of 306 bp were affiliated to the genus *Desulfotignum* showing 96 and 94 % similarity respectively. The phylogenic analysis of clones related to the OTU of 157 bp revealed the presence of several species within this SRB population. Clone A4-1-6 was closely related to the genus *Desulfotignum* while clone A15-1-2, A15-30-22, and A4-30-2 may constitute new taxa since they could not be related to *Desulfotignum* or *Desulfobacter* species.

DISCUSSION

T-RFLP analysis based on the *16S rDNA* gene allowed assessing the spatio-temporal distribution of the whole eubacterial communities in the Camargue mat during a diel cycle. Within the four millimeters of the mat, these communities showed an important complex dynamic probably in response to fluctuating physico-chemical gradients that have already been observed (Wieland *et al.*, 2003a). Similar behaviors were observed between the night and day, since eubacteria composing mid layers (1.5-2.2 mm) of the mat in the afternoon showed a downward migration to deep layers (2.6-4 mm) in the night. These populations might be intolerant to oxygen, since they were always located in anoxic zone. Moreover they tolerate higher concentration of sulfide in night than in day. Another cluster showed the same movement in the mat from the surface oxic zone (0.3-0.7 mm) in day to the anoxic and sulfidic zone (1.5-2.2 mm) in night. Environmental conditions of all these locations were really different, therefore these behaviors suggested a metabolic shift of bacteria composing these layers, and/or the search of optimal conditions by following the appropriate electron acceptor or carbon source. The first movement could correspond to the behavior of some sulfate-reducing bacteria aerotolerant attracted by oxygen as described for *Desulfovibrio* that could switch from sulfate-reduction in deep anoxic zone to an active aerobic respiration in mat surface (Krekeler *et al.*, 1997). This process could play a role of protection of the integrity of anoxic environment removing oxygen from oxic zone and then favoring the development of obligate anaerobic bacteria (Krekeler *et al.*, 1998; Krekeler *et al.*, 1997). The second behavior observed could correspond to the movement of versatile bacteria as the motile purple non sulfur *Rhodobacter sphaeroides*. Indeed during the day the conditions of the mid layer (1.5-2.2 mm), characterized by light, absence of oxygen and sulfide, favor anoxygenic photosynthesis of these phototrophic bacteria. When night occurred, they

orientated by chemotaxis towards chemoattractant as organic acids, and switch their metabolism to heterotrophic pathway (Jeziore-Sassoon *et al.*, 1998).

These complex dynamic patterns of the observed eubacterial diversity suggested that specific functional populations were involved in these different movements. In order to understand these processes, the study was focused mainly on sulfate-reducing bacteria. Considering the sub-group *Desulfonema, Desulfosarcina,* and *Desulfococcus*, T-RFLP patterns showed that some SRB went down into the mat at noon when oxygen penetration was optimal and sulfide content left surface layers of the mat. Some others SRB reached the mat surface during the day in spite of the high oxygen concentration; they could be correlated to a high sulfate-reduction rate inside mat surface since it was six times higher in afternoon than in night (Wieland *et al.*, 2003a). The OTU of 110 bp that could correspond to *Desulfonema* species revealed little upward movement in noon; its resultant zonation was for great part in oxic layers. Filamentous *Desulfonema* species were previously described in oxic area of mats (Minz *et al.*, 1999a; Minz *et al.*, 1999b; Teske *et al.*, 1998). Previous reports have demonstrated that this gliding bacterium was able to aggregate in order to survive under periodic exposure to oxic conditions, indicating probably the formation of anoxic micro-niches (Fukui *et al.*, 1999; Sigalevich *et al.*, 2000b).

The analysis of the sub-group *Desulfobacter* revealed the behavior of two major populations. T-RFLP and DNA sequences analysis of *16S rDNA* clones libraries showed important shift of these populations into the mat over a diel cycle. Numbers of sulfate-reducing bacteria have been described to be able to survive in diverse oxic zones (Minz *et al.*, 1999a; Minz *et al.*, 1999b; Teske *et al.*, 1998; Wieland *et al.*, 2003b; Wieringa *et al.*, 2000) and respire using oxygen as *Desulfovibrio* spp. (Cypionka, 2000; Krekeler *et al.*, 1998; Sigalevich *et al.*, 2000a) and few *Desulfobacter* species (Cypionka *et al.*, 1985; Dannenberg *et al.*, 1992). In this mat, one OTU (157 bp) was detected both in night and in day all over the 4 mm of the mat. Fluctuating environmental conditions did not seem to disturb the distribution of this OTU, particularly when the penetration of oxygen occurred in high concentration at the mat surface. This OTU, related to all species of the genus *Desulfobacter* so far described, showed a high tolerance to oxygen since it was located at the mat surface at 15:00h with oxygen concentration up to 907 µM (Wieland *et al.*, 2003a). Although this genus was described as strictly anaerobic bacteria (Widdel and Pfennig, 1981) some members could form clumps allowing them to tolerate oxygen. Phylogenetic analysis of *16S rDNA* sequences revealed that this SRB community could correspond to new species of the *Desulfobacteriaceae* family.

Vertical migrating behavior was observed for a second OTU corresponding to the T-RF of 306 bp. Indeed it moved downward from surface layers of the mat which are weakly oxic (around 16 µM) and sulfide rich (up to 123 µM) during the night to deepest sulfidic and anoxic zones of the mat containing up to 359 µM of total sulfide during the day (Wieland *et al.*, 2003a). Both predictive digestions and *16S rDNA* sequences analysis permitted to affiliate this OTU to the recently described genus *Desulfotignum* (Kuever *et al.*, 2001). The two species of this genus (Kuever *et al.*, 2001; Schink *et al.*, 2002) were characterized as strict anaerobes, non-spore forming bacteria. Only the type strain *Desulfotignum balticum* has been described as motile bacteria. The negative aerotactic behavior showed by this OTU was consistent with the anaerobic and motile characteristics of the genus *Desulfotignum*, despite that it was able to tolerate low concentrations of oxygen. Moreover, this observation could be correlated to great increase of the sulfate reduction rate (up to 6 to 10 times) in deep layers during the afternoon (Wieland *et al.*, 2003a) suggesting that chemotaxis to sulfide could also play an important role as cell attractant as already demonstrated (Cypionka, 2000).

Therefore, this study demonstrated the dynamic behavior of the sulfate-reducing bacteria within the few active metabolic millimeters of the Camargue microbial mat. The diel fluctuation of electron acceptors microgradients may control the bacterial migration.

ACKNOWLEDGMENTS

We acknowledge the financial support by the EC (MATBIOPOL project, grant EVK3-CT-1999-00010). The authors are grateful to the Company of Salins-du-midi at Salins-de-Giraud for facilitating access to the salterns, sampling and field experiments. AF is partly supported by a doctoral grant from the general council of Atlantic Pyrenees. Hervé REMIGNON from ENSAT (Toulouse- France) is gratefully thanked for the technical support.

Table 1. Primers sets used for *16S rDNA* amplification. Amplimer sizes for the different primer sets are as follows: *16S rDNA* eubacteria, 1481 bp; *16S rDNA Desulfococcus-Desulfonema-Desulfosarcina spp.*, 860 bp; *16S rDNA Desulfobacter spp.*, 1146 bp. All *16S rDNA* primer names are based on *E. coli 16S rDNA* sequence numbering.

Primer		**Target gene**	**Target group**	**Reference**
8F	AGA GTT TGA TCC TGG CTC AG	*ssu 16S rDNA*	*Eubacteria*	(Lane, 1991; Weisburg *et al.*, 1991)
1489R	TAC CTT GTT ACG ACT TCA	*ssu 16S rDNA*		
DCC305F	GAT CAG CCA CAC TGG RAC TGA CA	*ssu 16S rDNA*	*Desulfococcus, Desulfonema, Desulfosarcina*	(Daly *et al.*, 2000)
DCC1165R	GGG GCA GTA TCT TYA GAG TYC	*ssu 16S rDNA*		
DSB127F	GAT AAT CTG CCT TCA AGC CTG G	*ssu 16S rDNA*	*Desulfobacter*	(Daly *et al.*, 2000)
DSB1273R	CYY YYY GCR RAG TCG STG CCC T	*ssu 16S rDNA*		

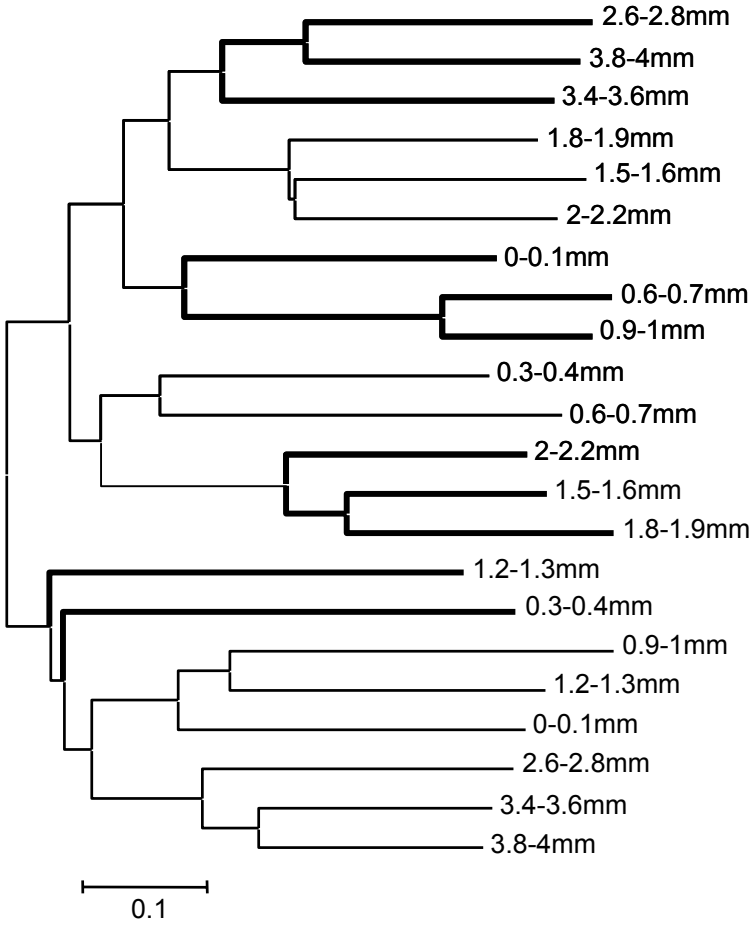

Figure 1. Dendrogram of Eubacterial communities showing the relatedness of each layer of the Camargue mat based on the Jaccard coefficient. It was constructed by stacking two individual 5'end T-RFLP patterns corresponding to the HaeIII, and Hin6I digests. Branches of the dendrogram related to 15:00h mat layers are represented by thin lines and those related to 4:00h thick lines.

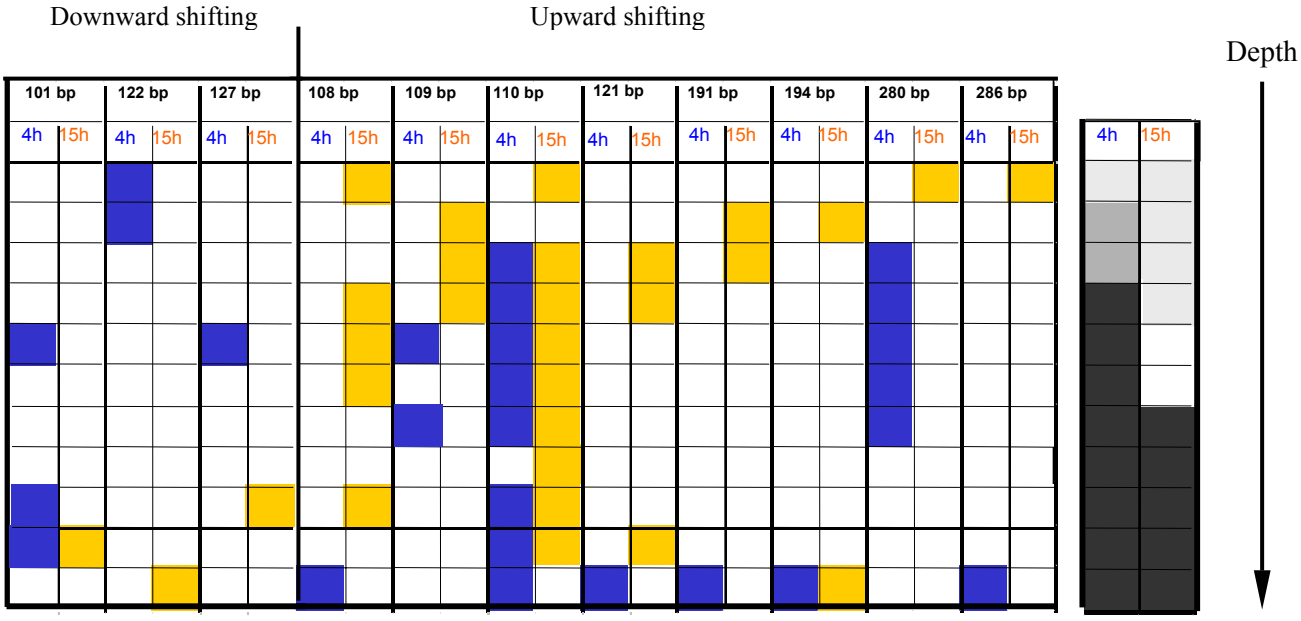

Figure 2. Comparison of the localization of common T-RFs within the mat during the diel cycle. The localization of the same population (T-RF) of *Desulfosarcina, Desulfococcus* and *Desulfonema* genera are compared between 4:00h and 15:00h at each layer studied. These data were obtained from 5'end *16S rDNA* terminal fragment digested with enzyme HaeIII. Each square corresponds to each layer studied along the 4 mm of the mat. Yellow squares show the presence of T-RF during the day, blue square the presence of T-RF during the night, and white square correspond to the absence of T-RF. The right outline corresponds to schematic oxygen profiles along the four millimeters of the mat, obtained from Wieland *et al.* (2003b). Oxic zone were colored in bright grey, oxygen-sulfide overlapped zone in mid grey, anoxic-sulfidic zone in dark grey, and anoxic zone without sulfide in white.

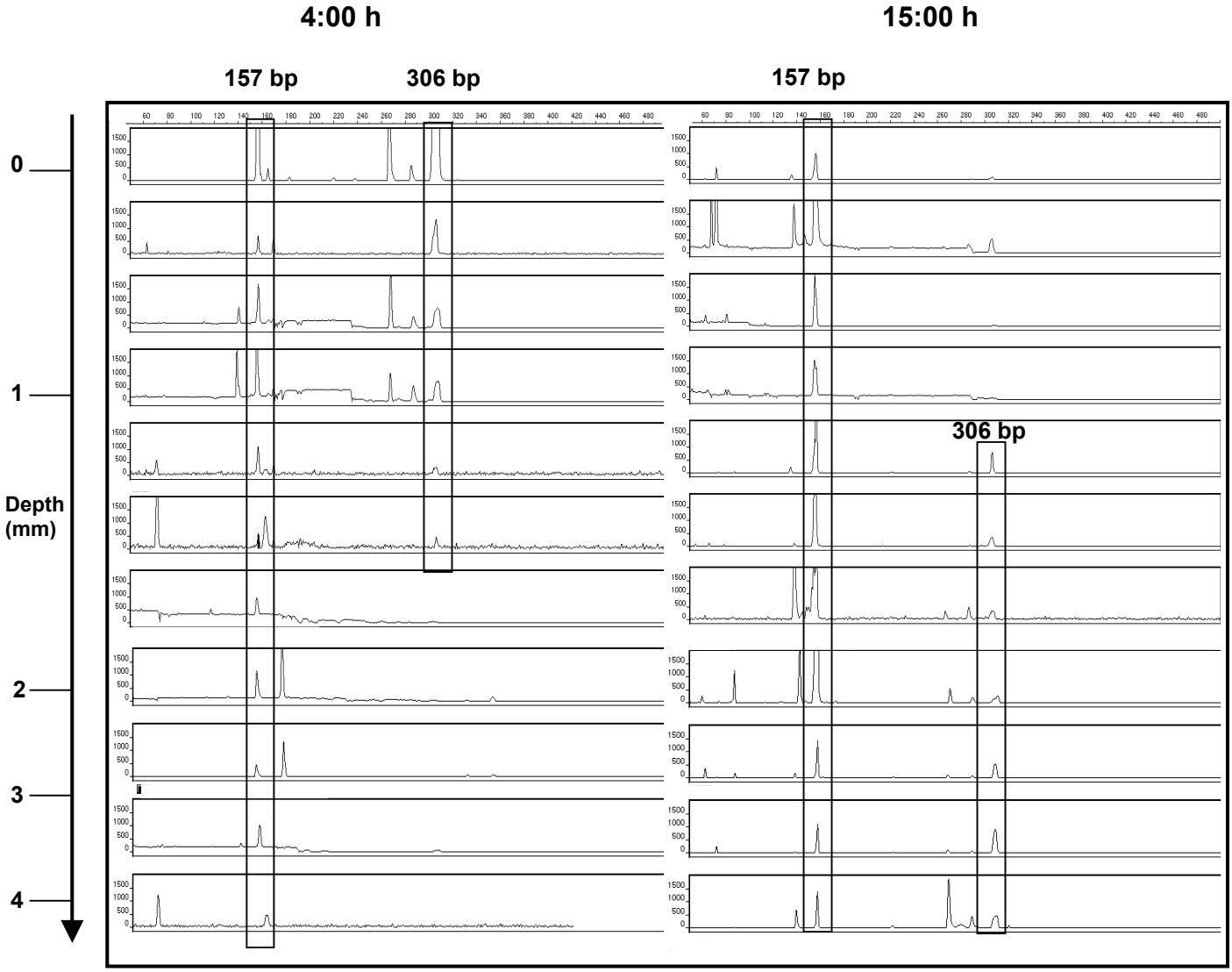

Figure 3. Comparison of sulfate reducing bacterial communities fingerprints between 4:00h and 15:00h for each layer studied within the four millimeters of the Camargue mat. Electropherograms of the 5' end T-RFLP profiles were obtained from HaeIII-digested *16S rDNA* amplified with primers DSB127F - DSB1273R.

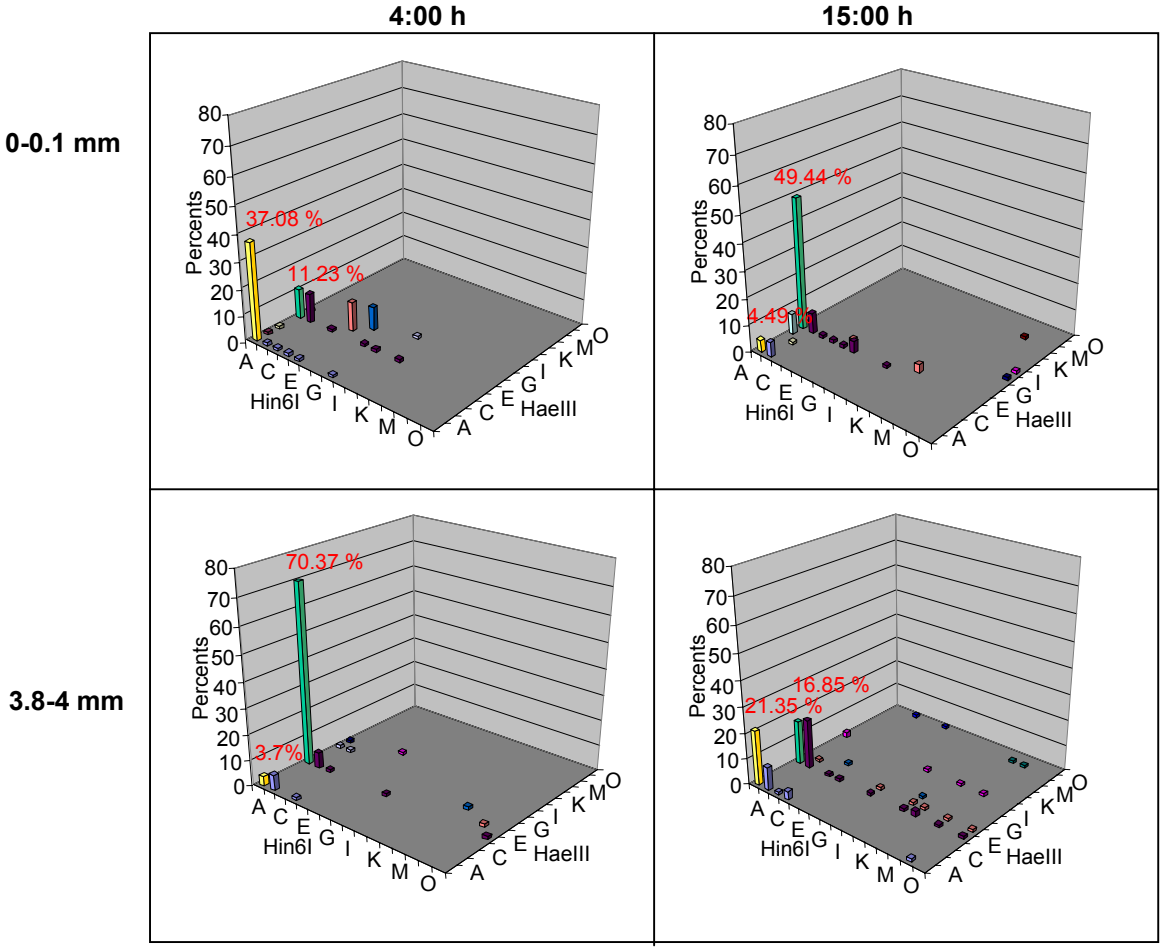

Figure 4. Comparison of *16S rDNA* clone libraries compositions. Histograms were obtained by combining two restriction profiles (HaeIII and Hin6I) of each clone analyzed at 4:00h and 15:00h, and for slices 0-0.1 mm and 3.8-4 mm. Green and yellow bars represent clones populations which *16S rDNA* sequences could be related to OTUs of 157 bp and 306 bp respectively.

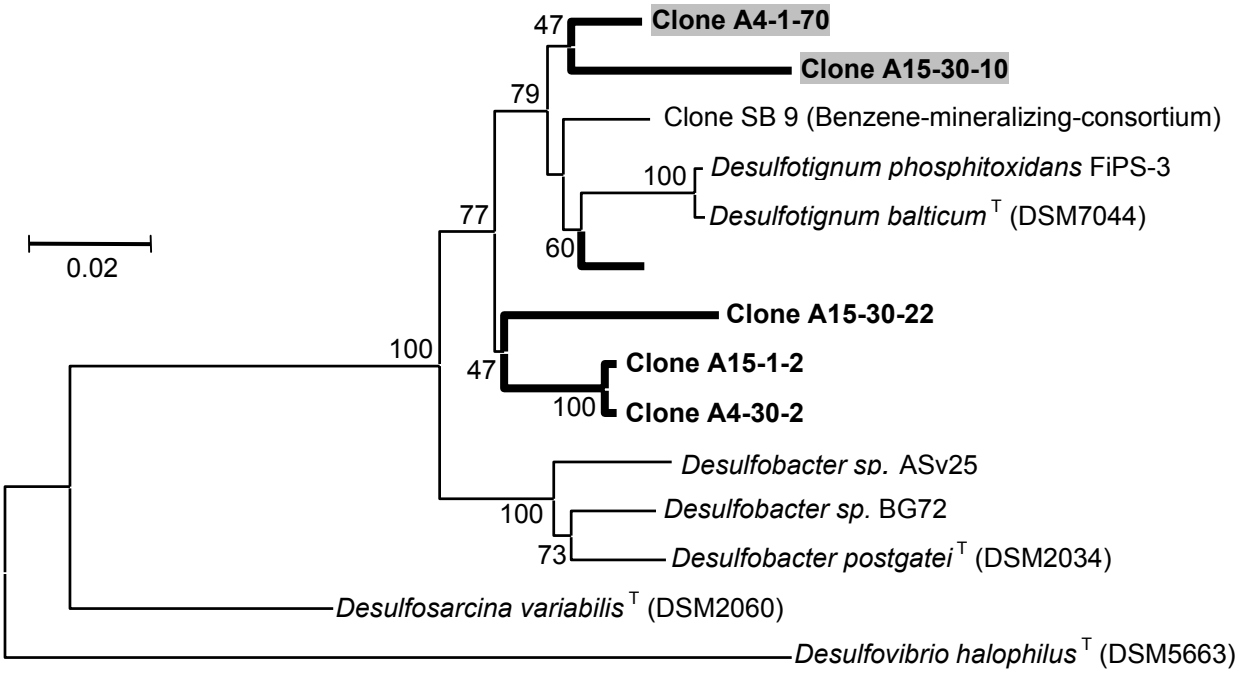

Figure. 5. **Phylogenetic position of *Desulfobacter* clones libraries. The tree is based on *16S rDNA* sequences analysis of each clone analyzed and type strains. Clone name corresponds to, respectively, hour of sampling (15 for 15:00h, and 4 for 4:00h), layer number (from 1 for 0-0.1 mm, to 30 for 3.8-4 mm), and clone number. Clone SB 9 derived from Phelps *et al.* (1998). Branches of the dendrogram related to clones from this study are shown bold. Clones corresponding to OTU of 306 bp are shaded and those corresponding to OTU of 157 bp in bold. Bootstrap values are marked at the junctions.**

REFERENCES

Canfield, D. E. & Des Marais, D. J. (1991). Aerobic sulfate reduction in microbial mats. *Science* **251**, 1471-1473.

Caumette, P., Matheron, R., Raymond, N. & Relexans, J. C. (1994). Microbial mats in the hypersaline ponds of Mediterranean salterns (Salins-de-Giraud, France). *FEMS Microbiology Ecology* **13**, 273-286.

Cypionka, H. (2000). Oxygen respiration by *Desulfovibrio* species. *Annual Review of Microbiology* **54**, 827-848.

Cypionka, H., Widdel, F. & Pfennig, N. (1985). Survival of sulfate-reducing bacteria after oxygen stress, and growth in sulfate-free oxygen-sulfide gradients. *FEMS Microbiology Letters* **31**, 39-45.

Daly, K., Sharp, R. J. & McCarthy, A. J. (2000). Development of oligonucleotide probes and PCR primers for detecting phylogenetic subgroups of sulfate-reducing bacteria. *Microbiology* **146**, 1693-1705.

Dannenberg, S., Kroder, M., Dilling, W. & Cypionka, H. (1992). Oxidation of H2, organic compounds and inorganic sulfur compounds coupled to reduction of O2 or nitrate by sulfate reducing-bacteria. *Archives of Microbiology* **158**, 93-99.

Ferris, M. J., Nold, S. C., Revsbech, N. P. & Ward, D. M. (1997). Population structure and physiological changes within a hot spring microbial mat community following disturbance. *Applied and Environmental Microbiology* **63**, 1367-1374.

Fourçans, A., Solé, A., Diestra, E., Esteve, I., Caumette, P. & Duran, R. (2004a). Vertical shift of phototrophic bacterial communities during a diel cycle in Salin de Giraud microbial mat (Camargue, France). *en préparation*.

Fourçans, A., García de Oteyza, T., Wieland, A., Solé, A., Diestra, E., van Bleijswijk, J., Grimalt, J. O., Kühl, M., Esteve, I., Muyzer, G., Caumette, P. & Duran, R. (2004b). Characterization of functional bacterial groups in a hypersaline microbial mat community (Salins-de-Giraud, Camargue, France). *FEMS Microbiology Ecology* **in press**.

Fründ, C. & Cohen, Y. (1992). Diurnal cycles of sulfate reduction under oxic conditions in cyanobacterial mats. *Applied and Environmental Microbiology* **58**, 70-77.

Fukui, M., Teske, A., Aßmus, B., Muyzer, G. & Widdel, F. (1999). Physiology, phylogenetic relationships, and ecology of filamentous sulfate-reducing bacteria (genus desulfonema). *Archives of Microbiology* **172**, 193-203.

Giani, D., Seeler, J., Giani, L. & Krumbein, W. E. (1989). Microbial mats and physicochemistry in a saltern in the Bretagne (France) and in a laboratory scale saltern model. *FEMS Microbiology Ecology* **62**, 151-162.

Jeziore-Sassoon, Y., Hamblin, P. A., Bootle-Wilbraham, C. A., Poole, P. S. & Armitage, J. P. (1998). Metabolism is required for chemotaxis to sugars in Rhodobacter sphaeroides. *Microbiology* **144**, 229-239.

Jørgensen, B. B. (1994). Sulfate reduction and thiosulfate transformations in a cyanobacterial mat during a diel oxygen cycle. *FEMS Microbiology Ecology* **13**, 303-312.

Krekeler, D., Teske, A. & Cypionka, H. (1998). Strategies of sulfate-reducing bacteria to escape oxygen stress in a cyanobacterial mat. *FEMS Microbiology Ecology* **25**, 89-96.

Krekeler, D., Sigalevich, P., Teske, A., Cohen, Y. & Cypionka, H. (1997). A sulfate-reducing bacterium from the oxic layer of a microbial mat from Solar Lake (Sinai), *Desulfovibrio oxyclinae* sp. nov. *Archives of Microbiology* **167**, 369-375.

Kuever, J., Konneke, M., Galushko, A. & Drzyzga, O. (2001). Reclassification of Desulfobacterium phenolicum as Desulfobacula phenolica comb. nov. and description of strain SaxT as Desulfotignum balticum gen. nov., sp. nov. *Int J Syst Evol Microbiol* **51**, 171-177.

Kumar, S., Tamura, K., Jakobsen, I. B. & Nei, M. (2001). MEGA2: molecular evolutionary genetics analysis software. *Bioinformatics* **17**, 1244-1245.

Lane, D. J. (1991). rRNA sequencing. In *Nucleic acid techniques in bacterial systematics.*, pp. 115-175. Edited by G. M. Stachenbradt E., (Eds): Wiley, Chichester.

Liu, W. T., Marsh, T. L., Cheng, H. & Forney, L. J. (1997). Characterization of microbial diversity by determining terminal restriction fragment length polymorphisms of genes encoding 16S rRNA. *Applied and Environmental Microbiology* **63**, 4516-4522.

Maidak, B. L., Cole, J. R., Lilburn, T. G., Parker, C. T., Jr., Saxman, P. R., Farris, R. J., Garrity, G. M., Olsen, G. J., Schmidt, T. M. & Tiedje, J. M. (2001). The RDP-II (Ribosomal Database Project). *Nucleic Acids Research* **29**, 173-174.

Minz, D., Fishbain, S., Green, S. J., Muyzer, G., Cohen, Y., Rittmann, B. E. & Stahl, D. A. (1999a). Unexpected population distribution in a microbial mat community: sulfate-reducing bacteria localized to the highly oxic chemocline in contrast to a eukaryotic preference for anoxia. *Applied and Environmental Microbiology* **65**, 4659-4665.

Minz, D., Flax, J. L., Green, S. J., Muyzer, G., Cohen, Y., Wagner, M., Rittmann, B. E. & Stahl, D. A. (1999b). Diversity of sulfate-reducing bacteria in oxic and anoxic regions of a

microbial mat characterized by comparative analysis of dissimilatory sulfite reductase genes. *Applied and Environmental Microbiology* **65**, 4666-4671.

Mouné, S., Caumette, P., Matheron, R. & Willison, J. C. (2003). Molecular sequence analysis of prokaryotic diversity in the anoxic sediments underlying cyanobacterial mats of two hypersaline ponds in Mediterranean salterns. *FEMS Microbiology Ecology* **44**, 117-130.

Namsaraev, Z. B., Gorlenko, V. M., Namsaraev, B. B., Buriukhaev, S. P. & Iurkov, V. V. (2003). [The structure and biogeochemical activity of the phototrophic communities from the Bol'sherechenskii alkaline hot spring]. *Mikrobiologiia* **72**, 228-238.

Nelson, D. C., Revsbech, N. P. & Jorgensen, B. B. (1986). Microoxic-anoxic niche of Beggiatoa spp. : microelectrode survey of marine and freshwater strains. *Applied and Environmental Microbiology* **52**, 161-168.

Phelps, C. D., Kerkhof, L. J. & Young, L. Y. (1998). Molecular characterization of a sulfate-reducing consortium which mineralizes benzene. *FEMS Microbiology Ecology* **27**, 269-279.

Ramsing, N. B., Ferris, M. J. & Ward, D. M. (2000). Highly ordered vertical structure of Synechococcus populations within the one-millimeter-thick photic zone of a hot spring cyanobacterial mat. *Applied and Environmental Microbiology* **66**, 1038-1049.

Revsbech, N. P., Jorgensen, B. B., Blackburn, T. H. & Cohen, Y. (1983). Microelectrode studies of the photosynthesis and O2, H2S and pH profiles of a microbial mat. *Limnology and Oceanography* **28**, 1062-1074.

Richardson, L. L. (1996). Horizontal and vertical migration patterns of *Phormidium corallyticum* and *Beggiatoa* spp. associated with black-band disease of corals. *Microbial Ecology* **32**, 323-335.

Richardson, L. L. & Castenholz, R. W. (1987). Diel vertical movements of the cyanobacterium *Oscillatoria terebriformis* in a sulfide-rich microbial mat. *Applied and Environmental Microbiology* **53**, 2142-2150.

Ruff-Roberts, A. L., Kuenen, J. G. & Ward, D. M. (1994). Distribution of cultivated and uncultivated cyanobacteria and Chloroflexus-like bacteria in hot spring microbial mats. *Appl Environ Microbiol* **60**, 697-704.

Schink, B., Thiemann, V., Laue, H. & Friedrich, M. W. (2002). Desulfotignum phosphitoxidans sp. nov., a new marine sulfate reducer that oxidizes phosphite to phosphate. *Arch Microbiol* **177**, 381-391.

Sigalevich, P., Baev, M. V., Teske, A. & Cohen, Y. (2000a). Sulfate reduction and possible aerobic metabolism of the sulfate- reducing bacterium Desulfovibrio oxyclinae in a chemostat coculture with Marinobacter sp. Strain MB under exposure to increasing oxygen concentrations. *Applied and Environmental Microbiology* **66**, 5013-5018.

Sigalevich, P., Meshorer, E., Helman, Y. & Cohen, Y. (2000b). Transition from Anaerobic to Aerobic Growth Conditions for the Sulfate-Reducing Bacterium Desulfovibrio oxyclinae Results in Flocculation. *Applied and Environmental Microbiology* **66**, 5005-5012.

Sorokin, D. I., Turova, T. P., Kuznetsov, B. B., Briantseva, I. A. & Gorlenko, V. M. (2000). [Roseinatronobacter thiooxidans Gen. Nov., sp. Nov., a new alkaliphilic aerobic bacteriochlorophyll-alpha-containing bacteria from a soda lake]. *Mikrobiologiia* **69**, 89-97.

Teske, A., Ramsing, N. B., Habicht, K., Fukui, M., Kuver, J., Jorgensen, B. B. & Cohen, Y. (1998). Sulfate-reducing bacteria and their activities in cyanobacterial mats of solar lake (Sinai, Egypt). *Applied and Environmental Microbiology* **64**, 2943-2951.

Thompson, J., Gibson, T., Plewniak, F., Jeanmougin, F. & Higgins, D. (1997). The CLUSTAL_X windows interface: flexible strategies for multiple sequence alignment aided by quality analysis tools. *Nucleic Acids Research* **25**, 4876-4882.

van Gemerden, H. (1993). Microbial mats : A joint venture. *Marine Geology* **113**, 3-25.

Weisburg, W. G., Barns, S. M., Pelletier, D. A. & Lane, D. J. (1991). 16S ribosomal DNA amplification for phylogenetic study. *Journal of Bacteriology* **173**, 697-703.

Whale, G. F. & Walsby, A. E. (1984). Motility of the cyanobacterium *Microcoleus chthonoplastes* in mud. *Phycol. J.* **19**, 117-123.

Widdel, F. & Pfennig, N. (1981). Studies on dissimilatory sulfate-reducing bacteria that decompose fatty acids. I. Isolation of new sulfate-reducing bacteria enriched with acetate from saline environments. Description of Desulfobacter postgatei gen. nov., sp. nov. *Archives of Microbiology* **129**, 395-400.

Wieland, A., Zopfi, J., Benthien, M. & Kühl, M. (2003a). Biogeochemistry of an iron-rich hypersaline microbial mat (Camargue, France). *Microbial Ecology* **in press**.

Wieland, A., Kuhl, M., McGowan, L., Fourçans, A., Duran, R., Caumette, P., Garcia De Oteyza, T., Grimalt, J. O., Solé, A., Diestra, E., Esteve, I. & Herbert, R. A. (2003b). Microbial mats on the Orkney islands revisited: microenvironment and microbial community composition. *Microbial Ecology* **46**, 371-390.

Wieringa, E. B., Overmann, J. & Cypionka, H. (2000). Detection of abundant sulphate-reducing bacteria in marine oxic sediment layers by a combined cultivation and molecular approach. *Environmental Microbiology* **2**, 417-427.

Chapitre V : Adaptation des populations bactériennes face à une pollution d'hydrocarbures

V. Adaptation des populations bactériennes face à une pollution d'hydrocarbures

V.1. Introduction

Depuis plusieurs décennies, l'essor de l'industrie a entraîné l'utilisation massive de pétrole comme source d'énergie ou matière première pour la production de produits chimiques divers. En conséquence, des risques nouveaux pour l'environnement sont apparus, par le biais des rejets de résidus toxiques accidentels ou non, mais aussi dus au transport maritime intensif de produits pétroliers des pays producteurs vers les pays utilisateurs. Les conséquences écologiques et économiques suite à de nombreux accidents pétroliers (Amoco Cadiz, Erika, Prestige, pollution pétrolière du golfe Arabo-Persique suite à la Guerre du Koweït, etc.), ont entraîné la recherche vers l'étude intensive des processus de bio-réhabilitation.

Le pétrole brut est essentiellement composé d'hydrocarbures, parmi lesquels les hydrocarbures saturés, les hydrocarbures aromatiques, les résines, et les asphaltènes (Harayama *et al.*, 1999). Ces composés sont fortement nocifs, puisqu'ils montrent des propriétés toxiques, mutagènes et carcinogènes. Dans l'environnement, et plus particulièrement dans les milieux marins, les principaux phénomènes intervenant dans le devenir des hydrocarbures sont soit abiotiques (évaporation, dissolution, dispersion, photo-oxydation et sédimentation) soit biotiques (biodégradation). Parmi ces processus, l'activité des microorganismes joue un rôle important soit direct par des réactions de biodégradation soit indirect en modifiant les conditions du milieu (Leahy and Colwell, 1990; Swannell *et al.*, 1996).

Les tapis microbiens sont considérés comme des écosystèmes compacts parfaitement organisés dans lesquels l'activité métabolique de chaque composante bactérienne dépend de l'activité des autres membres de la communauté (van Gemerden, 1993). Ainsi, comme production et consommation de matière organique ne sont séparées que de quelques microns à quelques millimètres, les tapis microbiens présentent un énorme potentiel métabolique pouvant être exploité pour des processus de bio-réhabilitation. En effet, pendant la guerre du Golfe, il a été démontré que les tapis microbiens pouvaient jouer un rôle important dans la biodégradation du pétrole des zones côtières contaminées (Höpner *et al.*, 1996).

Les connaissances actuelles sur la biodégradation des hydrocarbures proviennent principalement de l'étude de souches hydrocarbonoclastes en cultures pures (Rabus and Widdel, 1995; Harms *et al.* , 1999; Galushko *et al.*, 1999). Cependant les études récentes de tapis microbiens pollués portant sur la dynamique des communautés, la diversité bactérienne, et leurs potentiels de dégradation, participent à une meilleure compréhension des processus de dégradations biotiques (Abed *et al.*, 2002; Grotzschel *et al.*, 2002).

Ce chapitre porte sur l'étude de l'impact du pétrole sur les populations bactériennes issues de tapis microbiens, ainsi que de leurs capacités d'adaptation et donc de dégradation de ces hydrocarbures.

La première partie de ce chapitre, détaillée dans l'article intitulé "Dégradation of Erika fuel oil", concerne l'étude de l'impact du pétrole brut de l'Erika sur les microorganismes du tapis microbien des marais salants de Guérande (Bretagne), et de leurs potentiels de dégradation. L'analyse chimique par GC/MS du site pollué a mis en évidence l'influence des paramètres environnementaux dans la dégradation naturelle de ce pétrole, entre autres l'épaisseur de la couche de polluants, et le niveau de l'eau de mer par rapport aux zones analysées. Les tapis de Guérande maintenus en microcosme au laboratoire et pollués durant 3 mois avec le pétrole de l'Erika ont été analysé par T-RFLP. Cette analyse de la biodiversité moléculaire des eubactéries et des bactéries anoxygéniques phototrophes a permis de décrire l'impact réel de la pollution sur les communautés du tapis. Ainsi la succession de différentes communautés bactériennes révèle les capacités d'adaptation de ces écosystèmes face à ce stress.

Le deuxième article de ce chapitre "T-RFLP and functional analyses of bacterial communities changes in microbial mats following petroleum exposure" décrit l'impact de pétroles bruts sur deux tapis microbiens hypersalés : Salins-de-Giraud (Camargue) et Guérande (Bretagne). L'étude a été réalisée en polluant ces tapis maintenus en microcosme puis en suivant la diversité bactérienne au cours du temps par T-RFLP. Ainsi, les genres *Chloroflexus*, *Burkholderia*, *Desulfovibrio* et *Cytophaga* ont été observés comme faisant partie des OTUs les mieux adaptées à cette pollution. En parallèle, le potentiel métabolique de dégradation des hydrocarbures des différentes communautés de ces tapis a été appréhendé par l'étude de la diversité des gènes codant pour les dioxygénases. Ces enzymes impliquées dans la dégradation des hydrocarbures montrent dans cette étude une grande diversité, suggérant que les tapis microbiens possèdent un potentiel de dégradation important.

V.2. Tapis microbien de Guérande soumis à une pollution par le pétrole de l'Erika

Ce travail a été soumis au journal "Aquatic Living Ressources" sous le titre :

Degradation of Erika fuel oil

Par : Sylvain Bordenave[1], Ronan Jézéquel[2], Aude Fourçans[1], Héléne Budzinski[3], François Xavier Merlin[2], Tangi Fourel[2], Marisol Goñi-Urriza[1], Rémy Guyoneaud[1], Régis Grimaud[1], Pierre Caumette[1], Robert Duran[1]

ABSTRACT

Since March 2001, samples of remaining oil from Erika wreck were collected along the Atlantic coastline in order to assess the natural degradation. Four years after the wreckage, the chemical analyses of the oil revealed the influence of the environmental parameters on the degradation kinetics. Among the diverse parameters controlling the fate of crude oil in the environment, biodegradation by microorganisms is known to play an important role. To investigate the role of microorganisms on Erika fuel oil degradation, microbial mats from Guérande salterns were maintained in slurries containing the contaminant. From these slurries experiments, a low biodegradation by microorganisms of the Erika fuel oil could be suspected indicating the degradation capacities of microbial mats. To further understand the biodegradation processes biodiversity studies were conducted. Microbial mats from Guérande salterns were maintained in microcosms to evaluate the impact of Erika fuel oil on bacterial communities. Molecular analysis based on 16S rRNA and *pufM* encoding genes allowed to determine fingerprints on eubacterial and purple anoxygenic phototrophic bacterial (PAB) communities respectively. These studies revealed bacterial diversity and communities changes showing the adaptation of microorganisms to oil pollution.

[1] Laboratoire d'Ecologie Moléculaire EA3525, Université de Pau, BP 1155 F64013 Pau cedex France

[2] Cedre. 715 rue Alain Colas. CS 41836. 29218 Brest Cedex 1. France.

[3] Laboratoire de Physico-Toxico-Chimie - UMR 5472 CNRS, Université Bordeaux I, 351, crs de la Libération 33405 Talence France

INTRODUCTION

In late December 1999 the north of the French Atlantic coast was injured by an oil spill following the wreck of the Maltese oil tanker Erika. Crude oil is composed mainly by hydrocarbons, such as saturated hydrocarbons, aromatics, resins and asphaltenes [8], which are highly noxious, compounds as they exhibit toxic, mutagenic, and carcinogenic properties [3, 4]. Previous studies on the impact of oil spills report persistent effects during five to more than ten years [12, 24]. According to its composition of 90% of heavy residues and 10% of a light fraction, the Erika heavy fuel oil was found to be more resistant to natural degradation processes than light crude oils [19]. After the contamination the fate of petroleum hydrocarbon compounds in the environment depends on both physico-chemical and biological environmental variables that control different mechanisms such as photo and chemical oxidations, evaporation, dilution, sedimentation, and microbial activities. Among these processes, biodegradation by microorganisms is known to play an important role [14, 25]. Hydrocarbons differ in their susceptibility to microbial attack and generally degrade in the following order of decreasing susceptibilities: *n*-alkanes > branched alkanes > low-molecular-weight aromatics > cyclic alkanes [14]. For efficient remediation after oil spills, we need to evaluate kinetics and relative rates of natural degradation and estimate the active role played by microorganisms. For this purpose it is important to understand the behavior of microbial populations responsible for degrading crude oil. In coastal zone, photosynthetic microbial mats develop at the water-sediment interface [2, 27]. Since these vertically laminated structures show important bacterial diversity that present high metabolic potential for hydrocarbons degradation, they could be considered as relevant models to study crude oil impact on bacterial communities [1].

The specific aims of this research were: (1) to assess the kinetics of natural degradation processes of the Erika fuel oil according to the environmental parameters by monitoring *in situ* the fate of hydrocarbon compounds, (2) to evaluate the degradation capacities of bacterial communities present in microbial mats from the polluted area (Guérande, Brittany, France) using slurry experiments, and (3) to estimate the Erika fuel impact on these microbial structures by culture independent molecular analysis.

MATERIALS AND METHODS

Monitoring natural degradation of Erika fuel oil

To assess the natural degradation of the Erika fuel oil according to the environmental conditions, *Cedre* employees involved during the cleaning operations were asked to propose polluted areas following two main criteria: (1) area where no human cleaning operations were performed and (2) area with enough pollutant remaining to allow sampling round during several years. More than 75 sites were suggested for this study. After a survey of these selections, 21 sites were definitely selected and samples collected. For each site, samples were collected in triplicate, in various area according to solar - waves exposure and substrate nature. Samples were then frozen and stored at –20°C until analysis.

Sample extraction

For oil-sediment samples extraction, approximate 50 mg of the samples were weighed, dissolved in methylene chloride in a sonication bath during 10 minutes. The solvent was filtered through sodium sulfate then evaporated using a rotavapor. For mud samples extraction, a preliminary step before oil extraction was to evaporate the water at 40°C during 4 hours. The same procedure as cited above was then used. For sand samples extraction, approximate 150 ml of sand was mixed with sodium sulfate. Oil was then extracted using a soxhlet with methylene chloride during 4 hours.

Hydrocarbon composition analysis

Approximate 30 mg of the samples were purified through low-pressure liquid chromatography on an open silica-alumina column (saturates and aromatics were eluted simultaneously with a mixture pentane / methylene chloride 80/20). Solvent was then evaporated to 2 ml and the sample analyzed by gas chromatography equipped with a mass spectrometry detection (GC/MS). The GC was an HP 6890N (Hewlett-Packard, Palo Alto, CA, USA) equipped with a split/splitless injector (Pulsed Splitless time: 1 min, flow 50 $ml.min^{-1}$). The injector temperature was maintained at 270 °C. The interface temperature was 290°C and the GC temperature gradient was from 50°C (1 min) to 300°C (20 min) at $5°C.min^{-1}$. The carrier gas was Helium at a constant flow of 1 $ml.min^{-1}$. The capillary column used was an HP 5 MS (Hewlett-Packard, Palo Alto, CA, USA) : 60 m x 0,25 mm ID x 0,25 mm film thickness. The GC was coupled to an HP 5973 Mass Selective Detector (MSD) (Electronic Impact: 70 eV, voltage: 1200V). Saturates and PAHs

quantification were done using Single Ion Monitoring mode with the molecular ion of each compound at 1.4 cycles/s.

Quantification was performed with respect to an internal reference, the 17α (H), 21β(H)-hopane (m/z=191). This "biomarker" (non-biodegraded, non-photooxidazed, non-volatile and non-water-soluble) is currently used as a conserved internal marker within the oils to follow the disappearance of other components within the oils [11, 21, 23].

Microbial mat sampling and microcosms experiment set up

Guérande microbial mats were collected from a saltern near La Baule (Bretagne, France). Salterns provide environments of various salinities, ranging from the salt concentration of seawater up to those at which NaCl precipitates. The mean day light temperature in the area is 11°C to 12°C, with rainfall of 800 to 900 mm per year [7]. A freshly taken microbial mat sample was cut into pieces of equal size (20 cm^2) and placed in glass tubes without water. Half mat samples were not contaminated (control mats) and the remaining mat samples were contaminated with Erika fuel oil. Approximately equal amounts of oil (200 to 300 mg) were added on the surfaces of contaminated mats before adding synthetic seawater (salinity 70 ‰). Microbial mats microcosms were maintained at room temperature under a cycle of 16 h daylight / 8 h dark. Samples were taken every 15 days during 3 months. At each time, one contaminated microcosm and one control microcosm taken randomly, were sub-sampled in Pasteur micropipettes and then stored immediately at -80°C. Biodiversity was estimated by the T-RFLP method on two mixed sub-samples.

Genomic DNA extraction

Mixed community DNA was extracted from microbial mat fractions with the Ultraclean soil DNA isolation kit (Mo Bio Laboratories, Solana Beach, California), by using the recommended protocol with minor modifications as previously described [22].

PCR amplification and purification

Optimization of PCR was performed for each sample by adjusting the amount of genomic DNA extract used to obtain a strong band on an agarose gel, without visible non-specific product. PCR was performed using a reaction mixture of 200 µM each desoxynucleoside triphosphate (Qiagen), 1.5 mM $MgCl_2$, 1.25 U of Taq polymerase (Qiagen), 1X PCR Buffer (Qiagen), and 0.2 µM each primer. The first primers used were the general eubacterial primer

8-27F [13], and the universal primer 1472-1489R [18] amplifying specifically the 16S ribosomal gene. To assess specifically purple bacteria, *pufM* gene coding for the photosynthetic center was targeted with the primers: PB557F and PB750R [16]. Forward primers, 8-27F and PB557F were hexachlorofluorescein labeled. PCR (50µl) was performed in a MJ Research PTC-100 thermocycler by using an initial denaturation step of 95°C for 3 minutes, followed by 24 cycles of a program consisting of denaturation at 95°C for 30 seconds, primer annealing at 55°C for 30 seconds, and extension at 72°C for 30 seconds. A final extension at 72°C for 7 minutes was performed after the programmed numbers of cycles were completed. PCR products were then purified using the GFX DNA and Gel Band Purification kit (Amersham Biosciences) as directed by the supplier.

Restriction enzyme digestion and products purification

After a quantification of the purified PCR product by the "dots method", 300 ng of amplified DNA was mixed in a final volume of 30 µl of restriction enzyme mix containing 10 U of restriction enzyme (HaeIII) in 1X reaction buffer (New England BioLabs), were incubated for 3 h at 37°C.

T-RFLP analysis

Three microliters of the restricted PCR product was mixed with 1 µl of TAMRA500 size standard (Applied Biosystems Instruments, Foster City, California). DNA fragments were separated by size by capillary electrophoresis at 15,000 Volts for 30 minutes on an ABI PRISM 310 Genetic Analyzer (Applied Biosystems). The 5' terminal fragments were visualized by excitation of the hexachlorofluorescein molecule (hex) attached to the forward primer. The gel image was captured and analyzed by using Genescan version 3.1 analysis software (ABI). Negative controls (no genomic DNA) were conducted with every PCR and run on Genescan gels. Data sets were constructed by using peak which fluorescence was higher than 100 for at least one sample. Statistical analyses were done with a hierarchical cluster analysis; the unweighted-pair group method using arithmetic averages (UPGMA). Those statistical analyses were done with MVSP software (Multi-Variate Statistical Package 3.1, Kovach Computing Services).

In vitro Erika fuel oil biodegradation

To estimate the biodegradation potential of Guérande microbial mats, slurry experiments were conducted. Slurries consisted of grounded microbial mats maintained in synthetic seawater contaminated with Erika fuel oil (0.16 – 0.24 $g.l^{-1}$). Abiotic controls were done with sterilized microbial mats. Slurries were incubated in aerobic conditions at 30°C with shaking at 180 rpm under continuous light exposure. Samples were collected through the three months incubation period. Hydrocarbons composition of Erika fuel oil was analyzed as previously described [17].

RESULTS

Monitoring the natural degradation of Erika fuel oil

The results presented in this study were from "Baie de Bourgneuf" (Vendée-France) (Fig. 1A). Samples were collected in various areas according to solar-waves exposure and substrate nature (Fig. 1B). Table 1 shows the characteristics of the sampling sites. For each sample collected since March 2001, relative abundances (Hopane Unit) of *n*-alkanes (Fig. 2A), *n*-C30 (Fig. 2B), Benzothiophenes (parent and alkyl homologues) (Fig. 2C) and Chrysenes (parent and alkyl homologues) (Fig. 2D) were obtained.

In comparison with the other samples characterized by thin layer of pollutant, less *n*-alcanes degradation was observed for boulder breakwater samples (thick patches of oil at the surface and under rocks). Moreover, *n*-alkanes and *n*-C30 abundances increased in these samples. *n*-alkanes were degraded at a similar rate for samples 1, 4 and 5 despite the different level at which they were collected. Degradation of light PAHs (Benzothiophene) (Fig. 2C) was similar for all the samples. Heaviest PAHs such as Chrysenes (Fig. 2D) were degraded at different rates according to the environmental conditions: supratidal samples were more degraded than intertidal ones. Fig. 2D shows that the depletion of chrysenes was more important for the samples collected at a supratidal level (samples 4 and 5) compared to intertidal samples.

Evaluation of Erika fuel oil degradation capacities of Guérande microbial mats

Through the three months incubation period, modifications of Erika fuel oil composition were observed in both biotic and abiotic conditions (data not shown). However, although the results showed an important variation, a biotic degradation could be suspected. Phenanthrene and dibezothiophene derivatives compounds were among the most biodegraded hydrocarbons. High molecular weight compounds were less biodegraded.

Impact of Erika fuel oil on bacterial communities of Guérande microbial mats

T-RFLP analysis using specific primers targeting eubacterial 16S rRNA encoding genes allowed to obtain fingerprints with 22 operational taxonomic units (OTUs) revealing an important diversity. Although the bacterial communities structure changed through the experimental period in both contaminated and uncontaminated microcosms, the comparison between the different conditions showed that the evolution was different depending to the presence of the pollutant. Cluster analysis from the T-RFLP data showed that control samples from the 30th to the 75th day formed a separate cluster to the other samples (Fig. 3).

Purple anoxygenic phototroph community structure changes were analyzed by T-RFLP targeting *pufM* genes specific to these bacterial populations. T-RFLP fingerprints showed an abundant bacterial diversity characterized by the detection of 26 OTUs (Fig. 4). As observed with eubacterial community structure analysis, biodiversity changes were observed in both contaminated and uncontaminated microcosms during the experimental period. However the evolution of some bacterial populations was found to be different according to experimental conditions. Between the 15th and the 45th days, OTU with length of 132 base pairs (bp) was less developed in presence of Erika fuel oil rather than in control microcosms. In contrast during the same period OTU with length of 200 bp increased in contaminated microcosms while no changes were observed in uncontaminated conditions. From the 60th day to the end of the experiment (90th day), OTU with length of 82 bp was also increased in polluted mats. Comparison between the community fingerprints was obtained by cluster analysis (Fig. 5). Two main clusters were observed, cluster I with initial samples (from t0 to t15) and cluster II with samples of the rest of experiment. In cluster I contaminated sample Bt15 was separated from the other three samples. Similarly, contaminated sample Bt30 was found to be isolated in cluster II.

DISCUSSION

The *in situ* monitoring of the fate of Erika fuel oil indicated that *n*-alkanes were less degraded in thick patches of oil at the surface and under rocks than in samples characterized by thin layers of pollutant. Thus these results suggested that *n*-alkanes degradation could be related to the thickness of the pollutant layer. Moreover, the "increases" of *n*-alkanes and *n*-C30 abundances for samples from thick patches of oil were also due to the pollutant layer as all the processes of natural degradation are most effective on thin films of oil. The fact that samples characterized by a thin layer of pollutant showed that *n*-alkanes were degraded at

similar rates whatever the level at which they were collected suggest that biodegradation was probably the most significant process in the degradation of this compounds. Degradation of light PAHs (Benzothiophene) was related to evaporation, dissolution, and biodegradation processes, which are effective for all light compounds. Heaviest PAHs such as Chrysenes, known to be photosensitive compounds [6], were degraded at different rates according to the environmental light conditions.

Thus monitoring analysis revealed that the natural degradation was dependent of both the pollutant thickness and the level from the seawater at which the samples were collected. The degradation rate increase as the pollutant layer decreases and supratidal samples appears to be the most degraded. Nevertheless, although the assessment of natural degradation by using relative abundance of *n*-alkanes and PAH could be useful to establish which natural degradation process occur during an oil weathering, it does not show the "total" degradation of the pollutant since *n*-alkanes and PAH represent less than 4% of the Erika fuel oil [20].

Clustering analysis of T-RFLP fingerprints of eubacterial communities indicated that contaminated communities differ from uncontaminated communities suggesting that Erika fuel oil disturbs bacterial communities structure. Similar results have been previously reported showing the impact of toxic compounds to bacterial communities [1, 15]. To further analysis the impact of the Erika fuel oil on microbial mats, we focus our investigation on purple anoxygenic phototrophic bacterial (PAB) communities that play an important metabolic role in microbial mats [27]. Among this PAB community, T-RFLP fingerprints showed that a PAB population was sensitive to pollutant, i.e., OTU 132 bp related by predictive digestion of *pufM* genes to some purple non sulfur bacteria such as *Rhodoplanes elegans* or *Rubrivivax gelatinosus*. Other PAB populations (OTUs 82 and 200 bp) were capable to survive and/or utilize toxic contamination; predictive digestions of *pufM* genes could relate OTU 200 bp to two different bacterial types: *Erythrobacter* sp, or the purple sulfur bacteria *Halochromatium salexigens* SG3201. Therefore more *pufM* gene sequence data would be useful to improve the characterization of PAB populations by T-RFLP analysis. Furthermore, the impact on these OTUs was observed at different periods indicating that the microbial mats adapted in several steps by a succession of different communities. These observations were supported by clustering analysis that showed two main periods. First, a hydrocarbon impact during the first month characterized by a high divergence between contaminated and uncontaminated communities at t15 and t30 was observed. This first impact on PAB community would probably due to both hydrocarbon toxicity and opaqueness character of Erika fuel oil.

Second, for the rest of the experiment similarity between contaminated and uncontaminated PAB communities was found to increase progressively. In accordance with the appearance of the contaminated microcosms and the degradation results, these observations suggested that opaqueness and toxicity due to Erika fuel oil were less important. The observed Erika fuel oil modification could be explained by both abiotic and/or biotic degradations. Our degradation results indicated that biodegradation by microorganisms could be suspected. These results are consistent with preliminary observation demonstrating the low biodegradability of the Erika fuel oil [19]. However previous studies demonstrated that microorganisms produce surfactants that facilitate hydrocarbon solubilization and degradation [5, 10, 26]. It was also demonstrated that microbial mats from different origins were found to be rich in microorganisms with high biodegradative potential [1, 9]. To further understand biodegradation by microbial mats, it will be interesting to isolate key microorganisms and fully explore their potentials to degrade hydrocarbons.

ACKNOWLEDGEMENTS

We acknowledge the financial support by the Ministère de l'Ecologie et du Développement Durable (MEDD - LIT'EAU/Erika project, N° 01/1213857). The authors are grateful to the Salines de Guérande for facilitating access to the salterns, sampling and field experiments. SB and AF are partly supported by a doctoral grant from the Aquitaine region and the Conseil Général des Pyrénées Atlantiques respectively. We are grateful to Arnaud Verbaere for technical assistance for T-RFLP analysis and Alexia De Brondeau for slurry experiments.

Table 1. Environmental conditions and locations of samples collected from "Baie de Bourgneuf"

Samples	Location	Substrate nature	Solar radiation	Layer (mm) (*)	Tidal level
1	16	Mud	Exposed	5	Intertidal
2	15	Rocks (surface)	Exposed	> 10	Intertidal
3	15	Rocks (shade)	Non exposed	> 10	Intertidal
4	17	Concrete	Exposed	2	Supratidal
5	15	Rocks, soil	Exposed	5	Supratidal

(*) Pollutant layer was estimated visually at each sampling round.

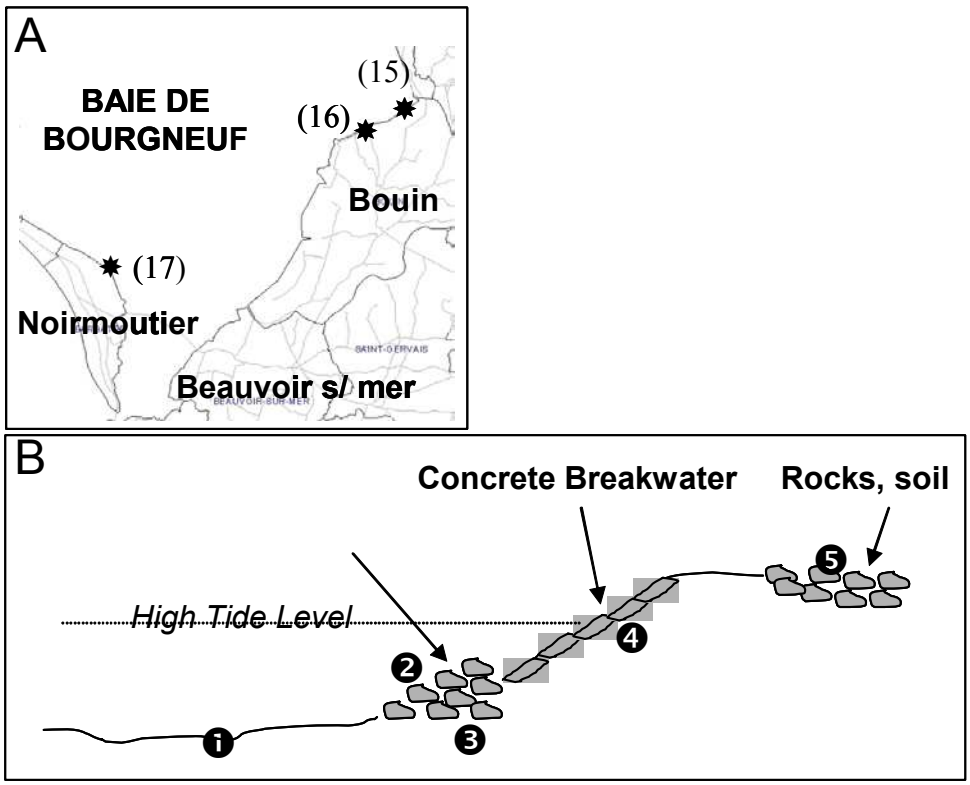

Figure 1: Location of sites sampled in "Baie de Bourgneuf" (A) and schematic representation of sampling areas (B).

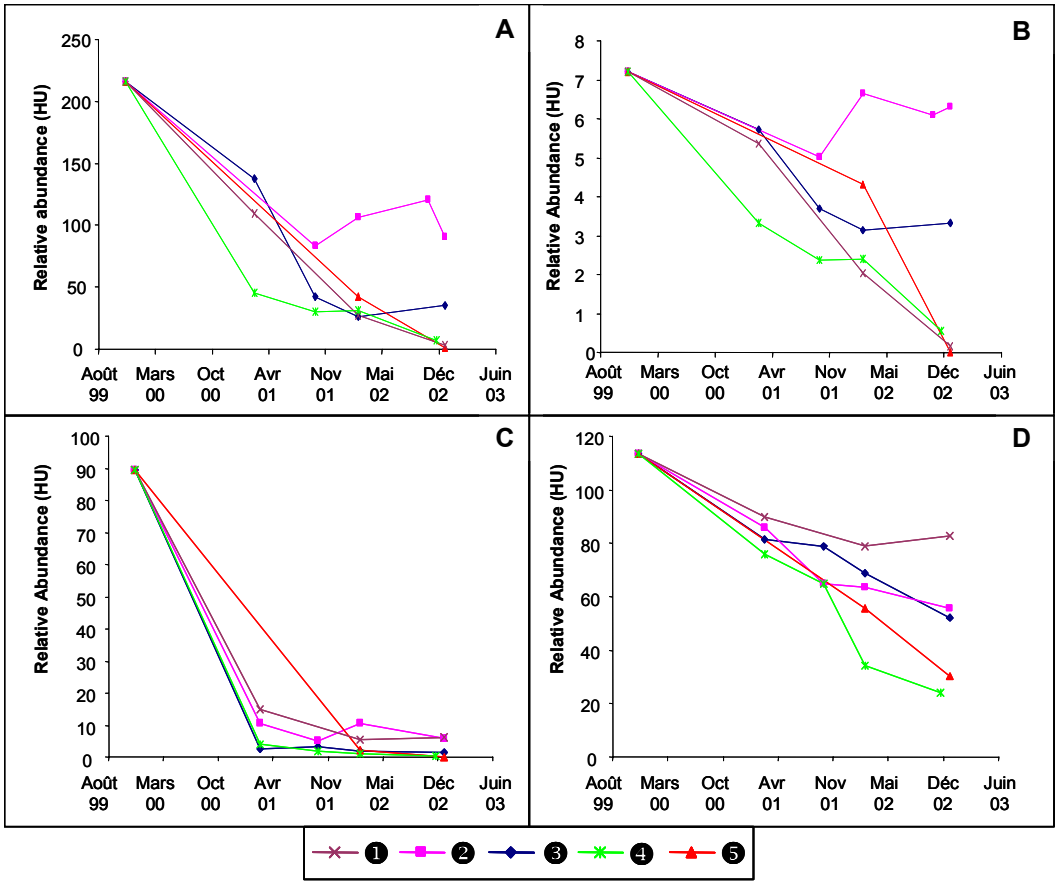

Figure 2: Relative Abundance (HU) of *n*-alcanes (A), *n*-C30 (B) benzothiophenes (parent and alkyl homologues) (C) and chrysenes (parent and alkyl homologues) (D) for samples collected since March 2001.

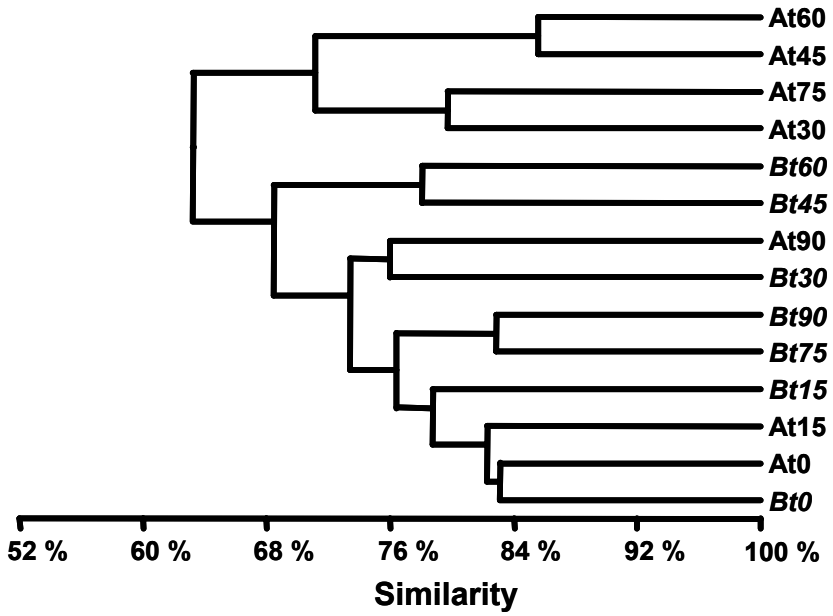

Figure 3: Clustering of eubacteria communities in uncontaminated (A samples) and contaminated (*B* samples) microbial mats microcosms during 90 days incubation period (from t0 to t90). The analysis was obtained from T-RFLP fingerprints of *16S rRNA* genes.

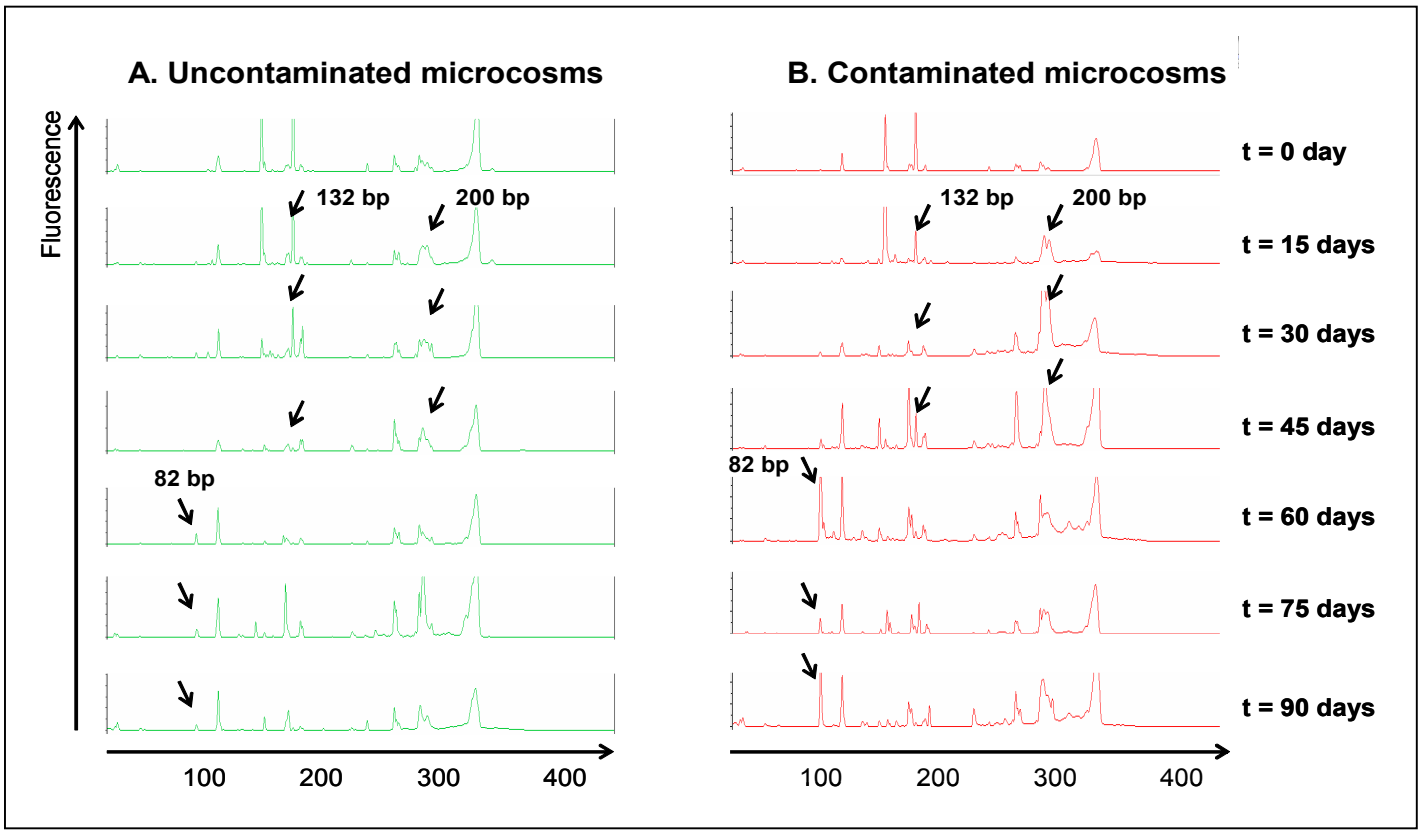

Figure 4: T-RFLP fingerprints of phototroph purple anoxygenic bacteria communities in uncontaminated (A) and contaminated (B) microbial mats microcosms during 90 days incubation period. 5' terminal restriction fragments were obtained after *pufM* gene enzymatic digestion by HaeIII. Arrows show OTUs discussed in the text. bp : base pairs

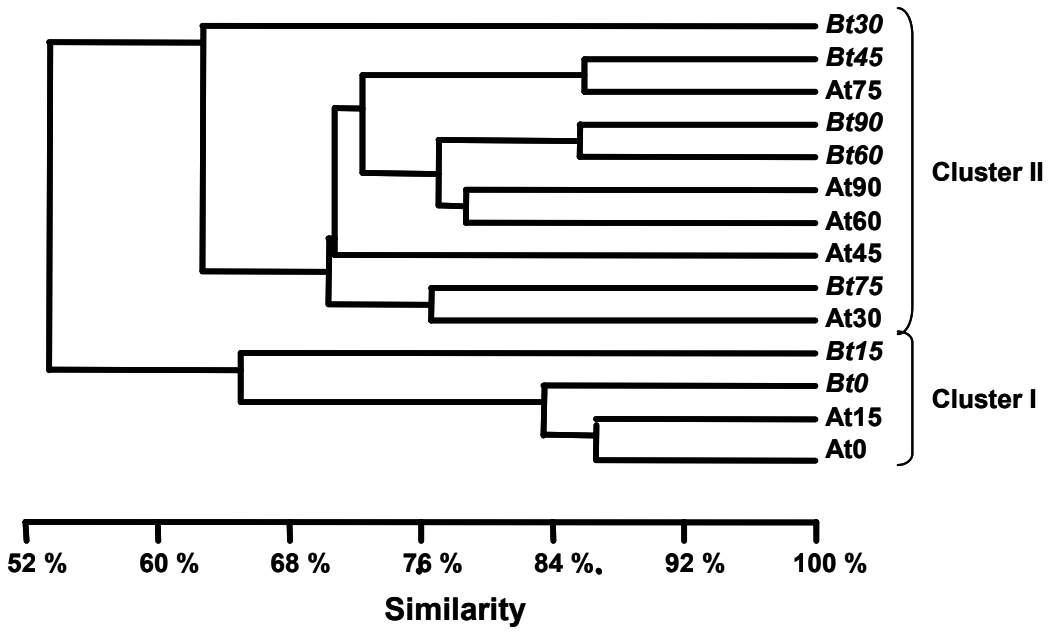

Figure 5: Clustering of phototroph purple anoxygenic bacteria communities in uncontaminated (A samples) and contaminated (*B* samples) microbial mats microcosms during 90 days incubation period (from t0 to t90). The analysis was obtained from T-RFLP fingerprints of *pufM* genes.

REFERENCES

[1] Abed, R.M., Safi, N.M., Koster, J., de Beer, D., El-Nahhal, Y., Rullkotter, J. and Garcia-Pichel, F., 2002. Microbial diversity of a heavily polluted microbial mat and its community changes following degradation of petroleum compounds. Appl. Environ. Microbiol. 68(4), 1674-1683.

[2] Caumette, P., Matheron, R., Raymond, N. and Relexans, J.C., 1994. Microbial mats in the hypersaline ponds of Mediterranean salterns (Salins-de-Giraud, France). FEMS Microbiol. Ecol. 13, 273-286.

[3] Churchill, S.A., Harper, J.P. and Churchill, P.F., 1999. Isolation and characterization of a Mycobacterium species capable of degrading three - and four-ring aromatic and aliphatic hydrocarbons. Appl. Environ. Microbiol. 65(2), 549-552.

[4] Coates, J.D., Woodward, J., Allen, J., Philp, P. and Lovley, D.R., 1997. Anaerobic degradation of polycyclic aromatic hydrocarbons and alkanes in petroleum-contaminated marine harbor sediments. Appl. Environ. Microbiol. 63(9), 3589-3593.

[5] Desai, J.D. and Banat, I.M., 1997. Microbial production of surfactants and their commercial potential. Microbiol. Mol. Biol. Rev. 61(1), 47-64.

[6] Garrett, R.M., Pickering, I.J., Haith, C.E. and Prince, R.C., 1998. Photooxidation of crude oils. Environ. Sci. Technol. 32, 3719-3723.

[7] Giani, D., Seeler, J., Giani, L. and Wolfgang, E.K., 1989. Microbial mats and physiochemistry in a saltern in the Bretagne (France) and in a laboratory scale saltern model. FEMS Microbiol. Ecol. 62, 151-162.

[8] Harayama, S., Kishira, H., Kasai, Y. and Shutsubo, K., 1999. Petroleum biodegradation in marine environments. J. Mol. Microbiol. Biotechnol. 1(1), 63-70.

[9] Hoffmann, L., 1996. Recolonisation of the intertidal flats by microbial mats after the Gulf War oil spill. In: Krupp, F., Abuzinada, A.H. and Nader, I.A. (Eds.) A marine wildlife sanctuary for the Arabian Gulf: environmental research and conservation following the 1991 Gulf War oil spill. Riyad, Saudi Arabia, and Seneckenberg Research Institue, Frankfurt, Germany, pp. 96-115.

[10] Hua, Z., Chen, J., Lun, S. and Wang, X., 2003. Influence of biosurfactants produced by Candida antarctica on surface properties of microorganism and biodegradation of n-alkanes. Water Res. 37(17), 4143-4150.

[11] Jézéquel, R. Menot, L. Merlin, F-X. Prince, R.C., 2003. Natural Cleanup of Heavy Fuel Oil on rocks: an in situ Experiment. Mar. Poll. Bull. 46(8), 983-990.

[12] Jones, D.A., Plaza, J., Watt, I. and Al Sanei, M., 1998. Long-term (1991-1995) monitoring of the intertidal biota of Saudi Arabia after the 1991 Gulf War Oil Spill. Mar. Poll. Bulletin. 36(6), 472-489.

[13] Lane, D.J., 1991. 16S/23S rRNA sequencing. In: Stackenbradt, E. and Goodfellow, M. (Eds.) Nucleic acid techniques in bacterial systematics. Wiley, Chichester, pp. 115-175.

[14] Leahy, J.G. and Colwell, R.R., 1990. Microbial degradation of hydrocarbons in the environment. Microbiol. Rev. 54(3), 305-315.

[15] MacNaughton, S.J., Stephen, J.R., Venosa, A.D., Davis, G.A., Chang, Y.J. and White, D.C., 1999. Microbial population changes during bioremediation of an experimental oil spill. Appl. Environ. Microbiol. 65(8), 3566-3574.

[16] Madigan, M.T., Carey, J.C., Milford, A.D., Jung, D.O. and Achenbach, L.A., 2000. New anoxygenic phototrophs from alkaline/cold environments.10th International symposium on phototrophic prokaryotes, Barcelona, Spain, August 26-31.

[17] Mazeas, L. and Budzinski, H., 2001. Polycyclic aromatic hydrocarbon 13C/12C ratio measurement in petroleum and marine sediments application to standard reference materials and a sediment suspected of contamination from the Erika oil spill. J. Chromatogr A. 923(1-2), 165-176.

[18] Muyzer, G., Teske, A., Wirsen, C.O. and Jannasch, H.W., 1995. Phylogenetic relationships of Thiomicrospira species and their identification in deep-sea hydrothermal vent samples by denaturing gradient gel electrophoresis of 16S rDNA fragments. Arch. Microbiol. 164(3), 165-172.

[19] Oudot, J., 2000. [Biodegradability of Erika fuel oil]. C R Acad Sci III. 323(11), 945-950.

[20] Oudot, J., Jézéquel, R., Le Floch, S. and Merlin, F-X, 2002. [Biodégradabilité du fuel de l'Erika], Proceedings of the 3rd R&D Forum on High-density Oil Spill Response, Brest, France. p. 228-234.

[21] Peters K.E. and Moldowan J.M., 1993. The Biomarker Guide; Interpreting molecular fossils in petroleum and ancient sediments. Englewood Cliffs, NJ: Prentice-Hall.

[22] Precigou, S., Goulas, P. and Duran, R., 2001. Rapid and specific identification of nitrile hydratase (NHase)-encoding genes in soil samples by polymerase chain reaction. FEMS Microbiol. Lett. 204(1), 155-161.

[23] Prince, R.C., Elmendorf, D.L., Lute, J.R., Hsu, C.S., Haith, C.E., Senius, J.D., Dechert, G.J., Douglas, G.S. and Butler, E.L., 1994. 17 α (H),21β (H)-hopane as a conserved

internal marker for estimating the biodegradation of crude oil. Environ. Sci. Technol. 28, 142-145.

[24] Southward, A.J., 1978. Recolonization of rocky shores in Cornwall after use of toxic dispersants to clean up the Torrey Canyon spill. Journal of Fisheries Research Board, Canada. 35, 682-706.

[25] Swannell, R.P., Lee, K. and McDonagh, M., 1996. Field evaluations of marine oil spill bioremediation. Microbiol Rev. 60(2), 342-365.

[26] Van Dyke, M.I., Lee, H. and Trevors, J.T., 1991. Applications of microbial surfactants. Biotechnol. Adv. 9(2), 241-252.

[27] Van Gemerden, H., 1993. Microbial mats: A joint of venture. Mar. Geol. 113, 3-25.

V.3. Tapis microbien de Camargue soumis à une pollution par différents pétroles

Ce travail a été soumis au journal "Ophelia" sous le titre :

T-RFLP and functional analyses of bacterial communities changes in microbial mats following petroleum exposure.

Par : Sylvain Bordenave[1], Aude Fourçans[1], Sophie Blanchard[1], Marisol Goni-Urriza[1], Pierre Caumette[1] et Robert Duran[1]

ABSTRACT

Microbial mats from Salins-de-Giraud (Camargue, France) and Guérande (Bretagne, France) were maintained in microcosm to determine the impact of crude oil contamination on bacterial communities. Terminal Restriction Fragment Length Polymorphism (T-RFLP) analyses revealed noticeable changes in the eubacterial community structures concomitant with petroleum degradation. The results demonstrate clearly different periods with a succession of different bacterial populations. OTUs with T-RFs that could be related to *Chloroflexus*, *Burkholderia*, *Desulfovibrio* and *Cytophaga* genera were found among the populations well adapted to crude oil exposure. To further evaluate the metabolic ability to degrade hydrocarbons of such oil contaminated microbial communities, we studied the diversity of the genes encoding two enzymes known to be involved in hydrocarbon compounds degradation: the naphthalene and phenanthrene dioxygenases. This analyses indicated that although the diversity of PAH dioxygenases encoding genes was important after a three month period of contamination, they were mainly represented by only three different types. Thus the combined analysis of the taxonomic diversity (16S rRNA encoding gene analysis) and the functional diversity (dioxygenases analysis) indicated that microbial community within saline microbial mats plays a role in hydrocarbon degradation.

[1] Laboratoire d'Ecologie Moléculaire, Université de Pau BP1155 - 64013 Pau cedex, France

INTRODUCTION

During the last decades, the extensively use of petroleum has increased the risk to release toxic compounds such as hydrocarbons into the environment. Among the mechanisms controlling the fate of hydrocarbons after contamination, biodegradation by microorganisms is known to play an important role (Hoffman, 1996; Leahy and Colwell, 1990; Narro *et al.*, 1992; Abed *et al.*, 2002). Most of our knowledge on oil biodegradation has been collected from isolated bacterial strains or consortia (Kanaly *et al.*, 2000; Kanaly *et al.*, 2002; Rios-Hernandez *et al.*, 2003; Cerniglia *et al.*, 1980). Improvement of bioremediation of polluted sites requests *in situ* knowledge on microbial diversity and communities dynamic (Kasai *et al.*, 2001; Macnaughton *et al.*, 1999; Nogales *et al.*, 2001).

In coastal zone, particularly exposed to accidental oil spillages and other improper practices, microbial mats develop at the water-sediment interface (Van Gemerden, 1993; Caumette *et al.*, 1994). Since these vertically laminated structures show important bacterial diversity that present high metabolic potential for hydrocarbons degradation, they could be considered as relevant models to study crude oil impact on bacterial communities (Abed *et al.*, 2002). Characterization of bacterial communities and their response to pollutants is now possible with recently developed culture-independent molecular techniques. These methods are suitable for bacterial fingerprinting based on either taxonomic (16S rRNA encoding gene) or functional analyses (Blackwood *et al*., 2003; Liu *et al*., 1997; Muyzer *et al.*, 1993; Dahllöf *et al*., 2002; Stach *et al.*, 2002; Moser *et al*., 2001). For the taxonomic approach, the T-RFLP (Terminal-Restriction Fragment Length Polymorphism) is a useful method to follow the bacterial communities adaptation since a high number of samples could be analyzed rapidly. For the functional purpose, genes involved in hydrocarbon degradation such as dioxygenases encoding genes are of special interest since their expression products play a key role in polyaromatic hydrocarbons degradation. Naphthalene and phenanthrene dioxygenases that catalyze the first step of Polycyclic Aromatic Hydrocarbons (PAH) degradation by introducing alcohol groups into the aromatic ring have been extensively studied (Ensley *et al*., 1982; Resnick *et al*., 1996). In consequence a large number of nucleic acid sequences of these genes have been obtained allowing the development of molecular tools for functional biodiversity studies (Brezna *et al.*, 2003; Olsen *et al*., 1986; Haddad *et al.*, 2001; Feng *et al.*, 1999; Kang *et al.*, 1998; Khan *et al.*, 2001; Contzen *et al.*, 2000).

Two types of hypersaline microbial mats from different environments, Camargue (Mediterranean French coast) and Guérande (Bretagne, Atlantic French coast), were

maintained in microcosms to evaluate the impact of crude oil exposure on microbial communities. Changes on communities' structure on the studied mats were followed by Terminal Restriction Fragment Length Polymorphism (T-RFLP) targeting 16S rRNA encoding genes. For the estimation of degradation capacities of the Camargue mat, a molecular method based on diversity analyses of dioxygenases encoding genes using specific primers has been developed.

MATERIALS AND METHODS

Microbial mat sampling and microcosms experiment set up

Camargue microbial mats develop in a hypersaline environment (salinity 70 to 110 ‰) under Mediterranean climatic conditions with temperatures from 3 to 25°C and annual rainfall of 750 to 1000 mm (Caumette *et al.*, 1994). Guérande microbial mats from a saltern near La Baule (Bretagne, France) providing environments of various salinities, ranging from the salt concentration of sea-water up to those at which NaCl precipitates (Giani *et al.*, 1989). The mean day light temperature in the area is 11°C to 12°C, with rainfall of 800 to 900 mm per year. Microbial mats from Salins-de-Giraud (Camargue, France) and Guérande (Bretagne, France) were maintained in microcosms at room temperature with sterilized synthetic seawater (salinity 70 ‰). A cycle of 16 H daylight / 8 H dark was applied. Approximately equal amounts of Maya oil (200 to 300 mg) were added on the surfaces of contaminated mats before adding synthetic seawater.

At different times of incubation, samples were taken randomly on microcosms with Pasteur micropipettes and conserved immediately at -80°C. Biodiversity was evaluated by the T-RFLP method and dioxygenases encoding genes diversity by RFLP method.

Genomic DNA extraction

Mixed community DNA was extracted from microbial mat fractions with the Ultraclean soil DNA isolation kit (Mo Bio Laboratories), by using the recommended protocol with minor modifications as previously described (Precigou *et al.*, 2001).

PCR amplification and purification

Optimization of PCR was performed for each sample by adjusting the amount of genomic DNA extract used to obtain a strong band on an agarose gel, without visible non-specific product. PCR was performed using a reaction mixture of 200 µM each desoxynucleoside

triphosphate (Qiagen), 1.5 mM $MgCl_2$, 1.25 U of Taq polymerase (Qiagen), 1X PCR Buffer (Qiagen), and 0.2 µM each primer. The first primers used were the general eubacterial primer 8-27F (Lane, 1991), and the universal primer 1472-1489R (Muyzer *et al*., 1995) amplifying specifically the 16S ribosomal gene. Forward primers 8-27F were hexachlorofluorescein labeled. PCR (50µl) was performed in a MJ Research PTC-100 thermocycler by using an initial denaturation step of 95°C for 3 minutes, followed by 24 cycles of a program consisting of denaturation at 95°C for 30 seconds, primer annealing at 52°C for 30 seconds, and extension at 72°C for 30 seconds. A final extension at 72°C for 7 minutes was performed after the programmed numbers of cycles were completed. PCR products were then purified by using the GFX DNA and Gel Band Purification kit (Amersham Biosciences) as directed by the supplier.

Restriction enzyme digestion and products purification

300 ng of amplified DNA were digested with 10 U of HaeIII restriction enzyme (New England BioLabs) in a final volume of 30 µl 37°C during 3h.

T-RFLP analysis

Restricted PCR product was mixed with 0.5 µl of TAMRA500 size standard (Applied Biosystems). DNA fragments were separated by size by capillary electrophoresis at 15,000 Volts for 30 minutes on an ABI PRISM 310 Genetic Analyzer (Applied Biosystems). The 5' terminal fragments were visualized by excitation of the hexachlorofluorescein molecule (hex) attached to the forward primer. The gel image was captured and analyzed by using Genescan version 3.1 analysis software (ABI). Negative controls (no genomic DNA) were conducted with every PCR and run on Genescan gels.

Data sets were constructed by using peak which fluorescence was higher than 100 Fluorescence units for at least one sample. Statistical analyses (canonical analysis) were done with MVSP software (Multi-Variate Statistical Package 3.1, Kovach Computing Services).

Estimating dioxygenases encoding genes diversity in microbial mats

Diversity of the α subunit of the PAH dioxygenases encoding genes in the microcosm mats were analyzed using degenerated primers designed for this experiment (FRT6A: TACCACGTBGGTTGGAC and FRT3B: CATGTCTTTTTCKACVATGGC). This set of

degenerated primers was used to amplify dioxygenases genes from DNA extracted before and after the contamination with crude oil. Then, the PCR products were cloned in *E. coli* (Topo cloning kit, Invitrogen). Inserts were amplified using specific vector primers and analyzed by HaeIII endonuclease restriction. Some of the inserts showing different restriction patterns were sequenced.

RESULTS

Changes of bacterial communities in Camargue microbial mat during crude oil contamination

Through the three months period of contamination, T-RFLP profiles of the eubacterial community (16S rRNA encoding gene) were obtained at different incubation times. In these bacterial fingerprints, biodiversity was represented by detected terminal restriction fragments (T-RFs or peaks); each of them could be associated to an operational taxonomic unit (OTU). According to the different incubation periods, approximately twenty OTUs could be considered for each sample (Figure 1). T-RFLP profiles from the contaminated mat were found more variable than those obtained from the uncontaminated control. Quite important modifications of the fingerprints were observed in contaminated microcosms during the incubation period. Some OTUs, as for example the T-RF with length of 35 bases pairs (bp), were detected during all the incubation period on T-RFLP profiles while others were found specifically on few profiles. OTUs with length of 291 bp and 62 bp were not observed respectively after the 3 and 12 first days of incubation. In contrast, from the 12th day of incubation new OTUs with length of 146, 200, and 314 bp were detected. OTUs with length of 146 and 200 bp T-RFs were then found in all the profiles obtained until the end of incubation period (103 days) whereas the OTU of T-RF 314 bp was found specifically in the 12th day profile. After 30 days of incubation a new OTU of T-RF 213 bp was detected and remained until the 103rd day of incubation. It is noteworthy that the T-RFLP profiles were not modified between the 30th and the 40th day of incubation. An important change of the T-RFLP fingerprint was observed at the 103rd day of incubation; three new OTUs with length of 221, 285, and 346 bp were detected.

Changes of bacterial communities in Guérande microbial mat during crude oil contamination

T-RFLP analysis allowed following the whole eubacterial community (16S rRNA encoding gene) changes in Guérande mat microcosms during the three months contamination period (Figure 2). At each sampling time T-RFLP fingerprints were characterized by twenty-two main OTUs that were considered for our analyses. These analyses showed that bacterial communities changes occurred in both contaminated and uncontaminated microcosms. However the modifications observed were found different according to the presence or the absence of crude oil. For example, between the 30th and the 75th day the abundance of the OTU with length of 376 bp remained stable on control mats while it decreased in polluted mts. Although T-RFLP fingerprints of Guérande microbial mats showed low variations, succession of bacterial populations during crude oil exposure was revealed with statistical analyses. Correspondence analyses (CA) based on T-RFLP data showed that bacterial communities were separated in three main clusters (Figure 3A). From both contaminated and uncontaminated mats, bacterial communities of the first 15 days (At0, Bt0, At15 and Bt15) were grouped in a first cluster with those of the last day of incubation (At90 and Bt90). Between the 30th and the 75th days, two other clusters were obtained separating bacterial communities from contaminated mats to those from uncontaminated mats. The cluster formed by the control samples was explained by the first axis, showing a high percentage (34,5%) of the variance corresponding to some OTUs (376 and 225 bp) that could not be identified (Figure 3B). The cluster formed by the contaminated samples was mostly influenced by the second axis (23,8%). This included OTUs with length of 199 bp corresponding to *Desulfovibrio* sp. and 238 bp that could be related to several bacterial strains.

Estimating dioxygenases encoding genes diversity in microbial mats

For the analyses of dioxygenases diversity by PCR based method, several couples of primers were designed and tested. Among them, the couple FRT6A-FRT3B amplifying a 413 bp PCR product was selected in order to determine the dioxygenases diversity in contaminated microbial mats by combining cloning, Restriction Fragment Length Polymorphism (RFLP) analyses and sequencing. The analyses of dioxygenases diversity in the Camargue microbial mat after 30 days crude oil exposure showed the presence of different RFLP patterns allowing the distribution of dioxygenases encoding genes in ten groups (Figure 4). The identity as dioxygenases encoding sequences of each pattern was demonstrated by

DNA sequencing. The main three groups corresponded to 85% (40, 25, and 20% respectively) of the whole detected genes. The other seven groups were found to be equally represented.

DISCUSSION

In the present study we used molecular based methods to monitor the impact of crude oil exposure on microbial communities. Microbial mats were maintained in microcosms under controlled conditions. During the contamination period changes on the petroleum composition were observed (data not shown). Although the degradation of petroleum composition could be attributed mainly to physico-chemical processes, chemical analysis showed that biodegradation by microorganisms could also be suspected (data not shown). From this experimental set up, biodiversity of the whole eubacterial community changes were found following hydrocarbon pollution.

In Camargue mat microcosms three principal periods were observed. Briefly, during the first period (0 to 12 days) several sensitive bacterial populations (OTUs) were eliminated, then a transient period (between the 30th and 40th days) revealed the domination of other OTUs, and finally at the 103rd day we observed the development of a novel dominant bacterial populations. During the first 12 days the fingerprint changes showed the first impact of the contamination on microbial community. This result indicated both the bacterial adaptation to pollutant and sensitivity of some OTUs. The sensitive OTU with length of 291 bp was no more detected after the 3rd day suggesting that this OTU was one of the first affected by the contamination. Interestingly, this OTU could be related to cyanobacteria species with Ribosomal Data Project (RDP; http://rdp.cme.msu.edu/html/) analyses. This result is consistent with previous observation of cyanobacteria species elimination associated to crude oil exposure in laboratory experiments (Abed *et al.*, 2002). The fact that some photosynthetic species were the first affected in our experiment was not surprising since light is no more available through the oil layer and petroleum compounds are known to inhibit cyanobacteria metabolism (Megharaj *et al.*, 2000; Radwan and Al-Hasan, 2000). In contrast during this first period, new OTUs became conspicuous in the fingerprints. Because microbial communities within contaminated ecosystems tend to be dominated by organisms capable of utilizing and/or surviving toxic contamination (Macnaughton *et al*., 1999), the marked rise of bacterial species presumes their important role in hydrocarbons biodegradation. Among them, the OTU with length of 200 bp could be related with RDP to the genus *Chloroflexus*. Similar observations have been reported in a recent study showing the possible role of these filamentous green bacteria in hydrocarbons degradation by a photoheterotrophic growth

(Abed *et al*., 2002). During the second period, between 30 and 40 days of incubation, a stability of the bacterial community structure of Camargue microbial mat was observed indicating that these populations were well adapted to both presence of crude oil and experimental conditions. This suggested that the dominant OTUs found in these fingerprints might play a role in hydrocarbons degradation. The third period, at the 103rd day of incubation, showed an important change in the bacterial community structure within the mat revealing the presence of three novel dominant OTUs of 221, 285, and 346 bp. These OTUs could be related to genera containing known hydrocarbon-degrading bacteria such as *Burkholderia* (221 bp) and *Cytophaga* (285 bp). Thus these important changes could be explained in part by the adaptation of the bacterial communities to the metabolites formed and the new physico-chemical conditions resulting from the degradation of crude oil.

Similarly, the succession of bacterial populations during crude oil exposure of Guérande microbial mats allowed showing the adaptation of bacterial communities in response to hydrocarbons pollutions. This impact was particularly observed between the 30th and 75th day since bacterial communities from contaminated and uncontaminated mats formed two distinct clusters. During this period of incubation, CA showed that noticeable OTUs in contaminated microcosm could be related to *Desulfovibrio* sp.. Species of this sulfate-reducing bacterium genus have been isolated from contaminated sites (Richardson *et al*., 2002; Wu *et al*., 2002; Watts *et al*., 2001) suggesting a possible role of such bacteria in hydrocarbon degradation.

The diversity of genes encoding naphthalene and phenanthrene dioxygenases was analyzed at the 30th day of incubation period when Camargue microbial mat showed stable and therefore adapted community. Obviously, the detection of diverse PAH dioxygenase genes demonstrate that Camargue microbial mat possesses a potential for PAH degradation. The fact that three dominants PAH dioxygenase genes were detected would suggest that these genes play an important role in hydrocarbons degradation. Therefore, bacterial species possessing these genes could be considered to be well adapted to crude oil exposure under the experimental conditions.

In conclusion the impact of crude oil contamination on the studied microbial mats was characterized by successive changes of bacterial communities with the replacement of sensitive species by more adapted or resistant species. These modifications are probably correlated to the evolution of direct and indirect pollutant effects. Furthermore, such alteration of the community composition could also be useful as a bioindicator of hydrocarbons

pollutions. To further understand biodegradation by microbial mats, it will be interesting to isolate key microorganisms and fully explore their potentials to degrade hydrocarbons.

ACKNOWLEDGEMENTS

We acknowledge the financial support by the EC (MATBIOPOL project, grant EVK3-CT-1999-00010) and the Ministère de l'Ecologie et du Développement Durable (MEDD - LIT'EAU/Erika project, N° 01/1213857). The authors are grateful to the Salines de Guérande and the company of Salins du Midi at Salins-de-Giraud for facilitating access to the salterns, sampling and field experiments. SB and AF were partly supported by a doctoral grant from the Aquitaine region and the Conseil Général des Pyrénées Atlantiques respectively.

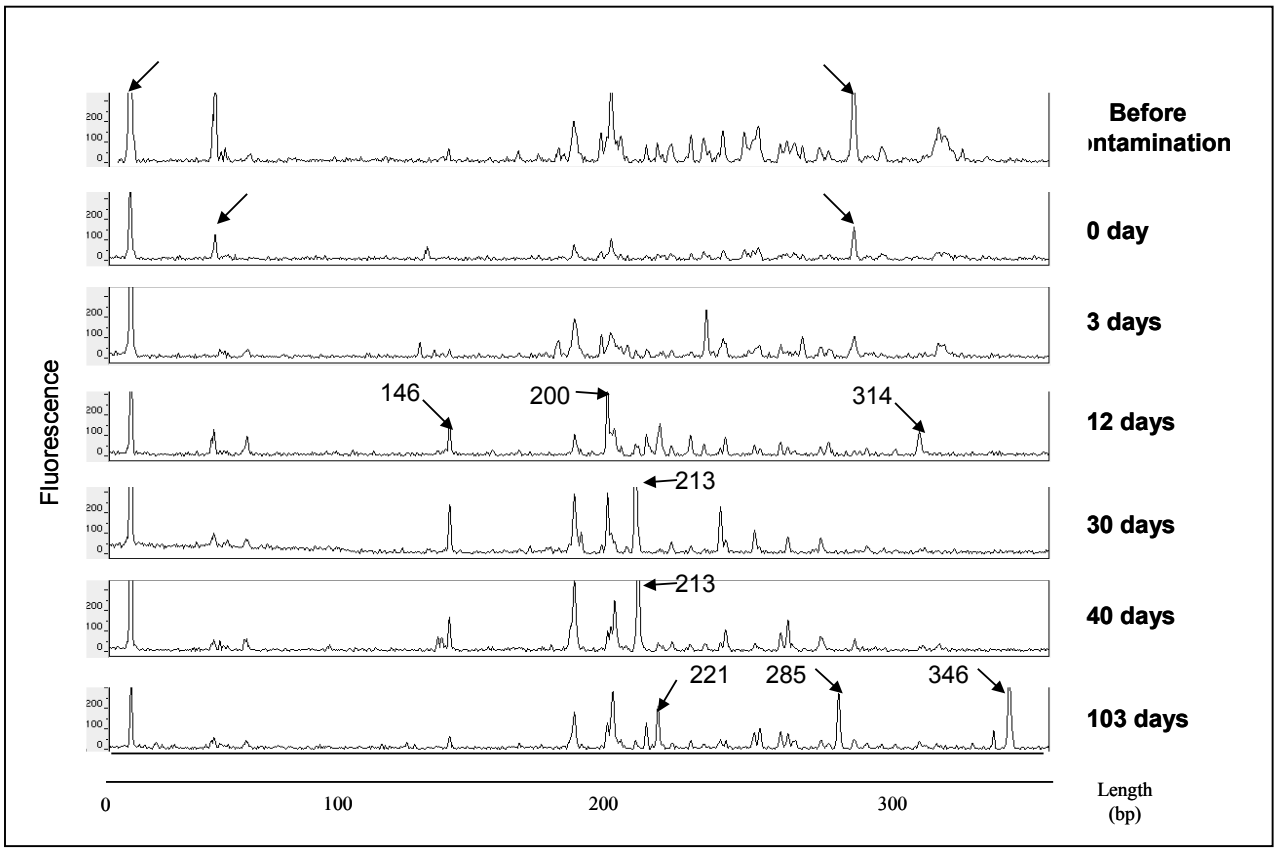

Figure 1: Eubacteria t-RFLP profiles of Camargue microbial mat microcosms based on 5' terminal restriction fragments (T-RFs) length of 16S rRNA encoding genes (HaeIII restriction enzyme) obtained at different incubation times through the 103 days of crude oil contamination. bp: bases pairs.

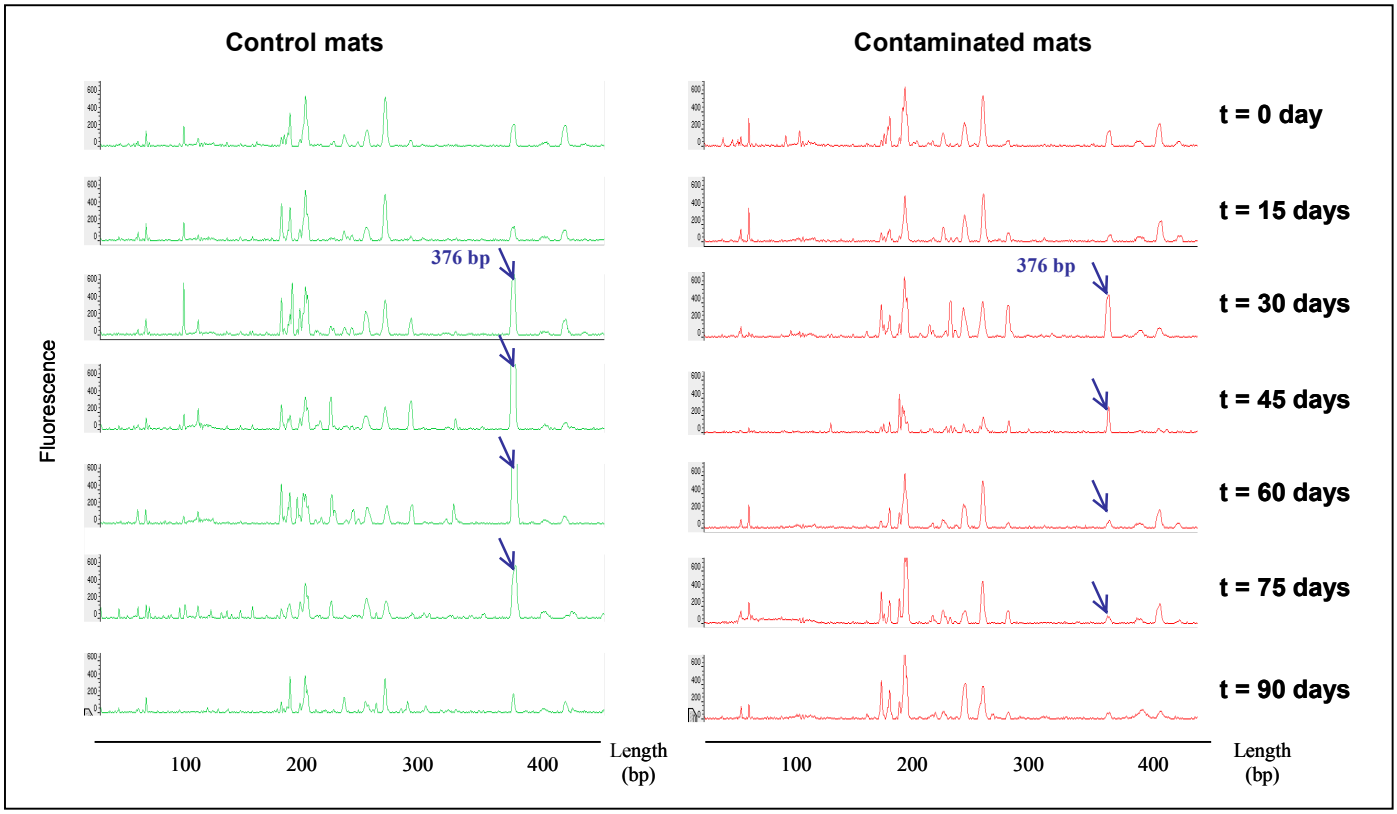

Figure 2: Eubacteria t-RFLP profiles of Guérande microbial mat microcosms based on 5' terminal restriction fragments (T-RFs) length of 16S rRNA encoding genes (HaeIII restriction enzyme) obtained at different incubation times through the 3 months of crude oil contamination. bp: bases pairs.

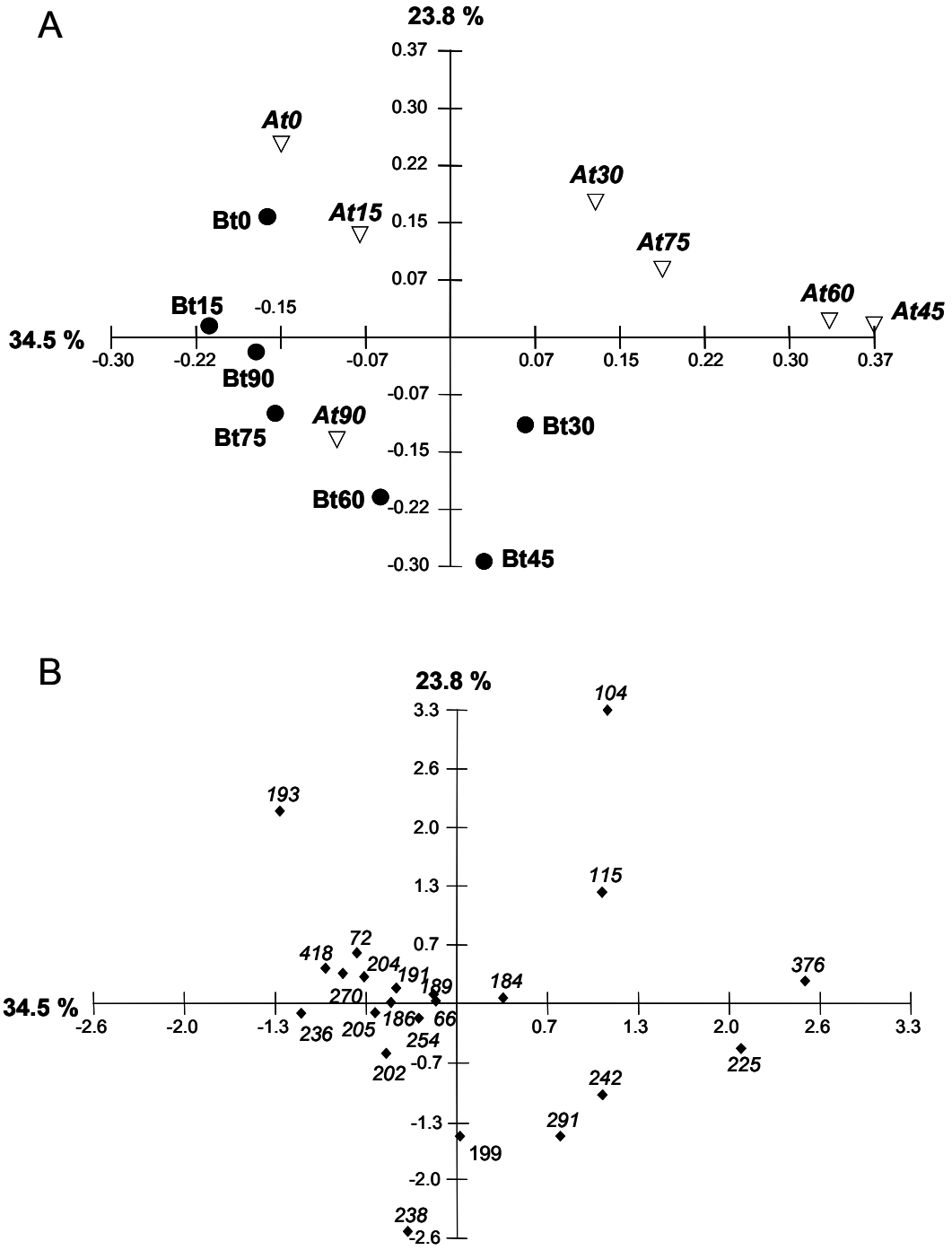

Figure 3: Correspondence analyses (CA) based on T-RFLP data of eubacteria (*16S rDNA*) from Guérande microcosms. (**A**) CA of contaminated (black circles) and control (white triangles) samples. The data analyzed correspond to 5' end T-RFLP pattern of the HaeIII digested *16S rDNA*. (**B**) CA of variables, i.e., T-RFs derived from CA in panel (A). Each number corresponding to the T-RF length in bases pairs.

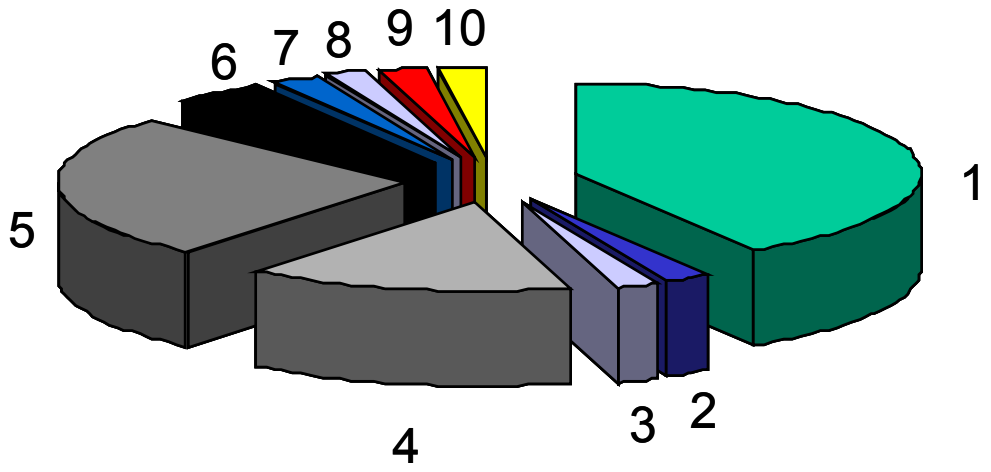

Figure 4: Distribution of the different dioxygenases RFLP patterns in Camargue microbial mats after 30 days of crude oil exposure.

REFERENCES

Abed, R.M., Safi, N.M., Koster, J., de Beer, D., El-Nahhal, Y., Rullkotter, J. and Garcia-Pichel, F. 2002. Microbial diversity of a heavily polluted microbial mat and its community changes following degradation of petroleum compounds. *Appl. Environ. Microbiol.* **68**(4): 1674-1683.

Al-Hasan, R.H., Al-Bader, D.A., Sorkhoh, N.A. and Radwan, S.S. 1998. Evidence for n-alkane consumption and oxidation by filamentous cyanobacteria from oil-contaminated coasts of the Arabian Gulf. *Mar. Biol.* **130**: 521-527.

Blackwood, C.B., Marsh, T., Kim, S.H. and Paul, E.A. 2003. Terminal restriction fragment length polymorphism data analysis for quantitative comparison of microbial communities. *Appl. Environ. Microbiol.* **69**(2): 926-932.

Brezna, B., Khan, A.A. and Cerniglia, C.E. 2003. Molecular characterization of dioxygenases from polycyclic aromatic hydrocarbon-degrading *Mycobacterium* spp. *FEMS Microbiol. Lett.* **223**(2): 177-183.

Caumette, P., Matheron, R., Raymond, N. and Relexans, J.-C. 1994. Microbial mats in the hypersaline ponds of Mediterranean salterns (Salins-de-Giraud, France). *FEMS Microbiol. Ecol.* **13**: 273-286.

Cerniglia, C.E., Van Baalen, C. and Gibson, D.T. 1980. Oxidation of biphenyl by the cyanobacterium, *Oscillatoria* sp., strain JCM. *Arch. Microbiol.* **125**(3): 203-207.

Contzen, M. and Stolz, A. 2000. Characterization of the genes for two protocatechuate 3, 4-dioxygenases from the 4-sulfocatechol-degrading bacterium *Agrobacterium radiobacter* strain S2. *J. Bacteriol*. **182**(21): 6123-6129.

Dahllof, I. 2002. Molecular community analysis of microbial diversity. *Curr. Opin. Biotechnol*. **13**(3): 213-217.

Ensley, B.D., Gibson, D.T. and Laborde, A.L. 1982. Oxidation of naphthalene by a multicomponent enzyme system from *Pseudomonas* sp. strain NCIB 9816. *J. Bacteriol*. **149**(3): 948-954.

Feng, Y., Khoo, H.E. and Poh, C.L. 1999. Purification and characterization of gentisate 1,2-dioxygenases from *Pseudomonas alcaligenes* NCIB 9867 and Pseudomonas putida NCIB 9869. *Appl. Environ. Microbiol*. **65**(3): 946-950.

Giani, D., Seeler, J., Giani, L. and Wolfgang, E.K. 1989. Microbial mats and physiochemistry in a saltern in the Bretagne (France) and in a laboratory scale saltern model. *FEMS Microbiol. Ecol.* **62**: 151-162.

Haddad, S., Eby, D.M. and Neidle, E.L. 2001. Cloning and expression of the benzoate dioxygenase genes from *Rhodococcus* sp. strain 19070. *Appl. Environ. Microbiol*. **67**(6): 2507-2514.

Hoffmann, L. 1996. Recolonisation of the intertidal flats by microbial mats after the Gulf War oil spill. *In*: Krupp, F., Abuzinada, A.H. and Nader, I.A. (Eds.) A marine wildlife sanctuary for the Arabian Gulf: environmental research and conservation following the 1991 Gulf War oil spill. Riyad, Saudi Arabia, and Seneckenberg Research Institue, Frankfurt, Germany, pp. 96-115.

Kanaly, R.A., Bartha, R., Watanabe, K. and Harayama, S. 2000. Rapid mineralization of benzo[a]pyrene by a microbial consortium growing on diesel fuel. *Appl. Environ. Microbiol*. **66**(10): 4205-4211.

Kanaly, R.A., Harayama, S. and Watanabe, K. 2002. *Rhodanobacter* sp. strain BPC1 in a benzo[a]pyrene-mineralizing bacterial consortium. *Appl. Environ. Microbiol*. **68**(12): 5826-5833.

Kang, B.S., Ha, J.Y., Lim, J.C., Lee, J., Kim, C.K., Min, K.R. and Kim, Y. 1998. Structure of catechol 2,3-dioxygenase gene from *Alcaligenes eutrophus* 335. *Biochem. Biophys. Res. Commun*. **245**(3): 791-796.

Kasai, Y., Kishira, H., Syutsubo, K. and Harayama, S. 2001. Molecular detection of marine bacterial populations on beaches contaminated by the Nakhodka tanker oil-spill accident. *Environ. Microbiol*. **3**(4): 246-255.

Khan, A.A., Wang, R.F., Cao, W.W., Doerge, D.R., Wennerstrom, D. and Cerniglia, C.E. 2001. Molecular cloning, nucleotide sequence, and expression of genes encoding a polycyclic aromatic ring dioxygenase from *Mycobacterium* sp. strain PYR-1. *Appl. Environ. Microbiol*. **67**(8): 3577-3585.

Lane, D.J. 1991. 16S/23S rRNA sequencing. *In*: Stackenbradt, E. and Goodfellow, M. (Eds.) Nucleic acid techniques in bacterial systematics. Wiley, Chichester, pp. 115-175.

Leahy, J.G. and Colwell, R.R. 1990. Microbial degradation of hydrocarbons in the environment. *Microbiol. Rev*. **54**(3): 305-315.

Liu, W.T., Marsh, T.L., Cheng, H. and Forney, L.J. 1997. Characterization of microbial diversity by determining terminal restriction fragment length polymorphisms of genes encoding 16S rRNA. *Appl. Environ. Microbiol*. **63**(11): 4516-4522.

MacNaughton, S.J., Stephen, J.R., Venosa, A.D., Davis, G.A., Chang, Y.J. and White, D.C. 1999. Microbial population changes during bioremediation of an experimental oil spill. *Appl. Environ. Microbiol*. **65**(8): 3566-3574.

Megharaj, M., Singleton, I., McClure, N.C. and Naidu, R. 2000. Influence of petroleum hydrocarbon contamination on microalgae and microbial activities in a long-term contaminated soil. *Arch. Environ. Contam. Toxicol*. **38**(4): 439-445.

Moser, R. and Stahl, U. 2001. Insights into the genetic diversity of initial dioxygenases from PAH-degrading bacteria. *Appl. Microbiol. Biotechnol*. **55**(5): 609-618.

Muyzer, G., de Waal, E.C. and Uitterlinden, A.G. 1993. Profiling of complex microbial populations by denaturing gradient gel electrophoresis analysis of polymerase chain reaction-amplified genes coding for 16S rRNA. *Appl. Environ. Microbiol*. **59**(3): 695-700.

Muyzer, G., Teske, A., Wirsen, C.O. and Jannasch, H.W. 1995. Phylogenetic relationships of *Thiomicrospira* species and their identification in deep-sea hydrothermal vent samples by denaturing gradient gel electrophoresis of 16S rDNA fragments. *Arch. Microbiol*. **164**(3): 165-172.

Narro, M.L., Cerniglia, C.E., Van Baalen, C. and Gibson, D.T. 1992. Metabolism of phenanthrene by the marine cyanobacterium *Agmenellum quadruplicatum* PR-6. *Appl. Environ. Microbiol*. **58**(4): 1351-1359.

Nogales, B., Moore, E.R., Llobet-Brossa, E., Rossello-Mora, R., Amann, R. and Timmis, K.N. 2001. Combined use of 16S ribosomal DNA and 16S rRNA to study the bacterial community of polychlorinated biphenyl-polluted soil. *Appl. Environ. Microbiol*. **67**(4): 1874-1884.

Olsen, G.J., Lane, D.J., Giovannoni, S.J., Pace, N.R. and Stahl, D.A. 1986. Microbial ecology and evolution: a ribosomal RNA approach. *Annu. Rev. Microbiol*. **40**: 337-365.

Precigou, S., Goulas, P. and Duran, R. 2001. Rapid and specific identification of nitrile hydratase (NHase)-encoding genes in soil samples by polymerase chain reaction. *FEMS Microbiol. Lett*. **204**(1): 155-161.

Radwan, S.S. and Al-Hasan, R.H. 2000. Oil pollution and cyanobacteria. *In*: B. A. Whitton and M. Potts (Eds.) The ecology of cyanobacteria. Kluwer Academic Publishers, Dordrecht, The Netherlands, pp. 307-319.

Resnick, S.M. and Gibson, D.T. 1996. Regio- and stereospecific oxidation of fluorene, dibenzofuran, and dibenzothiophene by naphthalene dioxygenase from Pseudomonas sp. strain NCIB 9816-4. *Appl. Environ. Microbiol*. **62**(11): 4073-4080.

Richardson, R.E., Bhupathiraju, V.K., Song, D.L., Goulet, T.A. and Alvarez-Cohen, L. 2002. Phylogenetic characterization of microbial communities that reductively dechlorinate TCE based upon a combination of molecular techniques. *Environ. Sci. Technol*. **36**(12): 2652-2662.

Rios-Hernandez, L.A., Gieg, L.M. and Suflita, J.M. 2003. Biodegradation of an alicyclic hydrocarbon by a sulfate-reducing enrichment from a gas condensate-contaminated aquifer. *Appl. Environ. Microbiol*. **69**(1): 434-443.

Stach, J.E. and Burns, R.G. 2002. Enrichment versus biofilm culture: a functional and phylogenetic comparison of polycyclic aromatic hydrocarbon-degrading microbial communities. *Environ. Microbiol*. **4**(3): 169-182.

Van Gemerden, H. 1993. Microbial mats: A joint of venture. *Mar. Geol.* **113**: 3-25.

Watts, J.E., Wu, Q., Schreier, S.B., May, H.D. and Sowers, K.R. 2001. Comparative analysis of polychlorinated biphenyl-dechlorinating communities in enrichment cultures using three different molecular screening techniques. *Environ. Microbiol*. **3**(11): 710-719.

Wu, Q., Watts, J.E., Sowers, K.R. and May, H.D. 2002. Identification of a bacterium that specifically catalyzes the reductive dechlorination of polychlorinated biphenyls with doubly flanked chlorines. *Appl. Environ. Microbiol*. **68**(2): 807-812.

Conclusions et perspectives

Conclusions et Perspectives:

Les travaux menés au cours de ces trois années de recherche ont été centrés sur le suivi de la diversité bactérienne de tapis microbiens soumis à des stress environnementaux. L'objectif de cette étude était donc de décrire à la fois l'organisation spatiale des tapis microbiens en terme de diversité des populations bactériennes, mais aussi de mettre en évidence la dynamique de cette structure hautement organisée en réponse à des stress récurrents que sont la salinité et les variations journalières des microgradients d'oxygène et de sulfure ou ponctuels comme les déversements de polluants.

Cette étude a été abordée par T-RFLP, approche moléculaire permettant le traitement et la comparaison d'un grand nombre d'échantillons. En effet, cette méthode a permis de décrire à une très petite échelle, de l'ordre d'une centaine de micromètres, la biodiversité bactérienne présente au sein de différents tapis microbiens et de mettre ainsi en évidence leurs fines organisations structurales. La comparaison des empreintes bactériennes ainsi obtenues a révélé une dynamique de la structure bactérienne de ces écosystèmes, autant sur le plan spatial que temporel, face à l'influence de gradients physico-chimiques verticaux ou de pollutions accidentelles. De plus, par le biais de collaborations au sein du projet MATBIOPOL, l'apport d'approches pluridisciplinaires a permis de compléter cette étude et d'aborder cette structure bactérienne en tant qu'écosystème dynamique capable de s'adapter aux conditions environnementales fluctuantes.

Dans un premier temps, la description de deux tapis microbiens photosynthétiques a été effectuée, à l'échelle du micromètre, en combinant différentes approches d'analyses. La biodiversité bactérienne des différentes communautés eubactéries, bactéries phototrophes anoxygéniques pourpres et bactéries sulfato-réductrices a été analysée par ribotypage moléculaire à l'aide de la T–RFLP, voire de la DGGE. Les résultats de ces approches moléculaires ont été corrélés à ceux des analyses biogéochimiques, des analyses de microscopie (CLSM), et des analyses des biomarqueurs lipidiques. L'alliance de ces différents résultats a permis de mettre en lien les communautés bactériennes présentes et leurs rôles écologiques au sein de ces écosystèmes complexes.

Le tapis microbien hypersalé des marais salants de Camargue révèle ainsi une organisation très fine, constituée de couches verticales distinctes de quelques micromètres, où s'agencent les populations bactériennes en fonction de leurs caractéristiques physiologiques et

des conditions environnementales. La surface de ces tapis est totalement dominée par les cyanobactéries filamenteuses, principalement *Microcoleus chthonoplastes*. De plus, la distribution des bactéries phototrophes pourpres et sulfato-réductrices est fonction des gradients mesurés de sulfure, d'oxygène et de lumière.

Le tapis photosynthétique marin des Iles Orcades montre une structure différente, dominée par les bactéries pourpres, très diversifiées et principalement représentées par le genre *Thiocapsa.* Les cyanobactéries y sont plus faiblement représentées. Comme pour le tapis microbien précédent, la structure de la diversité bactérienne des anoxyphototrophes et des sulfato-réducteurs est très finement organisée le long de gradients physico-chimiques.

Ainsi, l'analyse de ces deux écosystèmes microbiens a permis de mettre en évidence l'observation générale d'une fine structure des populations bactériennes au sein des tapis, quelle que soit la nature de ces populations. Cette organisation verticale se révèle être le reflet des divers métabolismes bactériens mis en jeu dans ces écosystèmes, induits par les conditions environnementales de l'habitat. Les principales populations fonctionnelles bactériennes composant ces tapis microbiens sont généralement comparables, cependant en terme de diversité leur variabilité se situe au niveau de leurs abondances et de leurs richesses en espèces. Dans notre étude, la salinité et les conditions climatiques, fort différentes entre les marais salants de Camargue et les plages des Iles Orcades, influeraient donc beaucoup sur le développement de certaines espèces bactériennes.

La seconde partie de cette étude s'est portée sur l'analyse de la distribution spatio-temporelle de groupes fonctionnels bactériens composant le tapis microbien de Camargue au cours d'un cycle nycthéméral. En effet, la fine organisation verticale des tapis microbiens observée, décrite dans le chapitre précédent, montre une structuration particulière des communautés bactériennes en fonction des conditions environnementales. Les microgradients verticaux d'oxygène, de sulfure, et de lumière présents au sein des tapis, fluctuent de manière importante au cours d'un cycle jour / nuit. Il s'agissait donc d'observer l'influence de ces facteurs physico-chimiques sur la localisation de ces communautés. Les comportements des principaux groupes fonctionnels composant ces tapis microbiens photosynthétiques, à savoir, les cyanobactéries, les bactéries anoxygéniques pourpres et les bactéries sulfato-réductrices, ont été mis en évidence par leur signature moléculaire ADNr 16S via l'approche de la T-RFLP.

Ceci a permis de montrer des comportements adaptatifs chez ces différentes populations. La composition et la structure du tapis microbien de Camargue, en terme de

diversité et d'abondance, que ce soit pour les communautés photosynthétiques ou les communautés sulfato-réductrices, est très différente au cours du cycle jour / nuit. Ceci révèle un fort impact des paramètres physico-chimiques sur la distribution verticale des bactéries du tapis. Ainsi, dues aux variations des microgradients au sein du tapis, différentes réponses des microorganismes à ce stress ont été observées : allant de la tolérance aux fluctuations, l'agrégation entre bactéries, à la mise en place de métabolismes versatiles permettant une meilleure adaptation de celles-ci. Néanmoins, le principal effet observé est la migration d'un grand nombre de ces microorganismes afin de se localiser où les conditions de croissance sont optimales ou de fuir les toxicités éventuelles. De ce fait, parmi les sulfato-réducteurs le genre *Desulfotignum* a montré une nette migration verticale vers le fond du tapis en journée, suivant ainsi le déplacement de la zone anoxique et fuyant l'oxygène riche en surface, du à une photosynthèse oxygénique active des cyanobactéries. Cette réponse adaptative par migration suggère fortement des mécanismes plus complexes d'«Energy» tactisme.

L'analyse de l'impact d'hydrocarbures sur les tapis microbiens de Guérande et de Camargue a été le troisième point abordé dans ce travail. L'effet de différents pétroles sur la biodiversité et donc la composition en communautés bactériennes de ces deux tapis microbiens a pu être étudié par la mise en place de microcosme. Ceci a permis le maintien de tapis microbiens en conditions contrôlées de pH, de salinité et de luminosité ; et de les incuber en présence de pétroles donnés.

Ainsi, l'influence des paramètres environnementaux sur la dégradation naturelle de ces pétroles a pu être démontrée. De plus, l'impact réel de la pollution sur les communautés du tapis a été observé, puisque l'étude a montré une adaptation séquentielle des différentes communautés bactériennes au cours de la période de pollution. En effet, au fur et à mesure des modifications de la composition des pétroles, différentes communautés bactériennes se succèdent révélant les capacités d'adaptation de ces écosystèmes face à ce stress d'hydrocarbures. Dans un premier temps, les communautés bactériennes sensibles aux hydrocarbures deviennent minoritaires, puis les communautés capables de résister et ou de dégrader les hydrocarbures présents deviennent majoritaires. Bien que les analyses chimiques aient montré l'évolution des pétroles, la dégradation par les micro-organismes n'a pu être clairement mise en évidence dans ces systèmes. Toutefois, l'analyse de la diversité des gènes codant pour les dioxygénases montre une grande diversité suggérant que les tapis microbiens possèdent un potentiel de dégradation important.

A la suite de cette étude, il apparaît que les microorganismes présents dans les tapis microbiens peuvent adopter différentes attitudes face à des stress environnementaux variés. Par conséquent, les microorganismes semblent posséder un panel de réponses adaptatives très diverses. Au cours de cette étude, différentes réponses ont pu être observées :

- Vis à vis d'un stress salin, les microorganismes sélectionnés par leur résistance et participant à la structuration des tapis microbiens sont des organismes taxonomiquement différents ayant des aptitudes halotolérantes à halophiles.

- Différents comportements sont induits par chimiotactisme tels que l'agrégation des bactéries entre elles afin de mieux résister aux mauvaises conditions environnantes.

- Chez les bactéries possédant des métabolismes versatiles, d'autres voies métaboliques mieux adaptées aux nouvelles conditions de l'habitat peuvent être mises en place.

- Le déplacement reste un comportement majeur d'adaptation chez les microorganismes. Les mécanismes permettant le déplacement sont également très variés. En effet, ils peuvent mettre en œuvre des flagelles, des systèmes de vacuoles de gaz ou des systèmes de glissement. Cette réponse est souvent régie par l'«Energy» tactisme guidant la migration de ces microorganismes vers des niches adaptées.

- Lorsque la pollution par des hydrocarbures constitue un stress environnemental chronique, elle induit aussi une sélection de microorganismes, soit tolérants aux hydrocarbures, soit capables de les dégrader possédant des activités hydrocarbonoclastes.

Afin d'approfondir ce travail et d'essayer de répondre aux diverses questions amenées par les observations faites au cours de ces recherches, il serait judicieux de compléter cette étude descriptive par des approches fonctionnelles.

En effet, l'analyse *in situ* de l'expression de gènes impliqués dans l'«Energy» tactisme, dans le métabolisme de dégradation des hydrocarbures ou bien dans l'osmorégulation, pourrait apporter de nombreuses informations. Les techniques de FISH (Fluorescence In Situ Hybrization), micro-arrays (ou puce ADN), RT-PCR (Reverse Transcription Polymerase Chain Reaction) pourraient être mises en œuvre pour suivre ces différentes réponses. Ceci permettrait une meilleure compréhension des mécanismes mis en jeux lors des réponses bactériennes face aux stress, et d'appréhender plus en détails la réponse dynamique de ces écosystèmes que sont les tapis microbiens.

Références bibliographiques

Références bibliographiques

Abed, R. M., Safi, N. M., Koster, J., de Beer, D., El-Nahhal, Y., Rullkotter, J. and García-Pichel, F. (2002). Microbial diversity of a heavily polluted microbial mat and its community changes following degradation of petroleum compounds. *Applied and Environmental Microbiology* **68**, 1674-1683.

Achenbach, L. A., Carey, J. and Madigan, M. T. (2001). Photosynthetic and phylogenetic primers for detection of anoxygenic phototrophs in natural environments. *Applied and Environmental Microbiology* **67**, 2922-2926.

Adler, J. (1988). Chemotaxis : old and new. *Botanica Acta* **101**.

Aeckersberg, F., Bak, F. and Widdel, F. (1991). Anaerobic oxidation of saturated hydrocarbons to CO2 by new type of sulfate-reducing bacterium. *Archives of Microbiology* **156**, 5-14.

Alexandre, G. and Zhulin, I. B. (2001). More Than One Way To Sense Chemicals. *Journal of Bacteriology* **183**, 4681-4686.

Alexandre, G., Greer-Phillips, S. and Zhulin, I. B. (2004). Ecological role of energy taxis in microorganisms. *FEMS Microbiology Reviews* **28**, 113-126.

Amann, R., Binder, B., Olson, R., Chisholm, S., Devereux, R. and Stahl, D. (1990). Combination of 16S rRNA-targeted oligonucleotide probes with flow cytometry for analyzing mixed microbial populations. *Applied and Environmental Microbiology* **56**, 1919-1925.

Barton, L. L. and Tomei, F. A. (1995). Characteristics and activities of sulfate-reducing bacteria. In *Sulfate-Reducing Bacteria*, pp. 1-32. Edited by L. L. Barton. New York: Peplum press.

Bebout, B. and Garcia-Pichel, F. (1995). UV B-induced vertical migrations of cyanobacteria in a microbial mat. *Appl. Environ. Microbiol.* **61**, 4215-4222.

Benlloch, S., López-López, A., Casamayor, E. O., Ovreas, L., Goddard, V., Daae, F. L., Smerdon, G., Massana, R., Joint, I., Thingstad, F., Pedros-Alio, C. and Rodriguez-Valera, F. (2002). Prokaryotic genetic diversity throughout the salinity gradient of a coastal solar saltern. *Environmental Microbiology* **4**, 349-360.

Benzécri, J. P. (1976). *L'analyse des données, l'analyse des correspondances.* Paris.

Bield, H. and Pfennig, N. (1978). Growth yields of green sulfur bacteria mixed cltures with sulfur and sulfate-reducing bacteria. *Archives of Microbiology* **117**, 9-16.

Blackwood, C. B., Marsh, T., Kim, S.-H. and Paul, E. A. (2003). Terminal Restriction Fragment Length Polymorphism Data Analysis for Quantitative Comparison of Microbial Communities. *Applied and Environmental Microbiology* **69**, 926-932.

Blankenship, R. E. and Hartman, H. (1998). The origin and evolution of oxygenic photosynthesis. *Trends in Biochemical Sciences* **23**, 94-97.

Brambilla, E., Hippe, H., Hagelstein, A., Tindall, B. J. and Stackebrandt, E. (2001). 16S rDNA diversity of cultured and uncultured prokaryotes of a mat sample from Lake Fryxell, McMurdo Dry Valleys, Antarctica. *Extremophiles* **5**, 23-33.

Canfield, D. E. and Des Marais, D. J. (1991). Aerobic sulfate reduction in microbial mats. *Science* **251**, 1471-1473.

Canfield, D. E. and Des Marais, D. J. (1993). Biogeochemical cycles of carbon, sulfur, and free oxygen in a microbial mat. *Geochimica et Cosmochimica Acta* **57**, 3971-3984.

Canosa, I., Sanchez-Romero, J. M., Yuste, L. and Rojo, F. (2000). A positive feedback mechanism controls expression of AlkS, the transcriptional regulator of the Pseudomonas oleovorans alkane degradation pathway. *Molecular Microbiology* **35**, 791-799.

Casamayor, E. O., Massana, R., Benlloch, S., Ovreas, L., Diez, B., Goddard, V. J., Gasol, J. M., Joint, I., Rodríguez-Valera, F. and Pedrós-Alió, C. (2002). Changes in archaeal, bacterial and eukaryal assemblages along a salinity gradient by comparison of genetic fingerprinting methods in a multipond solar saltern. *Environmental Microbiology* **4**, 338-348.

Castenholz, R. W. (1994). Microbial mats research: The recent past and new perspectives. In *Microbial Mats*, pp. 3-18. Edited by L. J. Stal and P. Caumette. Berlin Heidelberg: Springer-Verlag.

Castro, H. F., Williams, N. H. and Ogram, A. (2000). Phylogeny of sulfate-reducing bacteria. *FEMS Microbiology Ecology* **31**, 1-9.

Caumette, P., Baulaigue, R. and Matheron, R. (1988). Characterization of *Chromatium salexigens* sp. nov., a halophilic *Chromatiaceae* isolated from Mediterranean salinas. *Systematic and Applied Microbiology* **10**, 284-292.

Caumette, P., Baulaigue, R. and Matheron, R. (1991). *Thiocapsa halophila* sp. nov., a new halophilic phototrophic purple sulfur bacterium. *Archives of Microbiology* **155**, 170-176.

Caumette, P., Matheron, R., Raymond, N. and Relexans, J. C. (1994). Microbial mats in the hypersaline ponds of Mediterranean salterns (Salins-de-Giraud, France). *FEMS Microbiology Ecology* **13**, 273-286.

Cohen, Y. (2002). Bioremediation of oil by marine microbial mats. *International Microbiology* **5**, 189-193.

Cypionka, H. (2000). Oxygen respiration by *Desulfovibrio* species. *Annual Review of Microbiology* **54**, 827-848.

Cypionka, H., Widdel, F. and Pfennig, N. (1985). Survival of sulfate-reducing bacteria after oxygen stress, and growth in sulfate-free oxygen-sulfide gradients. *FEMS Microbiology Letters* **31**, 39-45.

Dade, W. B., Davis, J. D., Nichols, P. D., Nowell, A. R. M., Thistle, D., Trexler, M. B. and White, D. C. (1990). Effects of bacterial exopolymer adhesion on the entrainment of sand. *Geomicrobiological Journal* **8**, 1-16.

Daly, K., Sharp, R. J. and McCarthy, A. J. (2000). Development of oligonucleotide probes and PCR primers for detecting phylogenetic subgroups of sulfate-reducing bacteria. *Microbiology* **146**, 1693-1705.

D'Amelio, E. D., Cohen, Y. and Des Marais, D. J. (1987). Association of a new type of gliding, filamentous, purple phototrophic bacterium inside bundles of *Microcoleus chthonoplastes* in hypersaline cyanobacterial mats. *Archives of Microbiology* **147**, 213-220.

De Wit, R. and Caumette, P. (1994). Diversity of and interactions among sulfur bacteria in microbial mats. In *Microbial Mats*, pp. 379-391. Edited by L. J. Stal and P. Caumette. Berlin Heidelberg: Springer-Verlag.

de Wit, R., van den Ende, F. P. and van Gemerden, H. (1995). Mathematical simulation of the interactions among cyanobacteria, purple sulfur bacteria and chemotrophic sulfur bacteria in microbial mat communities. *FEMS Microbiology Ecology* **17**, 117-135.

Decho, A. W. (1990). Microbial exopolymer secretions in ocean environments : their role(s) in food webs and marine processes. *Oceanography and Marine Biology Reviews* **137**, 1369-1374.

Denome, S., Stanley, D., Olson, E. and Young, K. (1993). Metabolism of dibenzothiophene and naphthalene in Pseudomonas strains: complete DNA sequence of an upper naphthalene catabolic pathway. *Journal of Bacteriology* **175**, 6890-6901.

Donkor, V. and Häder, D. P. (1991). Effects of solar and ultra violet radiation on motility, photomovement and pigmentation in filamentous, gliding cyanobacteria. *FEMS Microbiology Ecology* **86**, 159-168.

Dunbar, J., Ticknor, L. O. and Kuske, C. R. (2001). Phylogenetic specificity and reproducibility and new method for analysis of terminal restriction fragment profiles of 16S rRNA genes from bacterial communities. *Applied and Environmental Microbiology* **67**, 190-197.

Duque, E., Segura, A., Mosqueda, G. and Ramos, J. L. (2001). Global and cognate regulators control the expression of the organic solvent efflux pumps TtgABC and TtgDEF of Pseudomonas putida. *Molecular Microbiology* **39**, 1100-1106.

Dutta, T. and Harayama, S. (2001). Biodegradation of n-alkylcycloalkanes and n-alkylbenzenes via new pathways in Alcanivorax sp. strain MBIC 4326. . *Applied and Environmental Microbiology* **67**, 1970-1974.

Egert, M. and Friedrich, M. W. (2003). Formation of pseudo-Terminal Restriction Fragments, a PCR-related bias affecting Terminal Restriction Fragment Length Polymorphism analysis of microbial community structure. *Applied and Environmental Microbiology* **69**, 2555-2562.

Esteve, I., Martínez, M., Mir, J. and Guerrero, R. (1992). Typology and structure of microbial mats communities in Spain: A preliminary study. *Limnetica* **8**, 185-195.

Farnleitner, A. H., Kreuzinger, N., Kavka, G. G., Grillenberger, S., Rath, J. and Mach, R. L. (2000). Comparative analysis of denaturing gradient gel electrophoresis and temporal temperature gradient gel electrophoresis in separating Escherichia coli uidA amplicons differing in single base substitutions. *Lett Appl Microbiol* **30**, 427-431.

Fauque, G. D. (1995). Ecology of sulfate-reducing bacteria. In *Sulfate-reducing bacteria*, pp. 217-241. Edited by L. L. Barton. New York: Peplum press.

Fenchel, T. (2002). Microbial behavior in a heterogeneous world. *Science* **296**, 1068-1071.

Ferris, M. J., Muyzer, G. and Ward, D. M. (1996). Denaturing gradient gel electrophoresis profiles of 16S rRNA-defined populations inhabiting a hot spring microbial mat community. *Applied and Environmental Microbiology* **62**, 340-346.

Fuenmayor, S., Wild, M., Boyes, A. and Williams, P. (1998). A gene cluster encoding steps in conversion of naphthalene to gentisate in Pseudomonas sp. strain U2. *Journal of Bacteriology* **180**, 2522-2530.

Fukui, M., Teske, A., Aßmus, B., Muyzer, G. and Widdel, F. (1999). Physiology, phylogenetic relationships, and ecology of filamentous sulfate-reducing bacteria (genus desulfonema). *Archives of Microbiology* **172**, 193-203.

Galushko, A., Minz, D., Schink, B. and Widdel, F. (1999). Anaerobic degradation of naphthalene by a pure culture of a novel type of marine sulphate-reducing bacterium. *Environmental Microbiology* **1**, 415-420.

Garcia-Pichel, F. and Pringault, O. (2001). Microbiology. Cyanobacteria track water in desert soils. *Nature* **413**, 380-381.

García-Pichel, F., Mechling, M. and Castenholz, R. W. (1994). Diel migrations of microorganisms within a benthic, hypersaline mat community. *Applied and Environmental Microbiology* **60**, 1500-1511.

Geissdorfer, W., Kok, R., Ratajczak, A., Hellingwerf, K. and Hillen, W. (1999). The genes rubA and rubB for alkane degradation in Acinetobacter sp. strain ADP1 are in an operon with estB, encoding an esterase, and oxyR. *Journal of Bacteriology* **181**, 4292-4298.

Giani, D., Seeler, J., Giani, L. and Krumbein, W. E. (1989). Microbial mats and physicochemistry in a saltern in the Bretagne (France) and in a laboratory scale saltern model. *FEMS Microbiology Ecology* **62**, 151-162.

Gibson, J. E., Stackebrandt, E., Zablen, L. B., Gupta, R. and Woese, C. (1979). A phylogenetic analysis of the purple photosynthetic bacteria. *Current Microbiology* **3**, 59-64.

Gloe, A., Pfennig, N., Brockmann, H. and Trowitchzsch, W. (1975). a new bacteriochlorophyll from brown-colored *Chlorobiaceae*. *Archives of Microbiology* **102**, 103-109.

Grant, A. and Ogilvie, L. A. (2003). Terminal restriction fragment length polymorphism data analysis. *Applied and Environmental Microbiology* **69**, 6342; author reply 6342-6343.

Grant, A. and Ogilvie, L. A. (2004). Name that microbe: rapid identification of taxa responsible for individual fragments in fingerprints of microbial community structure. *Molecular Ecology Notes* **4**, 133-136.

Grossman, A. R., Bhaya, D., Apt, K. E. and Kehoe, D. M. (1995). Light-harvesting complexes in oxygenic photosynthesis: diversity, control, and evolution. *Annu Rev Genet* **29**, 231-288.

Grotzschel, S., Koster, J., Abed, R. M. and de Beer, D. (2002). Degradation of petroleum model compounds immobilized on clay by a hypersaline microbial mat. *Biodegradation* **13**, 273-283.

Guerrero, R., Urmeneta, J. and Rampone, G. (1993). Distribution of types of microbial mats at the Ebro Delta, Spain. *Biosystems* **31**, 135-144.

Hamamura, N., Yeager, C. and Arp, D. (2001). Two distinct monooxygenases for alkane oxidation in Nocardiodes sp. strain CF8. *Applied and Environmental Microbiology* **67**, 4992-4998.

Harayama, S., Kishira, H., Kasai, Y. and Shutsubo, K. (1999). Petroleum biodegradation in marine environments. *Journal of Molecular and Microbiological Biotechnology* **1**, 63-70.

Harms, G., Zengler, K., Rabus, R., Aeckersberg, F., Minz, D., Rossello-Mora, R. and Widdel, F. (1999). Anaerobic oxidation of o-xylene, m-xylene, and homologous

alkylbenzenes by new types of sulfate-reducing bacteria. *Appl Environ Microbiol* **65**, 999-1004.

Herbert, R. (1985). Development of mass blooms of photosynthetic bacteria on sheltered beaches in Scapa Flow, Orkney Islands. *Proceedings of the Royal Society of Edinburgh* **87**, 15-25.

Hirschler-Rea, A., Matheron, R., Riffaud, C., Moune, S., Eatock, C., Herbert, R. A., Willison, J. C. and Caumette, P. (2003). Isolation and characterization of spirilloid purple phototrophic bacteria forming red layers in microbial mats of Mediterranean salterns: description of Halorhodospira neutriphila sp. nov. and emendation of the genus Halorhodospira. *International Journal of Systematic and Evolutionary Microbiology* **53**, 153-163.

Höpner, T., Yousef, M., Berthe-Corti, L., Felzmann, H., Struck, H. and AL-Thukair, A. (1996). Cyanobacterial mats on oil-polluted sediments - start of a promising self-remediation process ? *A marine wildlife sanctuary for the Arabian gulf.*, 85-95.

Imhoff, J. F. (1992). Taxonomy, phylogeny and general ecology of anoxygenic phototrophic bacteria. In *Photosynthetic bacteria*, pp. 53-92. Edited by N. H. Mann and N. G. Carr. New York: Peplum Press.

Johnson, H., Pelletier, D. and Spormann, A. (2001). Isolation and characterization of anaerobic ethylbenzene dehydrogenase, a novel Mo-Fe-S enzyme. *Journal of Bacteriology* **183**, 4536-4542.

Jørgensen, B. B. (1982). Ecology of the bacteria of the sulphur cycle with special reference to anoxic-oxic interface environments. *Philosophical Transactions of the Royal Society of London. serie B, Biological sciences* **298**, 543-561.

Jørgensen, B. B. and Des Marais, D. J. (1986). Competition for sulfide among colorless and purple sulfur bacteria in cyanobacterial mats. *FEMS Microbiology Ecology* **38**, 179-186.

Jørgensen, B. B. and Des Marais, D. J. (1988). Optical properties of benthic photosynthetic communities: Fiber-optic studies of cyanobacterial mats. *Limnology and Oceanography* **33**, 99-113.

Jørgensen, B. B., Revsbech, N. P. and Cohen, Y. (1983). Photosynthesis and structure of benthic microbial benthic microbial : microelectrode and SEM studies of four cyanobacterial communities. *Limnology and Oceanography* **28**, 1075-1093.

Kaine, B. P., Gupta, R. and Woese, C. R. (1983). Putative introns in tRNA genes of prokaryotes. *Proc Natl Acad Sci U S A* **80**, 3309-3312.

Kaplan, C. W. and Kitts, C. L. (2003). Variation between observed and true Terminal Restriction Fragment length is dependent on true TRF length and purine content. *Journal of Microbiological Methods* **54**, 121-125.

Kent, A. D., Smith, D. J., Benson, B. J. and Triplett, E. W. (2003). Web-Based Phylogenetic Assignment Tool for Analysis of Terminal Restriction Fragment Length Polymorphism Profiles of Microbial Communities. *Applied and Environmental Microbiology* **69**, 6768-6776.

Kieboom, J., Dennis, J. J., de Bont, J. A. M. and Zylstra, G. J. (1998a). Identification and molecular characterization of an efflux pump involved in Pseudomonas putida S12 solvent tolerance. *Journal of Biology and Chemistry* **273**, 85-91.

Kieboom, J., Dennis, J. J., Zylstra, G. J. and de Bont, J. A. M. (1998b). Active efflux of organic solvents by Pseudomonas putida S12 is induced by solvents. *Journal of Bacteriology* **184**, 6769-6772.

Kiko, H., Niggemann, E. and Ruger, W. (1979). Physical mapping of the restriction fragments obtained from bacteriophage T4 dC-DNA with the restriction endonucleases SmaI, KpnI and BglII. *Mol Gen Genet* **172**, 303-312.

Kim, I. S., Foght, J. M. and Gray, M. R. (2002). Selective transport and accumulation of alkanes by Rhodococcus erythropolis S_14He. *Biotechnol. Bioeng.* **80**, 650-659.

Kiyohara, H., Torigoe, S., Kaida, N., Asaki, T., Iida, T., Hayashi, H. and Takizawa.N. (1994). Cloning and characterization of a chromosomal gene cluster, pah, that encodes the upper pathway for phenanthrene and naphthalene utilization by Pseudomonas putida OUS82. *Journal of Bacteriology* **176**, 2439-2443.

Kniemeyer, O. and Heider, J. (2001). Ethylbenzene dehydrogenase, a novelhydrocarbon-oxidizing molybdenum/iron-sulfur/heme enzyme. *Journal of Biology and Chemistry* **276**, 21381-21386.

Koike, K., Ara, K., Adachi, S., Takigawa, P., Mori, H., Inoue, S., Kimura, Y. and Ito, S. (1999). Regiospecific internal desaturation of aliphatic compounds by a mutant Rhodococcus strain. . :. *Applied and Environmental Microbiology* **65**, 5636-5638.

Kovach, W. L. (1999).MVSP - a Multivariate Statistical Package for Windows. Wales U.K.: Kovack Computing Services.

Krekeler, D., Teske, A. and Cypionka, H. (1998). Strategies of sulfate-reducing bacteria to escape oxygen stress in a cyanobacterial mat. *FEMS Microbiology Ecology* **25**, 89-96.

Krumbein, W. E., Cohen, Y. and Shilo, M. (1977). Solar Lake (Sinai), 4. Stromatolitic cyanobacteria mats. *Limnology and Oceanography* **22**, 635-656.

Kruschel, C. and Castenholz, R. W. (1998). The effect of solar UV and visible irradiance on the vertical movements of cyanobacteria in microbial mats of hypersaline waters. *FEMS Microbiology Ecology* **27**, 53-72.

Kühl, M. (1992). Spectral light measurments in microbenthic phototrophic communities with a fiber-optic microbrobe coupled to a sensitive diode array detector. *Limnology and Oceanography* **37**, 1813-1823.

Kühl, M. and Fenchel, T. (2000). Bio-optical Characteristics and the Vertical Distribution of Photosynthetic Pigments and Photosynthesis in an Artificial Cyanobacterial Mat. *Microbial Ecology* **40**, 94-103.

Kumar, S., Tamura, K., Jakobsen, I. B. and Nei, M. (2001). MEGA2: molecular evolutionary genetics analysis software. *Bioinformatics* **17**, 1244-1245.

Kurkela, S., Lehvaslaiho, H., Palva, E. and Teeri, T. (1988). Cloning, nucleotide sequence, and characterization of genes encoding naphthalene dioxygenase of Pseudomonas putida strain NCIB9816. *Gene* **73**, 355-362.

Lane, D. J. (1991). rRNA sequencing. In *Nucleic acid techniques in bacterial systematics.*, pp. 115-175. Edited by G. M. Stachenbradt E., (Eds): Wiley, Chichester.

Larsen, H. (1986). Halophilic and halotolerant microorganisms-an overview and historical perspective. *FEMS Microbiology Letters* **39**, 3-7.

Lassen, C., Ploug, H. and Jørgensen, B. B. (1992). A fibre-optic scalar irradiance microsensor: application for spectral light measurements in sediments. *FEMS Microbiology Ecology* **86**, 247-254.

Laurie, A. and Lloyd-Jones, G. (1999). The phn genes of Burkholderia sp. strain RP007 constitute a divergent gene cluster for polycyclic aromatic hydrocarbon catabolism. *Journal of Bacteriology* **181**, 531-540.

Leahy, J. G. and Colwell, R. R. (1990). Microbial degradation of hydrocarbons in the environment. *Microbiological Reviews* **54**, 305-315.

Leuthner, B. and J., H. (1998). A two-component system involved in regulation of anaerobic toluene metabolism in Thauera aromatica. . :. *FEMS Microbiology Letters* **166**, 35-41.

Liu, W. T., Marsh, T. L., Cheng, H. and Forney, L. J. (1997). Characterization of microbial diversity by determining terminal restriction fragment length polymorphisms of genes encoding 16S rRNA. *Applied and Environmental Microbiology* **63**, 4516-4522.

Maidak, B. L., Olsen, G. J., Larsen, N., Overbeek, R., McCaughey, M. J. and Woese, C. R. (1996). The Ribosomal Database Project (RDP). *Nucleic Acids Research* **24**, 82-85.

Maidak, B. L., Olsen, G. J., Larsen, N., Overbeek, R., McCaughey, M. J. and Woese, C. R. (1997). The RDP (Ribosomal Database Project). *Nucleic Acids Research* **25**, 109-111.

Maidak, B. L., Larsen, N., McCaughey, M. J., Overbeek, R., Olsen, G. J., Fogel, K., Blandy, J. and Woese, C. R. (1994). The Ribosomal Database Project. *Nucleic Acids Research* **22**, 3485-3487.

Maidak, B. L., Cole, J. R., Lilburn, T. G., Parker, C. T., Jr., Saxman, P. R., Farris, R. J., Garrity, G. M., Olsen, G. J., Schmidt, T. M. and Tiedje, J. M. (2001). The RDP-II (Ribosomal Database Project). *Nucleic Acids Research* **29**, 173-174.

Maidak, B. L., Cole, J. R., Lilburn, T. G., Parker, C. T., Jr., Saxman, P. R., Stredwick, J. M., Garrity, G. M., Li, B., Olsen, G. J., Pramanik, S., Schmidt, T. M. and Tiedje, J. M. (2000). The RDP (Ribosomal Database Project) continues. *Nucleic Acids Research* **28**, 173-174.

Maidak, B. L., Cole, J. R., Parker, C. T., Jr., Garrity, G. M., Larsen, N., Li, B., Lilburn, T. G., McCaughey, M. J., Olsen, G. J., Overbeek, R., Pramanik, S., Schmidt, T. M., Tiedje, J. M. and Woese, C. R. (1999). A new version of the RDP (Ribosomal Database Project). *Nucleic Acids Research* **27**, 171-173.

Makkar, R. S. and Cameotra, S. S. (1998). Production of biosurfactant at mesophilic and thermophilic conditions by a strain of Bacillus subtilis. *Journal of industrial Microbiology and Biotechnology* **20**, 48-52.

Makkar, R. S. and Cameotra, S. S. (2002). An update on the use of unconventional substrates for biosurfactant production and their new applications. *Applied and Microbiological Biotechnology* **58**, 428-434.

Margulis, L., Barghoorn, E. S., Ashendorf, D., Banerjee, S., Chase, D., Francis, S., Giovannoni, S. and Stolz, J. (1980). The microbial community in the layered sediments at Laguna Figueroa, Baja California, Mexico: Does it have Precambrian analogues? *Precambrian Research* **11**, 93-123.

Marín, M. M., Smits, T. H. M., van Beilen, J. B. and Rojo, F. (2001). The alkane hydroxylase gene of Burkholderia cepacia RR10 is under catabolite repression control. *Journal of Bacteriology* **183**, 4202-4209.

Marsh, T. L. (1999). Terminal restriction fragment length polymorphism (T-RFLP): an emerging method for characterizing diversity among homologous populations of amplification products. *Current Opinion in Microbiology* **2**, 323-327.

Marsh, T. L., Saxman, P., Cole, J. and Tiedje, J. (2000). Terminal restriction fragment length polymorphism analysis program, a web-based research tool for microbial community analysis. *Applied and Environmental Microbiology* **66**, 3616-3620.

Marshall, K. C. (1989). Cyanobacterial-heterotrophic bacterial interactions. In *Microbial mats : physiological ecologyof benthic microbial communities.*, pp. 239-245. Edited by Cohen and E. Rosenberg. Washington DC, USA: ASM edition.

Martinez, A., Pibernat, I., Figueras, J. and Garcia-Gil, J. (1997). Structure and composition of freshwater microbial mats from a sulfur spring ("Font Pudosa", NE Spain). *Microbiologia* **13**, 45-56.

Matheron, R. (1976). Contribution à l'étude écologique, systématique et physiologique des *Chromatiaceae* et des *Chlorobiaceae* isolées de sédiments marins., pp. 193. Marseille: Université de Marseille.

Mengoni, A., Grassi, E. and Bazzicalupo, M. (2002). Cloning method for taxonomic interpretation of T-RFLP patterns. *Biotechniques* **33**, 990-992.

Minz, D., Fishbain, S., Green, S. J., Muyzer, G., Cohen, Y., Rittmann, B. E. and Stahl, D. A. (1999a). Unexpected population distribution in a microbial mat community: sulfate-reducing bacteria localized to the highly oxic chemocline in contrast to a eukaryotic preference for anoxia. *Applied and Environmental Microbiology* **65**, 4659-4665.

Minz, D., Flax, J. L., Green, S. J., Muyzer, G., Cohen, Y., Wagner, M., Rittmann, B. E. and Stahl, D. A. (1999b). Diversity of sulfate-reducing bacteria in oxic and anoxic regions of a microbial mat characterized by comparative analysis of dissimilatory sulfite reductase genes. *Applied and Environmental Microbiology* **65**, 4666-4671.

Mir, J., Martínez-Alonso, M., Esteve, I. and Guerrero, R. (1991). Vertical stratification and microbial assemblage of a microbial mat in the Ebro Delta (Spain). *FEMS Microbiology Ecology* **86**, 59-68.

Moezelaar, R., Bijvank, S. M. and Stal, L. (1996). Fermentation and sulfur reduction in the mat-building cyanobacterium *Microcoleus chthonoplastes*. *Applied and Environmental Microbiology*, 1752-1758.

Morgan, P. and Watkinson, R. J. (1994). Hydrocarbon degradation in soils and methods for soil biotreatment. *Critical Review in Biotechnology* **8**, 305-333.

Mouné, S. (2000). Analyse de la biodiversité bactérienne des sédiments anoxiques de milieux hypersalés (marais salants de Salins-de-Giraud, France), pp. 192. Pau: Université de Pau et des Pays de l'Adour.

Mouné, S., Caumette, P., Matheron, R. and Willison, J. C. (2003). Molecular sequence analysis of prokaryotic diversity in the anoxic sediments underlying cyanobacterial mats of two hypersaline ponds in Mediterranean salterns. *FEMS Microbiology Ecology* **44**, 117-130.

Mouné, S., Manac'h, N., Hirschler, A., Caumette, P., Willison, J. C. and Matheron, R. (1999). *Haloanaerobacter salinarius* sp. nov., a novel halophilic fermentative bacterium that reduces glycine-betaine to trimethylamine with hydrogen or serine as electron donors; emendation of the genus *Haloanaerobacter*. *International Journal of Systematic Bacteriology* **49 Pt 1**, 103-112.

Mouné, S., Eatock, C., Matheron, R., Willison, J. C., Hirschler, A., Herbert, R. and Caumette, P. (2000). *Orenia salinaria* sp. nov., a fermentative bacterium isolated from anaerobic sediments of Mediterranean salterns. *International Journal of Systematic and Evolutionnary Microbiology* **50 Pt 2**, 721-729.

Mullis, K., Faloona, F., Scharf, S., Saiki, R., Horn, G. and Erlich, H. (1986). Specific enzymatic amplification of DNA in vitro: the polymerase chain reaction. *Cold Spring Harb Symp Quant Biol* **51**, 263-273.

Muyzer, G. (1999). DGGE/TGGE a method for identifying genes from natural ecosystems. *Curr Opin Microbiol* **2**, 317-322.

Muyzer, G. and Smalla, K. (1998). Application of denaturing gradient gel electrophoresis (DGGE) and temperature gradient gel electrophoresis (TGGE) in microbial ecology. *Antonie Van Leeuwenhoek* **73**, 127-141.

Muyzer, G., de Waal, E. C. and Uitterlinden, A. G. (1993). Profiling of complex microbial populations by denaturing gradient gel electrophoresis analysis of polymerase chain reaction-amplified genes coding for 16S rRNA. *Appl Environ Microbiol* **59**, 695-700.

Muyzer, G., Teske, A., Wirsen, C. O. and Jannasch, H. W. (1995). Phylogenetic relationships of Thiomicrospira species and their identification in deep-sea hydrothermal vent samples by denaturing gradient gel electrophoresis of 16S rDNA fragments. *Arch Microbiol* **164**, 165-172.

Muyzer, G., Brinkhoff, T., Nübel, U., Santegoeds, C., Schäfer, H. and Wawer, C. (1998). Denaturing gradient gel electrophoresis (DGGE) in microbial ecology. In *Molecular microbial ecology manual*, pp. 1-27. Edited by v. E. J. Akkermans ADL, de Bruijn FJ (9eds). Kluwer, Dordrecht.

Nelson, D. C., Revsbech, N. P. and Jørgensen, B. B. (1986a). Microoxic-anoxic niche of Beggiatoa spp. : microelectrode survey of marine and freshwater strains. *Applied and Environmental Microbiology* **52**, 161-168.

Nelson, D. C., Jørgensen, B. B. and Revsbech, N. P. (1986b). Growth pattern and yield of a chemoautotrophic *Beggiatoa* sp. in oxygen-sulfide microgradients. *Applied and Environmental Microbiology* **52**, 225-233.

Nicholson, J. A. M., Stolz, J. F. and Pierson, B. K. (1987). Structure of a microbiol mat at Great Sippewissett Marsh, Cape Cod, Massachusetts. *FEMS Microbiology Letters* **45**, 343-364.

Nubel, U., Bateson, M. M., Madigan, M. T., Kuhl, M. and Ward, D. M. (2001). Diversity and Distribution in Hypersaline Microbial Mats of Bacteria Related to Chloroflexus spp. *Appl. Environ. Microbiol.* **67**, 4365-4371.

Nübel, U., García-Pichel, F. and Muyzer, G. (2000a). The halotolerance and phylogeny of cyanobacteria with tightly coiled trichomes (Spirulina Turpin) and the description of Halospirulina tapeticola gen. nov., sp. nov. *International Journal of Systematic and Evolutionnary Microbiology* **50**, 1265-1277.

Nübel, U., García-Pichel, F., Clavero, E. and Muyzer, G. (2000b). Matching molecular diversity and ecophysiology of benthic cyanobacteria and diatoms in communities along a salinity gradient. *Environmental Microbiology* **2**, 217-226.

Ogier, J. C., Son, O., Gruss, A., Tailliez, P. and Delacroix-Buchet, A. (2002). Identification of the bacterial microflora in dairy products by temporal temperature gradient gel electrophoresis. *Appl Environ Microbiol* **68**, 3691-3701.

Ollivier, B., Caumette, P., Garcia, J. L. and Mah, R. A. (1994). Anaerobic bacteria from hypersaline environments. *Microbiological Reviews* **58**, 27-38.

Osborn, A. M., Moore, E. R. and Timmis, K. N. (2000). An evaluation of terminal-restriction fragment length polymorphism (T- RFLP) analysis for the study of microbial community structure and dynamics. *Environmental Microbiology* **2**, 39-50.

Overmann, J. and van Gemerden, H. (2000). Microbial interactions involving sulfur bacteria: implications for the ecology and evolution of bacterial communities. *FEMS Microbiology Reviews* **24**, 591-599.

Overmann, J., Fischer, U. and Pfennig, N. (1992). A new purple sulfur bacterium from saline littoral sediments, Thiorhodovibrio winogradskyi gen. nov. and sp. nov. *Archives of Microbiology* **157**, 329-335.

Pandey, G. and Jain, R. K. (2002). Bacterial Chemotaxis toward Environmental Pollutants: Role in Bioremediation. *Applied and Environmental Microbiology* **68**, 5789-5795.

Panke, S., Meyer, A., Huber, C., Witholt, B. and Wubbolts, M. (1999). An alkane-responsive expression system for the production of fine chemicals. *Applied and Environmental Microbiology* **65**, 2324-2332.

Paterson, D. M. (1989). Shorts-trems changes in the erodibility of intertidal cohesive sediments related to the migratory behaviour of epipelic diatoms. *Limnology and Oceanography* **34**, 223-234.

Pfennig, N. (1967). Photosynthetic bacteria. *Annual Review of Microbiology* **21**, 285-324.

Pfennig, N. (1975). The phototrophic bacteria and their role in the sulfur cycle. *Plant and Soil* **43**, 1-16.

Pfennig, N. (1989). Ecology of Phototrophic purple and green sulfur bacteria. In *Autotrophic Bacteria*, pp. 97-116. Edited by H. G. Schlegel and B. Bowien. Berlin: Science Technique Publisher, Madison and Springer Verlag.

Pfennig, N. and Trüper, H. G. (1974). The phototrophic bacteria, 8th ed. In *Bergey's manual of determinative bacteriology*, pp. 24-64. Edited by R. E. Buchanan and N. E. Gibbons. Baltimore: Wiliams and Wilkins Co.

Pfennig, N. and Truper, H. G. (1983). Taxonomy of phototrophic green and purple bacteria: a review. *Ann Microbiol (Paris)* **134B**, 9-20.

Pfennig, N. and Trüper, H. (1992). *The family Chromatiaceae*. New-York: Springer-Verlag,.

Pierson, B., Oesterle, A. and Murphy, G. L. (1987). Pigments, light penetration, and photosynthetic activity in the multi-layered microbial mats of Great Sippewissett Salt Marsh, Massachusetts. *FEMS Microbiology Letters* **45**, 365-376.

Pinkart, H. C. and White, D. C. (1997). Phospholipid biosynthesis and solvent tolerance in Pseudomonas putida strains. *Journal of Bacteriology* **179**, 4219-4422.

Pringault, O. and Garcia-Pichel, F. (2003). Hydrotaxis of cyanobacteria in desert crusts. *Microbial Ecology* **12**, 12.

Rabus, R. and Widdel, F. (1995). Conversion studies with substrate analogues of toluene in a sulfate-reducing bacterium, strain Tol2. *Arch Microbiol* **164**, 448-451.

Ratajczak, A., Geibdorfer, W. and Hillen, W. (1998). Alkane hydroxylase from Acinetobacter sp. strain ADP1 is encoded by alkM and belongs to a new family or bacterial integral-membrane hydrocarbon hydroxylases. *Applied and Environmental Microbiology* **64**, 1175-1179.

Rehm, H. J. and Reiff, I. (1982). Regulation der mikrobiellen alkanoxidation mit hinblick auf die produktbildung. *Acta Biotechnolology* **2**, 127-138.

Revsbech, N. P., Jorgensen, B. B., Blackburn, T. H. and Cohen, Y. (1983). Microelectrode studies of the photosynthesis and O2, H2S and pH profiles of a microbial mat. *Limnology and Oceanography* **28**, 1062-1074.

Richardson, L. L. (1996). Horizontal and vertical migration patterns of *Phormidium corallyticum* and *Beggiatoa* spp. associated with black-band disease of corals. *Microbial Ecology* **32**, 323-335.

Rojas, A., Duque, E., Mosqueda, G., Golden, G., Hurtado, A., Ramos, J. L. and A., S. (2001). Three efflux pumps are required to provide efficient tolerance to toluene in Pseudomonas putida DOT-T1E. *Journal of Bacteriology* **183**, 3967-3973.

Romagnoli, S., Packer, H. L. and Armitage, J. P. (2002). Tactic Responses to Oxygen in the Phototrophic Bacterium Rhodobacter sphaeroides WS8N. *Journal of Bacteriology* **184**, 5590-5598.

Saiki, R. K., Scharf, S., Faloona, F., Mullis, K. B., Horn, G. T., Erlich, H. A. and Arnheim, N. (1985). Enzymatic amplification of beta-globin genomic sequences and restriction site analysis for diagnosis of sickle cell anemia. *Science* **230**, 1350-1354.

Saito, A., Iwabuchi, T. and Harayama, S. (2000). A novel phenanthrene dioxygenase from Nocardioides sp. strain KP7: expression in Escherichia coli. *Journal of Bacteriology* **182**, 257-261.

Sanger, F., Nicklen, S. and Coulson, A. R. (1992). DNA sequencing with chain-terminating inhibitors. 1977. *Biotechnology* **24**, 104-108.

Siefert, E. and Pfennig, N. (1984). A convenient method to prepare neutral sulfide solution for cultivation of phottotrophic sulfur bacteria. *Archives of Microbiology* **139**, 100-101.

Sigalevich, P., Baev, M. V., Teske, A. and Cohen, Y. (2000a). Sulfate reduction and possible aerobic metabolism of the sulfate- reducing bacterium Desulfovibrio oxyclinae in a chemostat coculture with Marinobacter sp. Strain MB under exposure to increasing oxygen concentrations. *Applied and Environmental Microbiology* **66**, 5013-5018.

Sigalevich, P., Meshorer, E., Helman, Y. and Cohen, Y. (2000b). Transition from anaerobic to aerobic growth conditions for the sulfate- reducing bacterium Desulfovibrio oxyclinae results in flocculation. *Applied and Environmental Microbiology* **66**, 5005-5012.

Simon, M., Bonner, J., McDonald, T. and Autenrieth, R. (1999). Bioaugmentation for the enhanced bioremediation of petroleum in a wetland. Polycyclic Aromatic Hydrocarbons 14-15:231-239. *Microbiology* **67**, 4353-4357.

Simon, M., Osslund, T., Saunders, R., Ensley, B., Suggs, S., Harcourt, A., Suen, W., Cruden, D., Gibson, D. and Zylstra, G. (1993). Sequence of genes encoding naphthalene dioxygenase in Pseudomonas putida strains G7 and NCIB 9816-4. *Gene* **127**, 31-37.

Smith, M. R. (1994). The physiology of aromatic hydrocarbon degrading bacteria. in Biochemistry of microbial degradation. pp. 347-372. Edited by C. Ratledge. Kluwer: Academic Publisher.

Stackebrandt, E. and Woese, C. R. (1984). The phylogeny of prokaryotes. *Microbiol Sci* **1**, 117-122.

Stal, L. J. (1994). Microbial mats in coastal environments. In *Microbial Mats*, pp. 21-32. Edited by L. J. Stal and P. Caumette. Berlin Heidelberg: Springer-Verlag.

Stal, L. J., van Gemerden, H. and Krumbein, W. E. (1985). Structure and development of a benthic marine microbial mat. *FEMS Microbiology Letters* **31**, 111-125.

Story, S. P., Parker, S. H., Kline, J. D., Tzeng, T. R. J., Mueller, J. G. and Kline, E. L. (2000). Identification of four structural genes and two putative promoters necessary for utilization of naphthalene, phenanthrene, and fluoranthene by Sphingomonas paucimobilis var. EPA505. *Gene* **260**, 155-169.

Swannell, R. P., Lee, K. and McDonagh, M. (1996). Field evaluations of marine oil spill bioremediation. *Microbiological Reviews* **60**, 342-365.

Taylor, B. L., Zhulin, I. B. and Johnson, M. S. (1999). Aerotaxis and other energy-sensing behavior in bacteria. *Annual Review of Microbiology* **53**, 103-128.

Teal, T. H., Chapman, M., Guillemette, T. and Margulis, L. (1996). Free-living spirochetes from Cape Cod microbial mats detected by electron microscopy. *Microbiologia* **12**, 571-584.

Ter Braak, C. J. F. (1986). Canonical correspondence analysis : a new eigenvector technique for multivariate direct gradient analysis. *Ecology* **67**, 1167-1179.

Teske, A., Ramsing, N. B., Habicht, K., Fukui, M., Kuver, J., Jørgensen, B. B. and Cohen, Y. (1998). Sulfate-reducing bacteria and their activities in cyanobacterial mats of solar lake (Sinai, Egypt). *Applied and Environmental Microbiology* **64**, 2943-2951.

Thar, R. and Kuhl, M. (2001). Motility of *Marichromatium gracile* in response to light, oxygen, and sulfide. *Applied and Environmental Microbiology* **67**, 5410-5419.

Tissot, B. P. and Welte, D. H. (1984). *Petroleum formation and occurence.* Berlin, Heidelberg, New York.

Treadway, S., Yanagimachi, K., Lankenau, E., Lessard, P., Stephanopoulos, G. and Sinskey, A. (1999). Isolation and characterization of indene bioconversion genes from Rhodococcus strain I24. *Applied and Microbiological Biotechnology* **51**, 786-793.

Trotha, R., Reichl, U., Thies, F. L., Sperling, D., Konig, W. and Konig, B. (2002). Adaptation of a fragment analysis technique to an automated high- throughput multicapillary electrophoresis device for the precise qualitative and quantitative characterization of microbial communities. *Electrophoresis* **23**, 1070-1079.

Tsitko, I. V., Zaitsev, G. M., Lobanok, A. G. and Salkinoja-Salonen, M. S. (1999). Effect of Aromatic Compounds on Cellular Fatty Acid Composition of Rhodococcus opacus. *Applied and Environmental Microbiology* **65**, 853-855.

van Beilen, J., Panke, S., Lucchini, S., Franchini, A., Rothlisberger, M. and Witholt, B. (2001). Analysis of Pseudomonas putida alkane degradation gene clusters and flanking insertion sequences: evolution and regulation of the alk genes. *Microbiology* **147**, 1621-1630.

van Gemerden, H. (1993). Microbial mats : A joint venture. *Marine Geology* **113**, 3-25.

van Gemerden, H., Tughan, C. S., de Wit, R. and Herbert, R. A. (1989a). Laminated microbial ecosystems on sheltered beaches in Scapa Flow, Orkney Islands. *FEMS Microbiology Letters* **62**, 87-101.

van Gemerden, H., de Wit, R., Tughan, C. S. and Herbert, R. A. (1989b). Development of mass blooms of Thiocapsa roseopersicina on sheltered beaches on the Orkney Islands. *FEMS Microbiology Ecology* **62**, 111-118.

Van Hamme, J. D. and Ward, O. P. (2000). Development of a method for the application of solid-phase microextraction to monitor the biodegradation of volatile hydrocarbons during bacterial growth on crude oil. *Journal of industrial Microbiology and Biotechnology* **25**, 155-162.

Van Hamme, J. D., Singh, A. and Ward, O. P. (2003). Recent Advances in Petroleum Microbiology. *Microbiology and Molecular Biology Reviews* **67**, 503–549.

Walter, M. R. (1976). Stromatolites. In *Developments in Sedimentology 20*, pp. 790. Amsterdam: Elsevier.

Walter, M. R., Grotzinger, J. P. and Schopf, J. W. (1992a). Proterozoic stromatolites. In *he proterozoic biosphere: a multidisciplinary study*, pp. 253-260. Edited by J. W. Schopf and C. Klein. Cambridge: Cambridge University Press.

Walter, M. R., Bauld, J., Des Marais, D. J. and Schopf, J. W. (1992b). A general comparison of microbial mats and microbial stromatolites: bridging the gap between the

modern and the fossil. In *The proterozoic biosphere: a multidisciplinary study*, pp. 335-338. Edited by J. W. Schopf and C. Klein. Cambridge: Cambridge University Press.

Weisburg, W. G., Barns, S. M., Pelletier, D. A. and Lane, D. J. (1991). 16S ribosomal DNA amplification for phylogenetic study. *Journal of Bacteriology* **173**, 697-703.

Whitman, B. E., Lueking, D. R. and Mihelcic, J. R. (1998). Naphthalene uptake by a Pseudomonas fluorescens isolate. *Canadian Journal of Microbiology* **44**, 1086-1093.

Widdel, F. (1980). Anaerober abbau von fettsäuren und benzoesäure durch neu isolierte arten sulfat-reduzierender bakterien. In *Insitut für Mikrobiologie*, pp. 443. Göttingen: Göttingen University.

Widdel, F. (1988). Microbiology and ecology of sulfate- and sulfur reducing bacteria. In *Biology of Anaerobic microorganisms*, pp. 469-585. Edited by A. J. B. Zehnder. New York: Wiley, J. and sons.

Widdel, F. and Bak, F. (1992). *Gram-negative mesophilic sulfate-and sulfur-reducing bacteria.* New York: Springer-Verlag.

Wieland, A. and Kühl, M. (2000). Short-term temperature effects on oxygen and sulfide cycling in a hypersaline cyanobacterial mat (Solar Lake, Egypt). *Marine Ecology Progress Series* **196**, 87-102.

Wieland, A., Zopfi, J., Benthien, M. and Kühl, M. (2004). Biogeochemistry of an iron-rich hypersaline microbial mat (Camargue, France). *Microbial Ecology* **in press**.

Wieland, A., Kuhl, M., McGowan, L., Fourçans, A., Duran, R., Caumette, P., Garcia De Oteyza, T., Grimalt, J. O., Solé, A., Diestra, E., Esteve, I. and Herbert, R. A. (2003). Microbial mats on the Orkney islands revisited: microenvironment and microbial community composition. *Microbial Ecology* **46**, 371-390.

Yen, K. and Serdar, C. (1988). Genetics of naphthalene catabolism in pseudomonads CRC. *Critical Review in Microbiology* **15**, 247-268.

Yuste, L. and Rojo, F. (2001). Role of the crc gene in catabolic repression of the Pseudomonas putida Gpo1 alkane degradation pathway. *Journal of Bacteriology* **183**, 6197-6206.